Investigation of the Removal and Recovery of Metal Cations and Anions from Dilute Aqueous Solutions Using Polymer – Surfactant Aggregates

Licheng Shen

Lady Margent Hall

University of Oxford

A thesis submitted for the degree of

Doctor of Philosophy

Trinity 2015

Statement of Originality

The work presented in this thesis is, to the best of the candidate's knowledge and belief, original and the candidate's own work, except as acknowledged in the text. The material has not been submitted, either in whole or in part, for a degree at this or any other university. This copy has been supplied on the understanding that it is copyright material and that no quotation from the thesis may be published without proper acknowledgement.

Investigation of the Removal and Recovery of Metal Cations and Anions from Dilute Aqueous Solutions Using Polymer – Surfactant Aggregates

Licheng Shen

Lady Margaret Hall, University of Oxford

A thesis submitted for the degree of Doctor of Philosophy in Engineering Science

Trinity 2015

Abstract

Dilute metallic ion treatment (<10 mg/L) remains a challenge in water purification and resource recovery. A novel and inexpensive treatment process that employs polymer–surfactant aggregates (PSAs) has been developed and applied to remove and recover dilute metallic ions, such as Cr^{3+}, Rh^{3+}, Cd^{2+}, $Fe(CN)_6^{3-}$ and CrO_4^{2-}, from industrial process and effluent. At the heart of this process is a material that comprises a colloidal structure of polymers and surfactants, named a polymer–surfactant aggregate (PSA), that trap metallic ions. The ion loaded PSAs then coalesce and settle out. The flocs are then treated separately by acid-base wash to recover the ions in a concentrated salt and regenerate the polymer and surfactant. The regenerated polymer and surfactant can then be recycled without a deterioration of removal ability in the next cycle. This process is simple, uses low energy, and generates little material loss or discharge.

The thesis is divided into three main parts: fundamentals, cation treatment and anion treatment. First, the mechanism of formation of PSAs and their interactions with metallic ions are investigated using surface tension and electrical conductivity measurements. Both measurements reveal that the PSA is formed by surfactant monomers binding to the oppositely charged polymer chains and forming micelle–like aggregates via hydrophobic and electrostatic forces. These aggregates, like micelles, can

bind to the oppositely charged metallic ions, but the surfactant concentration required is a few orders of magnitude lower than that required for micelle formation. The resulting nano-size PSA has a large surface area to volume ratio, and can effectively treat dilute aqueous streams. Each PSA consists of positive and negative charges. Within a near charge neutralisation range, they can quickly self-flocculate to simultaneously remove metallic ions and settle the flocs out of aqueous solutions. Correlating the removal efficiency of ions with surface tension and electrical conductivity measurements, the results suggest that the PSA is indeed responsible for removing the ions from the streams.

Based on the fundamentals, a PSA process consisting of three stages (removal, recovery and recycle) is developed to treat metal cations in dilute streams. At the removal stage, polymer and surfactant (i.e. removal agent) are used to form PSAs and trap 99% of 0.1 mM metal ions into flocs. At the recovery stage, a small amount of acid solution is added to leach out 95% of the trapped metal ions into a concentrated salt, and then using a base solution to completely dissolve and regenerate the removal agent. After that, the removal agent are recycled in the next cycle without the need for any make-up, and little deterioration of removal ability is found.

The same three-stage process is also applied to recover dilute metallic anions. As the targeted ions are negatively charged, the charge of polymer and surfactant used and the order of acid-base wash are reversed as compared with the cation treatment process.

The PSA process is robust under different conditions, e.g. pH, temperature, salinity and organic contaminants. Such a sustainable process thus has potential applications for the efficient removal and recovery of dilute metallic ions during process effluent water treatment.

Peer-Reviewed Papers

1. Shen, L. C., Nguyen, X. T. and Hankins, N. P. 2015. Removal of Heavy Metal Ions from Dilute Aqueous Solutions by Polymer–Surfactant Aggregates: A Novel effluent treatment process, *Separation and Purification Technology* 152, 101-107.
2. Shen, L. C., Lo, A., Nguyen, X. T. and Hankins, N. P. 2015. Recovery of Heavy Metal Ions and Recycle of Removal Agent in the Polymer–Surfactant Aggregate Process (under review)
3. Shen, L. C., Wu, J. Shivashkar, S. and Hankins, N. P. 2015. Removal of Anions from Dilute Aqueous Solutions by Polymer–Surfactant Aggregates (submitted)
4. Shen, L. C., Courtney, J. and Hankins, N. P. 2015. Recovery of Chromate and Recycle of Removal Agent in the Polymer–Surfactant Aggregate Process (in preparation)

Chapters in Book

- Shen, L. C., Hankins, N. P. and Singh, R. 2015. Surfactant and Polymer Based Technologies for Water Treatment, Chapter 10 in 'Emerging Membrane Technology for Sustainable Water Treatment and Supply', *Elsevier*, Amsterdam. (in press)
- Khan, J. S., Hankins, N. P. and Shen, L. C. 2015. Novel Membrane Bioreactor Configurations for Wastewater Treatment: Submerged and Attached Growth MBRs and Forward Osmosis MBRs, Chapter 11 in 'Emerging Membrane Technology for Sustainable Water Treatment and Supply', *Elsevier*, Amsterdam. (in press)
- Shen, L. C. and Hankins, N. P. 2015. Forward Osmosis, Chapter 3 in 'Emerging Membrane Technology for Sustainable Water Treatment and Supply', *Elsevier*, Amsterdam. (in press)

Patent Pending

- Shen, L. C. and Hankins, N. P., ‘Removal and recovery of a charged species’, no. 1420469.7GB – filing date: 18 November 2014.

Conferences

Oral presentation

- Shen, L. C., Lo, A. and Hankins, N. P. Dilute contaminant ion removal and recovery from wastewater by polymer–surfactant aggregates, oral presentation in the WEF-EESS Asia–Pacific Wastewater Treatment and Reuse Conference, the National University of Singapore, Singapore. June 28-July 1, 2015.
- Hankins, N. P. and Shen L. C. Removal and recovery of heavy metal ions from dilute aqueous solutions by recyclable polymer–surfactant aggregates, oral presentation in the 5th Oxford Water and Membrane Research Event – The Water, Food and Energy Nexus, Balliol College, Oxford, UK. June 28-30, 2015
- Shen, L. C. and Hankins, N. P. Removal of heavy metal ions from dilute aqueous solutions by polymer–surfactant aggregates, oral presentation in the Surfactants Workshop, Mathematical Institute, Oxford, UK. July 22, 2013.

Poster presentation

- Shen, L. C. and Hankins, N. P. Removal and recovery of heavy metal ions from dilute aqueous solutions by colloidal entities, poster presentation in the 5th International Colloidal Conference, Amsterdam, Netherland. June 21-24, 2015.

Acknowledgements

This work described in this dissertation was carried out in the Department of Engineering Science at the University of Oxford. I really enjoyed my research. This dissertation could not be accomplished without the co-operations of so many people. I extend my sincerest thanks and gratitude.

The long list of acknowledgement must begin with my supervisor Professor Nicholas Hankins. He gave me a lot of wonderful opportunities at the University of Oxford. He directed me into the fields of colloidal chemistry and water treatment, and supported my interests in the research directions. I enjoyed our discussion, which always brought me many inspirations. Thank you very much for all of this, I have learnt so much from you! I also would like to thank Professor Penny Smith, my college advisor, for her support and encouragement. Many people at the Department of Engineering Science helped me with my work at various stages.

It is also a pleasure to thank the people in Begbroke Science Park, especially Professor Ian Thompson, Dr Helen Townley, Dr Duane Ager, Dr Yaldah Azimi and Dr Yizhi Song for their help and guidance in laboratory. Xiafu S., Gabi G., Shivashkar S., Ana C., Fozia P., Ke Y., Cordelia R., Meg U., Naomi W., Mike M., Lakshmi A., Joan Z., Patrick T., Marimar B., Rachel M., Cindy H., Noel L., Adrian L., Tung N., Joshua C. and Ji W., thank you all and I'm extremely privileged to have you all as wonderful co-workers and friends. All my friends in Oxford, particularly Shivashkar Singh and Matthias Qian, are appreciated for their great friendships and contribution to many memorable and enjoyable occasions.

I also would like to thank Dr. Robert Thomas, Dr. Peixun Li, Dr. Hui Xu and Kun Ma who shared their insight in research directions and assisted me on surface tension experiments on top of their already busy schedule; Professor Christopher Breward and Dr. Christopher Bell for their inspirational contributions from mathematic modelling of the work; Dr. Chandra Ramanujan and Dr. Richard Holliday for their support of patent application and commercialisation, and the useful discussions and encouragement.

Most importantly, I express my greatest gratefulness to my parents and all my family members for their tremendous support. The very special thanks must be reserved for Jingjing Lou, for her ongoing and immense support throughout this work. Her unfailing belief keeps me going through ups and downs during my DPhil.

Financial support of Singapore-Peking-Oxford Research Enterprise scholarship is gratefully acknowledged. Thanks to my supervisor, Lady Margaret Hall and the department for the support of funds to attend conferences and workshops. I also thank Isis innovation for the support of patent application.

I hope that the water treatment process will be applied in the industry and improve the sustainability and resources management in the future.

Contents

List of Figures

List of Tables

Chapter 1

Introduction

1.1. Background and scope

Water is one of the planet's most precious natural resources, yet only 1% is available for human consumption. Today, 1.2 billion people in the world do not have access to clean drinking water, and 2.6 billion lack sanitation when 80% of developing world diseases are water-borne. Since the dawn of industrialisation, the number of both organic and inorganic contaminants in water supplies have increased steadily (Montgomery and Elimelech, 2007). In addition, due to stringent regulations driven by public health and environmental concerns, water previously considered as clean needs further treatment. With installed water distribution and purification infrastructure, maintenance of supply is a priority issue against a background of pressure to remediate and reduce pollution. The sustainable supply of potable water and the disposal of wastewater are thus among the major challenges of the 21st century. To address these challenges, a considerable amount

of research has been conducted to develop effective new technologies for water treatment at affordable cost and with minimum impact on the environment.

Metallic cation and anion contaminated streams, as one of the challenges and opportunities in wastewater treatment, have attracted extensive attention. All contaminant ion removal techniques have their inherent advantages and limitations in their various applications, which are summarised in Table 1.1. Chemical precipitation is a widely applied and straightforward process in high concentration streams due to its low capital cost. This process, however, is less cost–effective to treat dilute solutions, and the extra cost of handling and treating large amounts of sludge is substantial (Ku and Jung, 2001). Another commonly used process is ion exchange. This is highly effective in the removal of contaminants at high concentrations, but the cost and secondary pollution when regenerating the resin are critical. Thus, it is not an economical option to treat large volume of dilute metallic cation and anion wastewater (Ostroski et al., 2009, Athanasiadis and Helmreich, 2005). Electrochemical techniques are regarded as a rapid and well-controlled way to remove contaminant ions with fewer chemical additions and less sludge production. The drawbacks are high capital and operational costs (Kurniawan et al., 2006). Adsorption is an alternative way to treat dilute streams, but striking the balance between high cost and strong effectiveness of the physico-chemical adsorbent is an issue (Taffarel and Rubio, 2009). Biosorption has been proven as a promising and sustainable metal immobilisation method. The advantages are high removal selectivity, high overflow rate and production of concentrated sludge. The operation complexity and capital, maintenance and operational costs, however, cause great concern. The coagulation–flocculation method produces the sludge that has good settling and dewatering properties, but the amount of chemical dosages and their costs are the main disadvantages (Apiratikul

and Pavasant, 2008). Finally, membrane filtration technology is a high efficiency process, but high capital and operating cost, membrane fouling and low permeate flux are limitations (Rubio et al., 2002). In conclusion, each process has its own advantages and drawbacks. Selecting a suitable process according to the characteristics of the wastewater and the requirements of treatment is usually the best strategy.

Table 1.1: Summary of dilute metallic ion treatment processes.

	Cost	**Process complexity**	**Performance stability**	**Treatment speed**	**Selectivity**
Ion exchange	High	Medium	High	Medium	High
Membrane filtration	High	Low	High	Medium	High
Biosorption	Medium	High	Medium	Low	Medium
Adsorption	Medium	Medium	High	Low	Medium
Chemical precipitation	Low	Low	High	High	Low
Polymer–surfactant method	Low	Low	High	High	High

This thesis describes a novel wastewater treatment option to treat charged species from dilute aqueous solutions using polymer–surfactant aggregates (PSAs). It is an inexpensive, straightforward, reliable and quick process with a high selectivity (Table 1.1). At the heart of this process, the PSA is a nanostructured material with a large surface-volume ratio that forms in-situ by polymer and surfactant interactions, and contains both positive and negative charges. Forming millions of these nanostructures, while they are quickly binding the dilute metallic ions in the solution, all of them are flocculating with each other to form large and visible flocs. This process consists of three stages: removal, recovery and recycle. At the removal stage, a small amount of polymer and surfactant is

used to selectively bind the metallic ions and flocculate them out of solution. After gravity settling of the flocs from the treated clean water, a pH adjustment method is applied to recover these ions into a relatively pure and concentrated form before regenerating the removal agent. These regenerated removal agents are then recycled back into the process without a deterioration of removal ability in the next cycle. Such a sustainable metallic ion isolation process has a great application for process effluent water treatment, and opens up many potential applications in industries, such as textiles, fine chemicals, mining and pharmaceuticals.

1.2. Project objectives

- To develop a new, sustainable treatment process for removing and recovering both metallic cations and anions from dilute aqueous solutions, and recycling the polymer and surfactant (i.e. removal agent).
- To study the robustness of the process under different key variables at both removal and recovery stages.
- To explore the interaction mechanisms between oppositely charged polymers and surfactants in the presence of various metallic ions.

1.3. Thesis layout

The thesis consists of two major parts: the fundamentals of removal metallic ions from a scientific perspective, and a new treatment process (removal, recovery and recycle) for cations or anions from an engineering perspective.

Chapter 1 (this chapter) contains a background of wastewater treatment and available processes for metallic ion treatment in industry. It summaries the strengths and limitations of each process and the new process proposed in the thesis. The research objectives and outline of the whole thesis are also listed.

Chapter 2 reviews the existing techniques using polymer and/or surfactant for wastewater treatment and the interactions of polymer and surfactant at the air–water interface and in the bulk solution.

Chapter 3 presents experimental investigations on the interactions of polymer and surfactant in the presence/absence of metallic ions, and introduces the removal mechanism of metallic ions and the functional body: polymer–surfactant aggregate.

Chapter 4 and 5 contain the whole treatment process for dilute metal ions (removal, recovery and recycle), discuss the key variables in the process, and draw a comparison with closely related processes.

Chapter 6 and 7 contain the whole treatment process for metallic anions (removal, recovery and recycle), which is the mirror-image to the cation treatment process. The key variables and selectivity are also investigated. Both of the cation treatment and anion treatment process are compared and contrasted.

Chapter 8 summarises the whole presented process, discusses the potential applications of the process, and includes a flow sheet, mass balance and economic analysis of the process. Future work is also discussed.

Chapter 2

Literature Review of Surfactant and/or Polymer Based Technologies for Water Treatment

2.1. Introduction

Water provision is essential for domestic and industrial activity. With population growth and industrialisation, the access to affordable clean water has become a pervasive problem. To tackle the problem, a considerable amount of research has been targeted on developing robust decontamination technologies that can treat wastewater at lower cost, using less energy and with a minimum chemical usage and associated impact on the environment. Several technologies using polymers and/or surfactants for water treatment have been developed, two of which have attracted a great deal of research attention: micellar enhanced ultrafiltration and polymer enhanced ultrafiltration. Both these and their variations, such as ligand modification, the use of surfactant mixtures and copolymers, admicellar chromatography, adsorptive micellar flocculation and combined

polymer–surfactant based technologies, have been used to treat metallic ions and organic contaminants. Their commercial applications, however, are limited by operational cost, energy demands and/or the problem of membrane fouling. To overcome these limitations, a novel polymer-surfactant aggregate process has recently been developed to effectively and rapidly remove dilute contaminant ions, recover them into a concentrated salt, and then recycle the associated removal agent without the need for ultrafiltration.

In this chapter, the aim is to review the development of surfactant and/or polymer based technologies to treat both organic and inorganic contaminants in aqueous solutions over the past few decades, as well as the interactions between polymer and surfactant at air-water interface and in bulk solution.

2.2. Review of surfactant based technologies for water treatment

2.2.1. Micellar enhanced ultrafiltration

Micellar enhanced ultrafiltration (MEUF) technology was introduced 30 years ago by Dunn Jr et al. (1985). The technology has been used to treat many organic and multivalent inorganic contaminants from aqueous solutions, by hydrophobic forces and electrostatic/complex binding respectively. Due to the wide range of applicable industrials, including pesticides, pharmaceuticals, mining and mineral processes and the textile and battery industries, MEUF has strong potential in practical use. The main principle is that the contaminants are solubilised or bound onto micelles to increase their effective size; they can then be retained by ultrafiltration (Figure 2.1). The advantages of MEUF include relative ease of operation, relatively low energy input and capital cost,

simultaneous removal of organic molecules and charged ions and a high recovery efficiency for surfactants with a low critical micellar concentration (CMC). The technology, however, has its limitations, such as a low selectivity, sensitivity to ionic strength, monomer leakage/back contamination, and membrane fouling (e.g. formation of a gel layer).

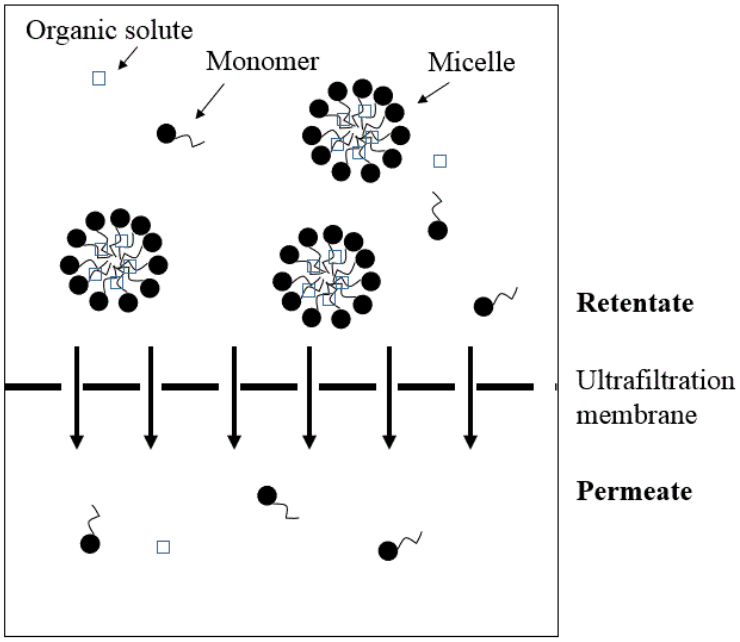

Figure. 2.1: Schematic of micellar enhanced ultrafiltration (modified from (Dunn Jr et al., 1985)).

To overcome these limitations, many modifications have been investigated, such as adding ligands, non-ionic surfactants, flocculants and activated carbon fibres and using polymeric surfactant. Low selectivity is one of the major barriers for commercialising the MEUF technology, because there are plenty of untargeted species in the solution and removing all of the charged or hydrophobic species can be problematic in terms of substrate usage efficiency and the later recovery process. Many types of ligand modified – micellar enhanced ultrafiltration (LM-MEUF), using so called chelating micelles, have

been proposed to increase the selectivity and binding strength for removing ions from aqueous solutions. LM-MEUF uses a certain number of hydrophobic ligands, which are obtained from suitable alkyl chains in common chelating molecules. For example, copper ions have been selectively removed by LM-MEUF (Shadizadeh et al., 1999). The low charge density of uranium(VI) inhibits the electrostatic binding with micelles. An auxiliary ligand (trioctylphosphine oxide) was used to complex uranyl ions and then strongly bind with micelles via the ligand (Pramauro et al., 1992).

In addition to reducing the monomer leakage in the permeate, the addition of non-ionic surfactants and flocculants and the use of low CMC surfactants have been investigated. The benefits of reducing the monomer leakage are not only to improve the quality of permeate solution, but also to increase the usage efficiency of the substrate. The surfactant leakage is caused by the nonmicellar monomers passing through the ultrafiltration membrane. For this reason, the concentration of surfactant monomers in the permeate is close to its CMC. Hence, decreasing the surfactant CMC is required to reduce its monomer leakage. In the case of the non-ionic surfactants, the CMC is generally much lower than ionic surfactant with the same length of alkyl chain because there is no electrostatic repulsion between their headgroups to inhibit the formation of micelles. Addition of non-ionic surfactant, therefore, can reduce the charge repulsion between ionic surfactant headgroups, which consequently decreases the CMC (Pramauro et al., 1992). Apart from adding nonionic surfactant, the CMC can also be decreased with increasing length of the alkyl chain and ionic strength of the solution. For a longer alkyl chain and different functional groups, the hydrophobicity of surfactant increases, so that the surfactant tends to form micelles at a lower CMC than shorter chains (Luo et al., 2010). With increasing ionic strength, the CMC is again reduced due to screening of the

electrostatic repulsion between headgroups. Thus, there are three main approaches to reducing the CMC of a surfactant and reducing the leakage of monomers: (1) adding nonionic surfactant, (2) using longer alkyl chain surfactants and (3) adding Fe^{3+} or Al^{3+} (Talens-Alesson et al., 2002) (to increase the ionic strength and act as flocculant).

However, all three approaches lead to some extent to either a decrease of micellar charge density or an increase of the binding competition with targeted ions. For this reason, the contaminant removal efficiency is somewhat compromised. On the other hand, the removal efficiency can be improved when the total amount of available micelles is increased due to the increased portion of surfactant forming micelles. Thus, there must be a critical balance between charged contaminant removal and surfactant usage efficiency by adjusting the degree of micellar charge density through the three approaches. For instance, at SDS concentration lower than its CMC, the removal efficiency of Ni^{2+} was improved from 88% to 96% with the addition of non-ionic surfactant (OP-10) (Yurlova et al., 2002). Lee et al. (2005) showed that a small addition of Triton-X to SDS increased Cu^{2+} removal efficiency from 18% to 70%; but once the molar fraction of Triton-X was over 30% of the total surfactant addition, the removal efficiency decreased. Yurlova et al. (2002) also found that with addition of nonionic surfactant, the permeate flux was decreased, because the configuration of micelles was changed from spherical to cylindrical or lamellar.

With regard to the ionic strength, a lot of research attention has been focussed on adding salt to the solution to reduce the CMC. Although the CMC and monomer leakage can be reduced, the competition between the charged contaminants and added salt cannot be ignored. Xu et al. (2007) showed a reduction of Cd^{2+} removal efficiency from 95% to 75% in the presence of less than 20mM NaCl. There may not be 20 mM NaCl in real

industrial effluent, but this is useful information since it is likely that a similar level of ionic strength would apply. However, the addition of Al^{3+} has been shown to induce a near flocculation of SDS in the presence of Zn^{2+} (Hankins et al., 2005). This means that the Zn^{2+} removal efficiency increases with less tendency for gel formation/membrane fouling. Apart from charged inorganic removal, the effects of ionic strength on organic removal in industrial effluents has also been widely researched. Naphthenic acids (Deriszadeh et al., 2009), olive mill wastewater (El-Abbassi et al., 2011) and soil washing solution (Jung et al., 2008) were effectively treated by MEUF. Lower dosages of surfactant were applied and less monomer leakage was found because some salt and organics existing in the effluent lowered the CMC of the applied surfactant in the wastewater. In summary, the ionic strength has a stronger effects on the charged inorganic removal than that of hydrophobic organics due to the different removal mechanisms, i.e. electrostatic versus solubilisation via hydrophobic forces.

Different binding removal mechanisms were employed for simultaneous removal of hydrophobic organics, such as aromatic compounds, and charged species, such as heavy metal ions, platinum-group metals and oxyanions. The simultaneous removal by MEUF has been tested firstly by Dunn Jr et al. (1985). They used SDS to remove phenol and o-cresol (as examples of organics) and Zn^{2+} and Ni^{2+} (as examples of inorganics). The results showed that removal of heavy metal ions was not strongly disrupted in the presence of organic solutes and vice versa. Other researchers have tested many different combinations of simultaneous removal, for example, chromate and chlorobenzene (Baek and Yang, 2004), chromate and trichloroethylene (Lee et al., 2005) and Cr^{3+} and phenol (Witek et al., 2006). Similar conclusions were reached. The important advantage of the simultaneous removal is the ability to enhance the economic viability of MEUF.

To further enhance the economic viability, some research has been conducted on removing precious metals and recycling the surfactant, e.g. gold(III) (Akita et al., 1997) and palladium(II) (Ghezzi et al., 2008). There are five main surfactant recycling processes: precipitation (Wu et al., 1998), acidification (Kim et al., 2006), chelating agents (Kim et al., 2006, Li et al., 2009), multistage foam fractionation (Tharapiwattananon et al., 1996, Boonyasuwat et al., 2003) and prevaporation (Jiang et al., 1997, Vane and Alvarez, 2002). The recycled surfactant did not perform as well as new materials most likely because it had deteriorated.

In conclusion, the MEUF is a promising technology for removing charged inorganic and hydrophobic organic contaminants from wastewater. Many modifications have been introduced and tested to improve the removal selectivity, reduce the surfactant usage and membrane fouling, and minimise contamination caused by the process itself.

2.2.2. Admicellar chromatography

Admicellar chromatography (AC) is a surfactant based separation and concentration technology to 'adsolubilise' organics within admicelles (adsorbed surfactant layers immobilised onto a solid surface) from aqueous solutions. After adsolubilisation of the organics, the surfactant can be recycled and the organics can be concentrated by adjusting the pH. The functional part of AC is the admicelles, which are formed as surfactant bilayer aggregates at a solid-liquid interface above a certain surfactant concentration (known as the hemimicelle or admicelle concentration). A schematic of AC process is shown in Figure 2.2.

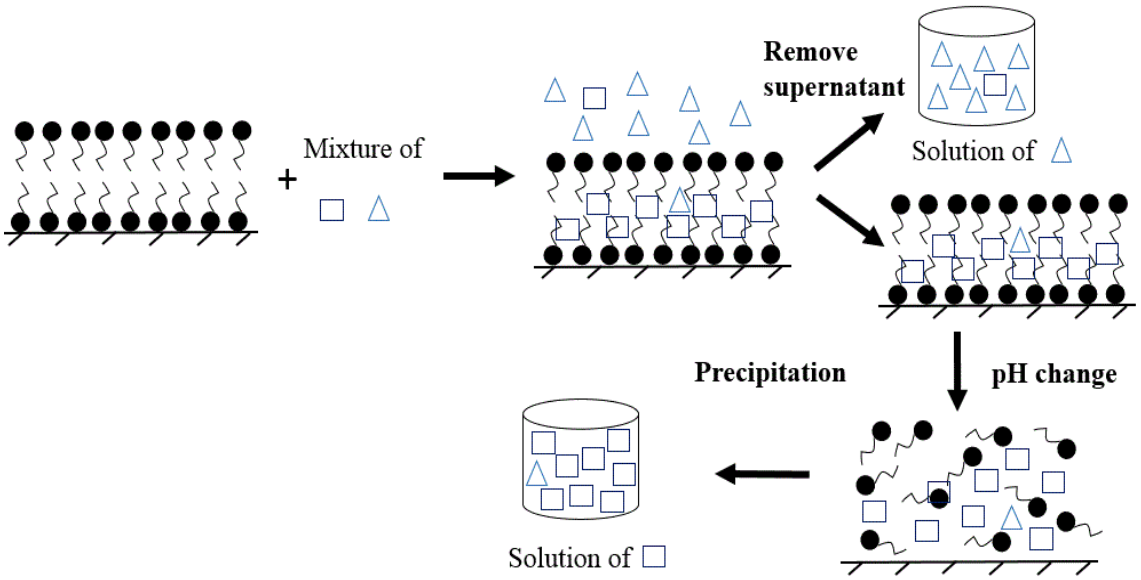

Figure 2.2: Schematic of a batch separation process using admicellar chromatography (modified from (Barton et al., 1988)).

The basis of AC is adsolubilisation, which is a partition phenomenon involving the solubilisation of organic species within an admicelle. The process was developed by Barton et al. (1988) as an alternative to activated carbon adsorption and conventional chromatographic separations and as a concentration/separation process for bio-products. Although AC has shown robust results in separating isomers of heptanol (Barton et al., 1988), crystal violet (Adak et al., 2005a, Adak et al., 2005b, Adak and Pal, 2006) and malachite green (Das et al., 2009), it still faces some limitations: the need for a continual surfactant feed, surfactant leakage into dilute solution, sensitivity to pH and salinity, relatively low processing capacity and slow adsorption kinetics. Some of the limitations have been addressed by modifying the AC process. Nayyar et al. (1994) operated the AC below the surfactant's Krafft temperature. At this condition, the admicelles were still effective in removing both polar and nonpolar organics from solution, and little leakage

of surfactant were observed. The limitations of the AC process, however, still need to be mitigated before scaling-up can be considered.

2.2.3. Adsorptive micellar flocculation

Adsorptive micellar flocculation (AMF) was originally proposed by Porras-Rodriguez and Talens-Alesson (1999) as an intensive surfactant-based technology to treat 2,4-dichlorophenoxyacetic acid by Al^{3+}-induced flocculation of lauryl sulphate micelles. During the AMF process, the organic pollutants bind with the highly positive charge of the Al^{3+} ion via ionic and complex binding. The Al^{3+} as a flocculant is also bound to the micellar surface and neutralises the surface charge. The charge neutralisation leads to a rapid decrease of electrostatic repulsive force between micelles resulting in a microscopic aggregation of the colloidal micelle (flocculation). The resulting flocs are then separated from solution by a coarse filter or even gravity settling. After that, the retentate/sediment is easily dewatered because of the open and porous structure of flocs. Finally, the organic pollutants can be separated from surfactant and flocculant via solvent extraction and then recycled back to the process (Talens-Alesson et al., 2006). The major advantages of AMF are fast kinetics and not using expensive membrane separation. However, it still has some drawbacks, such as 'back contamination' of surfactant and flocculant and inefficient removal for pollutants in dilute concentrations, as well as relatively low substrate recycle ratio (Sun et al., 2008) and selectivity. A schematic of AMF process is shown in Figure 2.3.

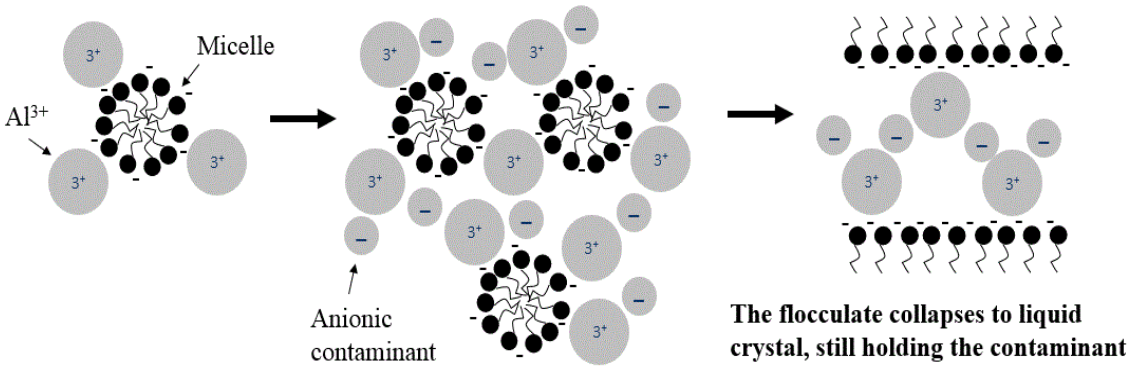

Figure 2.3: Schematic of adsorptive micellar flocculation process (modified from (Porras and Talens-Alesson, 1999)).

To overcome the drawbacks, attention has been focussed on improving the selectivity and removal efficiency of AMF. With regard to the selectivity, it was enhanced by adding a monovalent salt, such as NaCl over a narrow range of Al^{3+} concentrations (Anthony et al., 2007). The removal efficiency also improved by applying multistage separation (Talens-Alesson et al., 2006). To minimise the back contamination, marble dust as an adsorbent were used (Talens-Alesson et al., 2006). Apart from modifying the AMF process, finding a suitable application is equally important. AMF was employed to treat soil processing extract, which is a promising demonstration of its application (Svab et al., 2008).

Various combinations of surfactant and flocculant to treat organic pollutants at optimum operational conditions were investigated to extend the applications of AMF. Two surfactants (SDS and α-olefinsulfonates) (Porras and Talens-Alesson, 2000), their mixtures (Talens-Alesson, 2001), and two flocculants (Al^{3+} and Fe^{3+}) (Porras and Talens-Alesson, 1999, Talens-Alesson et al., 2002) were examined to remove organic pollutants, such as phenol, benzoic acid, 2,4-dichlorophenoxyacetic acid, 2,4-dichlorophenoxybutiric acid, phenylamine and catechol (Talens-Alesson et al., 2004,

Almeida and Talens-Alesson, 2006) and tetracycline (Saitoh et al., 2014). In addition, the AMF was also robust in the presence of Zn^{2+} (Paton-Morales and Talens-Alesson, 2002) and hydrocarbons (Paton-Morales and Talens-Alesson, 2000). For optimum operational conditions, the AMF worked effectively within a pH range of 5-8 and at flocculant and organic compound molar ratios of 6:1 and higher under certain mixing conditions (Paton and Talens-Alesson, 2001, Talens-Alesson et al., 2004, Talens-Alesson et al., 2010). Recently, a pilot-plant study of AMF was conducted, which demonstrated the feasibility of scaling-up to a continuously operated unit (Sun et al., 2008). Although there is little detailed work in the literature regarding the recovery of organic and recycling of surfactant and flocculant, it is important for the economical and sustainable viability of the AMF process. In conclusion, AMF is a promising but not yet fully developed process to (pre-) treat charged organic pollutants in aqueous solutions.

2.3. Review of polymer based technologies for water treatment

2.3.1. Polymer flocculation

Numerous applications of polymers in water treatment arise in coagulation and flocculation and in sludge conditioning. Separation processes such as sedimentation, filtration and flotation are often applied after polymer treatment. The main advantages of using polymers in water treatment are (1) low coagulation dosages, (2) reduction of other chemical use, (3) high treatment speed, (4) relatively low sludge generation, and (5) wide application ranges. Some disadvantages, however, still remain including relatively high costs, difficulty of selection of suitable polymers and sensitivity to incorrect dosages. Some excellent review articles have summarised the research and development of

polymer flocculation in water treatment over the last four decades (Bolto, 1995, Liu and Fang, 2003, Neyens et al., 2004, Bolto and Gregory, 2007, Zahrim et al., 2011). In this chapter, recently developed polymer based technologies are highlighted.

2.3.2. Polymer enhanced ultrafiltration

Polymer enhanced ultrafiltration (PEUF), also known as polyelectrolyte enhanced or polymer supported ultrafiltration, was proposed to remove metal ions from aqueous solutions by oppositely charged polyelectrolytes with the assistance of ultrafiltration (Sasaki et al., 1989). The applications of PEUF have also been extended to remove and concentrate ions, dyes, and organic materials from aqueous solutions as well as for desalination. The removal principle is as follows: enlarge targeted species by binding with polyelectrolytes to form macromolecular compounds, which are then ultrafiltered to remove the targeted species from aqueous solutions. The retentate is then treated to recover the target species into a concentrated form and to reuse the polymer in the next cycle. A schematic of PEUF process is shown in Figure 2.4.

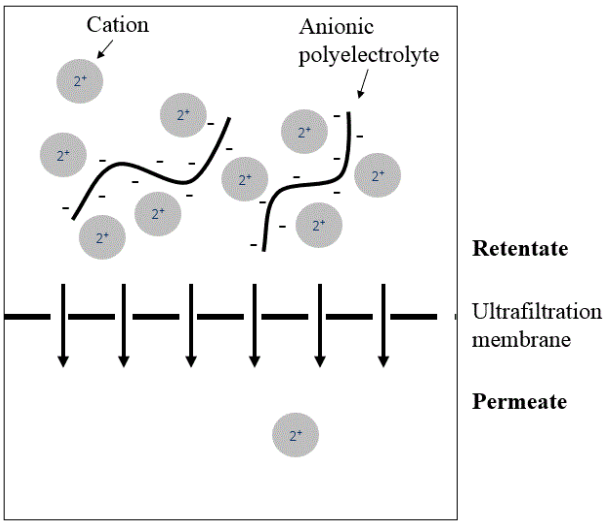

Figure 2.4: Schematic of polyelectrolyte enhanced ultrafiltration (modified from (Tabatabai et al., 1995)).

During the development of PEUF, polymers have been studied as the main functional component from three perspectives: (1) polymer binding (type of interactions), (2) polymer properties and (3) binding conditions. Ionic and complex bindings are the two binding mechanisms between polyelectrolyte and targeted species. With regard to the ionic binding, charged ions and the oppositely charged monomers in polymer are bound via electrostatic forces (Korkish, 1989). For this reason, the separation selectivity is low, as any similar charged ions can compete with the targeted ions. For example, 99% arsenic was removed from deionised water, but with increasing salt concentration in the solution up to 100 ppm NaCl, the removal efficiency was halved, and only 2% removal was achieved at 2000 ppm (Geckeler and Volchek, 1996). Many other anions were also studied by PEUF (Shkinev et al., 1989). Apart from removing anions, extensive work has focused on removing heavy metal ions from aqueous solutions. Most of the polyelectrolytes used in this case contain carboxylic functional groups that electrostatically bind with the heavy metal ions. As in the case of anion removal, relatively poor selectivity was reported for heavy metal ions due to mainly to the electrostatic binding mechanisms. However, more resistance to the effects of monovalent salt was demonstrated than in the case with anions (Dorra et al., 2010, Ennigrou et al., 2014).

With regard to complex binding, the selectivity is much higher than that of ionic binding. The reason for this is that the complex binding is mainly based on the chelation between the functional groups in the polymer and the targeted compounds as is the case with amine and imine groups, which form chelates with transition metal ions (Rivas et al., 2005). Examples using polyethylenimine (PEI) include removing mercury (Uludag et al., 1997), cadmium (Li et al., 2009), nickel (İslamoğlu and Yilmaz, 2006), chromium

(Aroua et al., 2007) and zinc (Islamoglu Kadioglu et al., 2009). However, alkali and alkaline earth metals cannot be removed by complex binding (Miretzky and Cirelli, 2009)

Apart from commercially available PEI, many other polymers are also applicable for PEUF. However, no single polymer has been found that can be applied universally. There are several reasons for this: (1) the different functional groups in the polymer need to have selectivity of the targeted species over the others, (2) the polymer needs to possess the properties of low toxicity and cost and (3) the polymer needs to be chemically and physically stable and easy to regenerate. Thus, the selection of polymer is tailored to each case (Almutairi et al., 2011). The polymers currently used are broadly divided into three groups. Firstly, alkaline polymers, such as PEI, which besides being commercially available have a relatively good selectivity among heavy metal ions. However, it shows moderate toxicity for water treatment. Scond, acidic polymers, like poly(acrylic acid), which are inexpensive and have low toxicity. However, due to the ionic bonding, the selectivity of heavy metals is low. Third, self-synthesised polymers have demonstrated a good selectivity, but the cost and toxicity for commercial usage remain unexplored.

Since the selection of a polymer is done on a case by case basis, the binding condition – binding degree required, pH value and solution composition – become a critical factor for this selection. For binding degree of the metal ion, with increase of polymer dosage, it was found that more metal was bound and then separated by ultrafiltration, which led to a high metal removal efficiency. However, when the polymer dosage was too high, the viscosity of the solution and concentration polarisation were increased; consequently, the metal removal efficiency and permeate flux were decreased (Shkinev et al., 1987, Scamehorn et al., 1990). Thus, a suitable polymer dosage is necessary to achieve both a high binding degree of metal ions and a high permeate flux. The value of pH can

fundamentally effect the suitability of targets and their removal and recovery efficiencies. A classic example is PEI. Since the amine groups in PEI can be protonated at an acidic pH, the formation of chelation bonds with cationic transition metals are not favoured. But the formation of an electrostatic bond with anions is enhanced. At a basic pH, since the amine groups can be deprotonated, and thus PEI becomes a neutral polymer, and hence, it becomes suitable for removing cations via chelation instead of anion removal via electrostatic binding (Bayer et al., 1985; Rivas and Geckeler, 1992; Li et al., 2008). Regarding solution composition, ionic strength and suspended solids contact may affect the treatment outcome. The portion of polymer which contributes to flocculation of the suspended solid in the presence of salt is hard to estimate, which may lead to an incorrect dosage (Soponvuttikul et al., 2003).

In conclusion, the binding mechanisms, the polymer properties, and the solution conditions are the main factors that can influence separation by PEUF.

The ultrafiltration membrane is another crucial part of the PEUF technology. Since PEUF is a separation process, the molecular weight cut-off is the key feature of the membrane rather than its material and shape. In most of the membrane separation processes, membrane fouling remains a key challenge. There are many reviews which discuss the fouling challenges as well as critical and sustainable flux (Belfort et al., 1994, Bacchin et al., 2006, Van der Bruggen et al., 2008). Hence, to prevent or minimise loss in flux and membrane fouling, technologies that do not require a membrane have been proposed such as polymer and additive synergic flocculation, surfactant induced polymer flocculation, and polymer-surfactant aggregate process, which will be discussed in detail later.

2.3.2.1. Polymer regeneration

The regeneration of polymer and the recovery of targeted ions are important for the economic and environmental viabilities of the PEUF technology. The polymers can be regenerated by chemical, electrochemical or thermal methods. Chemical regeneration has mainly been achieved by changing the retentate pH (Volchek et al., 1993) or adding a competitive binding chemical to the retentate (Korus et al., 2014). Electrochemical regeneration has been applied either by depositing the bound ions on an electrode and leaving the polymer in the solution for reuse (Camarillo et al., 2010) or using an ion-exchange membrane with electrolysis (Llanos et al., 2008). Finally, thermal regeneration was achieved by heating the retentate to break the bond between polymer and targeted metals. Given the development of successful recovery and regeneration methods, PEUF is becoming a more attractive technology, economically and environmentally. Minimising regeneration cost, however, remains a barrier for commercialisation. Therefore, it has been applied to treat industrial wastewater at the bench scale only (Canizares et al., 2005, Barakat et al., 2010), and no major full-scale case study has been published. In addition to the costly regeneration process, another barrier is the difficulty in selecting a polymer which possesses high selectivity, is inexpensive, has low toxicity and is easily reusable.

In conclusion, the PEUF could be an extremely promising technology for water treatment if the cost of regeneration can be reduced and more suitable polymers are developed.

2.3.3. Polymer and additive synergy ultrafiltration

Polymer and additive synergic treatment uses not only polyelectrolyte, but also other existing or added compounds to bind to the targeted species, followed by separation via

ultrafiltration or gravity settling. Examples of using existing compounds in the targeted solution to enhance the heavy metal and anionic organics removal performance of the polyelectrolyte include humic acid in natural waters (Hankins et al., 2006) and auxiliaries (anionic detergents, dispersing agents, thickeners) in textile wastewaters (Zemaitaitiene et al., 2003). Additional additives such as inorganic and organic ligands (Tuncay et al., 1994a, Tuncay et al., 1994b, Roach et al., 2003, Roach et al., 2009) and succinic acid (Nguyen et al., 1981) were also employed to enhance the performance of the polyelectrolyte. The difference when compared with PEUF is the use of more compounds, which can enhance the binding strength or selectivity for targeted species, and reduce the membrane fouling and energy consumption. In some cases, it may even eliminate using membranes. Compared with additive-metal complexation (Von Wandruszka, 2000, van den Hoop et al., 2002, Katsumata et al., 2004, Kim et al., 2005), the addition of polyelectrolytes increases the effective size of the targeted species, thereby, facilitating the use of less energy intensive filtration methods. In addition, the flocculation time is shortened, which consequently increases the treatment capacity of a plant. Therefore, the compounds in the three-way system acts in a synergistic fashion.

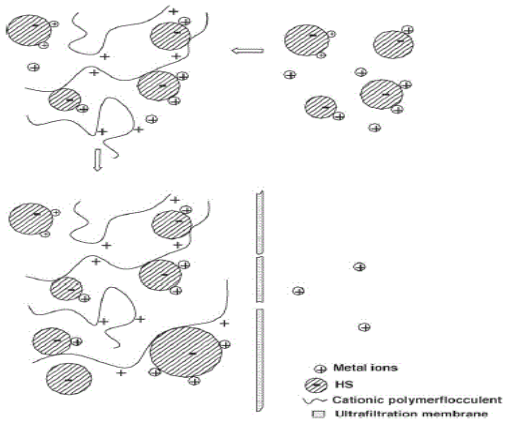

Figure 2.5: Schematic of humic acid and polyelectrolyte coagulation and flocculation (Adapted from (Hankins et al., 2006))

As an example, humic acid occurs naturally in ground water and shows a strong and stable binding with heavy metal ions to form complexes. The stability constant values of the complex were published by Lubal et al. (1998), which suggested a selective removal of heavy metal ions. Hankins et al. (2006) applied the phenomenon with polyelectrolyte to simultaneously remove humic acid and bound heavy metal ions by employing a cationic polyelectrolyte to sweep up the complexes by coagulation and flocculation (Figure 2.5). The polyelectrolyte thus allows the complexes to be removed by gravity settling. Although ultrafiltration was used during the bench scale process, its main role was to separate the extra polyelectrolyte from free ions in the solution. Due to the stable binding between humic acid and heavy metal ions, the process works effectively over a wider range of pH and higher ionic strength than PEUF. Therefore, complexation-flocculation has good and robust potential applications for the removal of metal ions in water treatment.

2.4. Polymer and surfactant interactions

2.4.1. Surface tension

Polymer–surfactant mixtures are widely used in paper making, oil recovery, detergency, surface conditioning applications and have received much attention in recent years due to their controllable behaviour in the bulk and at the interfaces (Goddard and Hannan, 1976; Goddard, 1986). There are two broad categories of the systems: neutral polymer and charged surfactant, named weak system; oppositely charged polymer and surfactant, named strong system.

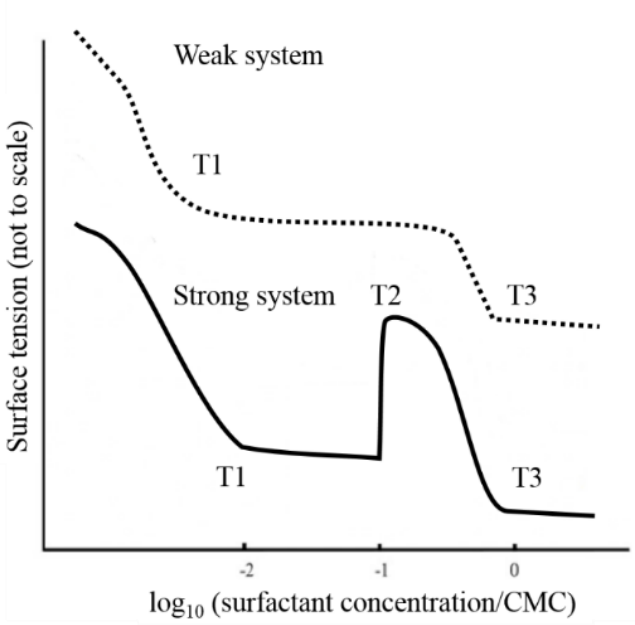

Figure 2.6: Sketched surface tension curves for weak and strong polymer and surfactant systems.

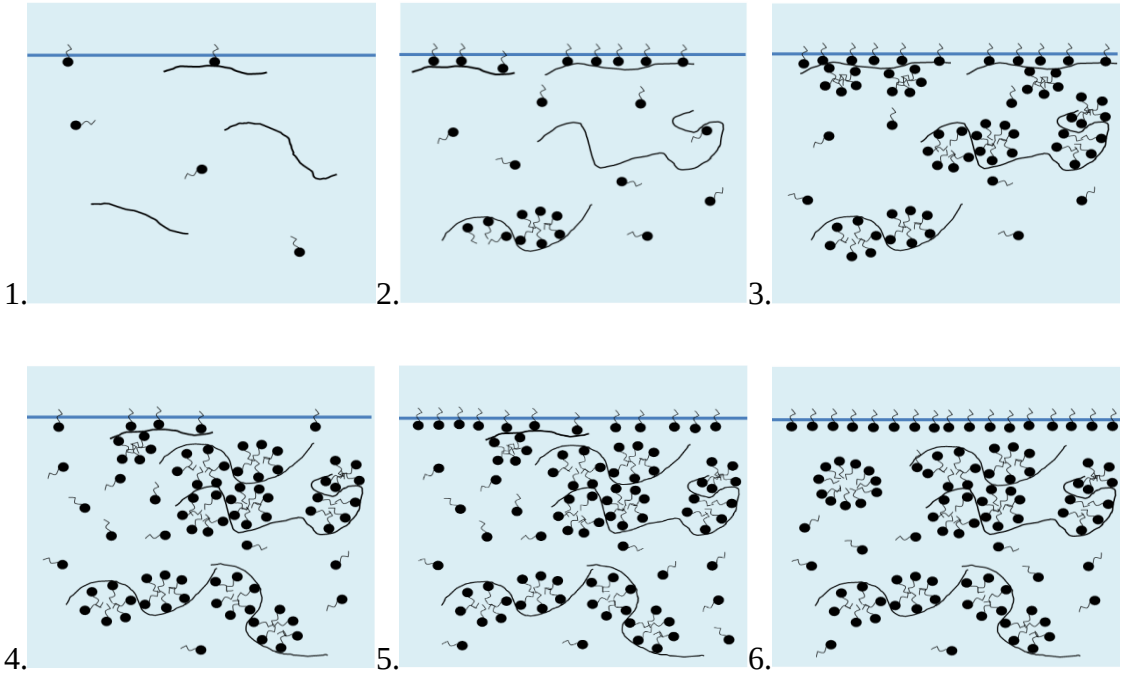

Figure 2.7. Schematic diagrams for the surface and bulk stuctures of the oppositely charged polymer and surfactant with increase of surfactant concentration from 1 to 6.

In weak systems, the neutral polymer and ionic surfactant mixtures lead to two break points at surfactant concentrations T1 and T3 in the dotted surface tension plot (Jones, 1967) (Figure 2.6). T1 is the critical aggregation concentration (CAC), which is the starting point for the formation of micelle-like aggregates on the polymer chains. T3 is the CMC, which is when the surfactant monomers start to form spherical or cylindrical micelles in the bulk solution.

In strong systems, oppositely charged polymer and surfactant mixtures result in complex surface tension behaviour (Figures 2.6 and 2.7). The Penfold and Thomas groups have made significant contributions to the understanding of the interactions of polyelectrolyte and ionic surfactant at the air–water interface by neutron reflectivity and surface tension (Taylor et al., 2007; Penfold et al., 2007a; Penfold et al., 2005). A classic example is the surface tension changes in SDS–polyDADMAC mixtures (Penfold et al., 2007b; Staples et al., 2002). With increasing SDS concentrations, a sharp decrease of surface tension was measured at various polymer concentrations. At low SDS concentrations until T1, the formation of SDS–polyDADMAC complexes at the interface enhances the air/water interface adsorption of SDS (Figures 2.6,and 2.7-1). After T1, the interface is almost saturated by the complexes, SDS forms micelle-like aggregates on the bulk polymer chains. The resulting structures, called polymer-surfactant aggregates (PSAs), occur at the CAC and arise, due to the presence of strong electrostatic and hydrophobic forces (Figure 2.7-2). Once the bulk polymers are saturated with surfactant, the additional SDS is energetically favoured to further saturate the surface polymer-surfactant complexes which then migrate to the bulk to form further PSAs (Figure 2.7-3). This migration leads to a partial depletion at the surface, which increases the surface tension value after the low plateau at T2 (Figures 2.6 and 2.7-4). At higher SDS

concentrations (after T3), a second low plateau in surface tension is measured, because the additional SDS forms micelles at the CMC and beyond, instead of moving to the interface (Figure 2.7-5-6). In conclusion, surface tension measurements can reveal the states of polymer and surfactant interactions.

Interactions in the strong system can be regarded as polymer-induced micellisation. The affecting properties of polymer in the interactions are molecular weight, polymer architecture, charge density, polymer hydrophobicity and polymer flexibility (Halacheva et al., 2012, Ritacco et al., 2003, Sokolov et al., 1996, Nizri and Magdassi, 2005). Regarding surfactants, the head group and length of hydrophobic chain are considered. Below the CAC, polymers are bound with individual surfactant monomers to form polymer–surfactant complexes, due to electrostatic attractions between oppositely charged polymer segments and surfactant headgroups. This process promotes hydrophobicity and shrinkage of the polymer chain. Given the exposed hydrophobic surfactant tails, they bind together under hydrophobic forces to minimise the contact area with water. The maximum charge neutralisation binding for polymer–surfactant complexes (below the CAC) is about 80% (Halacheva et al., 2012). This process tends to reduce flexibility of the polymer and raise the surface activity of the polymer–surfactant complexes (Staples et al., 2000). Thus, some of the polymer–surfactant complexes are present at the air–water interface at a very low surfactant concentration (Figure 2.7-1).

When the surfactant concentration reaches the CAC, about 20 to 40 monomers form a few stable open-network aggregates on the polymer chains (Figure 2.7-2), and the resulting structure is called PSA. The size of these PSAs is approximately 100 nm from cryo-TEM (Goldraich et al., 1997). At the same time, surface tension of the solution increases dramatically resulting a noticeable cliff–edge peak (Campbell et al., 2010). This

surface phenomenon offers a great way to determine the formation of PSA with minimum surfactant dosage, and will be explored in detail in Chapter 3. At a slightly higher surfactant concentration, the polymers are neutralised by these aggregates to form a 'necklace' structure, so the electrostatic repulsions between PSAs are minimised (close to zero) and flocculation occurs (Goddard, 2002). As a result, the turbid solution becomes clear and its viscosity close to that of water (Goddard, 1986).

At a higher surfactant concentration, below the CMC, the hydrophobic surface of flocs bind the hydrophobic tail of the extra surfactants to minimise the free energy, and these flocs may gain charge gain and re-dissolve in the solution (Figure 2.7-5) (Taylor et al., 2007). When the surfactant concentration reaches the CMC, micelles form in the bulk solution (Figure 2.7-6). The CMC is sensitive to the ionic strength, especially with multivalent ions, such as heavy metal ions. Thus, it is essential to review the effects of addition of metal ions on polymer and surfactant interactions.

The ionic strength has substantial effects on the association between polymer and surfactant, especially on the value of CAC, CMC and aggregation number (Petkov et al., 2010). Addition of electrolytes screens the electrostatic interactions between oppositely charged polymer and surfactant and the repulsions between the surfactant headgroups at the interface, in the aggregates and micelles. Charged polymer and surfactant also introduce electrolytes into the solution from their intrinsic counter ions. Thus, the ionic strength is elevated with the addition of electrolytes or the intrinsic counter ions from removal agent. With regards to the CAC, the effects of ionic strength depend mainly on the charge percentage of polymer (Fegyver and Mészáros, 2015). With regards to the CMC, the value decreases with increasing concentration of electrolytes. For example, in the PolyDADMAC-SDS system, both the CAC and CMC are lowered in the presence of

NaCl (Penfold et al., 2007b). The aggregation number notably increases with increasing electrolyte concentration (Petkov et al., 2010). In conclusion, the ionic strength is an important variable that could fundamentally change the position of the critical points.

The polymer structure changes from random coils to a more ordered structure by folding around the surfactant clusters, due to the hydrophobicity of surfactant tails (Chu and Thomas, 1986, Bulpin et al., 1987). The extent of reorganisation is affected by ionic strength, hydrophobicity and flexibility of polymer and surfactant concentration. Regarding a highly flexible polymer, such as polyDADMAC, it is relatively easy to form an intra-molecular association, but for a rigid polymer, inter-molecular association is favoured (Leung et al., 1985). Ohbu et al. (1982) report using nuclear magnetic resonance that in both polymer bound aggregates and free micelles, the surfactant chains experience the same environment. The results suggest that the chemical nature of aggregates in PSA and micelles are similar. At the pre- and post-flocculation zones, however, the aggregates are much less open and hydrated than that in micelles (Ananthapadmanabhan et al., 1985). A high charge density of polymer (Anthony and Zana, 1996), high ionic strength environment (Hansson and Almgren, 1996) and long chain of surfactant can result in a large aggregation number, because of the increase in co-operativity of the binding. On the other hand, an increase in the hydrophobicity and rigidity of polymer can result decrease in co-operativity, which leads to a smaller aggregation number (Bulpin et al., 1987).

The size of flocs is mainly controlled by the net charge in polymer and surfactant. Goldraich et al. (1997) report that the PSAs are in a phase of hexagonal liquid crystals. Due to the quaternary ammonium group in polyDADMAC, the aggregate formations are highly ordered (Nizri et al., 2008). In a non-ionic surfactant and anionic SDS mixture, the

increase in fraction of SDS from 0.24 to 0.36 increases the number of bound aggregates per polymer chain from 35 to 70, and also increase the overall molecular weight from 7 to 15 million, which is about an increase from 15 PSAs per flocs to 37 each (Xia et al., 1993). From Xia's findings, the inter- and intra-molecular interactions would be much stronger, if the aggregates are formed by a pure anionic surfactant, which is about 40. The size of each aggregate on the polymer chain is in the range of 15-30 nm and the average is 17 nm by number distribution, and the size of the PSA is in the range of 35-150 nm (Nizri et al., 2008).

A phase separation occurs when the polymer to surfactant ratio around the stoichiometric point. Before that point, turbidity occurs above a certain concentration of PSAs. Some flocs are not re-dissoluble because the charge density of polymer is high or surfactant has either branched chains or unusually shaped side groups (Goddard and Hannan, 1977). The flocs formed by polymer and surfactant, however, are in moderate charge densities and can usually be re-dissolved (Fegyver and Mészáros, 2015).

In this thesis, the focus is the oppositely charged polymer–surfactant system, which includes cationic polymer with anionic surfactant and vice versa. The cationic polymers are poly(diallyl dimethyl ammonium chloride) (PolyDADMAC) and poly(ethyleneimine) (PEI), and the anionic surfactant is sodium dodecyl sulphate (SDS). On the other hand, the anionic polymers are poly(sodium 4-styrenesulfonate) (PSS) and poly(acrylic acid) (PAA), and the cationic surfactant is myristyl trimethyl ammonium bromide (MTAB). The structures and chemical formulae of these polymers and surfactants are shown in Figure 2.8.

Poly (diallyldimethyl ammonium chloride)

(PolyDADMAC, $C_8H_{16}NCl$)

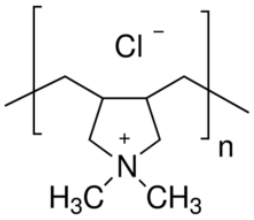

Poly (ethyleneimine)

(PEI, C_2H_5N)

Sodium dodecyl sulphate

(SDS, $CH_3(CH_2)_{11}OSO_3Na$)

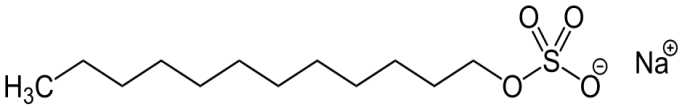

Poly (sodium 4-styrenesulfonate)

(PSS, $C_8H_7NaO_3S$)

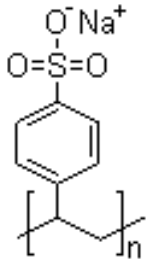

Poly (acrylic acid)

(PAA, $C_3H_4O_2$)

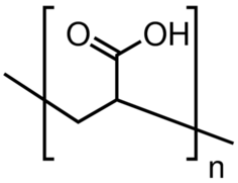

Myristyl trimethyl ammonium bromide

(MTAB, $CH_3(CH_2)_{13}N(Br)(CH_3)_3$)

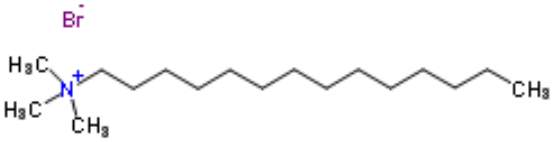

Figure 2.8: Structures and chemical formulae of the polymers and surfactants mainly used in this thesis.

2.5. Review of polymer and surfactant based technologies for water treatment

In this section, the focus is on the use of a mixture of polyelectrolytes and surfactants for water treatment. Colloid enhanced ultrafiltration (CEUF) is a broad concept including all the technologies that use a water-soluble colloid to associate with targeted pollutants, followed by ultrafiltration. The colloid can be a surfactant micelle, a polyelectrolyte or a mixture of both. The existing technologies, using two types of colloids are MEUF and PEUF. Uchiyama et al. (1994a and 1994b) first proposed the use of a combination of polyelectrolyte and surfactant micelles to solubilise the organic pollutants into the micelles, which is the same mechanism as MEUF. At solubilisation, the polyelectrolyte acts as a flocculant/scavenger to form polymer-surfactant complexes and reduces the surfactant monomer passage through the ultrafiltration membrane. In addition to less monomer leakage compared with MEUF, another advantage is that permeate flux is considerably higher than that of MEUF. Many organic pollutants have been treated by CEUF, such as o-cresol (Lee et al., 2000), p-tert-Butylphenol (Uchiyama et al., 1994a), trichloroethylene (Uchiyama et al., 1994b) and dyes (Petzold et al., 2006, Petzold et al., 2007). A schematic of so-called polyelectrolyte MEUF is shown in Figure 2.9.

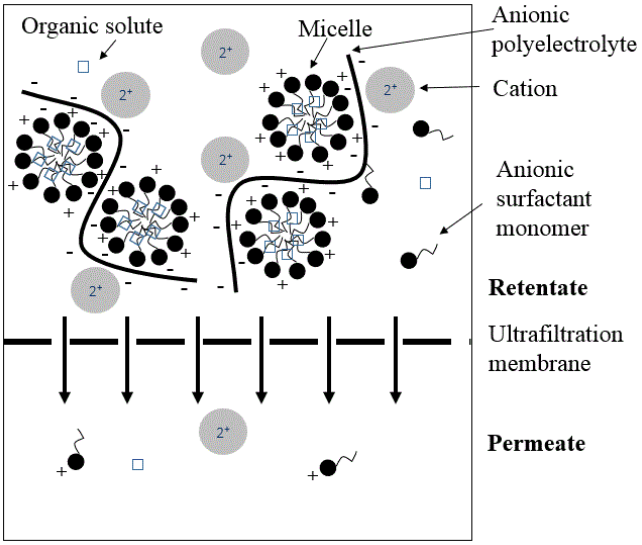

Figure 2.9: Schematic of colloid enhanced ultrafiltration, sometime know as polyelectrolyte micellar enhanced ultrafiltration (modified from (Komesvarakul et al., 2005b)).

In polyelectrolyte MEUF, the polyelectrolyte is used as a flocculant. Another technology, called surfactant-induced coagulation of polyelectrolyte, uses anionic surfactant as a coag-flocculant to neutralise the overcharge of cationic polyelectrolytes after they have bound with phenolic compounds (Saitoh et al., 2014). Thus, the dosage of surfactant depends on the valence of species and their concentrations in the solution, which is not easy to control. However, the rapid and effective removal of estrogens and phenolic compounds from solutions by this technology are beneficial for reducing the risk to ecosystems posed by these components.

The function of polyelectrolyte was further explored in CEUF to simultaneously solubilise molecular organic pollutants inside the micelle and bind metallic ions to the polyelectrolyte in solution (Guo et al., 1997). To increase the selectivity to metallic ions, a ligand-modified CEUF was proposed. The notion is similar to LM-MEUF, but the monomer leakage was much less due to the addition of polyelectrolyte. Systematic studies

were conducted by Komesvarakul et al. (2003, 2004, 2005a and 2005b) to purify phenolic-laden wastewater from the pulp and paper industries and to treat chlorophenols in wastewater. The effects of added salt, pH, ionic strength on organic solubilisation and surfactant leakage were also investigated.

Although the ligands were regenerated via pH adjustment, the regeneration of polymer-surfactant complexes received little attention. It was partially recognised that the formation of complexes is irreversible (Dubin and Davis, 1985, Berglund et al., 2004). For this reason, the CEUF (using polymer–micelle complexes) was less attractive than PEUF and MEUF. In addition, due to the extra dosage of polyelectrolyte plus a surfactant dosage above its CMC, the chemical intensity of the process is another barrier for wider applications.

2.6. Discussion and summary

The roles of surfactant and polymer in water treatment are well established. Surfactant and polymer based separation technologies have been developed over the past few decades and have good potential to treat industrial effluents. Each technology has its own strengths and limitations, and thus the applications of these technologies very much depends on the targeted ions, effluent characteristics, discharge requirements and cost. Much research has addressed the applications of polyelectrolyte or surfactant alone, but the usage of their mixture has shown some unique advantages in terms of chemical usage and stability, and has a great potential for a wider industrial application range. To fully explore the potential of polymer and surfactant mixture, it is important to understand the interaction between them in the solution.

Chapter 3

Experimental Investigation of Polymer–Surfactant–Ion Interactions at the Air-Water Interface and in the Bulk Aqueous Phase

3.1. Introduction

Adsorption of molecules at the air-water interface from polymer–surfactant mixtures and the bulk interactions of these systems have been studied extensively, because their wide applications in the pharmaceutical and detergent industries. However, little research attention has been focussed on the interfacial adsorption and bulk interactions in the presence of metal ions. This chapter is concerned with the preparation of the aqueous surfactant, polymer and metal ion solutions and their interactions at the interface and in the bulk phase, which underlies the fundamental basis of the polymer–surfactant based treatment process. The polymer–surfactant interactions in the presence of varying amounts of metal ions are studied via surface tension, phase diagram and electrical

conductivity measurements to develop the treatment process.

There are four reasons to conduct these measurements. Firstly, the surface tension measurements can reveal the extent of the formation of polymer–surfactant aggregates (PSAs), and estimate the binding capacity to the oppositely charged metal ions. Secondly, both surface tension and conductivity measurements can suggest a reasonably accurate optimum dosage ratio/range in the three way system, based on the transitional points in the plots. This is useful for the later optimisation experiments. Thirdly, correlating the changes of metal removal and removal agent usage efficiencies with the transitional points on the surface tension and conductivity plots can verify the mechanism for metal removal by the functional structures (i.e. the PSAs). Finally, the phase diagrams indicate the variation of polymer charge and the interaction status of polymer and surfactant at different dosage ratios.

Colloids consist of a dispersed phase distributed uniformly in a finely divided state in a dispersion medium (Everett, 1988). In the case of charged colloids, a layer of counter ions attach on the particle surface (stern layer), and the second layer contains free ions with a higher concentration of the counter ions that diffuse to the space surrounding the particle (diffuse layer).

The Deryagin-Landau-Verwey-Overbeek theory points out that the stability of colloids arise from counter activity Van der Waals attraction between two colloidal particles against the electrical double layer repulsion. The summation of these two contributions create a free energy barrier to prevent the elimination of the colloidal states i.e. stable colloidal dispersion. Brownian motion of particles is usually the reason for carrying the system over the barrier, originating from the random movement of the particles. When the energy barrier is a few times higher than thermal energy, flocculation is prevented.

When the energy barrier is close to thermal energy, flocculation can occur. (Lekkerkerker and Tuinier, 2011).

In this chapter, oppositely charged polymers and surfactants are investigated to enhance the understanding of the strong polymer–surfactant interactions at the interface and in the bulk phase and to build the fundamental knowledge of the effects of metal ions on such interactions.

3.2. Materials and methods

3.2.1. Preparation of aqueous surfactant, polymer and metal ion solutions

Poly (diallyl dimethyl ammonium) chloride (PolyDADMAC) solutions were prepared by diluting a stock PolyDADMAC solution (Sigma Aldrich, average molecular weight (MW)<100,000, 35 wt.% in H_2O, charge density 0.62eqv/mol). Poly (ethyleneimine) (PEI) solutions with MW 25K and 750K were prepared by diluting PEI stock solutions (Sigma Aldrich, average MW~25,000 and average MW~750,000, 50 wt.% in H_2O). Poly (acrylic acid) (PAA) solutions were prepared by diluting a stock PAA solution (Sigma Aldrich, average MW<100,000, 35 wt.% in H_2O). Poly (sodium 4-styrenesulfonate) (PSS) (average MW 1,000,000), sodium dodecyl sulphate (SDS) (purity ≥ 99.9%) and myristyl trimethyl ammonium bromide (MTAB) (purity ≥ 99%) were obtained from Sigma Aldrich. The SDS was further purified before use by recrystallization from an ethanol solution three times. Chromium (III) nitrate nonahydrate, cadmium sulphate, zinc sulphate, potassium chromate, potassium dichromate and potassium ferricyanide were purchased from Fisher Scientific (all purity ≥ 99%).

Polymer, surfactant and metal ion solutions were prepared from 2000-8000 ppm polymer, 0.1M surfactant and 0.01M ion stock solutions made in large volumetric flasks. A calculated amount of ions was added first and then diluted with deionised water. Polymer solution was added after the first dilution, and then diluted with deionised water. Finally, the surfactant solution was added and the mixture topped up with deionised water. The solution was stirred by a magnetic stir bar overnight to achieve equilibrium, indicated by a transparent solution with flocs at the bottom and on the beaker wall. After that, these solutions were then coarse-filtered. The pH of each solution was adjusted by adding small amounts of concentrated H_2SO_4 and NaOH solutions for the pH effect studies. The pH of solutions were measured by a Jenway pH meter.

3.2.2. Surface tension measurements

Changes in surface tension at the solution-air interface provide an insight into the status of the interactions between polymer and surfactant in the bulk solution. This insight can be used to determine the optimum dosage ratio between polymer and surfactant under different conditions. The optimum dosage ratio is then confirmed by experimentally measuring the heavy metal removal and removal agent usage efficiencies. The surface tension plots can also yield information about the critical aggregation concentration (CAC) and critical micellar concentration (CMC), which can be used to study and compare the effects of surfactant, polymer and heavy metal ion additions. Finally, the plots can be used to check the purity of surfactant.

The surface tension measurements were performed with a maximum pull digital tensiometer (K10T, Kruss) using the du Nouy ring method, with a platinum-iridium ring. Before each measurement, the ring was rinsed in ultra-high quality (UHQ) water and then

flame dried until no flame colour change was observed with a Bunsen burner. Each measurement was repeated until equilibrium was established and the variation in the surface tension was less than 0.2mN/m between the most recent three measurements.

3.2.3. Phase diagram measurements

The phase diagram measurements were based on plotting the turbidity of the prepared solutions in a systematic way. Each solution was prepared from the same stock solutions of polymer, surfactant and heavy metal ions. The solution was stirred by a magnetic stir bar at 200 rpm overnight to achieve equilibrium, which is indicated by no further changes in turbidity measured by a Turbidimeter (2100N, Hach).

3.2.4. Conductivity measurements

The conductivity of solutions was measured by a YSI professional plus conductivity meter, with an accuracy of ± 0.1 μs/cm in the range below 500 μs/cm and ±1 μs/cm in the range above. A 500 ml solution of PAA/PSS and/or anion was prepared from stock solutions; for the pH effect studies, the pH was adjusted by adding small amounts of concentrated H_2SO_4 or NaOH solution. The probe was calibrated with standards before each usage. 1ml of 0.01M surfactant solution was then added stepwise into the solution, containing a low concentration of polymer or adjusted pH for maintaining the polymer concentration or pH, and a reading was taken when the conductivity reading stabilised. A correction factor for the dilution was considered. In some relatively unstable zones, the readings could vary by 2 μs/cm in a few seconds. In this case, only the highest conductivity reading was taken to obtain consistent results. Due to the measurement accuracy, under a high ionic strength condition, some of the data was rounded-off to the nearest integer, and the trend of the change of increase of conductivity above 500 μs/cm

was less smooth than that below 500 μs/cm. Fortunately, the low surfactant concentration zone is the dosage range of interest.

3.3. Studies of surface tension

3.3.1. Importance of sample purity and sample environmental cleanliness

The bulk properties of a surfactant solution are not strongly affected by the presence of trace impurities, but the interfacial properties may be significantly affected. In the presence of a surface active impurity, the surface tension will be lowered, and may lead to some misleading interpretations of the interfacial structures. For example, a dip in surface tension around the CMC of a pure surfactant could be either caused by impurities or by an excess amount of metal ions. If there is a surface active impurity, the dip might be misinterpreted to be caused by the impurity rather than the compacted surface structures induced by the multivalent metal ions. Thus, it is important to consider the purity of materials and the cleanliness of the sample environment for the studies of interfacial behaviour. To ensure the cleanliness of the sample environment, all the glassware used in the surface tension studies, either for the preparation or purification of materials and samples, was cleaned by the following procedure. Firstly, 67% nitric acid was used to rinse the glassware to remove the oxidative contaminants. After using tap water to wash it thoroughly, it was left to soak for a few hours in a 2-3% solution of Decon 90 (a commercial alkaline detergent). Then it was washed with de-ionised water and then with UHQ water (Elgstat PS water purifier). The absence of long-lived bubbles at the surface of the rinsing water were considered to indicate the rinsing water was free from surface active impurities. Finally, the glassware was dried in a vacuum oven.

3.3.2. Heavy metal ion and SDS system

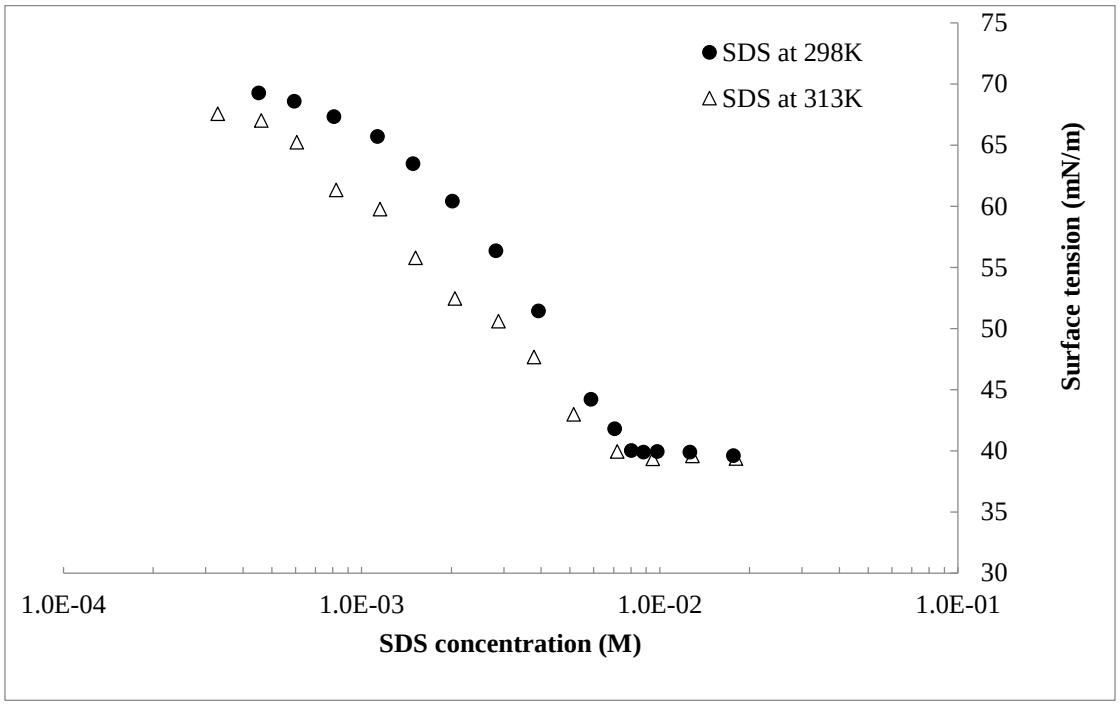

Figure 3.1: Surface tension plots for the SDS system at different temperature.

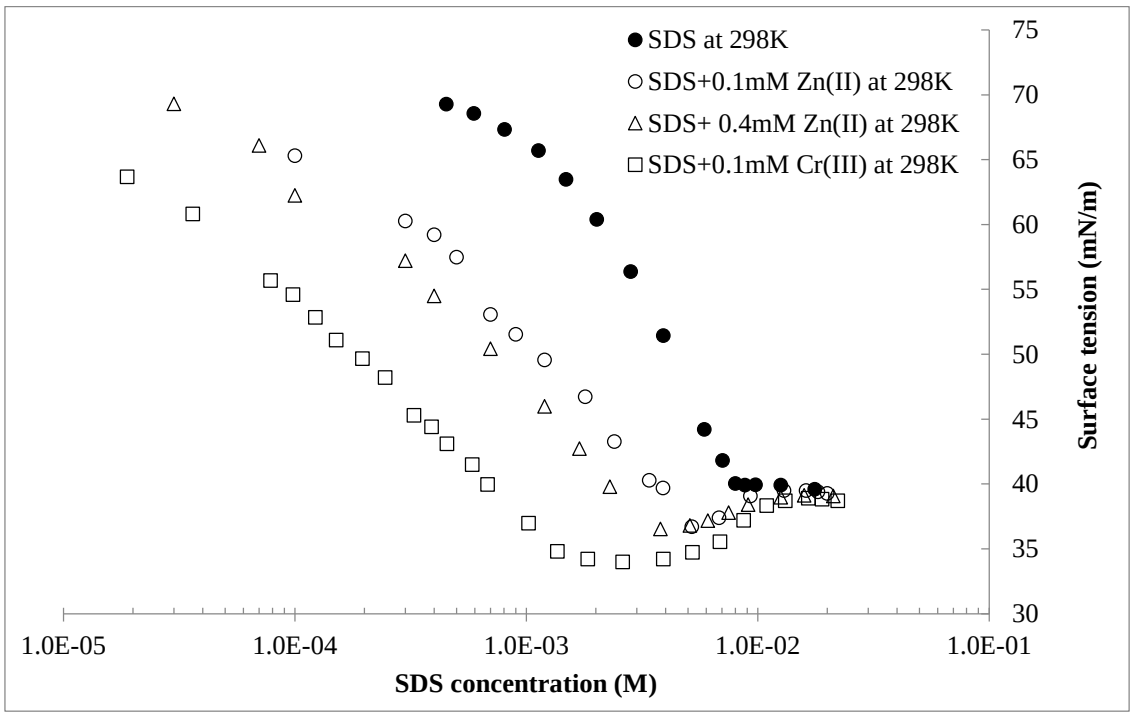

Figure 3.2: Surface tension plots for the SDS system at different metal ion concentrations.

From Figure 3.1, with an increase of temperature from 298K to 313K, it can be seen that the surface tension values decrease, and the CMC value decreases moderately. This is due to the increasing surface activity of SDS at a higher temperature, which leads to compacted air-water interfacial structures that further decrease the surface tension values. As shown in Figure 3.2, in the presence of heavy metal ions, the surface tension values decrease and dips appear around the shifted and apparent CMC. Since all the SDS used in the surface tension measurements was purified, and no surface active impurity was brought into the system from the metal ion stock solutions, the dips can only be caused by the addition of metal ions. The reasons of lower surface tension are that the multivalent metal ions can pull two SDS monomers closer via electrostatic forces and also reduce the repulsive force between them, which results in more compacted interfacial structures.

A minimum point (dip) is measured below the shifted CMC. At the SDS concentration below the dip, the decrease in the surface tension is due to compacted interfacial monomer arrangements induced by metal ions. The dip represents all the bulk metal ions have bonded with micelles, the surface bonded metal ions will start to migrate to the bulk solution to bond with the newly formed micelles, because the micelles have a higher charge density than that of interfacial monomers. This migration leads to relatively loose interfacial structures (less monomers are present at the interface), and consequently the surface tension increases. It is worth noting that the minimum point does not necessarily represent the CMC, because the metal ions not only exist at the interface, but also in the bulk solution. The very first micelle will be energetically more favoured to associate with the bulk metal ions rather than the interfacial ones. At this moment, the bulk associations cannot be measured via the surface tension method. The true CMC, therefore, is at a slightly lower SDS concentration than that of the dip. Moreover, all the surface tension

values above 0.02M SDS are almost at the same level, because all of the surface metal ions have migrated to the bulk solution.

The overall surface tension values, including the minimum value, decrease in the presence of metal ions (Figure 3.2). Comparing the surface tension curves of 0.1 mM and 0.4 mM Zn(II) addition, the 0.1 mM curve has a higher surface tension value at the same concentration of SDS. This is due to the Zn(II) equilibrium between the air-water interface and the bulk solution. At a higher Zn(II) concentration, a greater amount of Zn(II) ions are present at the interface to enhance the surface SDS adsorption, and consequently the surface tension value in general is decreased. This also leads to a lower minimum point value around the CMC, and the greater amount of surface Zn(II) will eventually migrate back to the bulk solution with an increasing amount of micelles. Apart from the dosage effects of added ions, the ionic valence itself also plays an important role. In the presence of 0.1mM trivalent Cr(III) ions, the changes of surface tension values are more obvious than with divalent Zn(II)'s, because the trivalent ion has a much stronger effect than that of the divalent ion. In conclusion, both the dosage and valence of metal ions have moderate effects on the values and the presence of a dip in the surface tension curve, and the extent of the effects increases with dosage and valence.

3.3.3. Polymer and SDS systems

3.3.3.1. PolyDADMAC and SDS system

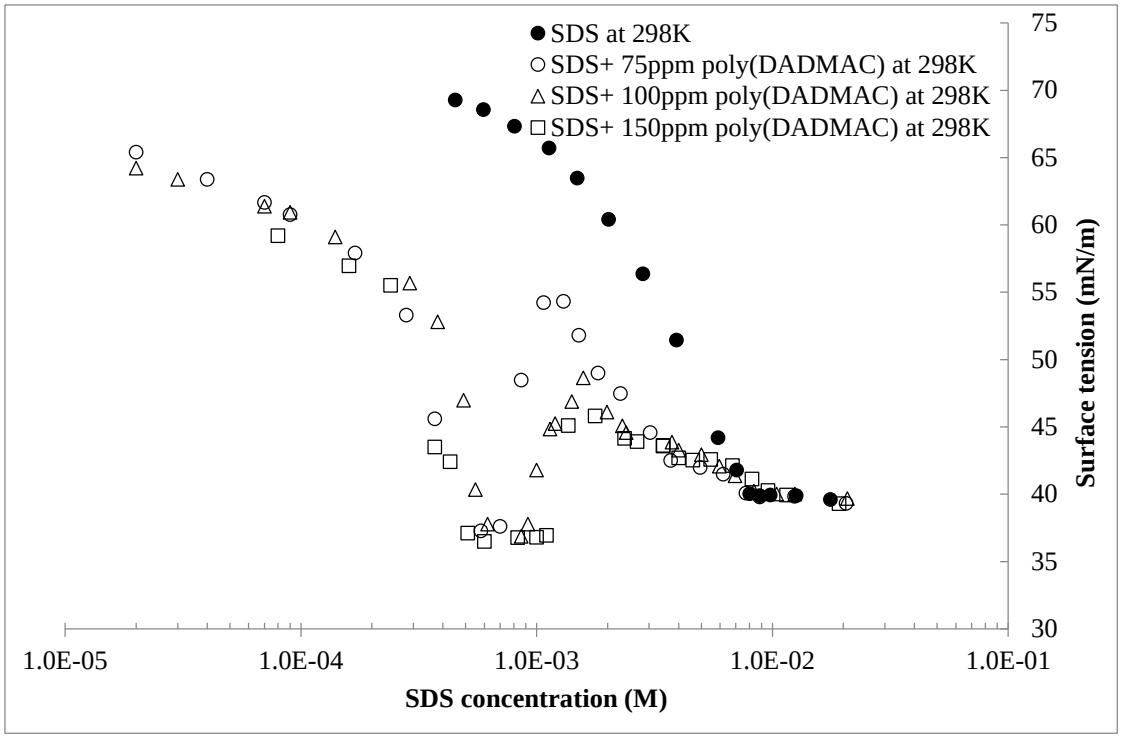

Figure 3.3: Surface tension plots for the SDS system with different polyDADMAC concentrations.

The surface tension of polyDADMAC and SDS mixtures were studied to investigate the general pattern of oppositely charged polymer–surfactant systems and to gain a fundamental knowledge for the metal ion addition studies later on. Figure 3.3 shows a classic surface tension plot for strong polymer–surfactant interactions, which has a distinct central peak. In the pure SDS system, little change is measured in surface tension at low surfactant dosage (about the same surface tension value as for the UHQ water), which means that little SDS monomer is present at the interface. However, in the polyDADMAC and SDS system, at the same surfactant dosage, the surface tension values drop quickly due to the formation of polymer–surfactant complexes at the air-water interface. This drop suggests that the presence of polyDADMAC promotes the adsorption of surfactant at the interface, and the surface activity of the resulting complexes are higher

than that of the surfactant monomers at the same surfactant concentration and solution temperature.

Apart from increasing the surface activity, the cationic polymer also causes a complex surface behaviour around the CAC. All three polyDADMAC–SDS plots show their first plateau after the CAC (approximately 0.5mM). The transitional points are independent of the concentration of polyDADMAC, because the interface has already been saturated with polymer–surfactant complexes even at a relatively low polyDADMAC concentration. Unlike the transitional point, however, the length of each plateau is proportional to the amount of polyDADMAC. This can be explained by the formation of PSAs, which is a structure formed by the micelle-like aggregates binding onto the polymer chain. They start to form at a particular surfactant concentration called the CAC. At and above the CAC, the local surfactant concentration reaches an energy threshold, which is a similar threshold in nature to that for the surfactant to form micelles in the bulk solution. Near to the bulk polymer chains, it becomes more favourable for surfactant to form a mini 'micelle-like' aggregate via hydrophobicity, rather than individual monomers bonding to the oppositely charged polymer chains (polymer–surfactant complexes). When all the bulk polymer chains are saturated with surfactant, the surface complexes start to migrate back to the bulk solution to form more PSAs, because polymer is favoured energetically to form PSAs to minimise the free energy. This leads to a partial depletion of surface at the interface, which increases the surface tension value. Hence, the end point of the first plateau is the saturation point of bulk polymer. For this reason, the length of this first plateau increases with the amount of polymer available in the bulk solution, which is proportional to the polyDADMAC concentration. After the first plateau, the height of the subsequent peak decreases with increasing polymer concentration. Thanks

to the increasing polymer concentration, the equilibrium of surface polymer–surfactant complexes and bulk PSAs is shifted towards the surface complexes side. This shift leads to an increased amount of surface polymer–surfactant complexes remaining at the interface, which lowers the surface tension values. In addition, the SDS concentration at the peak position is also moved to a higher concentration, due to the extra SDS needed to form the extra PSAs with the extra polyDADMAC amount.

At the peak, all the polymer chains either in aggregate or complex form, are saturated, with the majority of the polymers in PSA form. Further increasing the SDS concentration, the decrease of surface tension values is caused by the increasing amount of SDS monomers at the interface until reaching the second plateau. The transitional point is the CMC at which the micelles start to form in the bulk solution. The results suggest that the CMC values increase with increasing polymer concentration, for the same reason of increasing length of the first plateau and the peak position (Figure 3.3). On the other hand, the additional counter ions from the polyDADMAC can decrease the CMC by screening the repulsive force between the head groups of surfactant monomers. The results indicate that the screening effect on the CMC at the low polymer concentrations is negligible relative to the need for extra surfactants to form the PSAs. After the CMC, all four plots show a second plateau at the same surface tension values, because the air-water interface is now saturated by the monomers, and the amount of interfacial complexes is not significant when compared with the amount of interfacial monomers.

3.3.3.2. PEI and SDS system

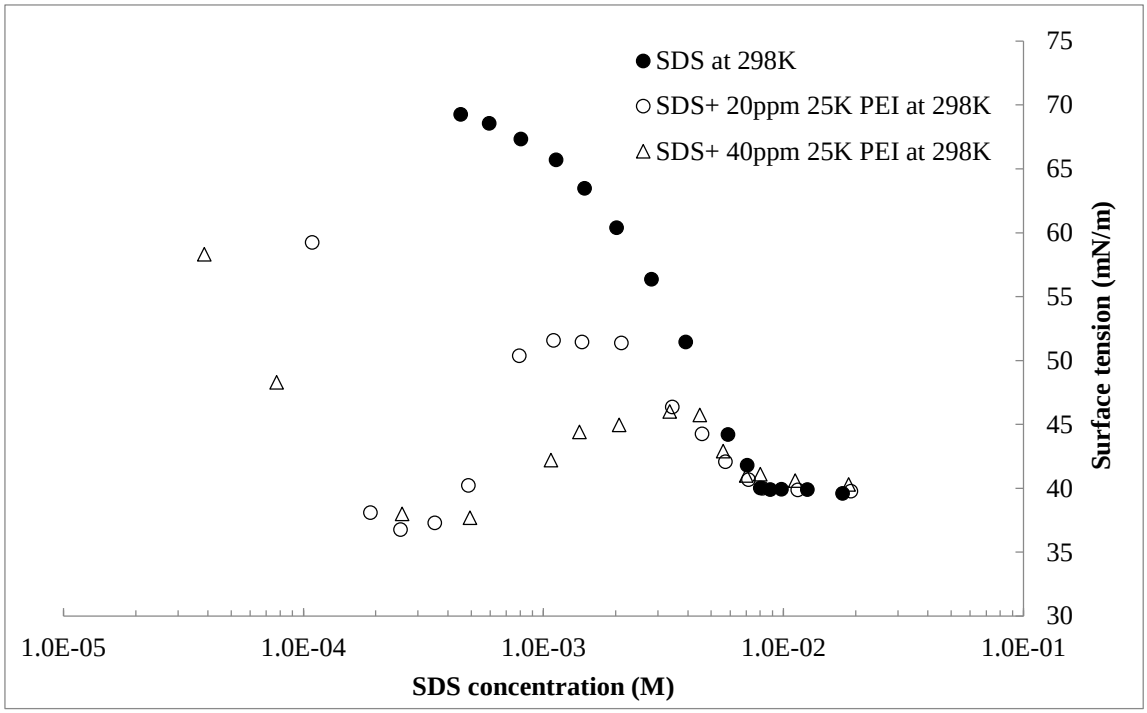

Figure 3.4: Surface tension plots for the SDS system with different concentrations of 25K PEI.

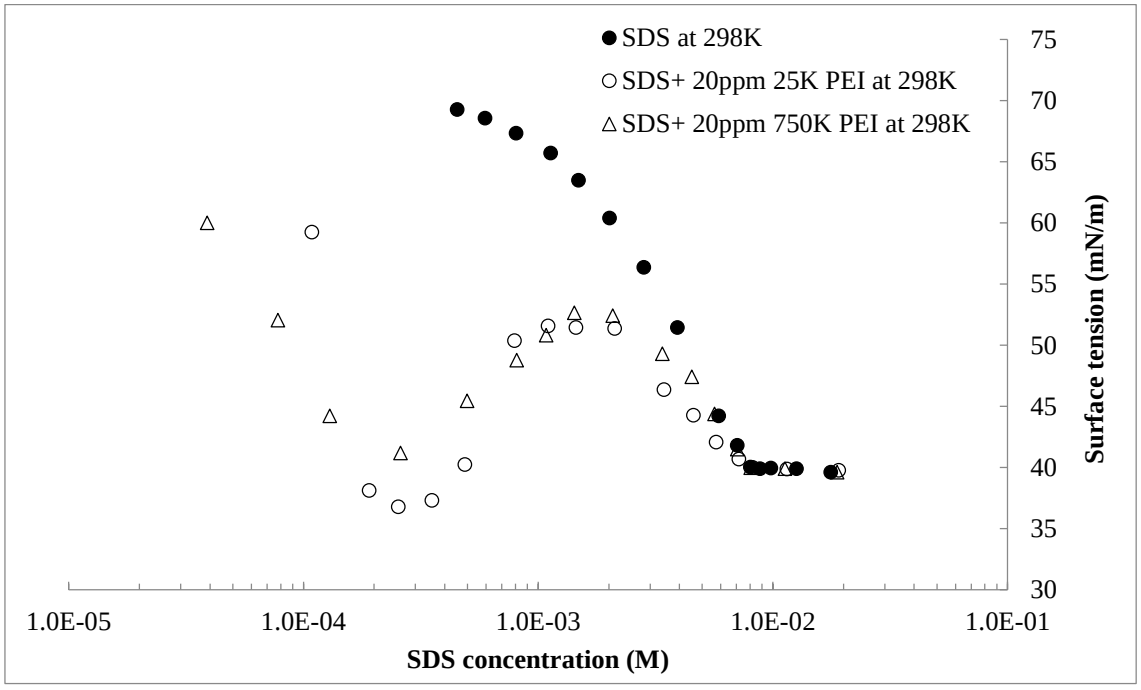

Figure 3.5: Surface tension plots for the SDS system with 20 ppm PEI with different molecular weights.

Another polymer (PEI) containing a secondary and tertiary amine group is also studied, which is positively charged at an acidic pH and neutral at a basic pH. This pH-sensitive property can be used to separate the polymer and bound surfactant for recovery and recycle, while the positive charge of the quaternary amine group in polyDADMAC is not reversible.

In Figure 3.4, the pattern of the PEI and SDS system is similar to that with the polyDADMAC and SDS system. With increasing PEI concentration, the surface tension values are slightly decreased; the peak position is also slightly postponed; and little difference is found after the CMC. Like the polyDADMAC–SDS system, the PEI–SDS system also demonstrate the formation of polymer–surfactant complexes before the CAC, after which the surface complexes migrate back to the bulk solution to form PSAs.

Two different MW PEIs (25KDa and 750KDa) are studied to reveal the MW effects on the interfacial behaviour (Figure 3.5). The results suggest that the surface tension values around the CAC are lower for the relatively low MW (short chain) PEI. The reason for this is that it forms more compact polymer–surfactant complexes than the high MW ones, which can reside at the interface with a higher packing density. Most importantly, the surface tension pattern and key points (CAC, peak and CMC) remain at the same SDS concentrations for the different MWs of PEI. This clearly demonstrate that the PEI also forms PSAs.

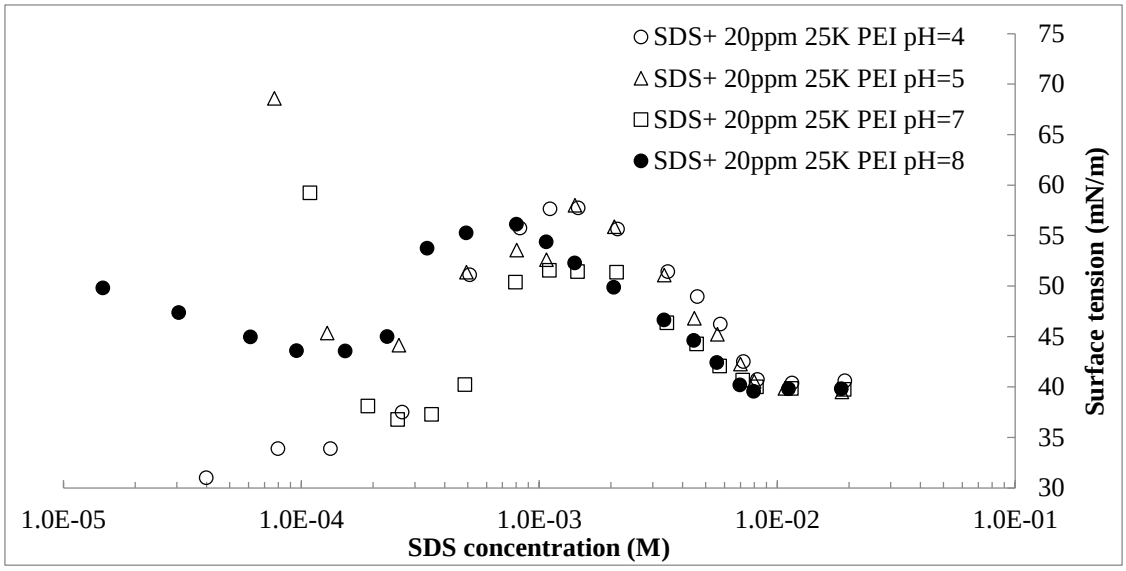

Figure 3.6: Surface tension plots for the SDS system with 20 ppm 25K PEI at different pHs.

As previously noted, the PEI is selected as a substitute for the polyDADMAC because it can be reused after neutralisation. This reusable property is due to the secondary amine group in the molecules of PEI. The amine group can not only be protonated at a low pH value to acquire a positive charge, but it also can be progressively deprotonated at a higher pH value to become a weakly positively charged or even a neutral polymer. This pH dependent behaviour offers a way to manipulate the charge of polymer via pH adjustment without damaging the polymer, and this can be used to recover and recycle the polymer.

To understand the PEI–SDS interactions in solution at various pH values, the surface tension measurements over a pH range from 4 to 8 were conducted. It is a surprise to notice that the surface tension plot for PEI–SDS at a pH of 8 is not a classic neutral polymer surface tension plot (no peak would be expected between the CAC and CMC), which indicates that the PEI at pH of 8 has not been completely deprotonated (Figure 3.6). For later recovery studies, a higher pH value should be used to neutralise the PEI, and to disassociate the flocculated PSAs. In addition, at lower pH values, a greater amount of

SDS is required to reach the same surface tension values between the CMC and the peak point. The reason is that with an increasing of screening effect allows a compacted SDS arrangement at the interface. The amount of available binding sites on the PEI is increased, so a greater amount of SDS is used to form more aggregates on each polymer chain. Due to the extra usage of SDS, the position of the peak point and the decrease of surface tension before the CMC are delayed. In summary, with decreasing pH values, an increasing amount of PEI segments are protonated to become positively charged, but the segments are not necessarily completely neutralised at a slightly basic condition.

3.3.4. Metal ion, polymer and SDS systems

3.3.4.1. Polymer and $ZnSO_4$ concentration effects

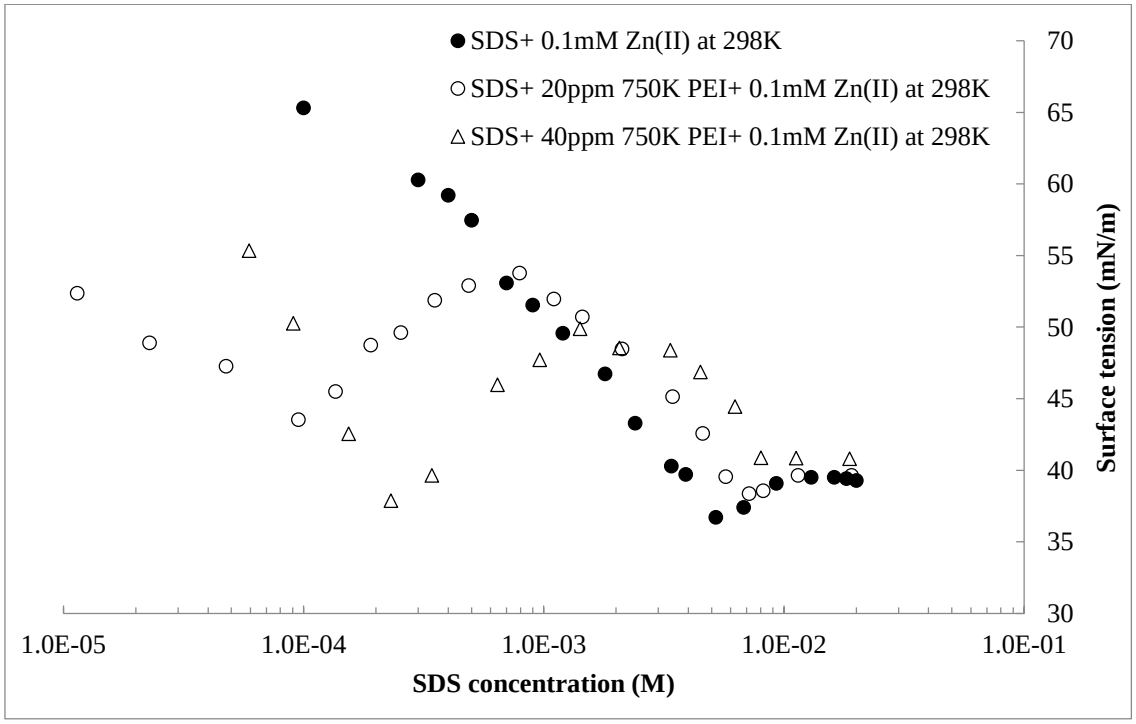

Figure 3.7: Surface tension plots at different SDS concentrations for 0.1 mM $ZnSO_4$ with different amounts of PEI.

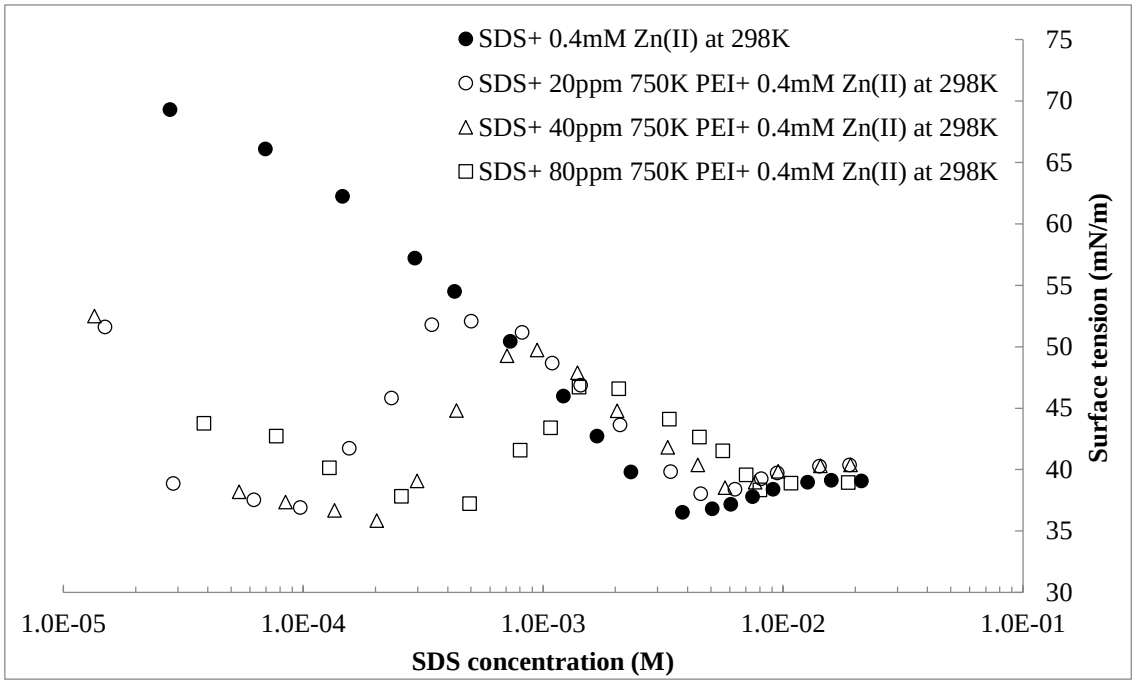

Figure 3.8: Surface tension plots at different SDS concentrations for 0.4 mM $ZnSO_4$ with different amounts of PEI.

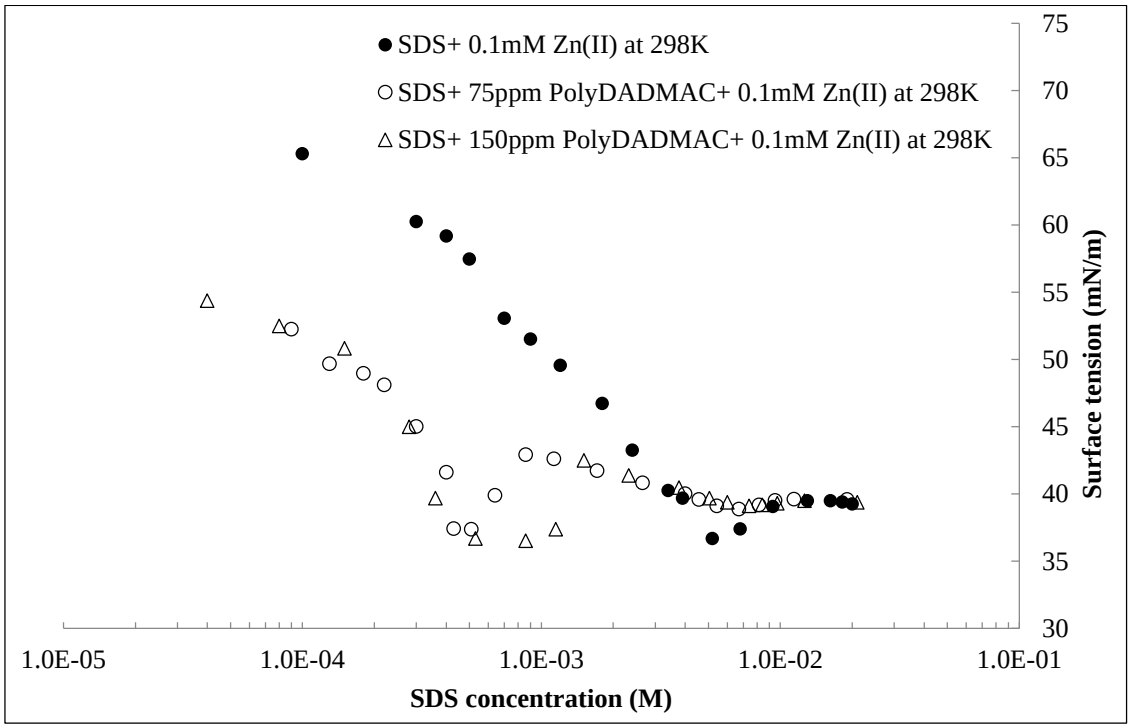

Figure 3.9: Surface tension plots at different SDS concentrations for 0.1 mM $ZnSO_4$ with different amounts of polyDADMAC.

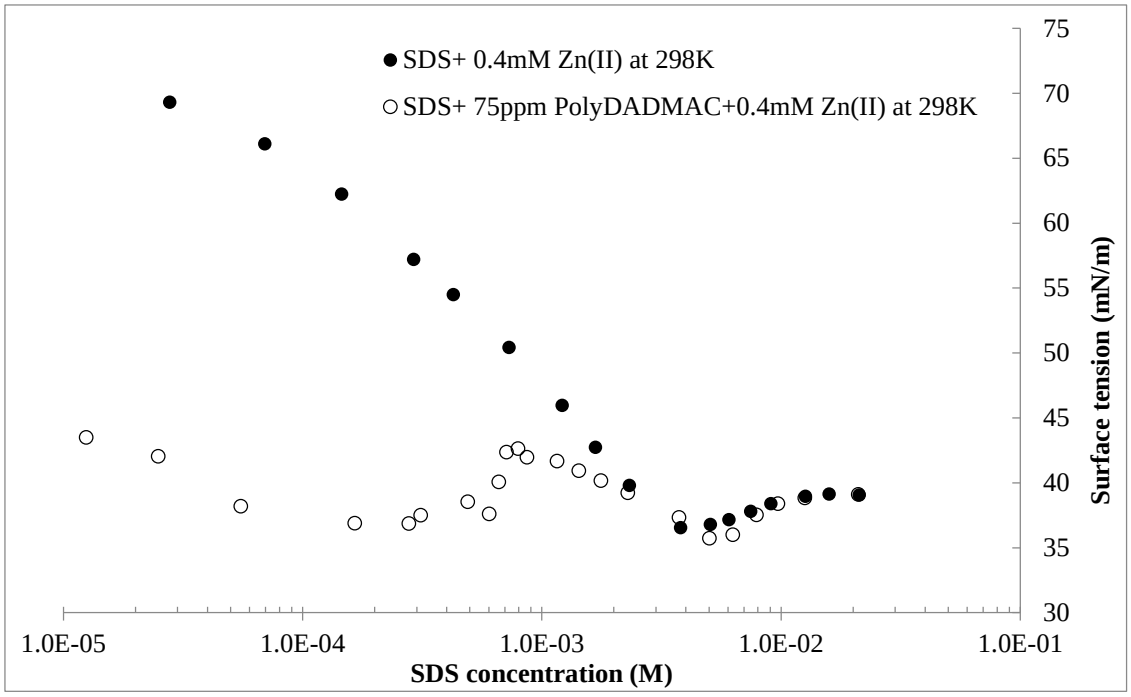

Figure 3.10: Surface tension plots at different SDS concentrations for 0.4 mM $ZnSO_4$ with different amounts of polyDADMAC.

To understand the effects of polymer and metal ion concentration on the interactions of polymer, surfactant and Zn(II) (an example of a metal ion) and on the formation of PSAs, two fixed concentrations of Zn(II) with various polymer (both PEI and polyDADMAC) concentrations are studied. At the same $ZnSO_4$ concentration, the surface tension plots (after the CAC) move in the direction of higher SDS concentration with increasing polymer concentration (Figure 3.7, Figure *3.8* and Figure *3.9*). This movement is caused by the formation of a greater amount of bulk PSAs, involving additional SDS. Since there are no PSAs formed before the CAC, the surface tension values in the polyDADMAC system are almost the same with increasing polymer concentration up to the CAC (Figure 3.9). In the PEI system, however, at the same SDS concentration, the CAC value increase with increasing polymer concentration. The reason for higher surface tension values is that the increasing amount of PEI binds with a great amount of free SDS

in the bulk solution, which leads to the surface-bulk SDS equilibrium moving toward the bulk. Thus, slightly less SDS movement are present at the surface, and this result in the increase of surface tension values at the same SDS concentration. $ZnSO_4$ has little effect on the surface tension above the CMC, because Zn(II) has a strong electrostatic binding affinity with micelles in the bulk solution as opposed to the surfactant at the surface (Figure 3.10).

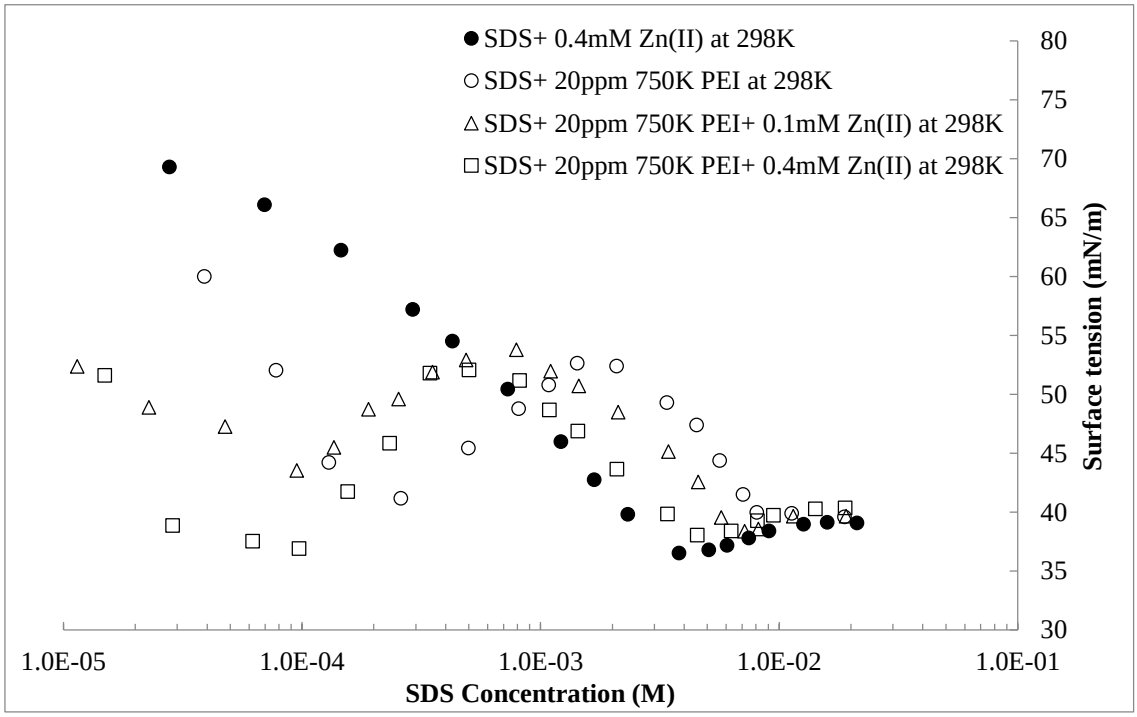

Figure 3.11: Surface tension plots at different SDS concentrations for 20 ppm 750K PEI with different amounts of $ZnSO_4$.

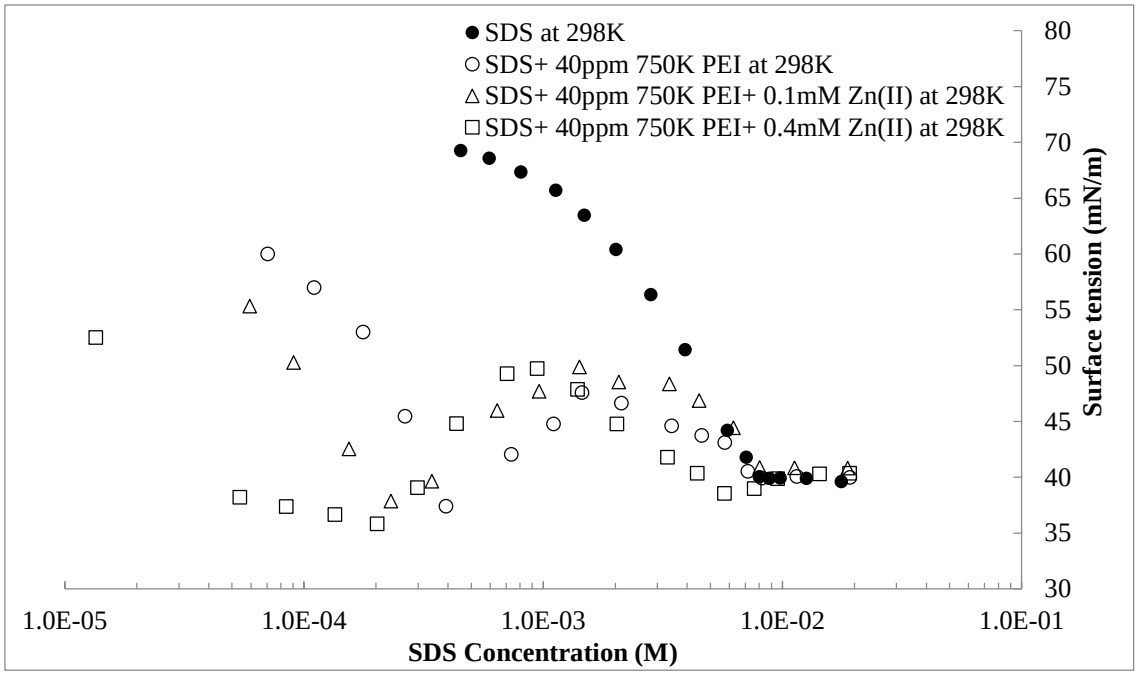

Figure 3.12: Surface tension plots at different SDS concentrations for 40 ppm 750K PEI with different amounts of $ZnSO_4$.

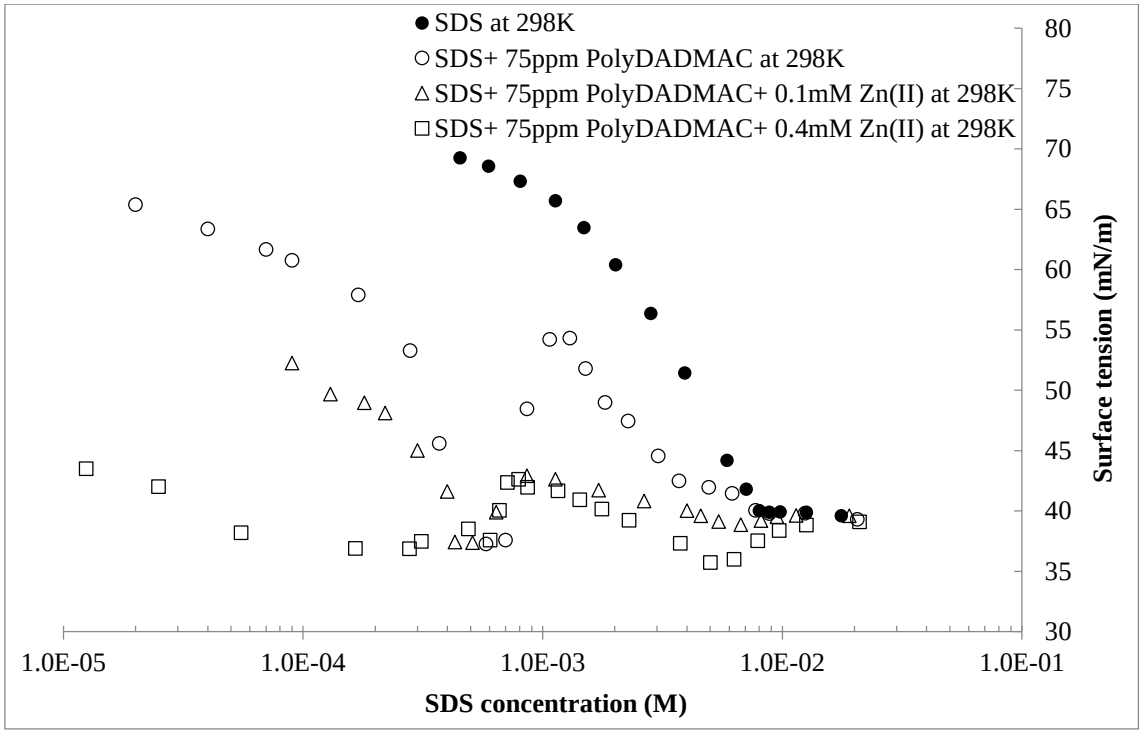

Figure 3.13: Surface tension plots at different SDS concentrations for 75 ppm polyDADMAC with different amounts of $ZnSO_4$.

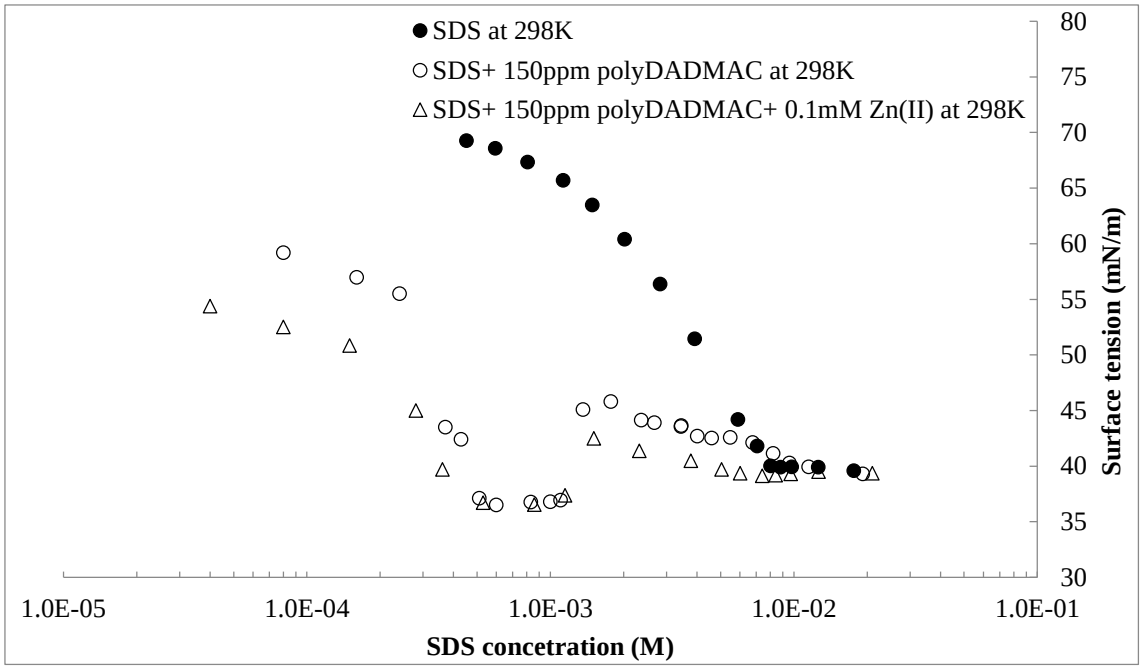

Figure 3.14: Surface tension plots at different SDS concentrations for 150 ppm polyDADMAC with different amounts of $ZnSO_4$.

To understand the effects of $ZnSO_4$ addition, the surface tension of solutions containing different amounts of cationic polymers in the presence of $ZnSO_4$ are measured as a function of SDS concentration. With the addition of $ZnSO_4$, even at 0.4 mM $ZnSO_4$, the surface tension of PEI and polyDADMAC systems follows a similar pattern. In Figure 3.12, Figure *3.13* and Figure *3.14*, although adding $ZnSO_4$ supress as the peak (and much more so in Figure 3.13), with increasing $ZnSO_4$ concentration the SDS concentration at the peak marginally decreases due to the charge screening of the surfactant headgroups. This relatively stable peak position suggests that the optimum dosage between polymer and SDS is not altered very much by adding 0.4 mM Zn(II). Further optimisation is conducted to achieve the highest metal removal efficiency with minimum total carbon residue left in the solution. Thus, in the later studies, the optimum dosages are kept the same for each metal ion. Apart from the stable peak position, the heights of the peak for

a consistent polymer concentration remains unchanged in the presence of increasing $ZnSO_4$ concentrations. This stable peak height may indicate that the surface components remain almost the same with increasing $ZnSO_4$ concentration i.e. a packed monolayer at the surface already is achieved.

Results from Figure 3.11, Figure *3.12* and Figure *3.13* indicate that, with increasing $ZnSO_4$ concentration, the surface tension values below 10^{-3} M SDS are lowered for both polymers at the same polymer and surfactant dosage. This suggests that increasing $ZnSO_4$ concentration promotes the presence of polymer–surfactant complexes at the surface via enhancing their surface activity, due to electrostatic screening. This presence, however, does not significantly affect the surface capacity of the complexes, so the surface tension values remains almost the same around the first dip at the CAC. However, in Figure 3.11, at low polymer–surfactant complex and high Zn(II) concentrations (20 ppm 750K PEI + 0.4 mM Zn(II), the surface tension values around CAC decrease. The reason is that the surface activity is probably affected by the amount of Zn(II) per complex rather than by the Zn(II) concentration alone.

The dip around the CMC is caused by the addition of Zn(II) which is not bound to PSAs (Figure 3.11, Figure *3.12* and Figure *3.13*). The Zn(II) increases the surface capacity of monomers at high surface concentration, through re-conformation or compaction of surface monomers under mainly charge screening and monomer chain hydrophobic associations at the surface. This compaction further lowers the surface tension value. After reaching the bottom of a dip (near the CMC), the Zn(II) is more energetically favoured to associate with micelles in the bulk than with the monomers at the surface. Hence, at a constant added Zn(II) concentration, the surface Zn(II) migrates into the bulk to bind with increasing amounts of newly formed micelles. At the surface, decreasing

amounts of Zn(II) shift the conformation of monomers back to that in a pure SDS solution, where monomers are more loosely compacted. Thus, the surface tension after the minimum point increases. The higher the concentration of Zn(II) is, the more the amount of Zn(II) is which could potentially be present at the surface and migrate into the bulk after the CMC is reached. Thus, the dip is deeper with increasing ZnSO4 concentration. After the CMC, surface tension plateau values are independent of ZnSO4 concentration. This reveals that there is little Zn(II) present at the surface at high SDS concentrations (a few times CMC).

One key finding from these four surface tension plots is that the dip in surface tension correlates with the Zn(II) adsorption capacity of PSAs. It was found that the dips around the CMC are less obvious with increasing concentrations of PEI at 0.4 mM $ZnSO_4$ (Figure 3.8). Moreover, the dip even disappears at 150 ppm PolyDADMAC (Figure 3.9), because almost all free Zn(II) is adsorbed by the PSAs and only a small portion of Zn(II) is able to form surface monomer-Zn(II) complexes. The reductions in the depth of the dip may well suggest that the Zn(II) is more energetically favoured to associate with bulk PSAs than the polymer–surfactant complexes at the surface. When a limited amount of $ZnSO_4$ is present in the solution, they preferably associate with the bulk PSAs. Thus, there are only a few zinc ions present at the surface, and even fewer Zn(II) could then subsequently leave the surface and migrate to the bulk and subsequently cause an increase of surface tension values. Therefore, the dip is much less obvious and even disappears in the presence of higher concentrations of polyDADMAC with a limited amount of $ZnSO_4$ (Figure 3.9). If the added $ZnSO_4$ is slightly greater than the adsorption capacity, the observable depth of the dip in surface tension is then caused by the $ZnSO_4$ which has not been captured by PSAs and micelles. The reduction of the depth of the dip depends on

the adsorption capacity of aggregates and micelles, and the amount of added multivalent ions. In conclusion, the observation of a dip in surface tension at the CMC may be correlated with an insufficient adsorption capacity of PSAs for the dosages of metal ions.

3.3.4.2. PEI molecular weight effects

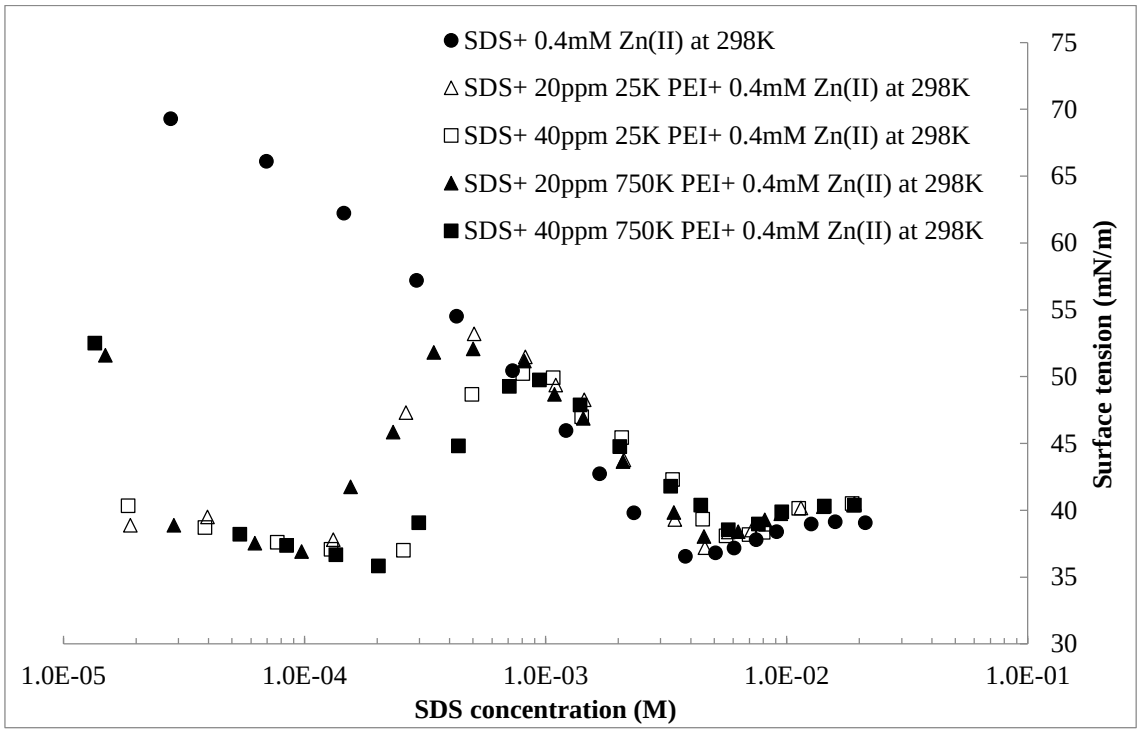

Figure 3.15: Surface tension plots at different SDS concentrations for 0.4 mM Zn(II) with different amounts of 25K and 750K PEI.

In Figure 3.15, both 25K and 750K branched PEI are also investigated to study the effects of different MW polymer on the surface–polymer interfacial behaviours. The results suggest that there is no noticeable difference between two different molecular weight PEI, in the presence of Zn(II), reaching the same conclusion as in the PEI–SDS system. That part per million (ppm) is a weight percentage concentration, thus even for different MW, the number of chargeable groups are the same at the same weight percentage concentration.

3.4.4.3. pH effects

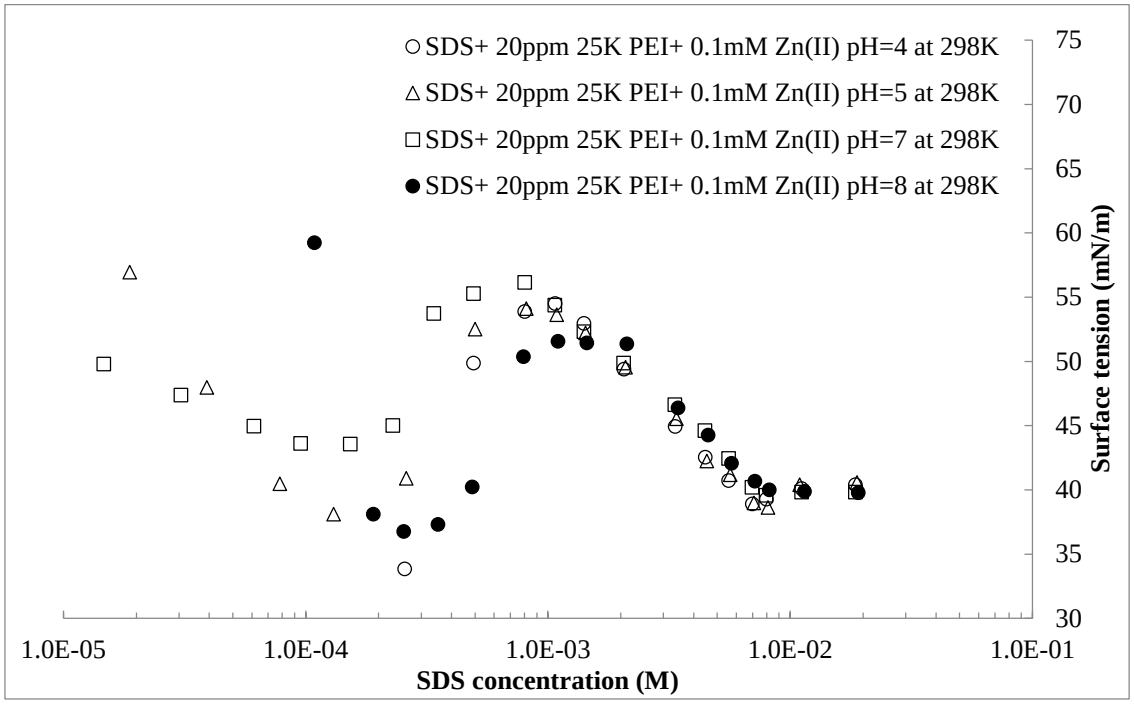

Figure 3.16: Surface tension plots at different SDS concentrations for 20 ppm 25K PEI and 0.1 mM Zn(II) with different pHs.

For different pH values, the overall pattern of surface tension plot remains the same. Generally, the surface activity of complexes increases with a decrease of pH, because the charge density of PEI is higher at a lower pH value (Figure 3.16). However, at a pH of 8, the surface tension is not as expected for a classic weak polymer–surfactant system (non-ionic polymer and surfactant). This unexpected behaviour suggests that the PEI segments are not completely neutralised in a weak basic solution, and can still form PSAs in the bulk solution. The same observation is made in the PEI–SDS system in the absence of Zn(II). In addition, the dip around the CMC is measured at pHs of 4 and 5, but not at pHs of 7 and 8. This means that most of the Zn(II) ions are removed at pHs 7 and 8, but a small amount of Zn(II) ions are still in the solution at pHs of 4 and 5, because the hydrogen ions in the acidic solution compete with the Zn(II) ions and result in a decrease

of binding between PSAs and Zn(II). The removal efficiencies of Zn(II) at different pHs are presented in Chapter 4.

3.3.4.4. Correlation of surface tension with the removal efficiencies of metal ions

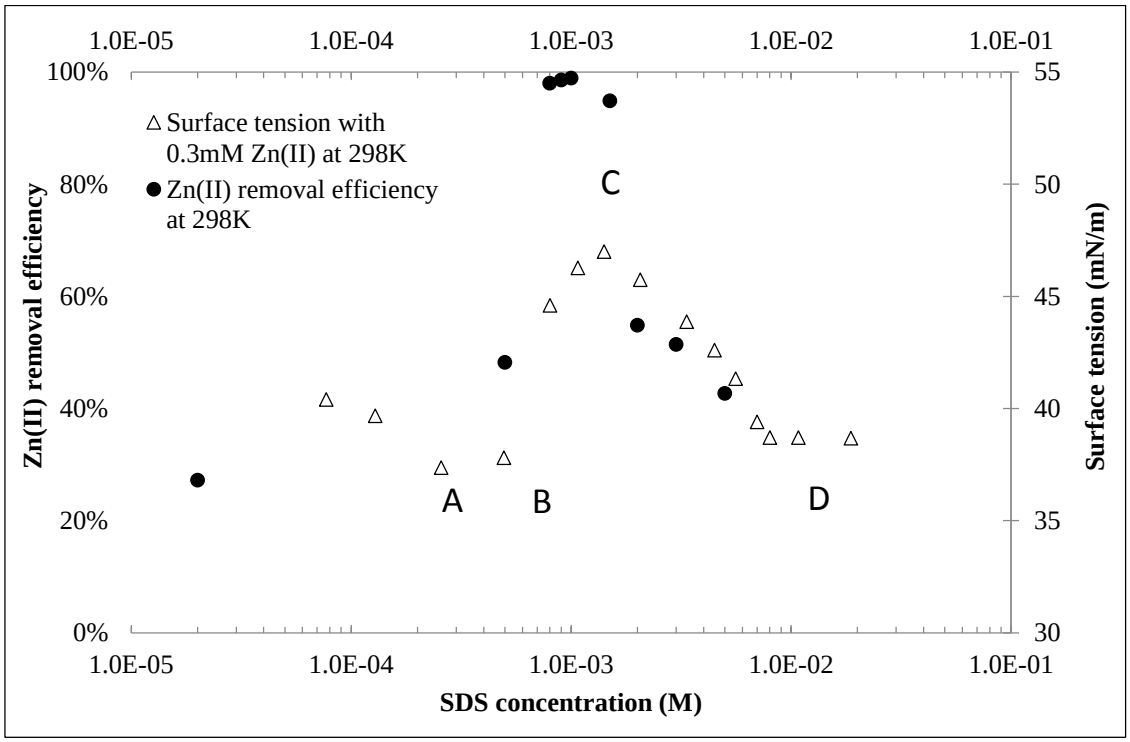

Figure 3.17: Surface tension and Zn(II) removal efficiency at 80 ppm PEI and 19 ppm/0.3 mM Zn(II) and varying SDS concentrations.

To understand the association mechanism of polyDADMAC/PEI, SDS and metal ions, and the effects of heavy metal ions on the surface and bulk interactions between polymer and surfactant, different amounts of PolyDADMAC/PEI, SDS and $ZnSO_4$ were mixed, and the surface tension of the system was measured (Figure 3.12 and Figure *3.17*).

With increasing SDS concentrations from zero to point A (Figure 3.17), the SDS binds to the PEI to form polymer–surfactant complexes at the interface, which lower the surface tension, until the PSAs form around point A. Over this SDS concentration range, 20% of

the Zn(II) is removed via chelation with ammonium groups in the PEI. This removal is in general agreement with the removal by the PEUF (Islamoglu Kadioglu et al., 2009). The plateau in surface tension from A to B indicates that the addition of SDS monomers between these concentrations contributes to the saturation of the bulk polymer to form more PSAs in the solution, and not to interface association.

After the polymer chains within the bulk phase have been saturated, further added SDS associates with the interface polymer–surfactant complexes. The increase in the surface tension is due to the transformation of polymer–surfactant complexes near the interface into PSAs, which then leave the air-liquid interface and are moved into the bulk solution. Thus, at peak C, the bulk solution contains the maximum amount of PSAs that are ever present in the solution.

The aggregates can interact with the free Zn(II) ions, and also to form flocs through intermolecular interactions with each other, because the PSA contains both positive and negative charges and the bound Zn(II) can act as a bridge between two PSAs to enhance the flocculation. Since Zn (II) adsorption is proportional to the number of PSA aggregates within the system, removal efficiency is found to be at a clear maximum (close to 100%) at the SDS concentration corresponding to peak position C (Figure 3.17). The results indicate that the position of the surface tension peak can be used to estimate the optimum dosage of polymer and surfactant for metal removal.

At SDS concentrations higher than the concentration at point C, it is observed that the surface tension once again begins to decline, and the removal efficiency also declines. The reduction of the surface tension is caused by excess SDS monomers migrating to the air-liquid interface, as a result of the polymer backbones becoming saturated and overall charge reverse of PSA. The reduction of the removal efficiency can then be explained by

the increase in the repulsive forces between the PSA aggregates as a result of the repulsive interactions between the electrical double layers. The repulsion between the electrical double layers of the PSAs inhibits the flocculation process; thus, in the tests, small, dispersed PSAs loaded with Zn(II) can pass through a 20 µm coarse filter. After point D, where the CMC is reached, further additional SDS forms micelles (Goddard, 2002). Concentrations of SDS above the CMC are in the MEUF working range, which is 10-20 times higher than the SDS concentrations used to optimise the polymer–surfactant aggregate process. The adsorption capabilities of micelles above the CMC are not the scope of this study.

3.4. Studies of phase diagram

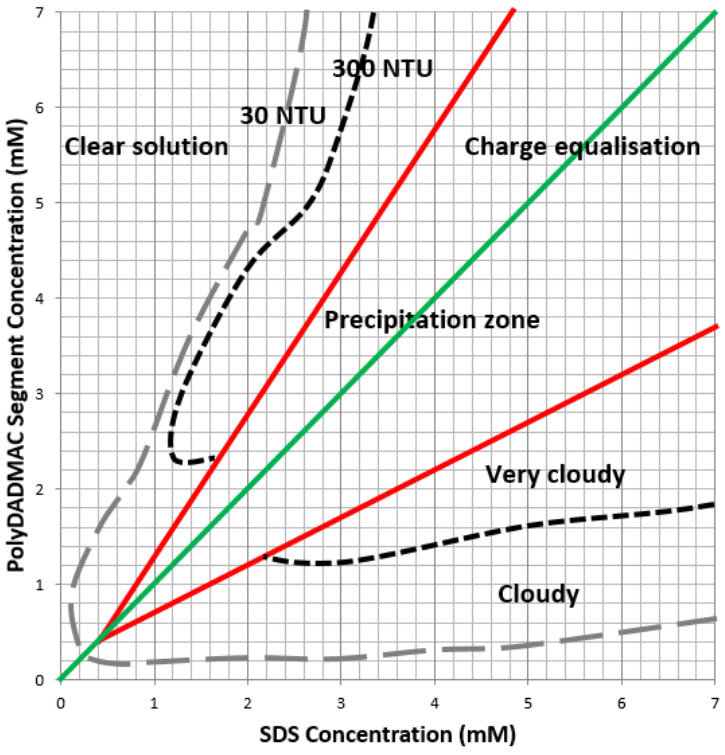

Figure 3.18: Phase diagram for polyDADMAC and SDS in the absence of $ZnSO_4$.

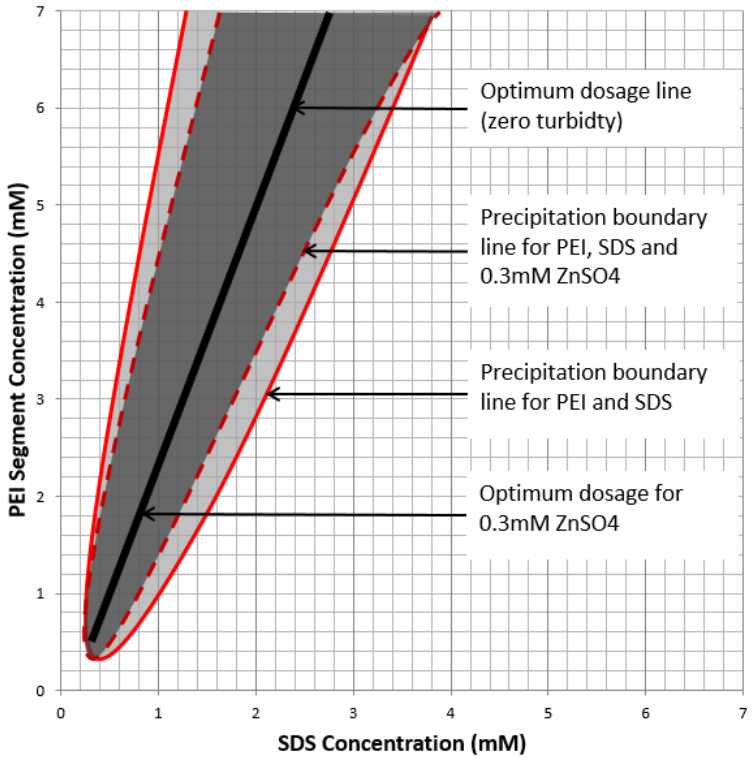

Figure 3.19: Phase diagram for PEI and SDS with $ZnSO_4$ (dark grey area) and without $ZnSO_4$ (light grey area) with the red line as a precipitation boundary (a pH of 7).

The phase behaviour of mixture of polyDADMAC/PEI with SDS have also been studied to understand the bulk interactions between fully or partially charged polymer and surfactant via turbidity changes. In Figure 3.18, the polyDADMAC and SDS completely settle out at the charge equalisation locus (zero turbidity), where the overall charge of SDS monomers are equal to the total number of polyDADMAC segments. It suggests that the polyDADMAC is fully charged at a neutral pH as expected. When the polymer–surfactant ratio is slightly shifted (1:2), the solution still remains transparent and some flocculation settle down at the bottom. When the ratio is moderately shifted (1:3), a colloidal suspension starts to form in the solution because of the formation of colloidal polymer–surfactant complexes and aggregates, and continues to build up until the flocculation zone is reached. Moreover, the turbidity increases with the total dosage of

polymer and surfactant due to the increasing amount of the colloidal structures. At a wide range of high polymer–surfactant ratios (top left of Figure 3.18), the solutions become clear again. Since most of the limited SDS molecules are neutralised, no PSAs form in the solution. The range of clear solution is much narrower at high SDS dosage (bottom right of Figure 3.18), because the limited amount of polymer can still form PSAs, which require a high ionic strength to destabilise the colloidal structures. Therefore, a carefully selected polymer–surfactant dosage ratio is important to effectively form PSAs that will ultimately settle down as flocs.

The phase diagram of PEI and SDS is somewhat different from the polyDADMAC and SDS systems. The optimum dosage line (zero turbidity) does not the follow charge equalisation locus, because the PEI is not completely charged at a pH of 7 (Figure 3.19). In fact, the extent of charge of PEI segments can be estimated from the phase diagram by calculation, which is approximately 40%. The addition of $ZnSO_4$ inhibits the phase separation, but the complete flocculation line does not change, which suggests 0.3 mM $ZnSO_4$ does not alter the optimum dosage. The reason is that the strength of the electrostatic interactions between polymer–surfactant complexes and PSAs are screened in the presence of divalent electrolytes. This screening effect can destabilise the colloidal structures; hence the flocculation zone is narrower. The turbidity zones are not present in this figure.

3.5. Studies of conductivity measurements

3.5.1. PolyDADMAC/PEI and SDS systems

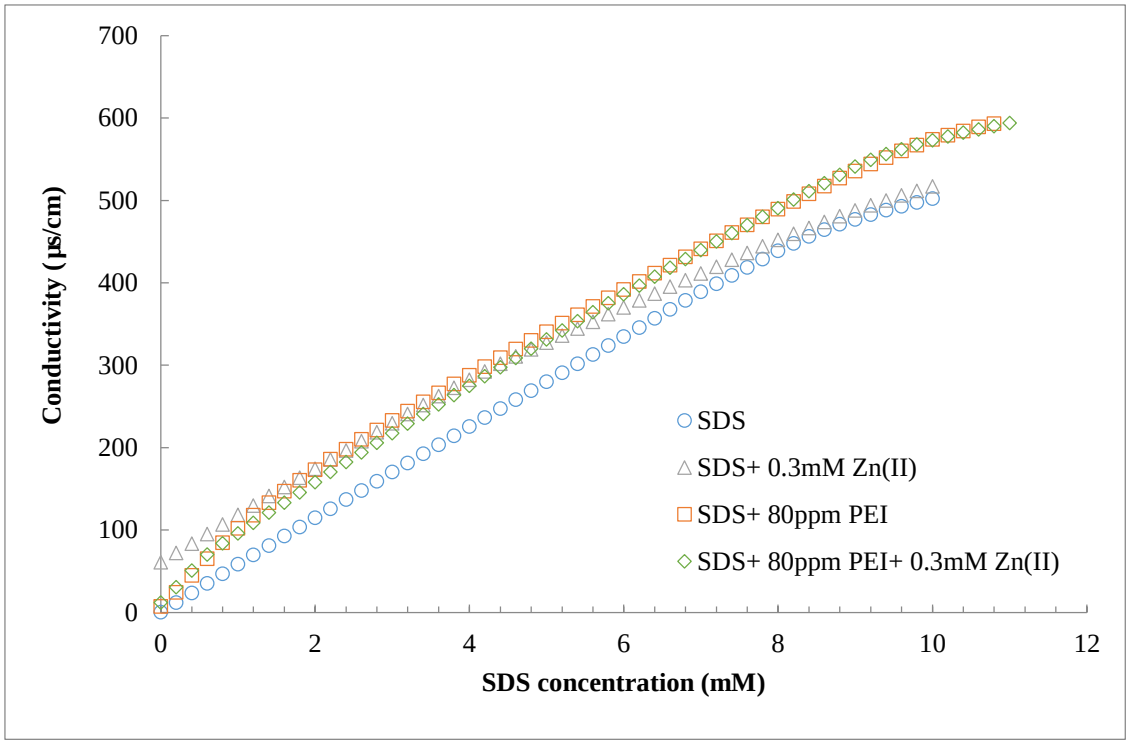

Figure 3.20: Conductivity changes for the SDS system with PEI and $ZnSO_4$.

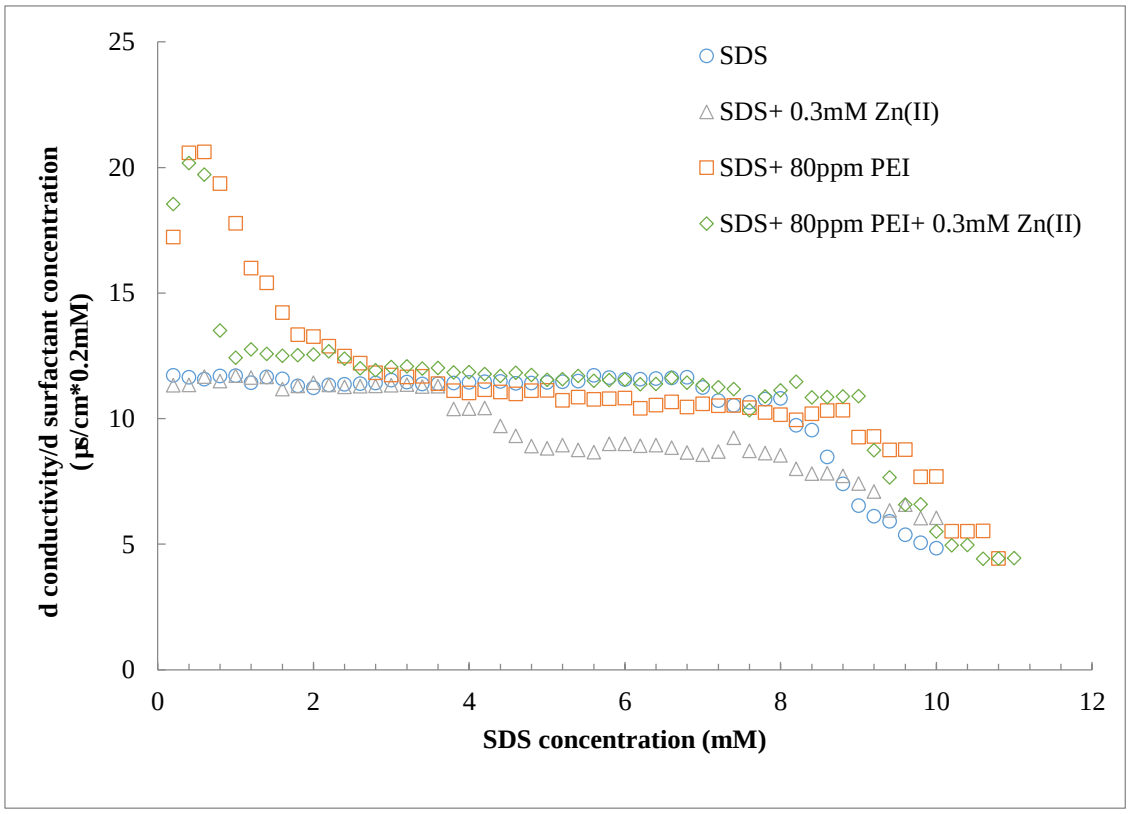

Figure 3.21: Change of increase of conductivity for the SDS system with PEI and $ZnSO_4$.

The electrical conductivity of the PEI–SDS system is studied to investigate the polymer–surfactant interactions in bulk solution directly. The results are initially plotted as conductivity versus SDS concentration, which it is hard to determine the subtle changes in the conductivity (Figure 3.20). Some workers have tried to plot the increasing conductivity as a function of the square root of the concentration (Nizri et al., 2008). In the presented work, the change of increase of conductivity per 0.2 mM SDS increase in concentration is plotted against the SDS concentration. The changes of the change of increase of conductivity represent the increase in the conductivity for that specific increase of 0.2 mM in SDS concentration, which can be used to indicate the formation of PSAs or the protonation of PEI. The detailed changes for each plot in Figure 3.21 are discussed as follows.

SDS plot: Before the CMC, the solution conductivity increases at a constant change of 11.3 ± 0.5 μs/cm with stepwise increases in SDS concentration of 0.2mM. The reason for this increasing conductivity is that the free SDS monomers can disassociate in the solution and conduct electricity. Above the CMC (~8 mM), further addition of SDS forms micelles in the solution which slows down the change of increase of conductivity, because the micelles confer a smaller electrical conductivity per monomer unit than free monomers. The gentle slope after the CMC point represents the transitional phase for the formation of micelle. The reason is that an increasing proportion of the added SDS contributes to form micelles.

SDS+ 0.3 mM $ZnSO_4$ plot: Before the SDS concentration increases to 3.5mM, the change of increase of conductivity is the same as the pure SDS system. After this constant change of increase, the change slows down due to the formation of micelles. This transitional point may be regarded as an estimation of the CMC in the presence of 0.3mM

$ZnSO_4$. A similar finding is made from the surface tension measurements, which suggest that the CMC of SDS in 0.4 mM $ZnSO_4$ is around 3 mM (Figure 3.2). The further gentle decrease in the change of increase of conductivity above may be 7 mM due to the dynamic equilibrium between micelles and monomers and the formation of different shapes and sizes of micelles under the charge screening effects of $ZnSO_4$.

SDS+ 80 ppm PEI plot: The hydrolysis of DS^- may induce the protonation of the amine on the PEI, which leads to both SDS and PEI being charged. Because of this, the change of increase of conductivity is twice as high as the pure SDS system at the same SDS total dosage. As the process of protonation continues, less and less neutral amine sites are available on the PEI, which slows down the change of increase of conductivity until most of the PEI are protonated. During the protonation, the PEI and SDS forms PSAs and start to form flocs, and most of the PE precipitate out of solution around 2.5 mM SDS. Consequently, the changes afterwards in conductivity follow the trend of the pure SDS system, because little PEI remains in the solution.

SDS+ 80 ppm PEI+ 0.3 mM $ZnSO_4$ plot: At a low SDS concentration (< 0.8mM), the SDS induced PEI protonation occurs as in the PEI–SDS system. The degree of protonation is slightly less strong due to the charge screening and chelation effects from $ZnSO_4$. Most importantly, when the concentration of SDS reaches 0.8 mM (the optimum dosage ratio for zinc removal), the flocs form in the solution. Most of the PEI and Zn(II) are in the flocs. Consequently, the behaviour of conductivity onwards follows the pure SDS system. Thus, the transitional point can be regarded as the optimum dosage point in the system. This again confirms that Zn(II) is removed by the PEI–SDS, and most of the PEI and Zn(II) are flocculated.

In conclusion, the electrical conductivity measurement offers another method, like the

surface tension measurements, to estimate the optimum dosage between polymer and surfactant.

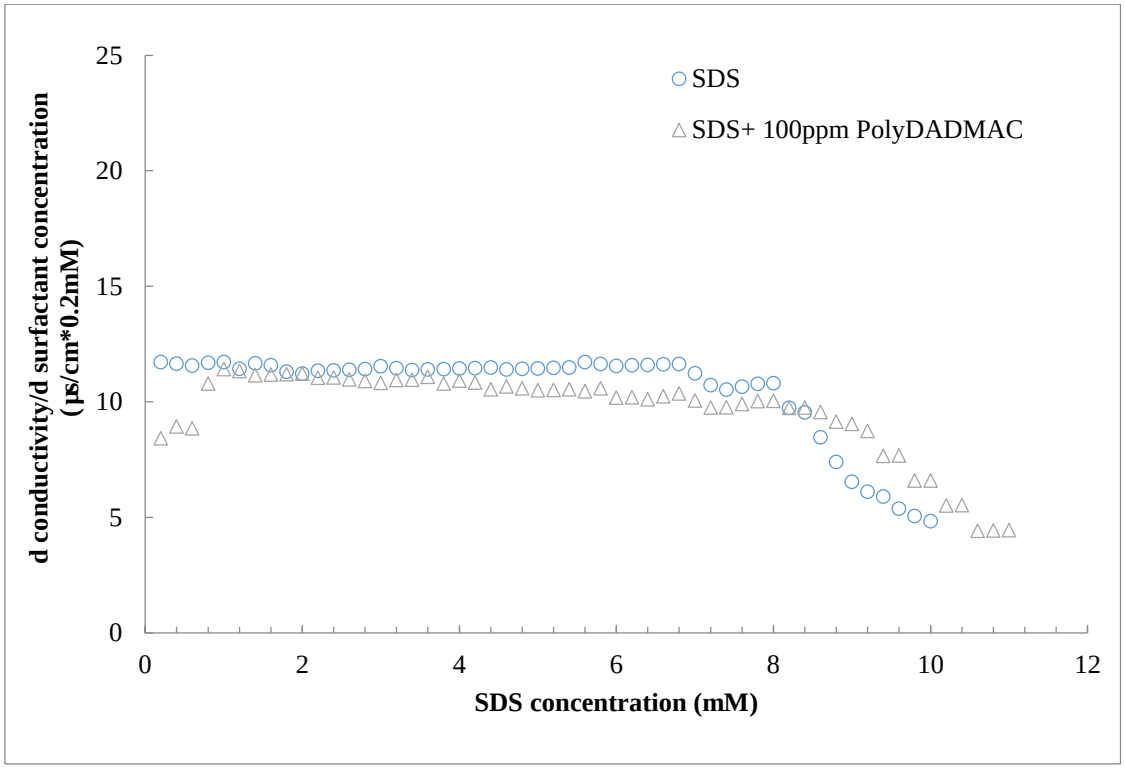

Figure 3.22: Change of increase of conductivity for the SDS system with 100 ppm polyDADMAC.

The polyDADMAC–SDS system behaves quite differently from the PEI–SDS system. The polyDADMAC is a permanently positively charged polymer, which cannot be protonated. For this reason, there is no peak in the change of increase of conductivity (Figure 3.22). The increase of the change of increase of conductivity at the low surfactant dosage may be due to the decreasing availability of positive segments in polyDADMAC to be electrostatically bind to added SDS. Once most of these segments are neutralised, the conductivity trend follows that of the pure SDS system. In addition, the SDS concentration at the transitional point is increased, because the extra SDS is consumed to neutralise the polyDADMAC.

3.5.2. PSS/PAA, MTAB and anion systems

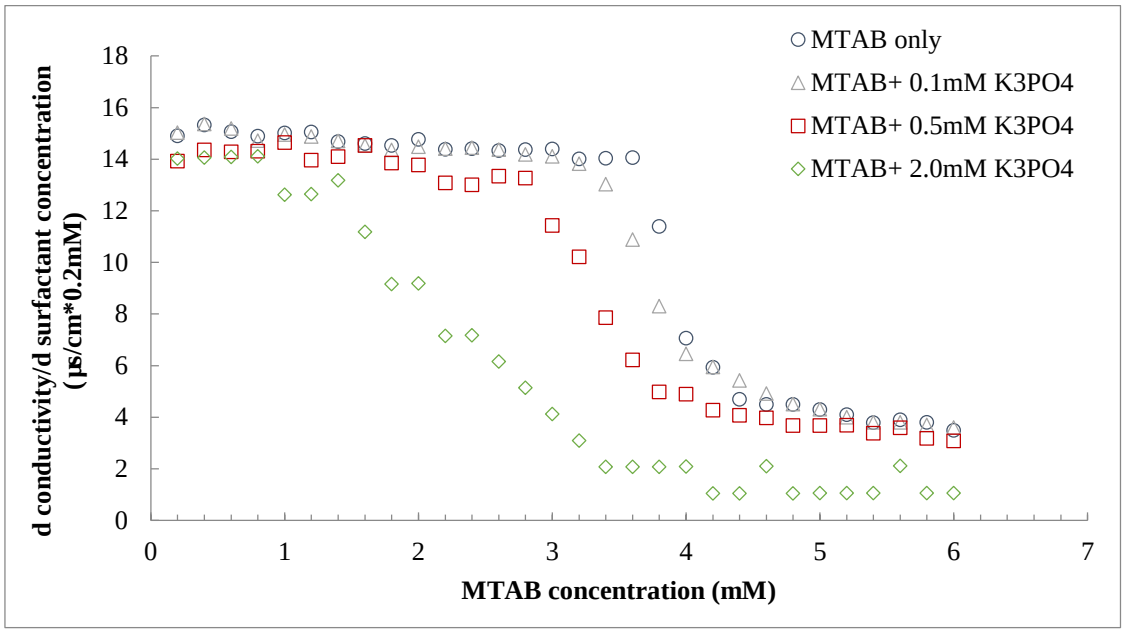

Figure 3.23: Change of increase of conductivity of the MTAB system with addition of different amounts of K_3PO_4.

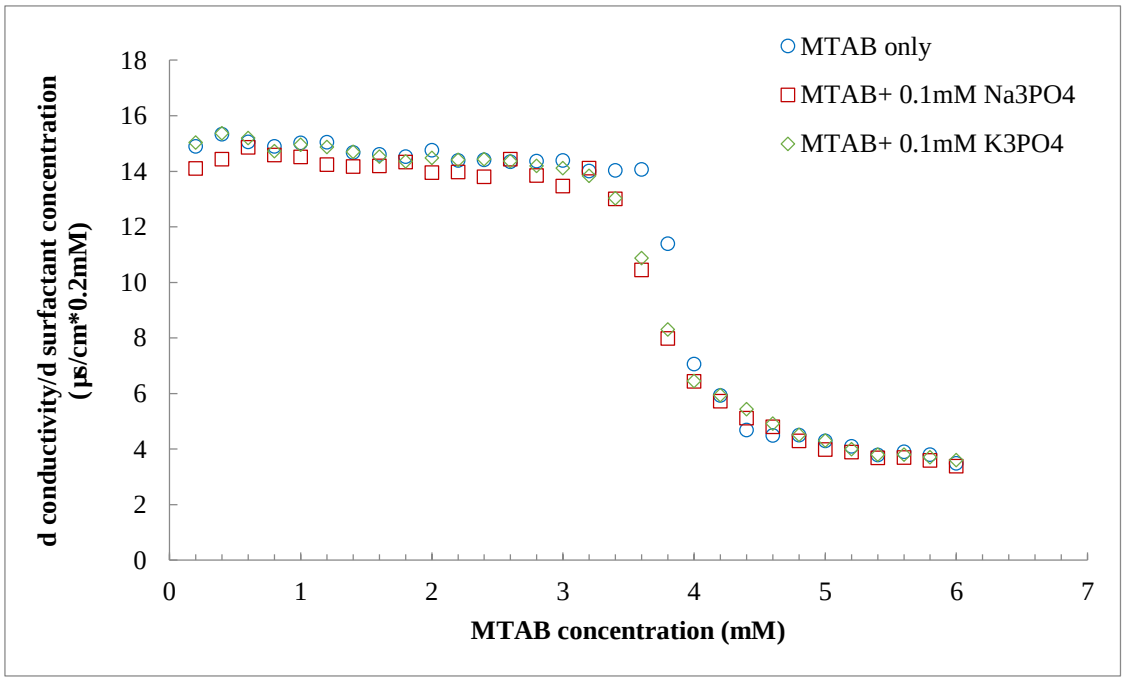

Figure 3.24: Change of increase of conductivity of the MTAB system with addition of 0.1 mM of different counter ions.

In the surfactant literature, the main uses of conductivity are to determine the CMC of a surfactant and by study the effects of additional salt on its CMC. In Figure 3.23, different amounts of K_3PO_4 were added to study its effect on the MTAB system, especially the CMC. The overall trend of conductivity changes is similar to that of the pure MTAB system, but there are three major changes with increasing amounts of K_3PO_4: a slower general change of increase, a lower CMC value and a longer transitional phase.

Firstly, the average change of increase at a higher K_3PO_4 concentration is slightly lower. This is due to the K_3PO_4 screening the charge of the MTAB monomers, which slightly decreases their charge density. The most important and distinct difference with increasing amounts of K_3PO_4 is the reduction of the CMC (falling point). This is due to the repulsive force of the quaternary amine group in the MTAB, which acts against the formation of micelles, being weakened by the screening effect of K_3PO_4. Thus, for a greater amount of K_3PO_4 in the bulk, the micelles are easier to form. The formation of micelles at a lower MTAB concentration is indicated by the decreasing CMC values, but the dynamic equilibrium between monomers and micelles is not significantly affected, so that the tailing off points remain at the same MTAB concentration. Therefore, the transitional phase (from the CMC point to the tailing off point) is prolonged with increasing amounts of K_3PO_4.

Different types of anion addition are carried out to examine the effects of different counter ions (Figure 3.24). The overall trend of K_3PO_4 is almost the same as for Na_3PO_4; hence the counter ions (K^+ and Na^+) have almost the same effect.

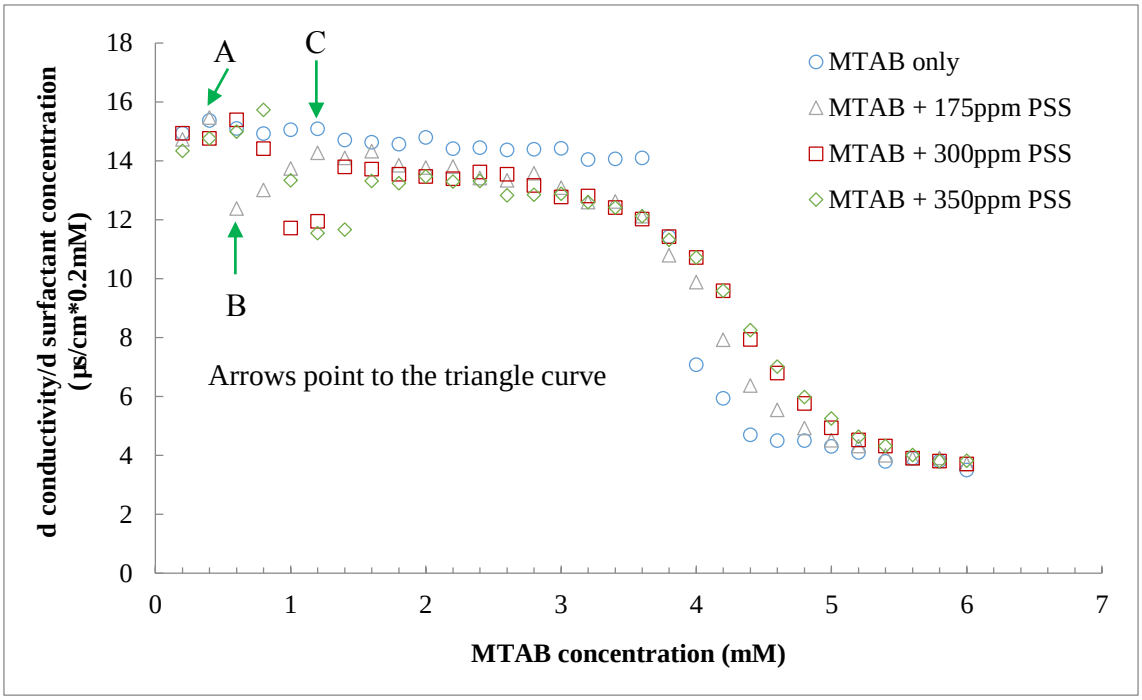

Figure 3.25: Change of increase of conductivity for the MTAB system at different amounts of PSS.

The conductivity of the PSS–MTAB system is studied to investigate directly the polymer–surfactant interactions in bulk solutions. In Figure 3.25, a distinct dip is observed in the plot with the addition of permanently charged polymer PSS. The different amounts of PSS in the MTAB solution do not change the overall pattern of plots, but the position of the salient points in the dip (A: the beginning, B: the bottom and C: the end) is shifted towards higher MTAB concentration with increasing PSS concentration.

Before point A, there is a short region of constant increase of conductivity at the low MTAB concentrations. At such low concentrations, the electrostatic and hydrophobic forces are not strong enough to cause interaction with PSS, so the added MTAB exists in the form of monomers only. Thus, the trend of change of increase of conductivity follows that of the pure MTAB system. Above point A, addition of MTAB forms aggregates on the PSS chains, and consequently the change of increase of conductivity diminishes. The

reason is that the aggregates (mini-micelles) on the PSS have a smaller mobility, charge and electrical conductivity per monomer unit than that of free monomers, which is similar to the slowdown in change of increase of conductivity which occurs after the CMC. The resulting structure is called a PSA. In addition, the transparent solution becomes turbid at point A, which indicates that some colloidal structures (i.e. PSAs) present in the solution. Point A, therefore, can be used to estimate the critical formation concentration (CFC) in the PSS–MTAB system, which is the concentration that PSA starts to quickly form and accumulate in the bulk solution.

The bottom of the dip (point B) represents where the largest proportion of the stepwise added MTAB is used to form the PSAs. Before the change of increase of conductivity returns to a constant level after point C, most of the PSS forms PSAs in the solution which can then bind with anions. Point C is regarded as the optimum dosage ratio between PSS and MTAB to form PSAs, and hence possibly for treating the anion solution. After that, the plots with PSS addition follow the pattern of the pure MTAB plot once again.

In a sense, point A to C represents a process of polymer saturation to form PSAs. It is important to note that all these transitional points occur at higher MTAB concentrations with increasing amounts of PSS because more MTAB is needed to saturate the PSS chain. Moreover, the change of increase of conductivity changes around the CMC (transitional zone) are less abrupt than for the pure MTAB system. The possible explanation for this might be that the dynamic balance between micelles and monomers is disrupted due to PSAs by hydrophobic binding of monomers with flocculated PSAs or with monomers of the PSS. In conclusion, the change of increase of conductivity offers a good method to estimate the status of polymer–surfactant interactions, such as the CFC, the optimum dosage for anion removal and the CMC.

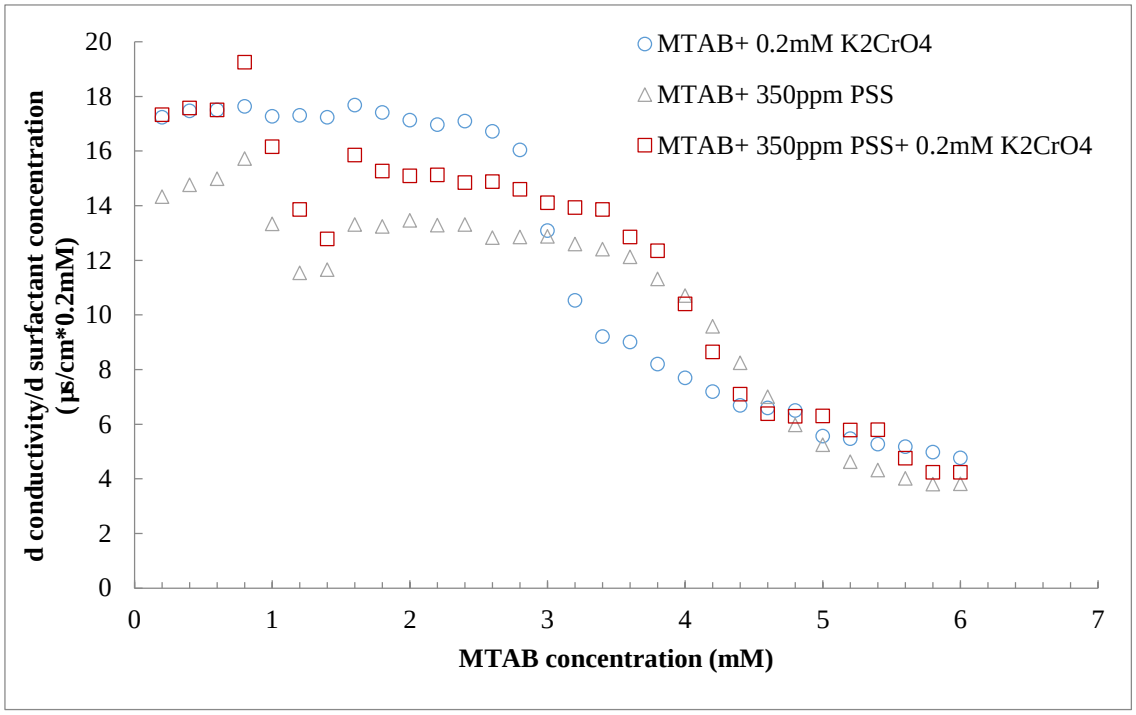

Figure 3.26: Change of increase of conductivity for the MTAB system with 350 ppm PSS at different amounts of K_2CrO_4.

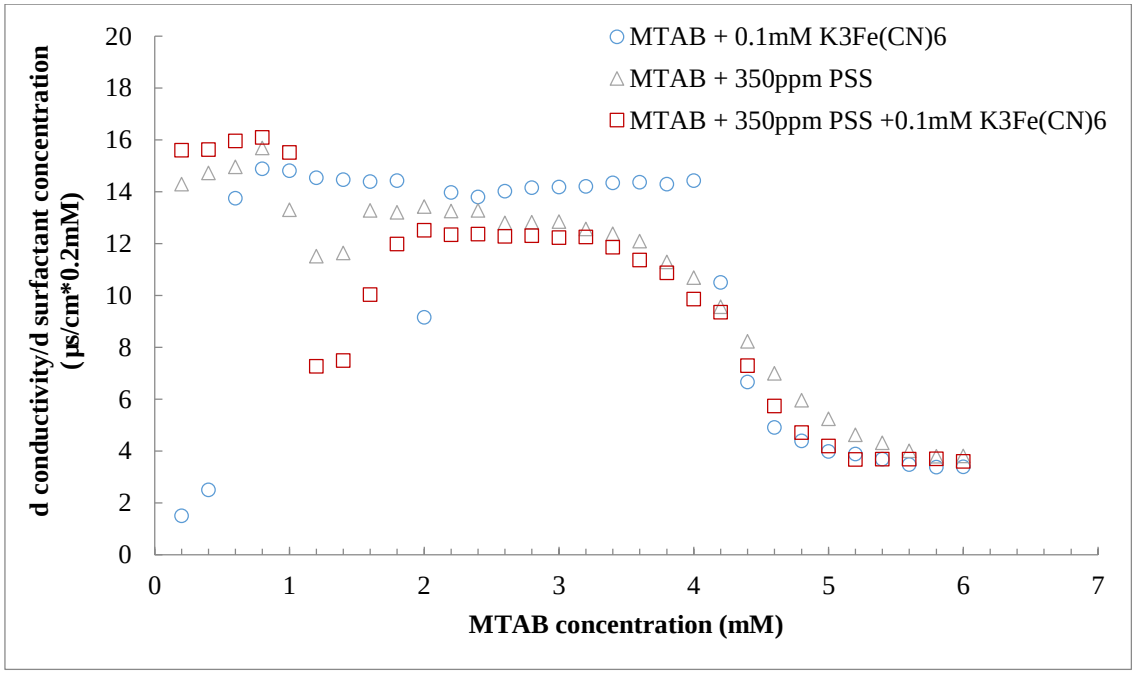

Figure 3.27: Change of increase of conductivity for the MTAB system with 350 ppm PSS at different amounts of $K_3Fe(CN)_6$.

The additions of anions of various valencies into the PSS–MTAB system are studied to understand their effects on the conductivity plots. The overall trend of the change of increase of conductivity does not change in the presence of a small amount of K_2CrO_4 (Figure 3.26) and $K_3Fe(CN)_6$ (Figure 3.27), especially the MTAB concentrations at the transitional points of the dip. The depth of the dip of trivalent is much deeper than that of the divalent. This might be caused by the strong electrical double layer of $Fe(CN)_6^{3-}$ ions decreasing the charge density of PSAs. After the dip, most of the anions and PSS are flocculated, so the trend of conductivity follows the pure MTAB system. The slightly higher change of increase for the K_2CrO_4 is probably due to the fact that room temperature was increased after the winter, and hence a systematic error was generated during the calibration without considering this fact. Thus, in the future, the conductivity measurement will be conducted in a water bath to avoid the effect of temperature shifts on the conductivity readings.

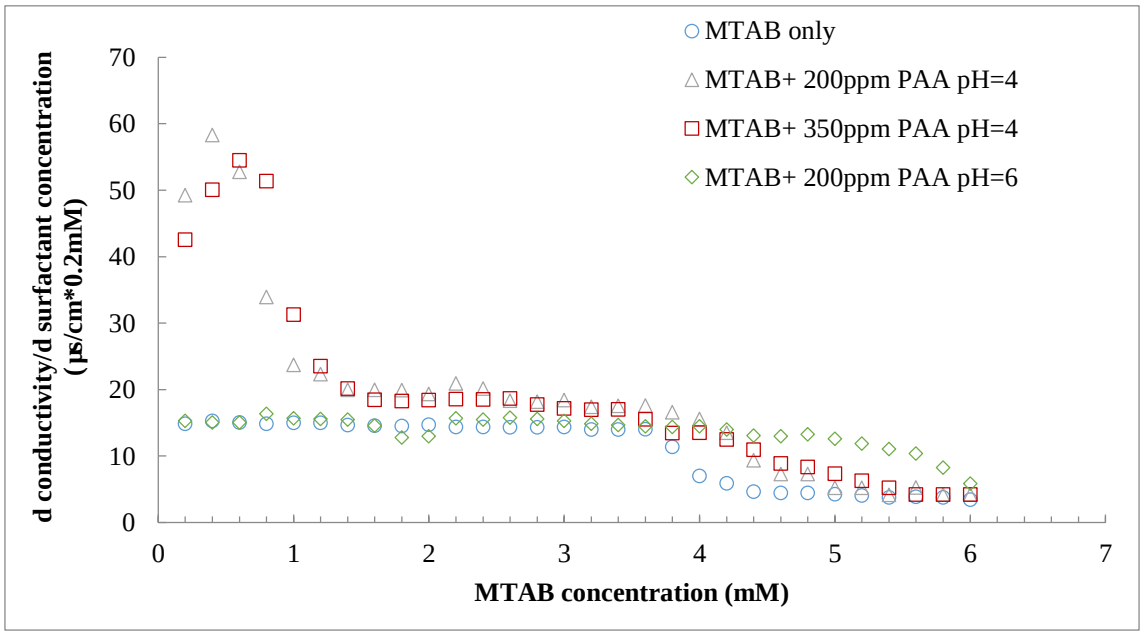

Figure 3.28: Change of increase of conductivity for the MTAB system with different amounts of PAA at different pH values.

Apart from studying the permanently charged polymer PSS, the weakly acidic polymer PAA is also investigated. The rationale for investigating the PAA is to explore the effects of the polymer charge density on the formation of PSAs and their treatment performance, because PSAs containing a pH-sensitive polymer such as PAA and monomer MTAB may be recycled by manipulating their charge density via pH. Figure 3.28 shows the effects of different amounts of PAA at different pH values on the interactions of PAA and MTAB.

The PAA is a weak acid, and the pH of the solution will decrease with increasing concentration of PAA if the pH is not adjusted. To evaluate the pH effects on the interactions, both adjusted and unadjusted samples are studied by conductivity measurements. Comparing the unadjusted 200 ppm and 350 ppm PAA plots (at a pH of 4), both of them have a high change of increase of conductivity at the beginning of the addition of MTAB (Figure 3.28). The reason for this is that the addition of MTAB induces the disassociation of PAA. Below the MTAB concentration at the peak, a portion of the addition of MTAB contributes to reach CFC and the other to promote the disassociation of PAA. With further addition of MTAB, the turbidity and flocculation are observed at the peak. After the peak, less and less PAA remains protonated and some of the PA^- forms flocs which is less conductive than the free PA^-, so that the change of increase diminishes. Eventually, all of the PA^- ions are either in PSAs or flocs.

Apart from the notable peak, no dip is measured in the pH unadjusted PAA–MTAB system. The possible explanation is that the appearance of a dip is due to the binding of MTAB to PAA and the formation of PSAs, and the relatively subtle associated changes in conductivity are offset by the rapid increase of the conductivity. To confirm this explanation, the pH of the solution is adjusted to 6 to dissociate the majority of PAA (pKa=4.2). As expected, the peak disappears after the pH adjustment, and the dip is

measured. This may seem less obvious in Figure 3.28, because the scale of the Y axis is more than 3 times larger than in Figure 3.30 or Figure 3.29. In short, the disassociation of PAA is induced by MTAB and the two can form PSAs, and the extent of disassociation can be manipulated by pH.

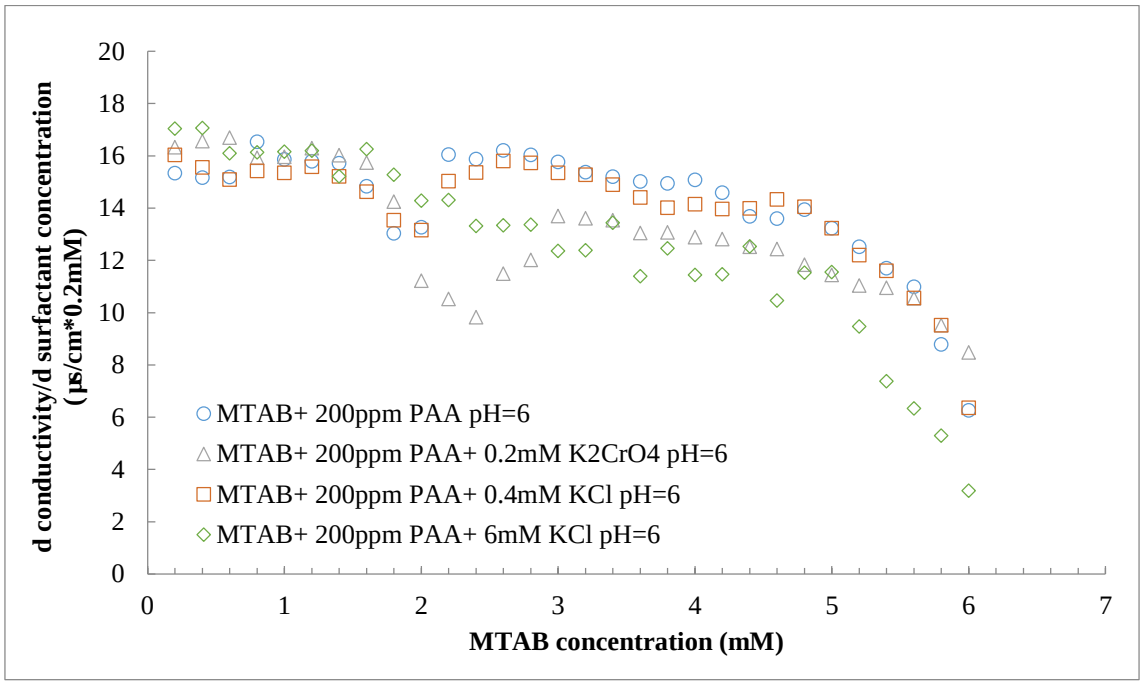

Figure 3.29: Change of increase of conductivity for the MTAB system with 200 ppm PAA at a pH of 6 with different amounts of K_2CrO_4 or KCl.

With regard to the pH adjusted PAA–MTAB system, the effects of CrO_4^{2-} and Cl^- are studied in Figure 3.29. The purposes of testing 0.4 mM and 6mM KCl are to investigate the effects of the ionic strength on the position and depth of the dip. The results suggest that the position of dip is independent with the ionic strength, because the initial drop for the 0.2 mM chromate plot is at the same MTAB concentration for the 0.4 mM and 6mM KCl (Figure 3.29). The increasing depth of the dip is affected by the charge density of ions rather than the ionic strength. In the presence of $Fe(CN)_6^{3-}$, a deep dip is found in Figure 3.30, and a shallow depth in the KCl addition and a moderate one in the chromate

addition in Figure 3.29.

In conclusion, the change of increase of conductivity can reveal more detailed information about the bulk interactions between polymer, surfactant and ions, such as the CFC, the optimum dosage and the CMC. It also demonstrates that the removal of anions is due to the PSAs, and establishes the foundation for studying the dosage optimisation, robustness and removal selectivity of anions.

3.5.3. Correlations with the removal efficiency of metallic anions

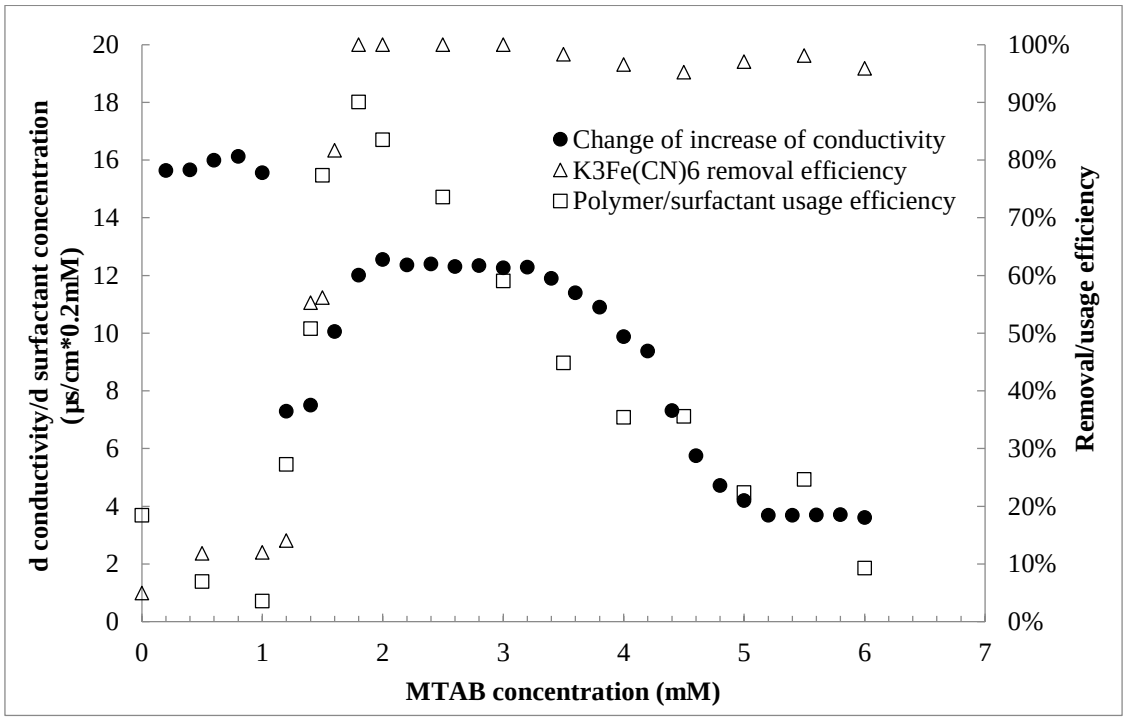

Figure 3.30: Change of increase of conductivity and $Fe(CN)_6^{3-}$ removal and removal agent usage efficiencies at 300 ppm PSS, 0.1 mM $Fe(CN)_6^{3-}$ and varying MTAB concentrations.

To confirm the interpretation of the change of increase of conductivity, the results are plotted against removal efficiency and removal agent usage efficiency (Figure 3.30). The removal and polymer surfactant usage efficiencies start to increase rapidly at the first

falling point in the conductivity change plot, which is the equivalent to point A in Figure 3.25. With the formation of PSAs after 1 mM MTAB, the efficiencies increase towards the highest level, which is at the transitional point to the second plateau of conductivity change (equivalent to point C in Figure 3.25). This confirms that the optimum dosage can be estimated by conductivity measurements. After the optimum dosage, the removal efficiency remains at a high level, but the removal agent usage efficiency starts to decrease, because the polymer chains are saturated and most of the additional monomeric MTAB passes directly through the filter to the filtrate. The removal agent usage efficiency continues to decrease after the second falling point (CMC), because the pore size of the filter is much bigger than the size of the micelles, so that the micelles can also pass through into the filtrate.

3.6. Discussion and conclusions

The studies of the surface tension, the phase diagram and the electrical conductivity measurements have enhanced the understanding of interactions between the oppositely charged polymers and surfactants in the presence of metallic ions. Various amounts of different molecular weight polymers and metallic ions are investigated at different pHs to reveal their effects on the interactions. Most importantly, the results from both surface tension and conductivity measurements via correlation with the ion removal efficiency suggest that the PSAs are the functional structures responsible for removing the metallic ions. Moreover, the CFC, the optimum dosage and the CMC of the polymer–surfactant systems can be estimated from surface tension and conductivity measurements, and the results show a good agreement. For example, in the PEI–SDS system, both measurements

suggest the optimum dosage for 80 ppm PEI is about 1 mM SDS. In the later studies, the optimum dosage for 80 ppm PEI is confirmed to be 0.8 mM SDS (Figure 4.5), which is close to the estimates of both measurements. It is worth noting that a surface tension measurement may take at least 8 hours to complete, while a conductivity measurement takes less than 2 hours, showing the latter has the potential to be widely applied as a fast and low capital cost method to estimate the optimum dosage for polymer and surfactant.

Apart from studying the polymer–surfactant interactions, the phase behaviour of polymer and surfactant and the effects of adding heavy metal ions on the phase diagram should also be highlighted. The results of phase diagram studies show that there is a fine balance between the dosage of polymer and that of surfactant to achieve a transparent solution as the final product. In addition, it also provides valuable information about the optimum ratios between polymer and surfactant to treat various concentrations of heavy metal ions. The main drawback, however, is the time taken; it takes days, if not weeks, to complete a phase diagram. In the later removal experiments, the optimum dosage between polymer and surfactant will be studied in more detail based on the removal and polymer–surfactant usage efficiencies.

In conclusion, in the surface tension measurements, two transitional points (the dip and the peak) can reveal the interaction status of polymer and surfactant. The dip in both surfactant and polymer–surfactant systems is caused by the addition of multivalent ions. The depth of dip can reveal the adsorption capacity of PSAs in the polymer and surfactant system. The surfactant concentration at the peak is regarded as the optimum dosage ratio to form PSAs. In the phase diagrams, the complete flocculation occurs around the charge equalisation locus. Outside the locus, there is a turbidity zone, which can be narrowed in the presence of divalent electrolytes that destabilising the colloidal structure. In the

conductivity measurements, plotting the conductivity as change of increase of conductivity verse surfactant concentrations can clearly reveal a dip. The first falling point of the dip is regarded as the CFC and the transition plateau point is regarded as the optimum dosage ratio to form PSAs. Both surface tension and conductivity measurements containing these transitional points can correlate with the removal efficiency of metallic ions. This confirms the interaction status of polymer and surfactant and the optimum dosage ratio to form PSAs. All three methods have established a foundation for obtaining a clear picture about the interactions between polymer, surfactant and metal ions, both at the interface and in the bulk.

Chapter 4

Investigation of the Removal of Metal Cations from Dilute Aqueous Solutions using Polymer–Surfactant Aggregates

4.1. Introduction

Heavy metals, such as zinc, cadmium, and chromium, are included on the EPA list of priority pollutants (El-Abbassi et al., 2011). These ions tend to accumulate in organisms, causing numerous diseases and disorders (Kim et al., 2006). In wastewater treatment, processes for metal-contaminated water have received much interest in recent years in order to comply with stringent regulations (Kurniawan et al., 2006). Due to the requirement of discharge concentrations for heavy metal ions to be at ppb levels, dilute heavy metal ion removal processes, such as chemical precipitation (Charerntanyarak, 1999; El-Samrani et al., 2008), ion exchange (Alyüz and Veli, 2009), adsorption (Saiano, 2005), biosorption (Ajjabi and Chouba, 2009) and membrane filtration (Hafiane et al.,

2000; Hankins et al., 2005, Hankins et al., 2006), have been widely researched. Specifically, the uses of surfactant and polymer systems have each been individually investigated for their abilities to remove heavy metal ions from aqueous solutions with the aid of ultrafiltration (Cañizares et al., 2008, Fillipi et al., 1999).

Micellar or polymer enhanced ultrafiltration, which individually use surfactant or polymer, can achieve a high removal efficiency in dilute solutions. However, the chemical dosage, energy consumption, and membrane cost remain as challenges (Fu and Wang, 2011). No previous research has tested polymer surfactant aggregates (PSAs) to remove metal ions from aqueous solutions. Instead of using micelles to bind metal ions, the mini micelle–like aggregates in the PSAs are used to bind the metal ions. The PSAs start to form at the CAC which is a few orders of magnitude lower in concentration than the CMC. The removal, therefore, can be achieved with much less surfactant and a small amount of polymer addition. Another important characteristic of this strong polymer/surfactant system is the phase behaviour in the bulk solution. A flocculation zone occurs under the mixing of polymer and surfactant in the correct stoichiometric ratio. The overall charge of the PSAs is neutral, leading to hydrophobic structures which are then flocculated. In addition, a turbidity zone occurs at a wider range of dosage ratios between polymer and surfactant, because the induced repulsions of electrostatic double layers present on the PSAs allows for them to act as a dispersed phase, i.e. a stable colloidal system (Voisin and Vincent, 2003). This flocculating characteristic means that the process has the potential to obviate the need for an ultrafiltration membrane to separate metal ion loaded PSAs from solution. The formation of large, visible flocs due to intra-molecular interactions allows them to be settled out or coarse filtered. Therefore, as a PSA–based process is proposed to effectively remove dilute metal ions from solution using low

chemical dosage and no membrane.

In this chapter, the filtration method is modified, and the optimum dosages for each metal ion and their mixtures are determined. The adsorption limits and kinetics as a function of dosages of polymer, surfactant and metal ions are investigated. The pH, salt, organic contaminants and residence time effects on the metal removal efficiency were also investigated. Finally, the removal efficiency was compared with that from micellar enhanced ultrafiltration (MEUF) and polymer enhanced ultrafiltration (PEUF), being the two most similar processes, under the same conditions.

4.2. Experimental techniques

4.2.1 Modification of filtration method

4.2.1.1 Modified filtration setup

The energy usage in membrane filtration increases with decrease in membrane pore size. From reverse osmosis to nano-filtration then to ultra-filtration (UF), the pore size of membrane increases, which leads to an increase in the particle size in the permeate, but the energy demand, filtration time, manufacturing cost and fouling tendency are decreased. If there is a method to increase the size of targeted species, the incentive of using relatively large pore size membrane will be much greater, maybe even obviating the need for a membrane.

The PSAs are used to increase the overall size of metal ions in order to reduce the requirement of pore size of membrane. The UF was tested first to study the effects of membrane pore size on the PSA-based process. After that, the metal removal efficiencies

via micro-filtration (MF), and subsequently coarse-filtration (CF) are compared with that of UF, and treatment performance remains almost the same under the optimum dosage.

A new filtration procedure, therefore, is developed. The procedure uses the same Millipore model 8050 dead-end filtration cell, but without the pressure addition. The feed passes through a 20µm filter under gravity, such that solutes larger than the filter pore size are retained in the cell, while water and solutes smaller than the pore size pass into the filtrate. The purpose is to separate polymer–surfactant flocs with bound metal ions from the solution containing free metal ions, surfactant monomers and free polymers. For time series experiments, the solution is filtered at each time point to study the kinetics of the metal ion adsorption process.

4.2.1.2. Effects of different pore sizes of membrane/filter

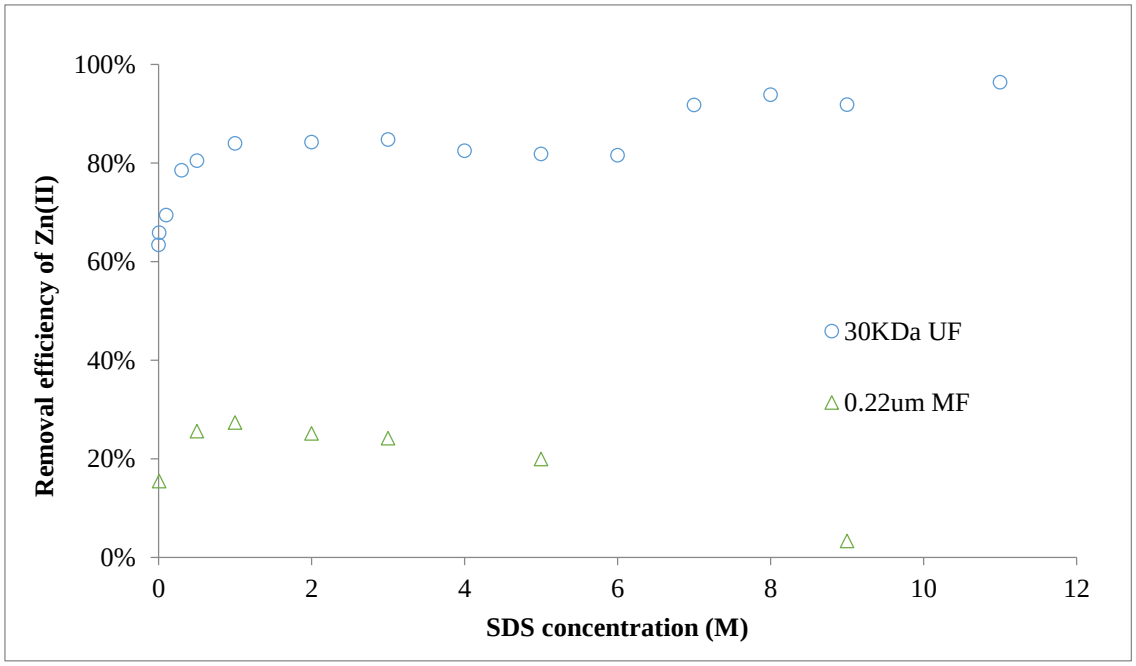

Figure 4.1: Removal efficiency of Zn(II) for MF and UF as a function of SDS concentrations at 20 ppm PEI and 7 ppm Zn(II).

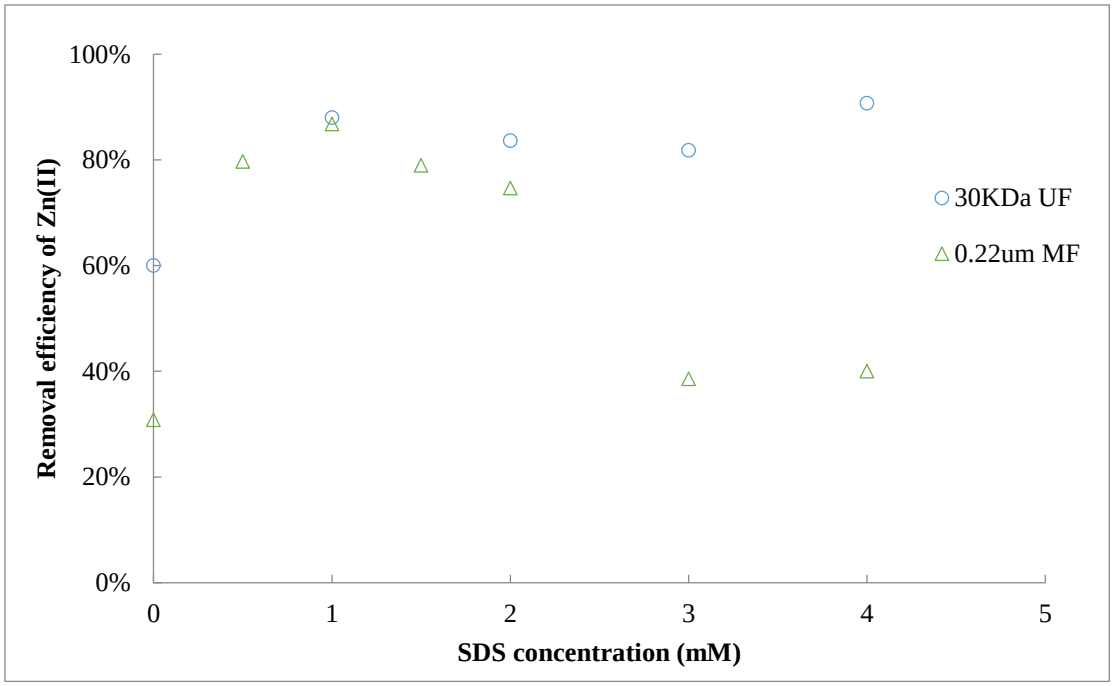

Figure 4.2: Removal efficiency of Zn(II) for MF and UF as a function of SDS concentrations at 60 ppm PEI and 21 ppm Zn(II).

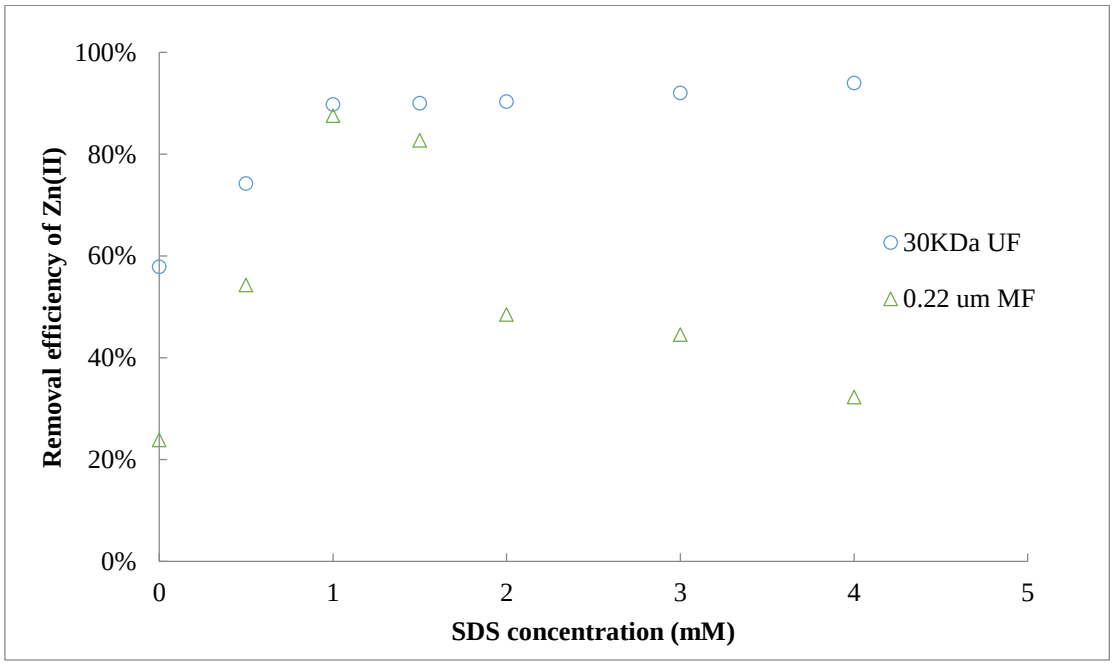

Figure 4.3: Removal efficiency of Zn(II) for MF and UF as a function of SDS concentrations at 80 ppm PEI and 28 ppm Zn(II).

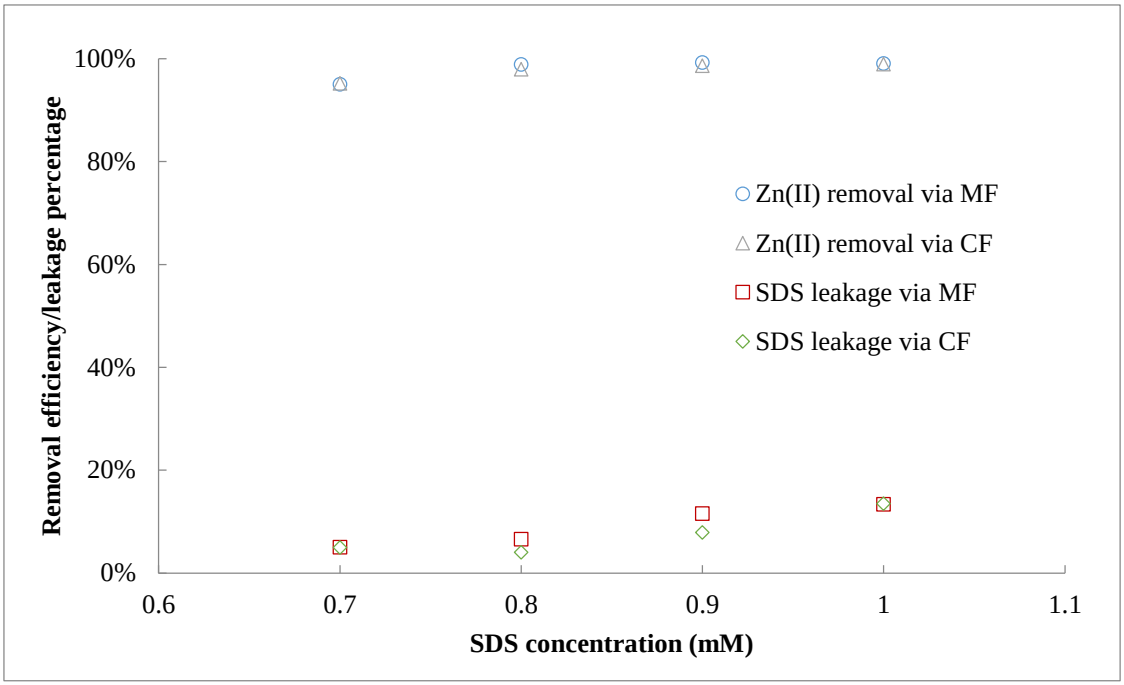

Figure 4.4: Removal efficiency of Zn(II) for CF and MF as a function of SDS concentrations at 80 ppm PEI and 21 ppm Zn(II).

The removal efficiency of Zn(II) after UF (30KDa, approximately 5nm) and MF (0.22 μm) are compared at the same dosage of polymer–surfactant–Zn(II). At a low dosage (20 ppm PEI), the removal efficiency after UF is higher than that after MF, because the concentration of PSAs in the bulk solution is not high enough to form larger size of flocs via intra-molecular interactions (Figure 4.1). At 60ppm and 80ppm PEI, however, the removal efficiencies after UF and MF are almost the same under the optimum dosages (Figure 4.2 and Figure 4.3). This indicates that it is achievable to substitute the UF membrane with the MF.

To further reduce the pore size, the results of removal efficiency after CF (20 μm) is compared with the MF (0.22 μm) in Figure 4.4. No obvious difference is found in the efficiencies of Zn(II) removal and polymer-surfactant usage. The results suggest that the majority of the size of flocculated PSAs is larger than the pore size of MF (0.22 μm),

even larger than that of CF (20 μm). Thus, in the thesis, the CF is used as the filtration method, as a method to accelerate the gravity settling as a separation process between flocs and treated solution.

4.2.2. Rate of mixing and shear rate

In a sense, the process using polymer surfactant aggregates is a coagulation and flocculation process. Thus, the shear rate is an important variable to determine the mixing and energy consumption. In this thesis, for the constant power input, the agitation speed is around 200 revolution per minute (rpm).

$$P = P_0 \rho N^3 D^5 \tag{4.1}$$

Equation 4.1: Calculation of the power input of mixing.

$$\gamma = \sqrt{\frac{P}{V\mu}} \tag{4.2}$$

Equation 4.2: Calculation of shear rate of mixing.

Where P is the power input, P_0 is the coefficient of impeller shape = 1, ρ is the density of solution = 1000 kg/m^3, N is the agitation speed = 3.3 revolution per second, D is the impeller diameter = 0.05 m, V is the volume of solution = 1.5-3*10^{-4} m^3, μ is the viscosity of solution = 10^{-3} kg/sm and γ is the shear rate in kg/ms^2. Using these estimated data, the calculated shear rate using equation 4.1 and 4.2 is about 200-300 per second, which depends on the volume of the solution. This is in the region of rapid mixing. Ideally, to minimise the power input, the mixing process should start with a few minutes of rapid mixing to enhance the coagulation, and then applying a slow mixing to enhance the flocculation.

4.2.3 Two–phase mixed indicator titration

The two phase mixed indicator titration was used to measure the SDS concentration in the solution through the calculation in Equation 4.3. To perform the titration, 6ml of filtrate sample was taken and diluted to 25 ml by deionized water. 9-10 ml chloroform was poured into each beaker in the fume cupboard. 0.4 ml dimidium bromide/disulphine blue solution was added into the solution as a colour indicator while stirring vigorously with a magnetic stir bar; 4 mM hyamine 1622, acting as a titrant, was slowly added to the solution by a 20 μl pipette until the bottom phase (chloroform phase) turned from pink to blue. The filtrate concentration of SDS was calculated from the volume and concentration of hyamine 1622 (a cationic surfactant) used. For some low SDS concentration samples, the dilution step was eliminated to obtain more accurate results. The reproducibility of this titration is 3%.

$$C_{\text{SDS filtrate}}\,(\text{mM}) = \frac{C_{\text{hyamine}} \times V_{\text{hyamine}}}{V_{\text{before dilution}}} = \frac{4\text{mM} \times V_{\text{hyamine}}(\text{ml})}{6\ \text{ml}} \qquad (4.3)$$

Equation 4.3: Calculation of SDS concentration.

4.2.4. Total organic carbon analyser and atomic absorption spectroscopy

The total carbon values of solutions were measured by a total organic carbon analyser (TOC–VCPH, Shimadzu) to reveal the degree of flocculation and de-flocculation (regenerate), because the only two carbon sources in the solution are PEI and SDS. A small amounts of total carbon in the filtrate indicates that most of the PEI and SDS formed flocs and were retained in the retentate. Having the knowledge of the SDS concentration from titration, the PEI concentration weight concentration was calculated from the total carbon minus the carbon associated with the SDS, and then divided by the carbon

molecular weight by percentage of the total for PEI (Equation 4.4).

$$C_{\text{PEI filtrate}}(\text{ppm}) = \frac{\text{Total carbon}_{\text{filtrate}} - C_{\text{SDS filtrate}} * \text{Carbon content}_{\text{SDS}}}{\text{Carbon Molecular weight by percentage}_{\text{PEI}}} =$$

$$\frac{\text{Total carbon}_{\text{filtrate}}(\text{ppm}) - C_{\text{SDS filtrate}}(\text{mM}) * 144\text{g/mol}}{0.326} \quad (4.4)$$

Equation 4.4: Calculation of PEI concentration.

The concentrations of different metal ions were analysed by an atomic adsorption spectrometer (200 Series AA, Agilent Technologies). Some interferences from polymer and surfactant have been found in the measurements of Zn(II), Cd(II) and Cr(III). An interference mitigation method, acidifying the samples and standards, was developed to obtain accurate results of the concentration of metal ions.

Assuming the volume of solution before and after treatment is consistent, the polymer–surfactant usage efficiency and anion removal efficiency are defined by Equation 4.5.

$$\text{Polymer– surfactant usage efficiency } = (1 - \frac{\text{Total carbon}_{\text{filtrate}}}{\text{Total carbon}_{\text{original}}}) \times 100\%$$

$$\text{Metal removal efficiency } = (1 - \frac{C_{\text{filtrate}}}{C_{\text{original}}}) \times 100\% \quad (4.5)$$

Equation 4.5: Calculations of polymer–surfactant usage and metal removal efficiency.

4.3. Variables in the removal of metal ions by PolyDADMAC/PEI and SDS

4.3.1 Polymer and surfactant dosages and ratio

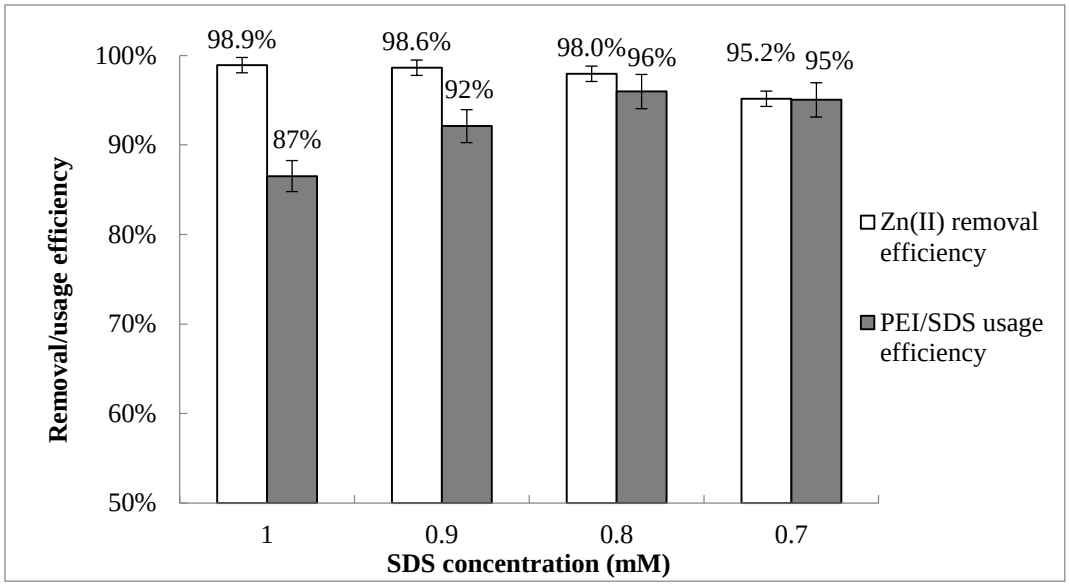

Figure 4.5: Optimisation of the dosage of 80 ppm PEI and varying concentrations of SDS to remove 19 ppm Zn(II).

The surface tension and electrical conductivity measurements have revealed an estimated optimum dosage between PEI and SDS. In Figure 4.5, the removal and PEI–SDS usage efficiencies are directly measured to identify the optimum dosage between PEI, SDS and Zn(II) for the later experiments. At 80 ppm PEI and 19 ppm Zn(II), with increasing SDS concentration from 0.7 mM to 1mM, the removal efficiency increases, but the PEI–SDS usage efficiency decreases. The reason is that part of the increased amount of SDS are formed more PSAs that can remove the metal ions, and the rest of SDS reports in the filtrate. The 80 ppm PEI and 0.8 mM SDS is selected as the optimum dosage for 19 ppm Zn(II) (0.3 mM), considering the balance between the removal and removal agent usage efficiencies. If the leakage of removal agent is relatively high, their concentrations in the filtrate will be higher, which can be regarded as contaminants. In this case, the process uses two contaminants (PEI and SDS) to replace another contaminants, such as Zn(II). The polymer–surfactant usage efficiency, therefore, is as important as the removal efficiency.

The optimum dosages for each metal ions are also studied and listed in Table 4.1. From all three individual optimum dosages for metal ions, 20 ppm PEI are needed to effectively remove each 0.1 mM metal ion, and the SDS concentration is about the valence of the metal ion times its concentration, and then plus 0.1-0.3 mM.

Table 4.1: Optimum dosages for removing metal ions using PSAs.

Metal ion	Ion concentration (mM)	PEI (ppm)	SDS (mM)	Removal efficiency %
Zn(II)	0.3	80	0.8	98+
Cr(III)	0.2	60	0.7	99+
Cd(II)	0.1	40	0.5	99+
Rh(III)	0.2	60	0.7	99+

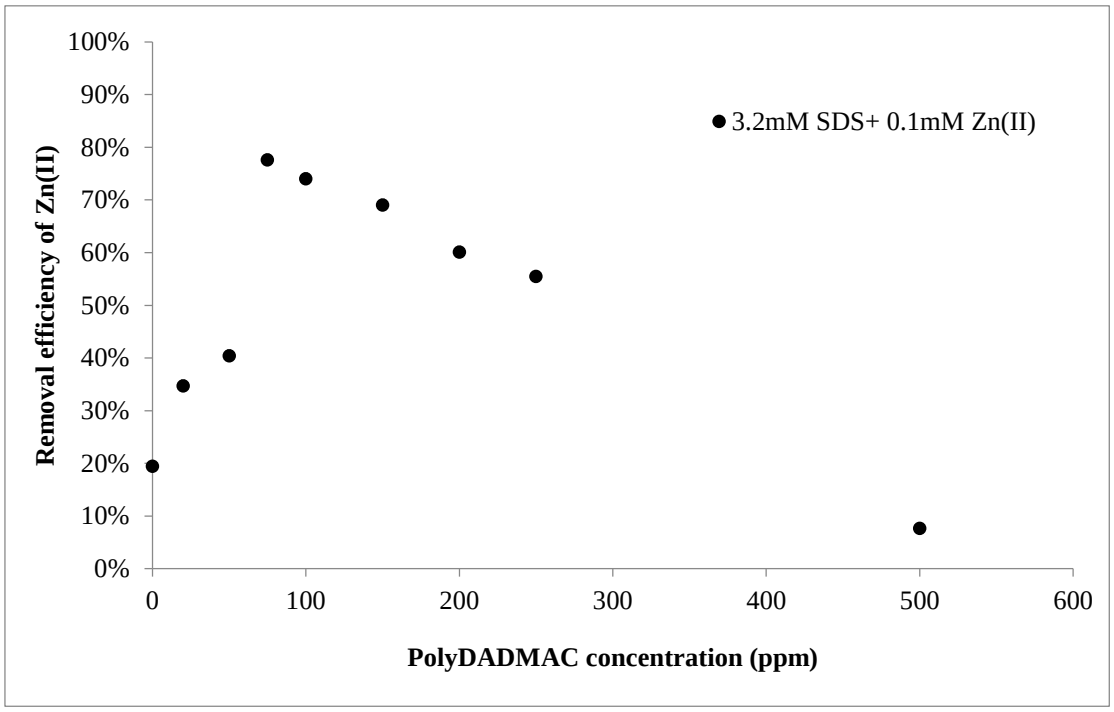

Figure 4.6: Optimisation of the dosage between 3.2 mM SDS and varying amounts of polyDADMAC to remove 6.5 ppm Zn(II).

The polyDADMAC and SDS system has been briefly studied to prove that the PSAs can also be formed by other types of polymer, such as polyDADMAC. The reason for only studying the polyDADMAC briefly is that the positive charge in polyDADMAC cannot be easily regained via pH adjustment. This means that once the quaternary amine groups in polyDADMAC are neutralised, they lost the charge forever, so they cannot be reused easily. The development of the recovery method is discussed in Chapter 5 and 7.

In Figure 4.6, the optimum dosage corresponds with the peak position at its surface tension plots (Figure 3.3). This proves that the PSAs form over a particular range of polymer–surfactant ratio, and is responsible for removing the metal ions. The range of polymer–surfactant ratio is relatively narrow for achieving the highest removal efficiency. In industrial application, the ratio has to be carefully controlled to obtain desired treatment results.

4.3.2. Metal cation removal limits

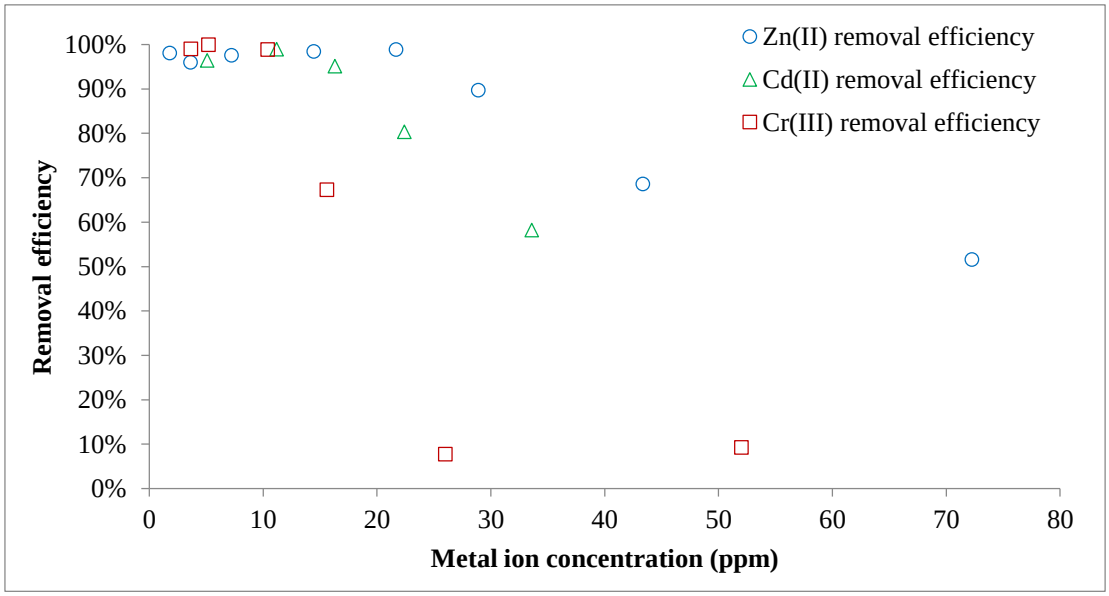

Figure 4.7: Adsorption capacities of the PSAs for metal ions at their optimum dosages in the PEI-SDS system.

To directly investigate the adsorption capacities and removal limits of PSAs for each metal ion, a series of qualitative studies are conducted at optimum polymer/surfactant concentrations with increasing amounts of targeted single species metal ions. Each metal ion has a slightly different optimum polymer-surfactant dosage ratio to comply with their individual effluent concentration and discharge limits. In Figure 4.7, the treated concentrations of metal ion in the filtrate under the optimum dosages in Table 4.1 are as low as 30 ppb for Cr(III), 40 ppb for Zn(II) and 10 ppb for Cd(III). The decreases in removal efficiency at higher metal ion concentrations are caused by the limit in adsorption capacity of the PSAs at a fixed dosage of polymer and surfactant. This dosage can be modified to fit the purpose of treating higher or lower concentrations of metal ions in solution; the dosage mass ratio between polymer and surfactant is in the range of 1:2.8-3.6.

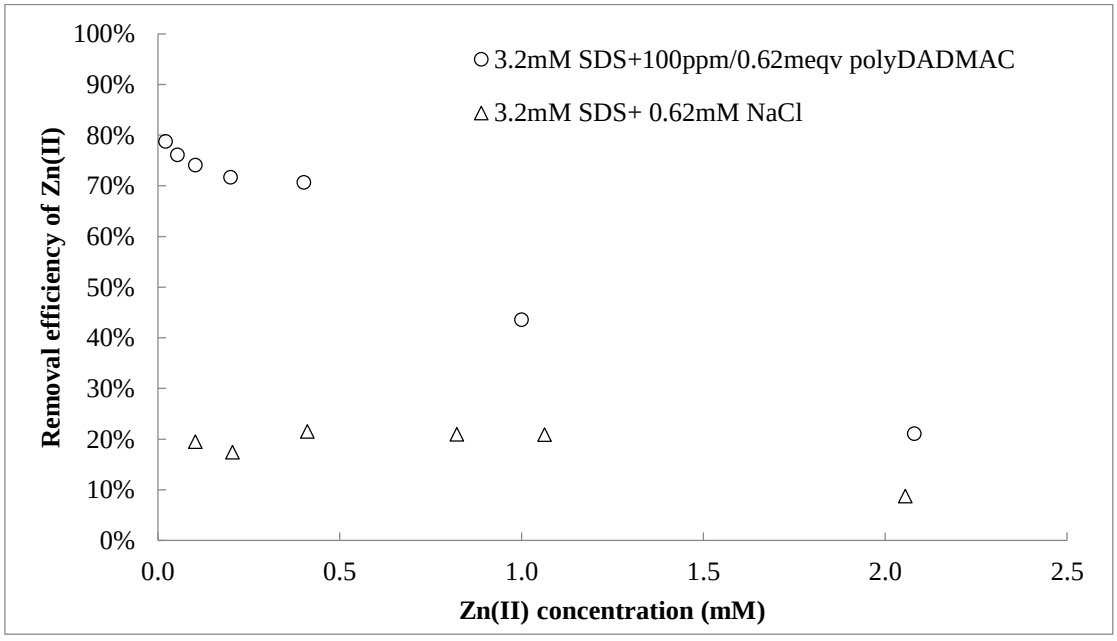

Figure 4.8: Zn(II) removal efficiency at the same ionic strength in the SDS/polyDADMAC system and the SDS/NaCl system with increase of Zn(II) concentrations.

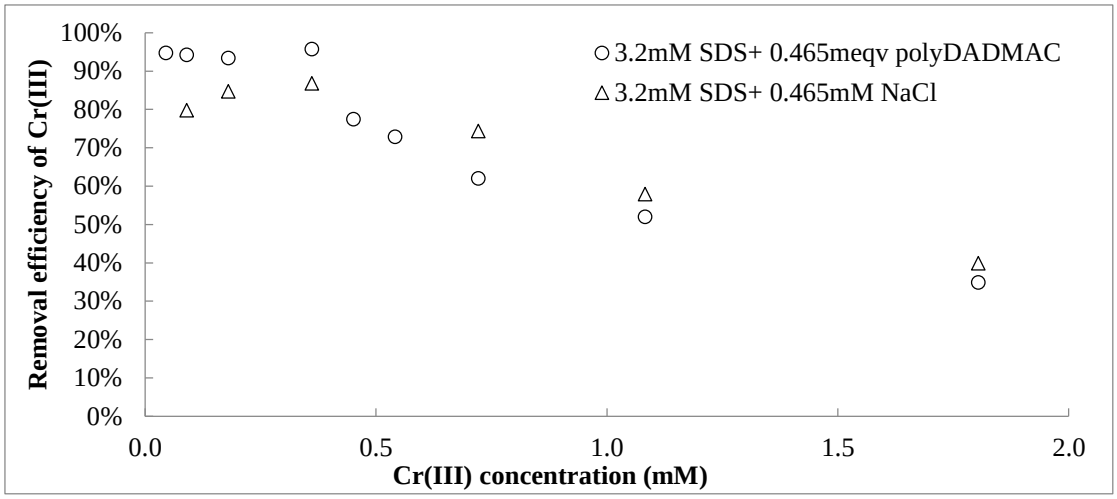

Figure 4.9: Cr(III) removal efficiency at the same ionic strength in the SDS/polyDADMAC system and the SDS/NaCl system with increase of Cr(III) concentrations.

The polyDADMAC–SDS system and the pure SDS system are tested to confirm that the PSAs are more effective for removing dilute metal ions than the SDS does, and to prove that the removal is mainly caused by the PSAs rather than the micelles formed in the vicinity of the membrane (Figure 4.8). For these purposes, the estimated optimum polymer–surfactant dosage ratio from the optimisation test (Figure 4.6) is used in the presence of the same ionic strength of SDS and NaCl. The NaCl is to simulate the addition of intrinsic counter ions when adding polyDADMAC. For a fair comparison, all solutions are filtered by 30kDa cellulose membranes to retain the micelles. This ultrafiltration step can be obviated with the addition of polymer because of the formation of flocs.

The removal efficiency of Zn(II) is almost four times higher than that of the pure SDS system at low zinc concentrations, which shows the PSAs are more effective for removing Zn(II), especially from dilute solutions. At low zinc concentrations, the gradual decrease of efficiency may well suggest that the existence of dynamic binding equilibrium between PSAs and Zn(II), which slows down the linear decline of the removal efficiency. A steep

decline is found above 0.5 mM Zn(II), suggesting most of the PSAs has been saturated by Zn(II).

In Figure 4.8, it is surprise to find that about 20% of Zn(II) is removed under the concentration of SDS around 40% of its CMC (8 mM). Theoretically, this removal efficiency should be zero. This is likely caused by the formation of micelles in the vicinity of the membrane due to the concentration polarisation (i.e. the local SDS concentration in the vicinity of the membrane approaches the CMC). A small amount of Zn(II) can bind to these micelles. Similar finding on the heavy metal removal efficiency in the MEUF below CMC is also reported (Samper et al., 2009). The 30kDa membrane should theoretically allow all the micelles to pass through, as the size range of a micelle is 18 to 22kDa. This is, however, too close to the Nominal Molecular Weight Limit of the membrane: 30kDa. Thus, it seems highly likely that the Zn(II) loaded micelles block some of the smaller pores inside the membrane, as the size of pores in a cellulose membrane are not uniformly distributed (Chan et al., 1984). The micelles can be trapped in the retentate and/or inside the membrane. Because of the dynamic equilibrium between free Zn(II) and bound Zn(II) in the vicinity of the membrane, with increasing zinc concentration, the removal efficiencies of Zn(II) in the SDS–NaCl system remain almost the constant value (Figure 4.8). Upon further increasing Zn(II) concentration, the final decline of removal efficiency is due to the limited binding capacity of micelles.

The Cr(III) removal efficiency of the SDS–polyDADMAC system is higher than the SDS–NaCl system under a low concentration range (< 0.4 mM $Cr(NO_3)_3$) (Figure 4.9). This suggests that the binding affinity of PSAs is higher than that of micelles at a low chromium concentration. The slightly increasing trend of removal efficiency in the SDS–NaCl system is because of the dramatic decrease of CMC with increasing $Cr(NO_3)_3$

concentration. This is supported by the results from surface tension measurements in Chapter 3 (Figure 3.2). For example, the CMC of SDS in the presence of 0.1 mM $Cr(NO_3)_3$ is about 3.1 mM (i.e. the micelles existed in the bulk at 0.1 mM $Cr(NO_3)_3$). Thus, with increasing $Cr(NO_3)_3$ concentration, the proportion of SDS forming micelles increases as well, which rises the binding capacity of Cr(III).

Above 0.4 mM $Cr(NO_3)_3$, the linear decline of efficiencies are due to the saturation of PSAs and micelles. It is worth noting that the Cr(III) removal efficiency is slightly lower in the presence of polyDADMAC. This is caused by the neutralization of polyDADMAC by a small amount of SDS, which should otherwise form micelles to bind Cr(III). This implies that the usage efficiency of SDS in the presence of polyDADMAC is lower than pure SDS micelles, when the SDS concentration is a few times higher than CMC. However, for the SDS concentration lower or slightly higher than CMC, the PSAs have a similar binding capacity and stronger binding affinity than that with micelles.

4.3.3. pH

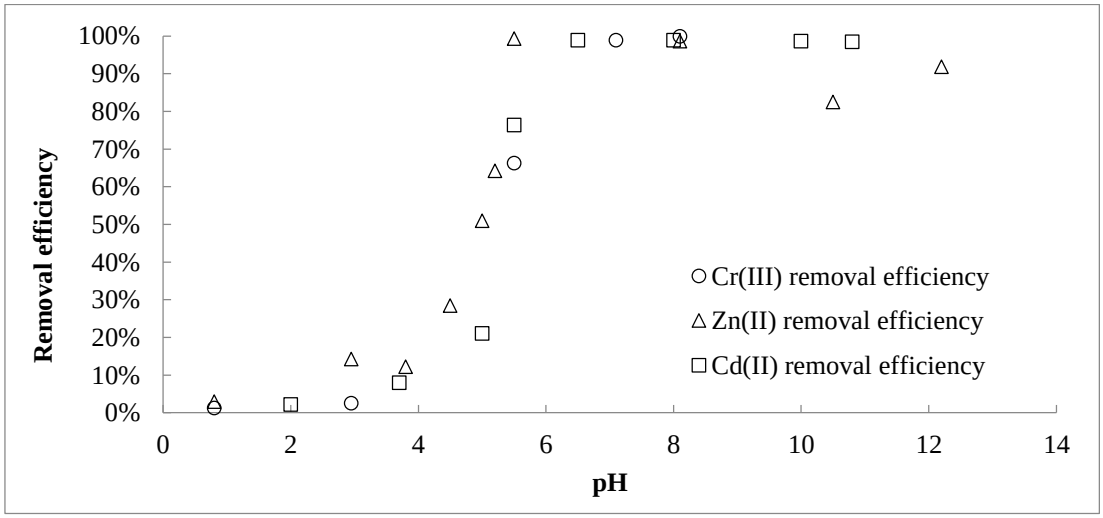

Figure 4.10: Cr(III)/Zn(II)/Cd(II) removal efficiencies at their optimum dosages in the PEI–SDS system versus different pH values.

The polymer–surfactant process works effectively around pH of 5-9. As shown in Figure 4.10, below a pH of 5, the removal efficiency dramatically decreases because the hydrogen ions compete with the metal ions for the binding sites on the PSAs. Below a pH of 2, there is little removal of the metal ions at all, since the adsorption sites on the PSAs are fully occupied by the excess hydrogen ions. At high alkaline pH values, the metal removal is caused by hydroxide precipitation.

All the metal ions have a very similar trend in the removal efficiency at various pH values. This suggest that the binding ability of the metal ions are similar, which may lead to a low selectivity at the removal stage. This is discussed in detail in Section 4.5.1.

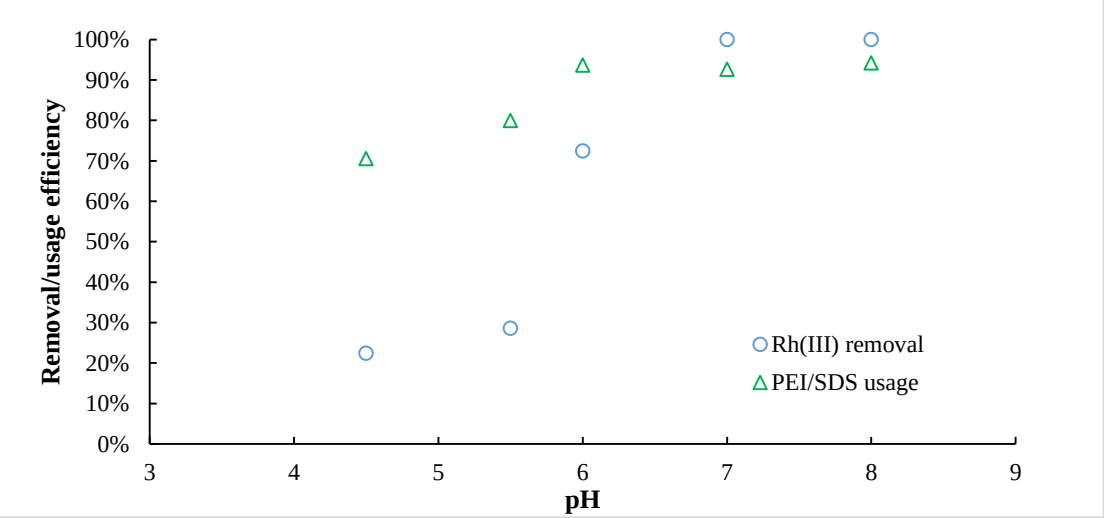

Figure 4.11: Rh(III) (0.2 mM) removal efficiency changes at different pH values under 60 ppm PEI and 0.7 mM SDS.

In Figure 4.11, the Rh(III) is completely removed at a pH of 7 and above, which is a bit narrower than the other metal ions. The reason is that the charge density for the Rh(III) is relatively small compared with the other metal ions as it is a relatively large atom. Thus, the proposed PSA process is suitable to treat a range of industrial effluents, the tolerance to extreme pH environment depends on the charged density of targeted metal ion.

4.3.4. Salinity and organic contaminants

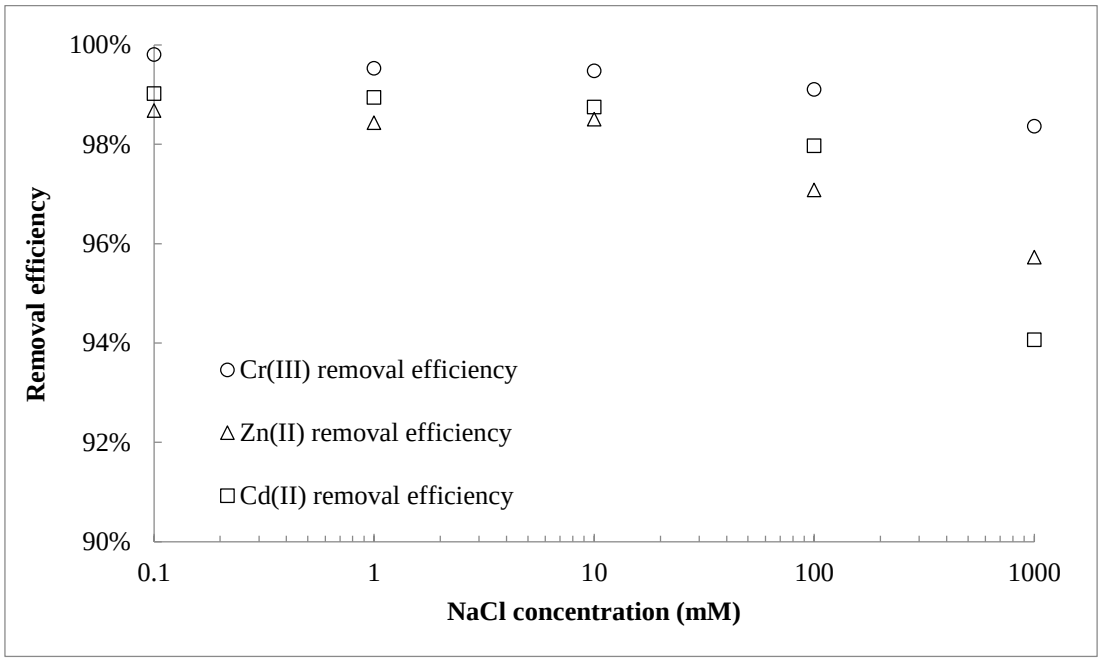

Figure 4.12: Cr(III)/Zn(II)/Cd(II) removal efficiencies versus the presence of different NaCl concentrations at optimum removal dosages for the PEI–SDS system.

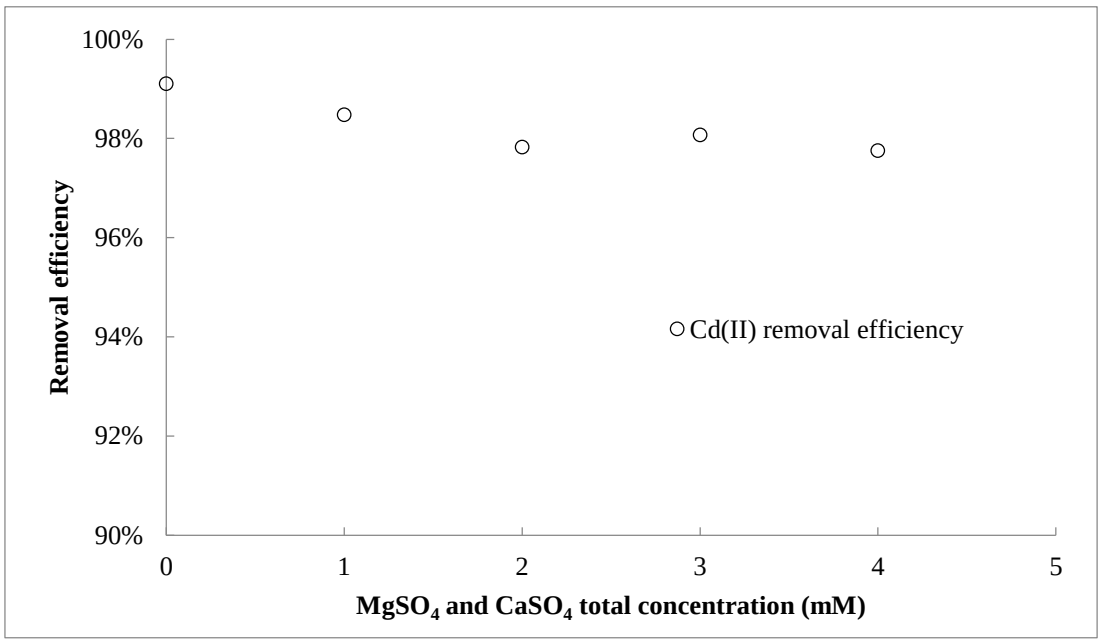

Figure 4.13: Cd(II) removal efficiencies versus various $MgSO_4$ and $CaSO_4$ (1:1 molar ratio) total concentrations at the optimum removal dosage for the PEI–SDS system.

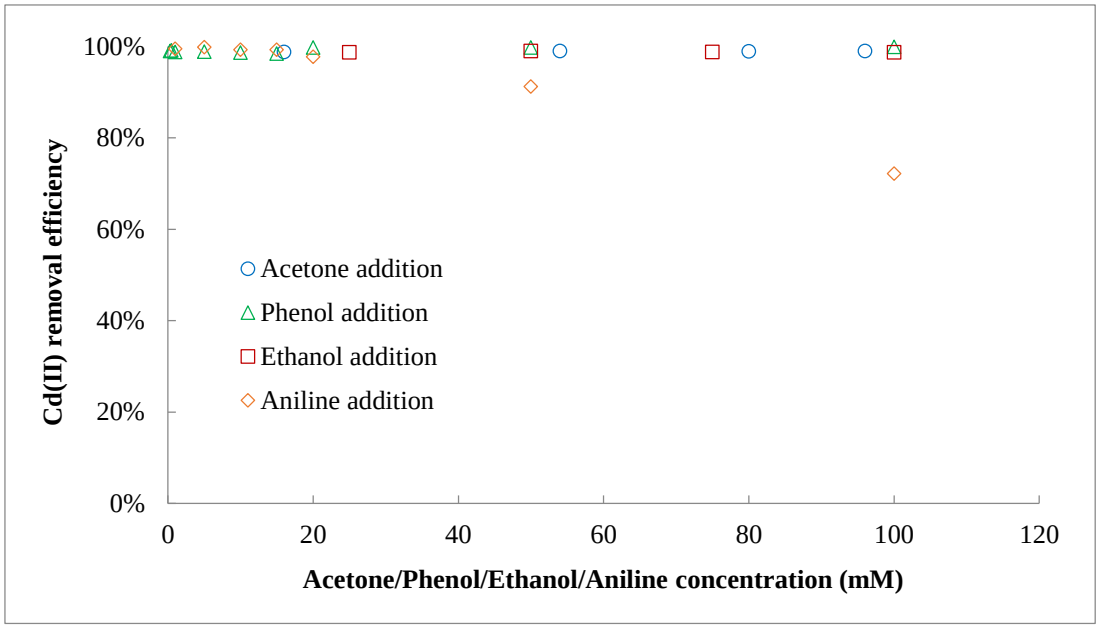

Figure 4.14: Cd(II) removal efficiencies versus the presence of various types of different concentrations at the optimum removal dosage for the PEI–SDS system.

The salinity effects on the removal of metal ions at the optimum dosages is also investigated. There is little decrease in metal removal efficiency until the NaCl concentration increase above 0.1 M, and only a 3% decrease arise when the concentration was 1 M (Figure 4.12). Cr(III) has less impact by NaCl than the other two divalent metal ions, because the electrostatic attraction between SDS headgroups and Cr(III) ions is stronger than that between SDS headgroups and the divalent ions. In addition, the water hardness are also studied, which is represented by $MgSO_4$ and $CaSO_4$ in this case (Figure 4.13). No notable decrease of removal efficiency is found up to 2 mM of each compound, which is about 4 times than the common hardness in water. Thus, the salinity in solution do not have a strong effect on the removal efficiencies.

With regard to the organic effects, the metal ion removal efficiencies remain the same with the addition of acetone, phenol and ethanol up to 100 mM (Figure 4.14). The addition of aniline, however, decreases the metal removal efficiency after the concentration above

20 mM. As a weak base containing an amino group, it can precipitate the Cd(II) to some extent, but it also may disrupt the formation of PSAs with the increase of pH. The disruption may due to the fact that some of the SDS tails bind with hydrolysed aniline via hydrophobic and electrostatic forces. Therefore, with addition of the weak base, the removal mechanism is slowly shifted from binding with PSAs to precipitation. At a higher aniline concentration (>100 mM), the removal may be dominated by the precipitation.

These results suggest that the process is not affected by some inorganic and organic components at moderate concentrations, and gives confidence in the robustness of applying the PSAs to real world industrial effluents.

4.3.5. Residence time

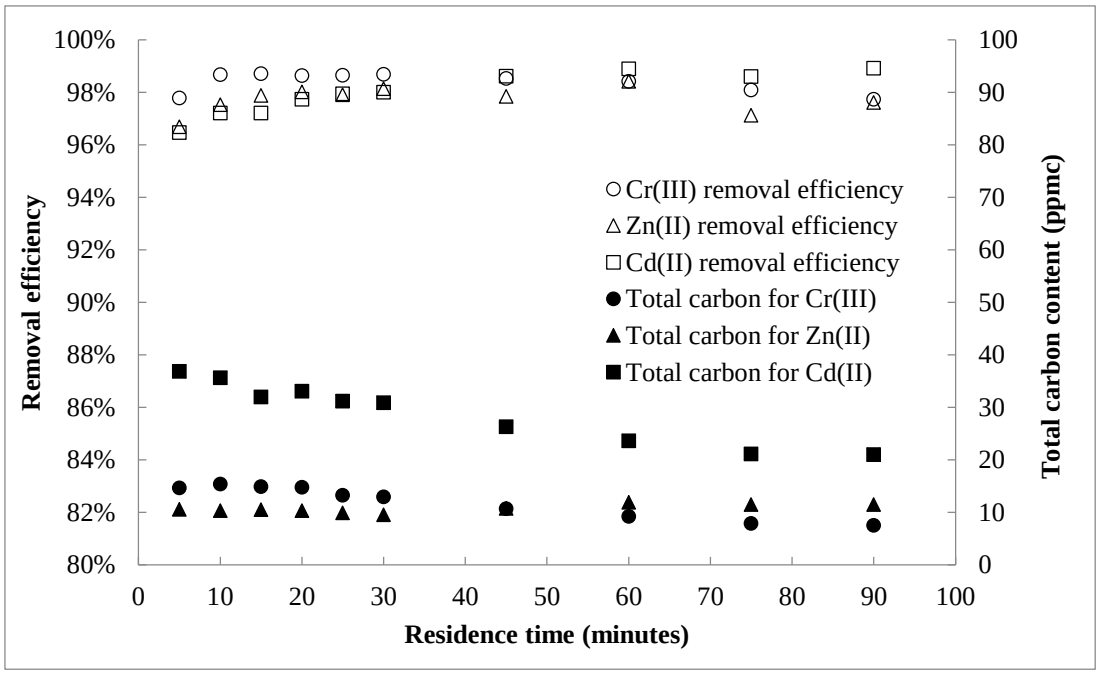

Figure 4.15: Removal efficiencies of metal ions and changes in the amount of total carbon in the filtrate with residence time for the PEI–SDS system.

Apart from effectively treating dilute metal ion solutions to a ppb level, this PSA process is largely completed within 20 min (Figure 4.15). A series of time studies are conducted to study the kinetics of the process. Within 20 min, 99% of each metal ion is adsorbed by the PSAs. The total carbon in the filtrate indicates the degree of flocculation between polymer and surfactant, since they are the only two carbon sources in this system. Thus, the decrease of total carbon suggests the flocculation process continued up to one hour of stirring at 200 rpm, but it is calculated that 85-95% of the PEI and SDS formed flocs within 20 min. This corresponds with the attainment of maximum metal removal efficiency.

4.4. Comparison with MEUF and PEUF

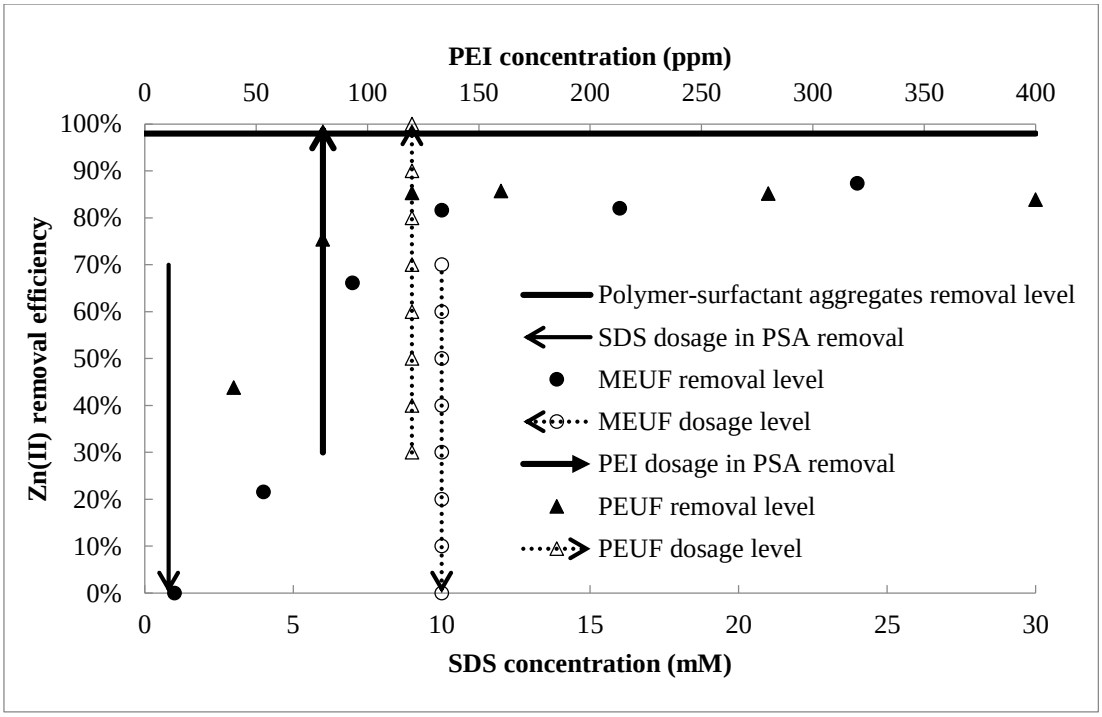

Figure 4.16: A comparison between MEUF and PEUF performance with that of the PSA process to treat 0.3 mM $ZnSO_4$ in aqueous solutions. The solid line at the top presents the

Zn(II) removal efficiency for the PSAs, the solid arrow lines represent the PEI and SDS dosages in this process, and the dotted arrow lines with triage and circle represent the PEI and SDS dosages in the PEUF and MEUF, respectively.

A comparison with two closely related techniques is conducted to remove 0.3 mM $ZnSO_4$ from aqueous solutions. Regarding PEUF, the highest Zn(II) removal efficiency (86%) is achieved around 120 ppm PEI, and further increases of PEI concentration does not enhance the performance. Regarding MEUF, the removal efficiency is about 87%, when the SDS concentration is three times higher than its CMC. This SDS dosage is approximately 50 times higher than is used in the PSA process. At the PSAs surfactant dosage with 80 ppm PEI, the Zn(II) removal efficiency (marked as a solid horizontal line in Figure 4.16) is as high as 99%, which is higher than the highest removal efficiency achieved either by MEUF or PEUF. Moreover, the separation method for MEUF and PEUF is ultrafiltration, but the PSA process uses a coarse filter which is much cheaper in capital and running costs and yields much higher filtration fluxes and therefore process intensity. In conclusion, the PSA process is quick and effective in removing dilute (ppm) metal ions, and overall requires much less polymer and surfactant dosages than the competing process of MEUF and PEUF.

4.5. Optimum dosage for removing metal cation mixtures

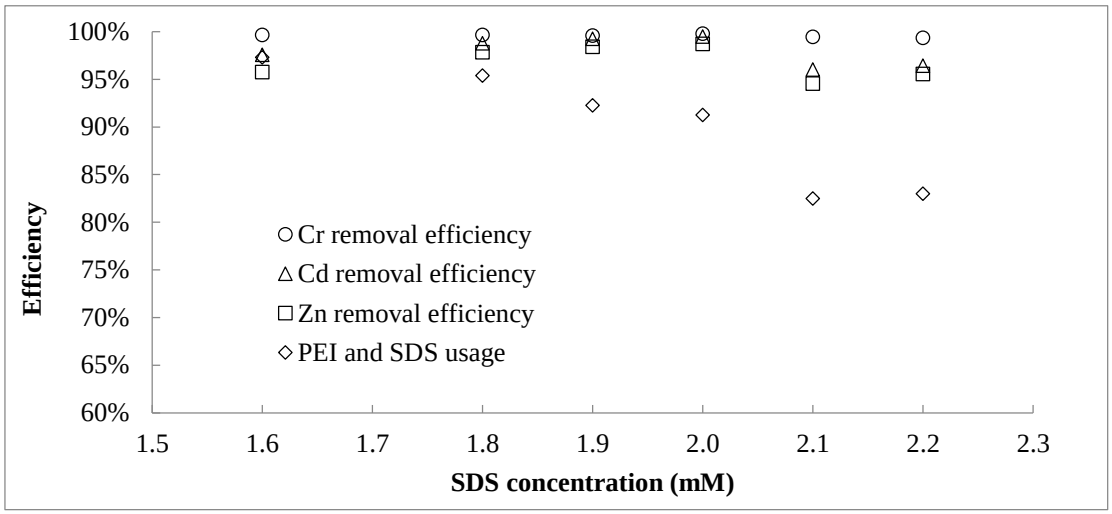

Figure 4.17: Optimisation of dosage ratio of PEI and SDS for the mixture of 0.1 mM $CdSO_4$, 0.2 mM $Cr(NO_3)_3$ and 0.3 mM $ZnSO_4$ at fixed 180 ppm PEI.

The mixtures of heavy metal ions are removed together using PSAs for the later selective recovery studies in Chapter 5. In the mixture system, the metal ion removal efficiencies are almost the same, but the polymer–surfactant usage efficiency decreases with increasing SDS concentration (Figure 4.17). The reason is that part of the increasing amount of SDS are formed more PSAs which push the dynamic binding balance towards the bound PSAs side.

Most importantly, the optimum dosage for the mixture systems also follows the PEI–SDS–metal ion dosage ratio, which is discussed in Section 4.3.1. All removal efficiencies of metal ions are above 95%, the highest removals are at 2 mM SDS, but the highest PEI–SDS usage efficiency is at 1.6 mM SDS. If the PEI–SDS usage efficiency is not high, the removal agent passes through the filter and cause contamination of the cleaned waste stream. Considering both of the removal and usage efficiencies, 1.8 mM SDS is regarded as the optimum dosage for the metal ion mixtures. The 1.8 mM SDS is close to the sum

of three individual optimum SDS concentrations (1.9 mM). The results prove that, for dilute metal mixture streams, the dosages between PEI and SDS is scalable by simply adding the optimum dosages for individual metal ions to estimate the optimum dosage of the mixtures at the same concentrations. Thus, excessive optimisation tests are not required for the dosages between PEI and SDS for each waste stream containing metal mixture.

4.6. Discussion and summary

A novel treatment process for effluent streams that employs PSAs has been developed and applied to remove dilute metal ions, such as Cr(III), Zn(II) and Cd(II), from aqueous solutions. This process uses cationic polymers, such as polyDADMAC or PEI, as a backbone structure onto which anionic surfactants, such as SDS, can form micelle–like aggregates. The resulting structures, PSAs, have the ability to remove metal ions from solution, and to form larger flocculated aggregates through a process of intermolecular association. The flocculated aggregates can then be separated from the effluent stream through a settling or coarse filtration step. In the work presented, it is shown that 99% of 11.2 ppm Cd(II) was removed under optimum dosage using 40 ppm PEI and 0.5 mM SDS. The results show that this process is quick and effective at metal ion removal for a pH range from 6 to 9, and is also effective in the presence of organic contaminants and in the presence of inorganic contaminants. This overall process requires about 35% less polymer and 90% less surfactant dosages than the competing process of MEUF and PEUF. Such a PSA process thus has potential application for the efficient removal of dilute metal ions during process effluent water treatment.

Chapter 5

Investigation of the Recovery of Metal Cations and Recycle of Removal Agent in the Polymer–Surfactant Aggregate Process

5.1. Introduction

Many industrial wastewaters contain heavy metals; those associated with mining and mineral processing, as well as textile and battery industries pose particular challenges. The incentives for removal of heavy metals include not only progressively stricter legislation on effluent quality standards, but also their potential economic value as non-renewable (and increasingly rare) natural resources. Further benefits include toxicity elimination, and the prevention of metal biological accumulation.

Many papers have been published regarding the removal and recovery of metal ions from effluent. The popular removal methods for treating such effluent are chemical

precipitation (Charerntanyarak, 1999; Mógora et al., 2013), adsorption (Najafi et al, 2012, Hilal et al., 2005), biosorption (Ajjabi and Chouba, 2009), ion exchange (Inglezakis et al., 2005) and membrane filtration (Hafiane et al., 2000; Hilal et al., 2004; Hankins et al., 2006). Chemical precipitation and adsorption are relatively cheap and widely used methods, but the heavy metal concentrations in treated effluents hardly meet the discharge limits. Adsorption and biosorption are sustainable methods for heavy metal treatment, but these methods only transfer the metal ions from effluent to other materials that are difficult to be reused and/or require stricter disposal procedures. Ion exchange and membrane filtration possess high removal efficiency, but the resin, membrane and energy costs are relatively high. To overcome these limits, a novel heavy metal ion removal process using polymer–surfactant aggregates (PSAs) has been introduced in a previous chapter. However, a method to recover the metal ions and recycle the polymer and surfactant has not yet been proposed.

One of the widely researched recovery methods, acidification, is used to displace the bound metal ion from adsorbents consisting of natural or waste materials, such as algal biomass (Darnall et al., 1986), fruit peel (Ajmal et al., 2000), lignite (Mohan and Chander, 2006), rice husk (Ajmal et al., 2003), and crop milling waste (Saeed et al., 2005). The purity of the recovered metal ions, however, is relatively low and the used natural materials may need stricter disposal procedures. Other methods which have a similar treatment process (acidification recovery) use polyelectrolytes (Jellinek and Sangal et al., 1972, Onsosyen, and Skaugrud, 1990, Rether and Schuster, 2003) or surfactant (Li et al., 2009, Liu and Li, 2004) with ultrafiltration. Unlike those using natural materials, the polyelectrolytes or surfactants can be reused by replenishing a notable amount of material lost in the removal and acidification steps and maybe accompanied by a small deterioration

of removal ability. Although chelation agents, such as EDTA (Allen and Chen, 1993) and potassium ferricyanide (Kim et al., 2006), have been applied to effectively recover metal ions, the stable chelate – metal complexes have limited applications by themselves and it is hard to justify the economic case for further purification. Some work has focussed on recovering SDS by foam fractionation or chemical precipitation for micellar enhanced ultrafiltration, but only about 70% SDS is recovered and the removal efficiencies of the reclaimed SDS from precipitation after each cycle are deteriorated (Boonyasuwat, et al., 2003, Tharapiwattananon et al., 1996, Juang et al., 2003). Thus, effectively recovering the substrates without a deterioration of removal ability from one cycle to the next still remains a key problem, which limits the sustainable development of metal ion treatment process.

In the previous chapter, a PSA process is developed and applied to remove heavy metal ions from dilute aqueous solutions. This process uses a cationic polymer, such as polyethylenimine (PEI), and an anionic surfactant, such as sodium dodecyl sulphate (SDS), to form micelle-like aggregates on the oppositely charged polymer chains, thus forming PSAs. The PSA can bind with heavy metal ions from dilute effluents and form flocs, which can be separated by coarse filtration or gravity settling. The results show that 99% of 11.2 ppm Cd(II) is removed under optimum dosage using 40 ppm PEI and 0.5 mM SDS in the presence of inorganic and organic contaminants.

In this chapter, a new recovery and recycle process is presented to recover bound metal ions from flocculated PSAs into a highly concentrated solution by acidification and to recycle the polymer and surfactant by basification. The recovery method within the whole PSA process has been investigated, and the recovery efficiencies are studied at various values of pH, concentration factor, residence time, salinity, and cycle number. In addition, PEI and SDS were recycled up to 6 times by sequential acidification, basification and

neutralisation. This work completes the whole treatment process for the PSA process, which is divided into three stages: removal, recovery and recycle.

5.2. Materials and methods

5.2.1. Materials and the removal stage

Poly(ethyleneimine) (PEI) solutions with MW 750K were prepared by diluting PEI solution (Sigma Aldrich, average MW~750,000, 50 wt.% in H_2O). Sodium dodecyl sulphate (SDS) (purity ≥ 99.9%), dimidium bromide/disulphine blue solution, and hyamine 1622 solutions (4mM, pH 5.5-7.5) were obtained directly from Fisher Scientific. Chromium (III) nitrate nonahydrate, cadmium sulphate and zinc sulphate were purchased from Fisher Scientific (all purity ≥ 99%). Sodium sulphate (ACS reagent, ≥ 99.0%), sulphuric acid (ACS reagent, 95-98%) and sodium hydroxide (reagent grade, ≥ 98%, pellets) were obtained from Sigma Aldrich. 30kDa regenerated cellulose membranes and 20 μm mixed cellulose ester membrane filters were obtained from Millipore.

The solution preparation, filtration, SDS, total carbon and metal concentration measurements follow Sections 3.2.1., 4.2.1., 4.2.3 and 4.2.4.

5.2.2. Metal ion recovery by acidification

A calculated amount of acid solution was added to the flask and then stirred at 200 rpm for at least 20 min to treat the flocs stuck on the flask walls until the flocs where floating on the surface. The filtrate outlet of the filtration cell was lifted above the level of solution in the cell. The solution in the flask was then decanted (leaving some flocs behind) into

the filtration cell, and stirred at 200 rpm for another 20 min before the filtration was started by lowering the outlet under gravity. The filtration stopped when all solution had passed through the 20 µm filter. The experiments were carried out by adding recovery solution at concentration factors of 10 and 40. The concentration factor is defined in Equation 5.1. The recovered filtrate was analysed directly by total organic carbon analyser and two-phase mixed indicator titration. It was then diluted by deionised water before measuring the final metal ion concentrations by atomic adsorption spectrometry. The metal ion recovery efficiency was calculated by Equation 5.2. The salinity is defined as the inorganic salt (Na_2SO_4) concentration in the solution.

$$\text{Concentration factor} = \frac{\text{Volume of treated effluent (ml)}}{\text{Voulume of added acid or base solution (ml)}}$$

Equation 5.1: Calculation of the concentration factor.

$$\text{Metal ion recovery efficiency} = \frac{C_{\text{recovered ion}}(\text{mg/l}) \times V_{filtrate}(\text{ml})}{C_{\text{original effluent}}(\text{mg/l}) \times V_{\text{effluent}}(\text{ml})} \times 100\%$$

Equation 5.2: Calculation for the metal ion recovery efficiency from acidification.

5.2.3. Polymer and surfactant recovery by basification

A calculated amount of base solution was added to the original flask and then stirred at 200 rpm for 20 min until all the flocs dissolved. The solution was then poured into the filtration cell, and stirred at 200 rpm for another 20 min to recover the polymer and surfactant in the cell. The filtration started when all the flocs in the cell had dissolved. The filtration stopped when all solution had passed through the 20 µm filter, which became 2nd filtration filtrate. The method for the residence time experiments is the same as in the acidification step (Section 5.2.2.). The recovered filtrate was analysed directly

by atomic adsorption spectrometry, and was diluted before analysis by total organic carbon analyser and two-phase mixed indicator titration. The polymer–surfactant and surfactant recovery efficiencies were calculated by Equation 5.3.

$$\text{Polymer} - \text{surfactant recovery efficiency} = \frac{\text{Total carbon}_{\text{recovered}}(\text{ppm}) \times \text{V}_{\text{2nd filtration filtrate}}(\text{ml})}{\text{Total carbon}_{\text{added removal agent}}(\text{ppm}) \times \text{V}_{\text{effluent}}(\text{ml})} \times 100\%$$

$$\text{Surfactant recovery efficiency} = \frac{\text{C}_{\text{recovered SDS}}(\text{mM}) \times \text{V}_{\text{2nd filtration filtrate}}(\text{ml})}{\text{C}_{\text{added SDS}}(\text{mM}) \times \text{V}_{\text{effluent}}(\text{ml})} \times 100\%$$

Equation 5.3: Calculation for the polymer–surfactant and surfactant recovery efficiencies from basification.

5.2.4. Residence time and salinity effect experiments

With regard to residence time experiments, a calculated amount of acid/base solution was stirred in the flask for a desired period of time (the residence time), and then decanted into the filtration cell to stir for the same period of time before the filtration was started in order to study the kinetics of the metal ions desorption process. Na_2SO_4 was used as a sample salt to represent different salinities. Salinity experiments were carried out in the same recovery procedure under 15 min residence time and a concentration factor of 20, but at the previous removal stage, the metal contaminated solution contains different amounts of Na_2SO_4.

5.2.5. PEI and SDS recycle

The regenerated PEI–SDS basic solution was directly recycled back into the original solution as a batch process, and then the pH was neutralised by adding H_2SO_4. After

stirring the solution overnight, the next cycle was performed by filtration (Section 4.2.1), acidification (Section 5.2.2) and basification (Section 5.2.3) methods and repeated. A portion of the regenerated PEI–SDS solution was consumed by analysing the total carbon and SDS concentration and no make-up was added, so that the total amount of the PEI and SDS in the process was reduced after each cycle. Thus, the treatable volume after each cycle was also reduced until the 7th cycle when the regenerated filtrate volume was no longer enough for further analytical measurements.

5.3. Overview of the whole cation treatment process

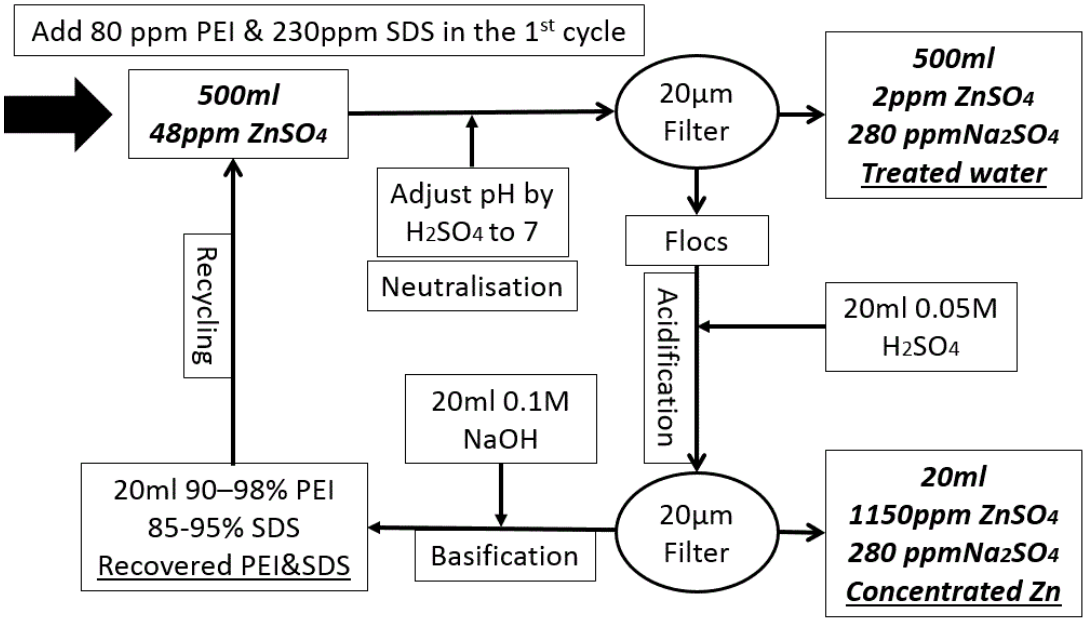

Figure 5.1: Flow sheet diagram of the whole cation treatment process using PSAs.

The removal stage of metal ions using PSAs is reported in the previous chapter, and is followed here by recovery and recycle stages to reclaim and concentrate the removed metal ions and regenerate the removal agent (i.e. polymer and surfactant) for recycle.

These purposes are fulfilled by an acid-base wash method, which is shown in the flow sheet diagram (Figure 5.1). From experimental observations, the blockage of the coarse filter at the removal stage can be cleaned up by the acid-base method, which could consequently avoid the need for filter cleaning. With the addition of recovery and recycle stages, the treatment process is completed, chemical cost is greatly reduced, and the sustainability of the process is enhanced. In addition, no disposal of flocs is required. In short, having developed the polymer and surfactant recycling in the process, the feed of the process are simply the heavy metal containing effluent/wastewater and the acid and base solutions, and the outputs are the treated clean water with a small amount of salt, and the reclaimed highly concentrated metal ion solution. The latter can be either recycled back into a manufacturing process or sold directly.

In the example process, an effluent containing 48 ppm (0.3 mM) $ZnSO_4$ is treated by 80 ppm PEI and 230 ppm SDS (0.8 mM) mixtures, which are added in the first cycle. Neither PEI nor SDS need to be replenished in the following cycles. At the removal stage, the Zn(II) loaded flocs are formed and separated from the treated effluent. The treated effluent is a product of the process and contains some Na_2SO_4, which is generated from the acid and base neutralisation at the recycle stage. To recover and concentrate the Zn(II) as a secondary product, a small amount of 0.05 M H_2SO_4 is added to the flocs to leach out the Zn(II) as a highly concentrated Zn(II) solution. After that, the flocs are further treated by dissolving in a small amount of 0.1 M NaOH to displace the SDS from the PEI, which leads to the regeneration of PEI and SDS. The regenerated PEI and SDS are then added in the next cycle before neutralising the pH of the solution.

5.4. Orders of acidification and basification and pH effects

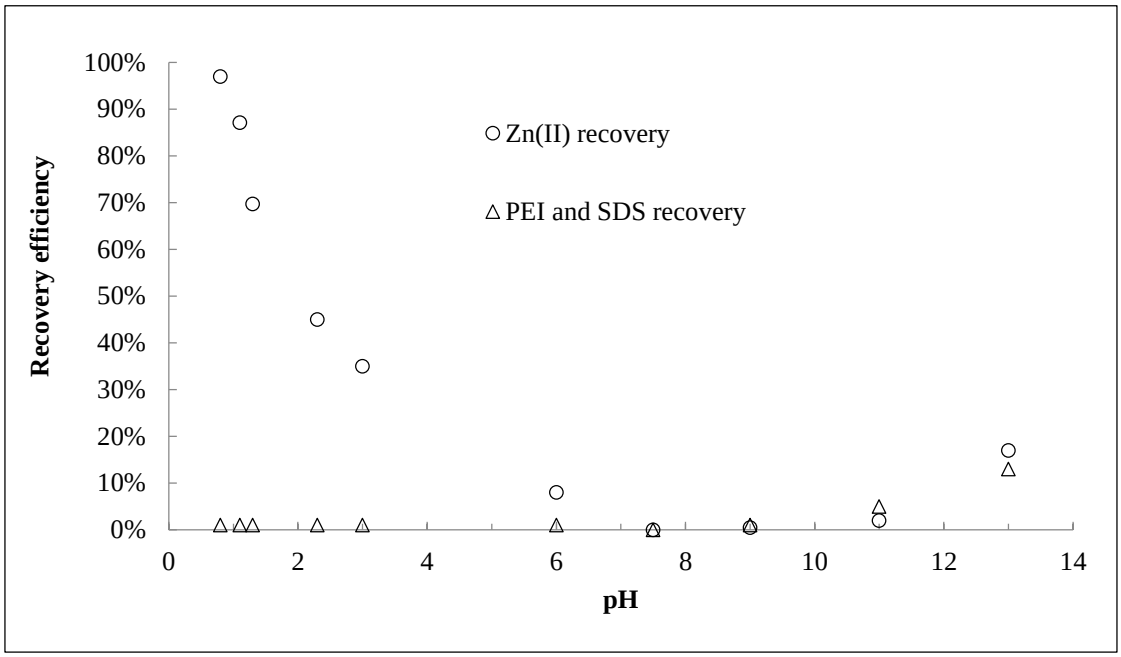

Figure 5.2: Zn(II) and PEI–SDS recovery efficiencies as a function of pH.

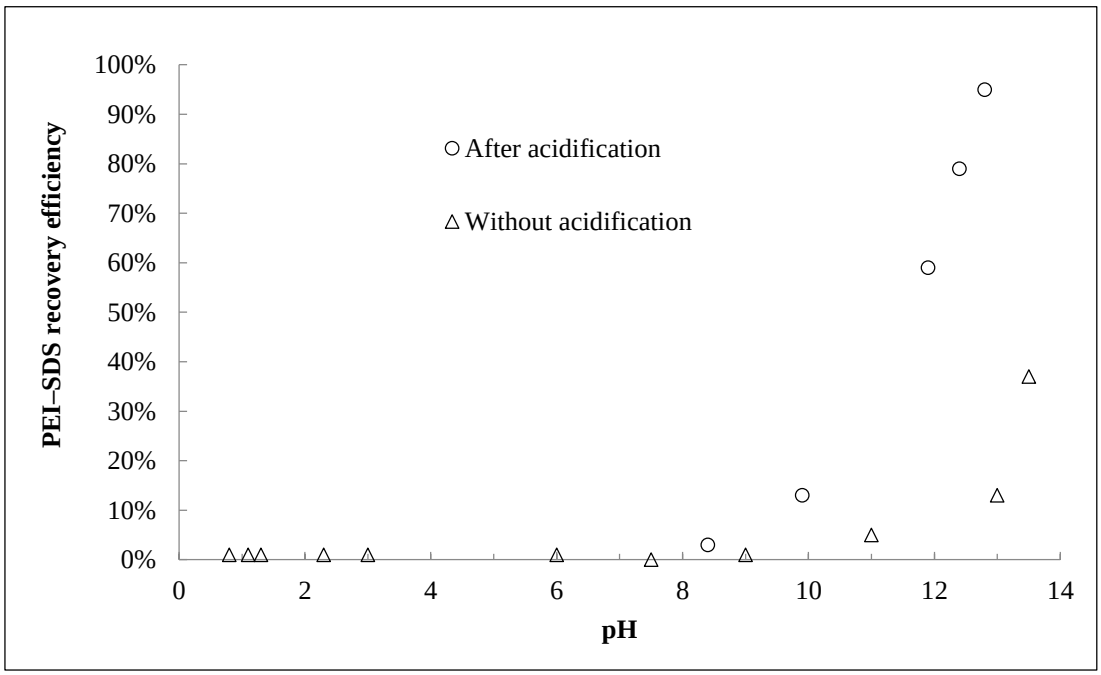

Figure 5.3: Effects of acidification (at a pH of 1) on the subsequent PEI–SDS regeneration efficiency via basification at various pH values.

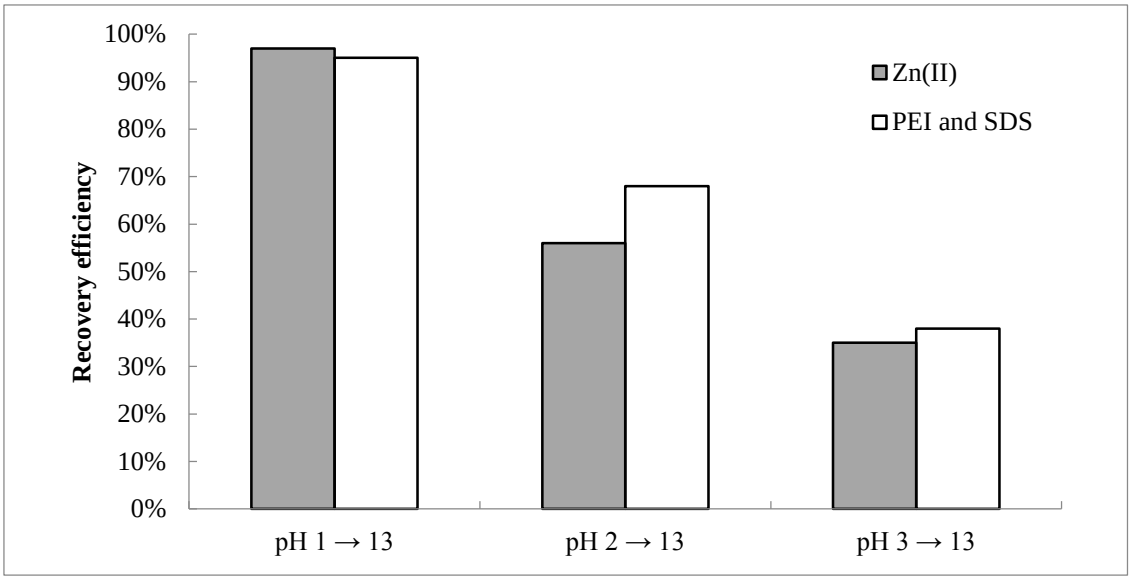

Figure 5.4: Effects of the pH at the acidification step on the subsequent PEI–SDS regeneration efficiency by basification using 0.1 M NaOH (a pH of 13).

The orders of addition of acid and base solutions are investigated to develop the recovery procedure and further understand the interactions between PEI, SDS and metal ions. High metal ion and PEI–SDS recovery efficiencies are found when 0.05 M H_2SO_4 is added first before 0.1 M NaOH. The results in figure 5.2 show that the Zn(II) recovery efficiency increases with the decrease of pH values, because the kinetics of displacing the Zn(II) that are bound to the PSAs are promoted with increasing concentration of hydrogen ions. Importantly, little PEI and SDS in Zn(II) loaded PSAs is recovered in the acid solution, and less than 15% of them is recovered even at a pH of 13. The reasons are probably that at an acidic condition, the PEI is fully protonated as a cationic polymer, which strengthens the electrostatic binding with SDS. At a basic condition, the bridging effects from divalent zinc ions inhibit the disassociation of PSAs, because the zinc ions may bind to two aggregates on different PSAs that can strengthen the associations between PSAs. Thus, the base solution should be added after the acidification; the latter is to displace the Zn(II) from flocs and mitigate the bridging effects. The PEI–SDS

recovery efficiency consequently increases to a high level with the increase of pH values (Figure 5.3), because now a greater amount of hydroxide ions can enhance the kinetics of displacing SDS from PEI chains. To further confirm the bridging theory, various pH values of acid solutions are used to displace the Zn(II) to varying extents to obtain flocs containing different amounts of bound Zn(II) (Figure 4). After acidification, the flocs are treated with pH 13 NaOH solutions. The results in figure 5.4 suggest that less PEI–SDS is regenerated in the presence of a higher amount of Zn(II) in the flocs. In conclusion, the pHs of 1 and 13 solutions are used in sequence to recover more than 95% of the metal ions and the PEI–SDS respectively. It is a win-win situation as higher recovery of zinc allows higher recycle of PEI–SDS.

5.5. Variable effects on recovery efficiency (concentration factor, residence time, Na_2SO_4 concentration and cycle number)

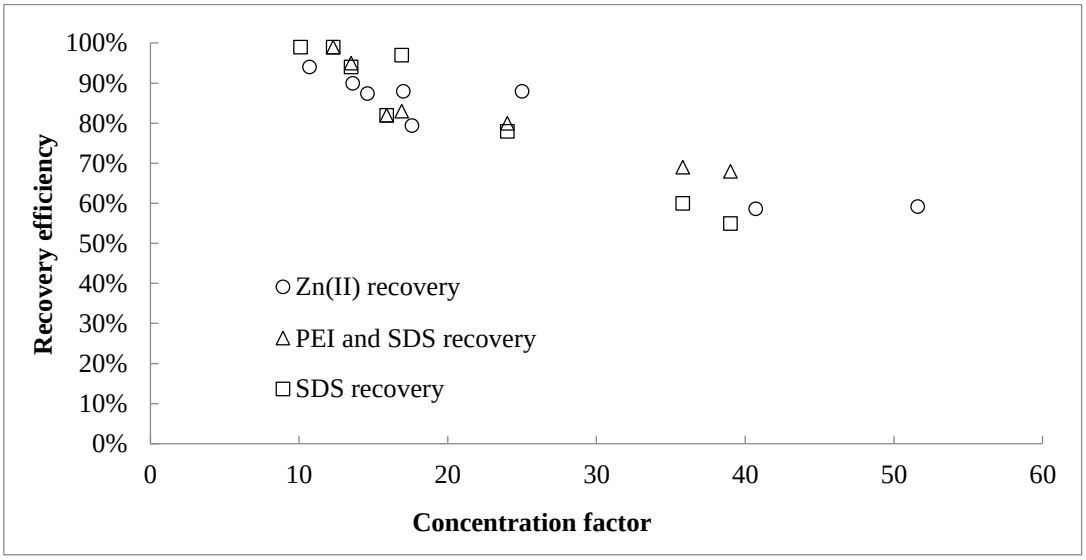

Figure 5.5: Recovery efficiency of Zn(II) at a pH of 1 and that of PEI–SDS and SDS at a pH of 13 in 15 min at different concentration factors.

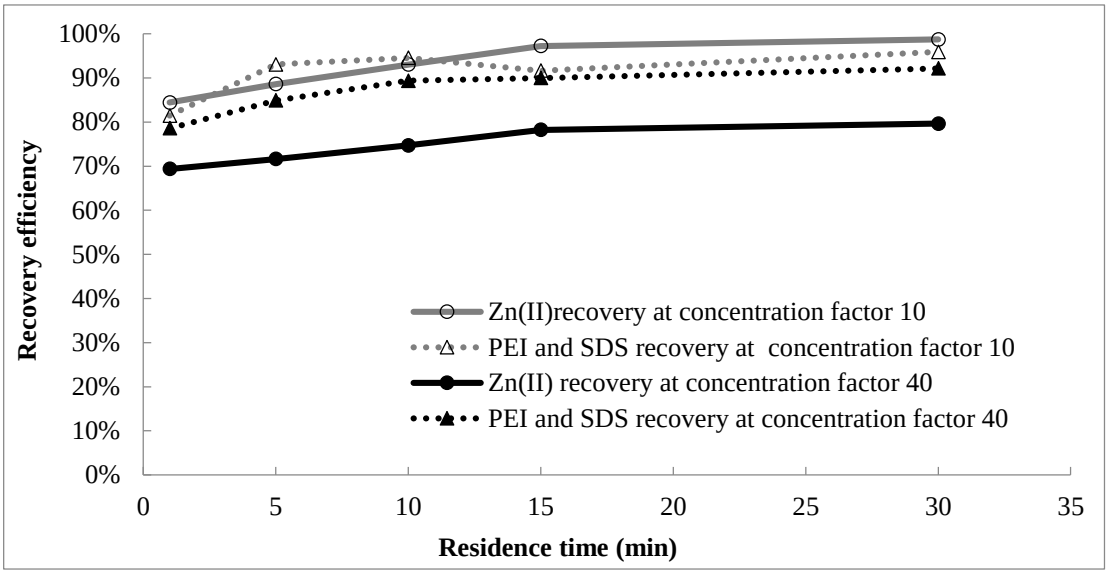

Figure 5.6: Recovery efficiencies of Zn(II) at pH 1 and that of PEI–SDS at a pH of 13 for a different period of residence time at concentration factors of 10 and 40.

The effects of concentration factor, residence time, salinity and number of cycles on the metal ion and PEI–SDS recovery efficiencies are also investigated to determine the optimum operational environment and robustness of the recovery and recycle stages. Apart from the pH effects on the recovery, the concentration factor also plays a key role. The concentration factor is the ratio of the total volume of the treated effluent to the volume of the added acid or base solution (Equation 5.1). With increase of concentration factors, the PEI, SDS and Zn(II) recovery efficiencies decrease (Figure 5.5). The decrease at a higher concentration factor may be primarily caused by the recovered $ZnSO_4$ in the acidic solution approaches to the saturation at the room temperature, leading to the equilibrium of the recovery process slows down dramatically. Thus, at the same residence time, the recovery efficiency decreases with increasing concentration factor (i.e. slow kinetics/dissolution rate). To further understand the kinetics, in figure 6, the correlations between recovery efficiency and residence time suggest that the kinetics is fast at the first 5 min, and slows down afterward, particularly after 15 min. The rate of increase recovery

efficiencies for the concentration factor of 10 is quicker than that of 40, much clearer for the removal agent regeneration in the first 5 min (Figure 5.6). This suggests that the increasing concentration factor indeed reduces the dissolution rate/kinetics of the recovery process.

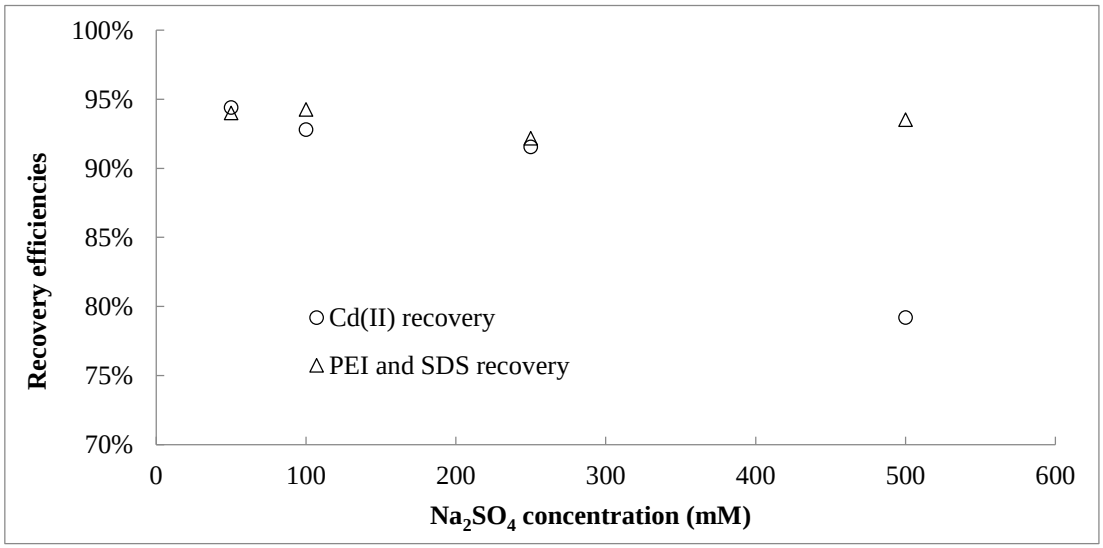

Figure 5.7: Effects of different concentrations of Na2SO4 on the recovery efficiency of Cd(II) at a pH of 1 and that of PEI–SDS at a pH of 13 under 15 min residence time and a concentration factor of 20.

At the recycle stage, the pH neutralisation generates a small amount of Na_2SO_4 that will accumulate in the process at each cycle. Thus, the effects of various amounts of Na_2SO_4 on the PEI–SDS and metal ion recovery efficiencies are examined (Figure 5.7). The results show that no effect is found when the Na_2SO_4 remains below 250 ppm. When the Na_2SO_4 concentration reaches 500 mM (71,000 ppm), the Cd(II) recovery efficiency decreases by less than 20%. The decrease is partially due to the weakening effect on the overall charge of PSAs due to the double layer compression. Thus, less Cd(II) is removed in a high salinity condition, which agrees with the results in Figure 4.12 in Chapter 4. The charge screening effects may also act on the charge repulsion between surfactant

headgroups and leads to more monomers forming each aggregate on the polymer chain, but this effect is dominated by screening effects on the PSAs. This overall reduction in removal efficiency therefore contributes to a part of the reduction in the recovery efficiency at 500 mM Na_2SO_4. Another important effect is the changes in equilibrium and kinetics of Cd(II) recovery in a high salinity. At 500 mM Na_2SO_4, the dissolution rate of Cd(II) slows down which leads to less Cd(II) is recovered at the given residence time.

Most importantly, the majority of bound Cd(II) ions are still displaced by hydrogen ions in the presence of Na_2SO_4. After the acid leaching, the results suggest that in the presence of up to 500 mM Na_2SO_4, the Cd(II) unloaded PSAs are fully disassociated in 0.1 M hydroxide ions. In conclusion, more than 98% of the Cd(II) ions are recovered, even in the presence of 200 mM Na_2SO_4, into a 20 times more concentrated acidic solution in 15 minutes; no notable effects due to the presence of Na_2SO_4 are found on the recovery of PEI and SDS.

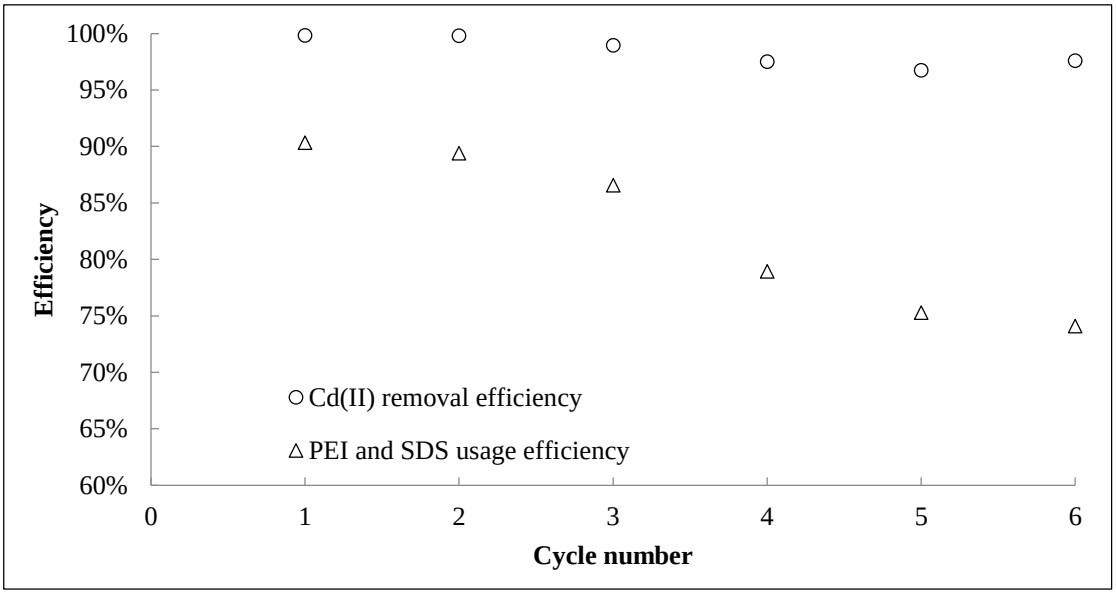

Figure 5.8: Cd(II) removal and PEI–SDS usage efficiencies in 6 cycles using regenerated PEI and SDS.

Recycling of the regenerated PEI and SDS was examined for up to 6 cycles of removing 11 ppm (0.1mM) Cd(II) from solution without any make-up of PEI and SDS. The purpose is to evaluate the extent of deterioration of the regenerated PEI–SDS after each cycle. The Cd(II) removal efficiency remains above 98% after 6 cycles. This removal is the result of the polymer–surfactant aggregate process, and not cadmium hydroxide precipitations – the pH is neutralised before stirring. Since the PSA removal capacity is almost twice the added amount of Cd(II) shown in the previous chapter, the removal efficiency does not decrease with a small decrease of the available PSAs.

The PEI–SDS usage efficiency, however, decreases from 90% in the first cycle to 74% in the sixth cycle (Figure 5.8). This may seem like a notable decrease, but the value of total carbon in the treated clean water only increases from 8 ppm to 22 ppm, which is still at a low level. The total carbon in the filtrate is mainly due to the leakage of SDS monomers, because the coarse filter cannot retain the surfactant monomers which are caused by the critical aggregation concentration (CAC) and a slow shifting of the optimum dosage for PSA formation. When the concentration of free SDS monomers is above its CAC, further SDS monomers then form more aggregates on the polymer chains, which bind to metal ions. In other words, there must be a small amount of SDS monomers which exist in the solution to build up the surfactant concentration to allow for the formation of PSAs, which will consequently pass through the coarse filter into the filtrate. The ratio between PEI and SDS, therefore, is slowly shifted away from the optimal dosage after each cycle. The SDS titration results also suggest that the carbon content of the SDS in the filtrate is almost equal to the total carbon measured, so the polymer is absent. To further confirm this, the filtrate is further filtered by a 30K ultrafiltration to completely reject the possibly leaked 750K PEI. The results show no difference in the total carbon

content before and after ultrafiltration. Thus, little PEI is present in the coarse-filtered filtrate.

In summary, the stable removal efficiency over 6 cycles demonstrates that PEI and SDS can be recycled multiple times without a deterioration of removal ability, which enhances the sustainability of the process and saves on the chemical costs. As previously noted, the relatively pure concentrated metal ion solution as a secondary product may be recycled back into a manufacturing process or sold as a revenue stream.

5.6. Recovery of metal ion mixtures

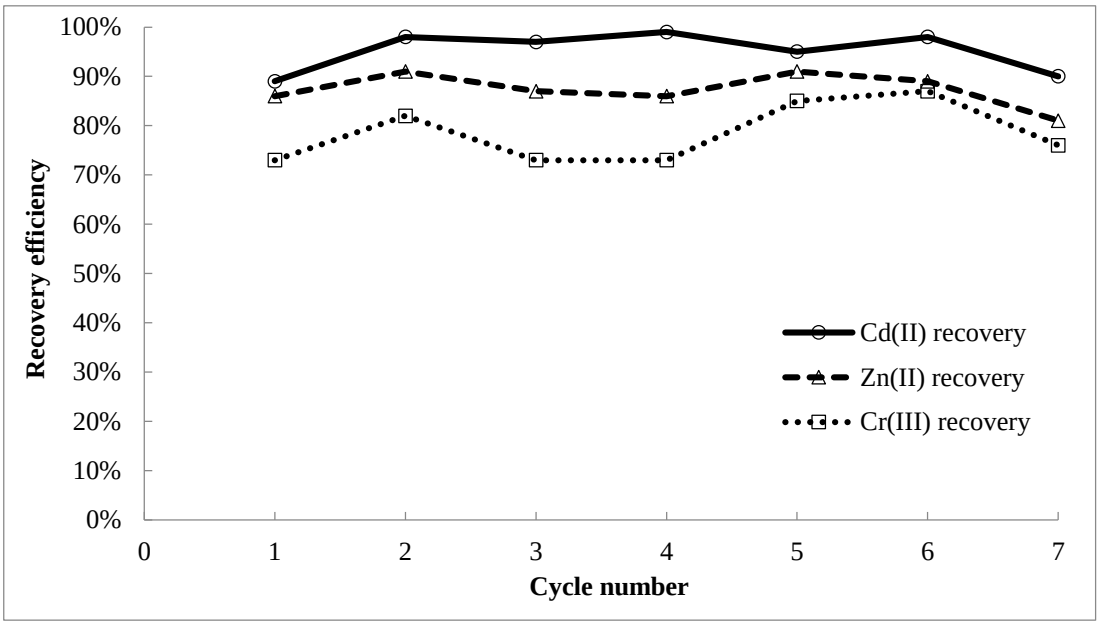

Figure 5.9: Recovery efficiencies of PSAs with metal ion mixtures in 7 cycles at 0.1 M hydrogen ions and a concentration factor of 15.

As well as validating the removal ability of the regenerated PEI and SDS, the recovery ability is also investigated with cycle number. Overall, the recovery efficiencies remain stable at a high level over 7 cycles (Figure 5.9).

At a pH of 1, no strong selectivity among the metal ions is found. The order of recovery efficiency is Cd(II) > Zn(II) > Cr(III), because the electrostatic interactions between SDS headgroups and Cd(II) are weaker than for Zn(II). In addition, the Cr(III) has the strongest interaction among the metal ions as it has the highest charge density among them. The selectivity at the recovery stage could be improved, if a relatively moderate pH solution is used to recover Cd(II) first, and then the acidity level is increased to recover higher charge density ions sequentially. This order of mixture recovery efficiency implies that the selective recovery of metal ion mixtures is achievable, which is a subject of future study.

In conclusion, the pH adjustment method works effectively for recovering metal ion mixtures into a highly concentrated metal ion solution and regenerating PEI and SDS to treat the next cycle of metal ion mixtures without a deterioration in removal ability.

5.7. Discussion and summary

A novel process to remove metal ions from dilute aqueous solutions was previously presented. A metal ion recovery and polymer–surfactant recycle method has now been developed. This method uses an acid solution to recover the heavy metal ions from the flocculated PSAs, and then coarse filters the highly concentrated metal ion solution from the flocs. After that, the metal unloaded flocs are completely dissolved in a base solution to regenerate PEI and SDS, which is recycled into the next process cycle without a deterioration in removal ability. Finally, the pH of the solution is neutralised by adding a small amount of H_2SO_4 to optimise the formation of PSAs in the next cycle.

Due to the neutralisation step at the beginning of each cycle, salt (Na_2SO_4) is formed and accumulated in the process, which leads to the treated filtrate and recovered metal solution containing about 280 ppm and 100 ppm of Na_2SO_4 after 10 cycles, respectively. To minimise the salt formation and accumulation without compromise the treatment performance, a high concentration factor (> 20) and a long residence time (15-20 min) are suggested at the recovery stage.

The removal and recovery performance of metal ion mixtures using regenerated PEI and SDS are also studied. The results suggest that a pH of 1, a concentration factor of 20, and 15 min residence time are the operational conditions for optimal metal recovery, which can recover more than 95% of bound heavy metal ions into a 20 times more concentrated acidic solution. This solution can be either recycled back into a manufacturing process or sold directly. Most importantly, the metal removal and recovery efficiencies remain at high levels after using 6 process cycles involving recycle of the regenerated PEI and SDS without any make-up.

These recovery and recycle stages, therefore, complete the whole treatment process of the PSA process, and significantly save the chemical usage and enhance the sustainability of the process.

Chapter 6

Investigation of the Selective Removal of metallic anions from Dilute Aqueous Solutions by the Polymer–Surfactant Aggregates

6.1. Introduction

Metallic anions are widely used in the plating and pigment industries. Like metal cations (e.g. chromium and iron), their metallic anions can also be present in a stable and multivalent form in aqueous solutions, such as oxyanions and bound with cyanide ions, such as CrO_4^{2-}, $Cr_2O_7^{2-}$ and $Fe(CN)_6^{3-}$. They usually exist in a dilute concentration within a wide range of solutions, and can accumulate in ecological systems to cause health disorders. Because of this, their presence in aqueous effluent has also attracted a great deal of attention with respect to the development of mitigation techniques.

All metallic anion removal techniques have their inherent advantages and limitations

in their various applications, depending upon the characteristics of the wastewater and the treatment requirements. Ion exchange is highly effective in the removal of small amounts of contaminants at high concentrations (Higgins, 1973, Jorgensen and Weatherley, 2003, Vaaramaa and Lehto, 2003), but the cost and secondary pollution when regenerating the resin are critical. Thus, it is not economical to treat large amounts of dilute metallic anion wastewater by ion exchange. Electrochemical techniques are regarded as rapid and well-controlled methods to remove both metallic cations and anions with fewer chemical additions and less sludge production (Gözmen et al., 2003). The drawbacks are high capital and running costs. Adsorption is an alternative method to treat dilute systems, but striking the balance between high cost and strong effectiveness of the physico-chemical adsorbent is an issue (Xu et al., 2002, Hilal et al., 2005, Boukhalfa, 2010). Biosorption has proven a promising and sustainable removal method. The advantages are high overflow rate and production of concentrated sludge. However, the capital, maintenance and operational cost are high (Loukidou et al., 2003, Deng and Ting., 2005). Finally, membrane filtration technology is an efficient method, but high capital and operating cost, membrane fouling and low filtrate flux are limitations (Gzara and Dhahbi, 2001, Sato et al., 2002, Tangvijitsri et al., 2002, Hilal et al., 2004, Shafiquzzaman et al., 2011). Therefore, treating dilute anion contaminated aqueous streams remains as a challenge with no clear and effective solution.

To face the challenge and fill the resulting niche, polymer–surfactant aggregates have been applied for treating cations from dilute aqueous streams (Shen et al., 2015). This process essentially uses a structure called a polymer surfactant aggregate (PSA), which is formed under a certain range of dosage ratio between oppositely charged polymer and surfactant ions (Penfold et al., 2006, Bell et al., 2007). PSA has been successfully applied

to remove metal ions from dilute aqueous solutions, and surface tension measurements have been used to show that the PSA is responsible for removing the metal ions (Shen et al., 2015). Electrical conductivity measurement is one of the common methods used for investigating the interactions between polymer and surfactant in the bulk solution (Winnik et al., 2000, Nizri et al., 2008). For example, the CMC of a surfactant can be measured by the break point in the increase of conductivity with concentration (Fuguet et al., 2005). The PSAs form at low surfactant and polymer concentrations (<250 ppm cationic surfactant; <100 ppm anionic polymer) due to electrostatic and hydrophobic interactions, and contain both positive and negative charges (Taylor et al., 2002, Taylor et al., 2003, Zhang et al., 2005, Fegyver and Mészáros, 2015). In the removal process, many individual nano-scale PSAs with a high surface-volume ratio then bind to dilute anions via electrostatic forces and chelation. Due to their containing both positive and negative charges, while binding with the metallic anions, they also intermolecularly associate with each other at charge neutralisation to form large flocs and settle down. After settling or coarse filtering from the treated streams, the PSA flocs are potentially dissolvable and recyclable and the anions recoverable in a concentrated form. Because of these features, the PSA process has the benefit of using a small amount of recyclable removal agent to remove anions from dilute aqueous streams without the need for a membrane or other expensive processing.

In this chapter, the PSA has been applied to remove metallic anions from dilute aqueous solutions. The effects of different charge density of the polymer on the treatment performance, and the adsorption limits and kinetics as a function of polymer, surfactant and anion are studied. Finally, the effects of separation method, pH, temperature, salt and organic contaminant on the anion removal efficiency are investigated. The selectivity

between multivalent anions is also explored.

6.2. Materials and methods

Poly (acrylic acid) (PAA) solutions were prepared by diluting stock PAA solution (Sigma Aldrich, average MW <100,000, 35 wt.% in H_2O). Poly (sodium 4-styrenesulfonate) (PSS) (average MW 1,000,000), sodium dodecyl sulphate (SDS (purity ≥99.9%) and myristyl trimethyl ammonium bromide (MTAB) (purity ≥99%) were obtained from Sigma Aldrich. Potassium chromate, potassium ferricyanide, and potassium chloride were purchased from Fisher Scientific (all purity ≥99%).

The solution preparation, filtration, total carbon and metallic anion concentration measurements follow Sections 3.2.1., 4.2.1., 4.2.3 and 4.2.4. For the temperature adjustment, a hotplate stirrer (UC152, Stuart) was used to maintain the desired temperature of solution. The MTAB concentration was measured by two-phase mixed indicator titration. The method is discribed in Section 4.2.3., but the titrant here was SDS and the ending point was when the bottom phase turns from blue to pink. Having the measurement of MTAB concentration from titration, the PAA concentration in the filtrate was calculated from Equation 6.1.

$$C_{\text{PAA filtrate}}(\text{ppm}) = \frac{\text{Total carbon}_{\text{filtrate}} - C_{\text{MTAB filtrate}} * \text{Carbon content}_{\text{MTAB}}}{\text{Carbon Molecular weight by percentage}_{\text{PAA}}} = \frac{\text{Total carbon}_{\text{filtrate}}(\text{ppm}) - C_{\text{MTAB filtrate}}(\text{mM}) * 204\text{g/mol}}{0.5} \quad (6.1)$$

Equation 6.1: Calculation of PAA concentration in the filtrate.

The concentrations of chromate and ferricyanide were measured by an atomic adsorption spectrometry (200 Series AA, Agilent Technologies) and a UV-VIS spectrometry (UV-1800, Shimadzu). The phosphate concentrations were measured by

Hach-Lange LCK349 cuvettes. Assuming the volume of solution before and after treatment is consistent, the polymer surfactant usage efficiency and anion removal efficiency are defined by Equation 6.2 .

$$\text{Polymer surfactant usage efficiency } = (1 - \frac{\text{Total carbon}_{\text{filtrate}}}{\text{Total carbon}_{\text{original}}}) \times 100\%$$

$$\text{Anion removal efficiency } = (1 - \frac{\text{C}_{\text{filtrate}}}{\text{C}_{\text{original}}}) \times 100\% \quad (6.2)$$

Equation 6.2: Calculations of polymer surfactant usage and anion removal efficiencies.

The binding selectivity between anions is evaluated by binding coefficient, which is calculated by Equation 6.3.

$$PSA + Anion\ 1 \leftrightarrow PSA - Anion\ 1$$

$$K_{PSA-anion\ 1} = \frac{[PSA - Anion\ 1]}{[PSA][Anion\ 1]}$$

$$PSA + Anion\ 2 \leftrightarrow PSA - Anion\ 2$$

$$K_{PSA-anion\ 2} = \frac{[PSA - Anion\ 2]}{[PSA][Anion\ 2]}$$

$$PSA - Anion\ 1 + Anion\ 2 \leftrightarrow PSA - Anion\ 2 + Anion\ 1$$

$$K_{anion\ 1,2} = \frac{[PSA-Anion\ 2][Anion\ 1]}{[PSA-Anion\ 1][Anion\ 2]} = \frac{K_{PSA-anion\ 2}[PSA][Anion\ 1][Anion\ 2]}{K_{PSA-anion\ 1}[PSA][Anion\ 1][Anion\ 2]} =$$

$$\frac{K_{PSA-anion\ 2}}{K_{PSA-anion\ 1}} = \frac{\frac{[PSA-Anion\ 2]}{[PSA][Anion\ 2]}}{\frac{[PSA-Anion\ 1]}{[PSA][Anion\ 1]}} = \frac{[PSA-Anion\ 2][Anion\ 1]}{[PSA-Anion\ 1][Anion\ 2]} \quad (6.3)$$

Equation 6.3: Calculations of selectivity coefficient between anion 1 and anion 2.

6.3. Variables in the removal of metallic anions by PSS/PAA and MTAB

6.3.1. Polymer and surfactant dosage and ratio

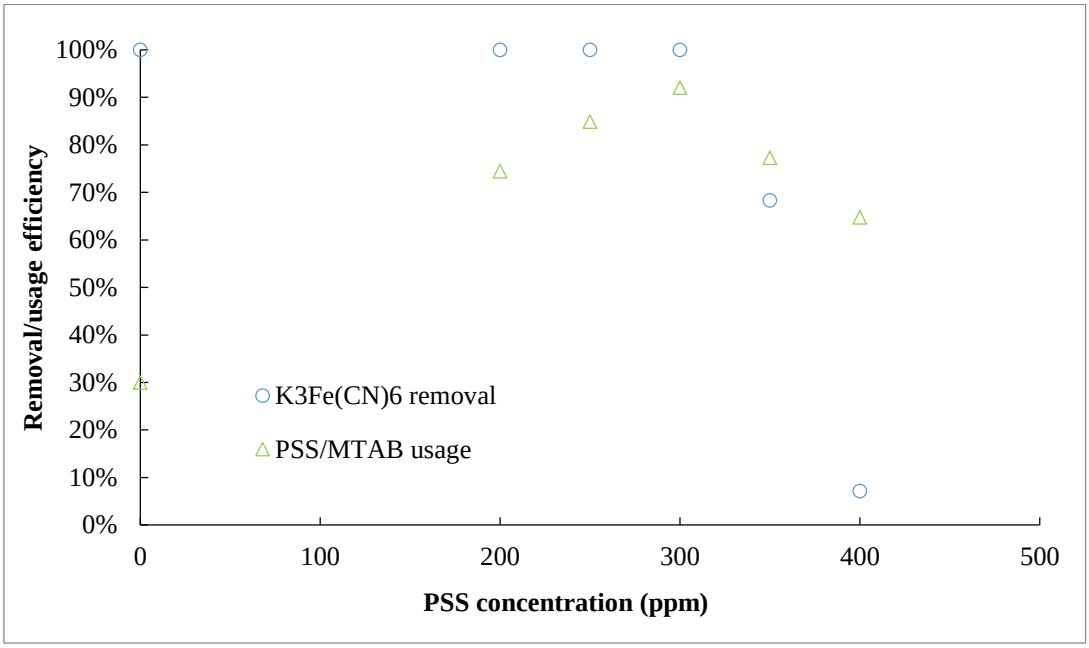

Figure 6.1: Dosage optimisation for 1.5 mM MTAB and varying amounts of PSS to remove 0.1 mM $K_3Fe(CN)_6$.

PSS and PAA are mixed individually with MTAB to remove anions from dilute solutions. In Figure 6.1, it may seem that the addition of PSS is unnecessary, because $Fe(CN)_6^{3-}$ can act as a flocculant to precipitate with MTAB as $(MTA^+)_3Fe(CN)_6^{3-}$, and lead to a complete removal of itself in the absence of PSS; however, nearly 70% of the added MTAB passes through coarse filtration, and reports in the filtrate. Without the addition of PSS, the process only replaces one unwanted species ($Fe(CN)_6^{3-}$) with another species (MTAB) in the solution, which is not ideal for the quality of treated effluents and the polymer surfactant usage efficiency.

With increasing amounts of PSS in the solution, the $Fe(CN)_6^{3-}$ removal efficiencies

remain at a high level, but more importantly the polymer surfactant usage efficiency increases from 30% to around 95% at 300 ppm PSS. The increase of the efficiency is due to the formation of PSAs by PSS and MTAB, which is demonstrated in Figure 3.31. When both the removal and usage efficiencies reach the highest value, the polymer and surfactant dosage is at its optimum ratio. Upon further increasing the PSS concentration, the amount of surfactant is now not enough to saturate all the PSS to form PSAs. Thus some of the surfactant monomers are moved from PSAs, and bound to polymer chains in the form of polymer–surfactant complexes rather than in aggregates. The polymer–surfactant complex is not as effective as the PSA in binding $Fe(CN)_6^{3-}$ ions, because its overall charge is almost neutralised by monomers. Therefore, the removal efficiency of $Fe(CN)_6^{3-}$ decreases rapidly.

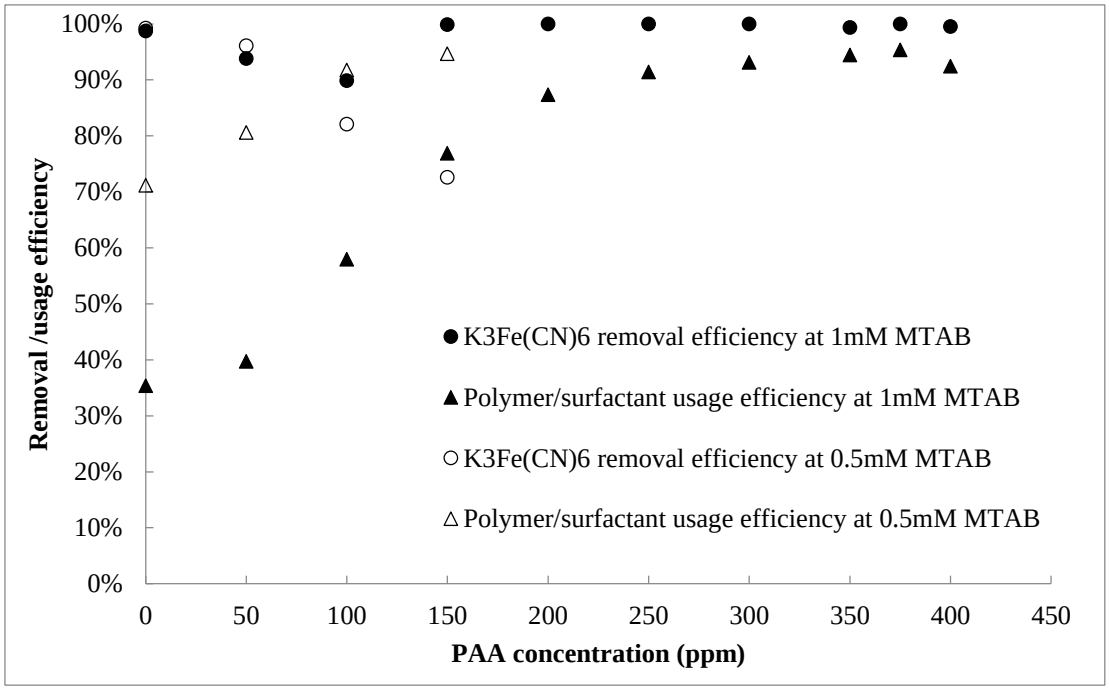

Figure 6.2: Dosage optimisation for 0.5 mM and 1 mM MTAB and varying amounts of PAA to remove 0.1 mM $K_3Fe(CN)_6$.

With regard to the PAA-MTAB system, the removal performance of $Fe(CN)_6^{3-}$ is

broadly similar to that for the PSS-MTAB system (Figure 6.2). The reason to test PAA is that the charge percentage of PAA strongly depends on the pH of the solution, which can be used to manipulate the charge density and the interactions between PAA and MTAB. This manipulation may be the key for recycling the polymer and surfactant. In Figure 6.2, 0.5 mM and 1 mM MTAB are tested with varying amounts of PAA without adjusting pH. Without any addition of PAA, at 0.5 mM MTAB, almost 100% of $Fe(CN)_6^{3-}$ and 70% of MTAB are retained by the filter in the form of the $Fe(CN)_6^{3-}$-MTAB precipitates. In other words, 30% of MTAB passes into the filtrate as an unwanted species Interestingly, with increasing PAA concentration to 150 ppm, the removal efficiency decreases from 100% to 70%, because some of the MTAB that was used to form the $Fe(CN)_6^{3-}$-MTAB precipitates is now bound with the PAA. Thus, the remaining MTAB monomers are insufficient to from precipitates with all of the $Fe(CN)_6^{3-}$.

In a higher MTAB concentration curve (1mM), the decrease in the initial removal efficiency still occurs for the same reason as that in the 0.5 mM MTAB curve. However, upon further increase of the PAA concentration, the removal efficiency returns to above 99%, and the main mechanism is probably shifted from precipitating with the MTAB to electrostatic binding with the PSAs. The polymer surfactant usage efficiency gradually increases with the increase of PAA concentration until 350 ppm; after that, the PAA-MTAB ratio is not optimal for the formation of PSAs to bind the anions. The ratio seems rather high in terms of the PAA usage, because the PAA is not fully dissociated or charged in the original solution (~ a pH of 4) without adjusting the pH, and only the charged segments in PAA can electrostatically interact with MTAB. Thus, increasing the charge percentage of PAA by adjusting the pH is a way to reduce the PAA usage.

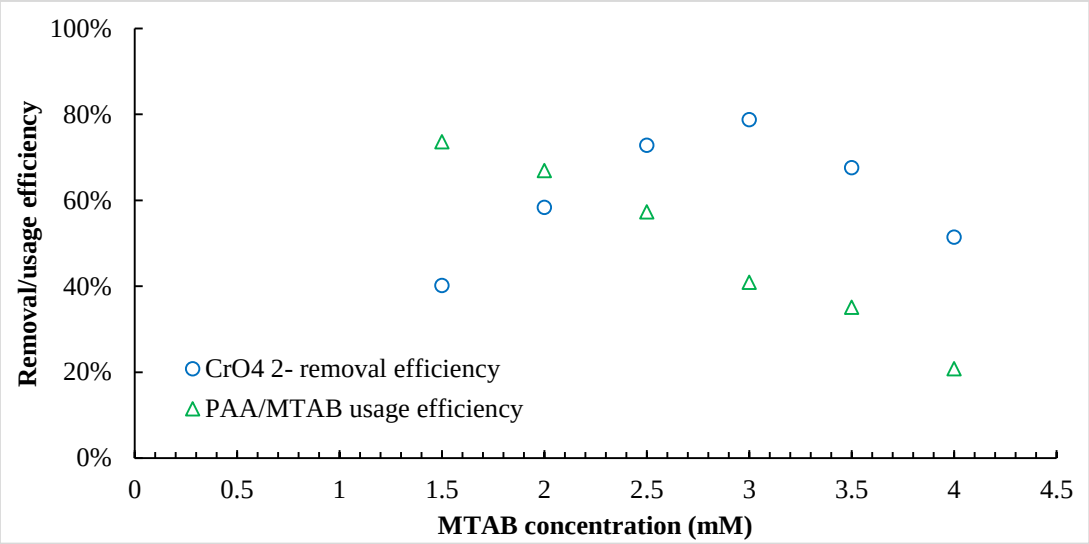

Figure 6.3: Dosage optimisation for 100 ppm PAA and varying amounts of MTAB to remove 0.2 mM K_2CrO_4 at a pH of 5.3.

CrO_4^{2-} is also removed in the PAA-MTAB system. The charge density of the chromate group is lower than that of the $Fe(CN)_6^{3-}$ group, which results in a relatively weak binding strength to MTAB. For this reason, without increasing the charge percentage of PAA, only 5% of the 0.2mM chromate is removed at the optimum dosage which applies for removing 0.1 mM $Fe(CN)_6^{3-}$ (350 ppm PAA and 1.5 mM MTAB in Figure 6.2). To increase the charge percentage of the PAA, the pH of the original solution is increased from 4 to 5.3 to disassociate PAA above 90%, as the pKa of PAA is 4.2. This latter value means that 50% of PAA is disassociated at a pH of 4.2, and 90% of PAA at a pH of 5.2. When most of the PAA is negatively charged, the highest chromate removal efficiency increases from 5% to about 80% using only 100 ppm PAA (see Figure 6.3). Considering both the removal and usage efficiencies, the optimum dosage for removing 0.2 mM chromate is 100 ppm PAA and 2.5 mM MTAB (Figure 6.3). After adjusting the pH, the PAA usage in the optimum dosage decreases from 350 ppm to 100 ppm, owing to the increase of charge percentage. The polymer surfactant usage efficiency is only 60%. The calculated results

from MTAB titration and total carbon analysis in the filtrate suggest that almost all carbon leakage comes from the MTAB, which is about 1.2mM. This leakage at 100 ppm PAA is probably equivalent to the critical flocculation concentration (CFC); note the CFC is about 1.6 mM in the 200 ppm PAA curve via the conductivity measurements (Figure 3.30).

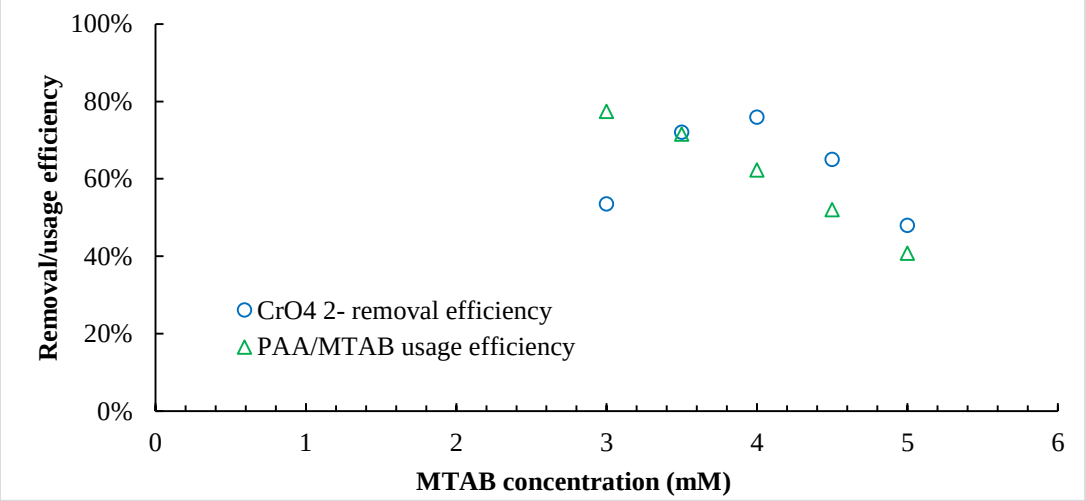

Figure 6.4: Dosage optimisation for 200 ppm PAA and varying amounts of MTAB to remove 0.2 mM K_2CrO_4 at a pH of 5.3.

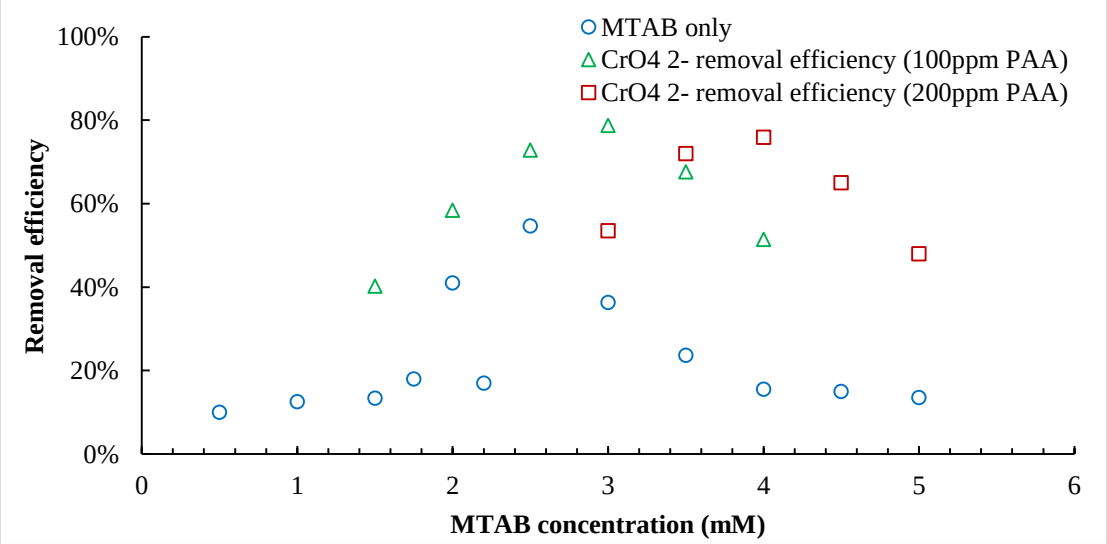

Figure 6.5: Effects of different PAA dosages and varying amounts of MTAB on the removal efficiency of 0.2 mM K_2CrO_4 at a pH of 5.3.

Due to the incomplete removal of chromate at 100 ppm PAA, a higher dosage of PAA (200 ppm) is optimised with MTAB to understand the effects of total PSA amount on the chromate removal efficiency, and to confirm the correlation between the leaked (filtrate) MTAB concentration and its CFC. In Figure 6.5, the highest removal (~80%) with 200 ppm is almost the same as it is using 100 ppm PAA.

It is worth noting that, at 3 mM MTAB, the 100 ppm curve shows a higher removal efficiency of chromate than for 200 ppm. If the PAA only acted as a flocculant to increase the size of MTAB-chromate precipitates, the chromate removal efficiency would increase with increasing PAA concentration from 100 to 200 ppm. On the contrary, the removal efficiency actually decreases, because the extra PAA neutralises the limited amount of MTAB which might be used to form PSAs, instead forming polymer–surfactant complexes. In this case, therefore, the amount of available PSAs decreases with the addition of PAA, and this leads to the decrease in chromate removal efficiency.

At the highest removal efficiency for both the 100 ppm and 200 ppm plots, most of the PAA is saturated to form PSAs (Figure 6.5). The removal efficiency plot for 100 ppm PAA could be moved to the right by 1 mM superimpose on the plot for 200 ppm PAA. This may well suggest that the extra 100 ppm PAA consumes approximately 1 mM MTAB to form the extra amount of PSAs; these PSAs do not increase the removal efficiency, only the total removal capacity. Thus, the incomplete maximum chromate removal is not caused by the quantity of available PSAs. The possible cause of this incomplete removal is discussed in detail in the section on removal limits (Section 6.3.3.).

In the absence of PAA, less than 60% of the chromate is also removed after coarse filtration, but more than 95% of added MTAB are reported in the filtrate (Figure 6.5). This is caused by the same reason (precipitation) as the $Fe(CN)_6^{3-}$-MTAB system, but the

removal efficiency of chromate is lower as a result of its low charge density. The MTAB leakage is severe (95%), but can be reduced to 30% with the addition of PAA. One way of further reducing the leakage of MTAB is to decrease its CFC by increasing the charge percentage of PAA, which is discussed in Sections 6.3.3 and 6.3.4.

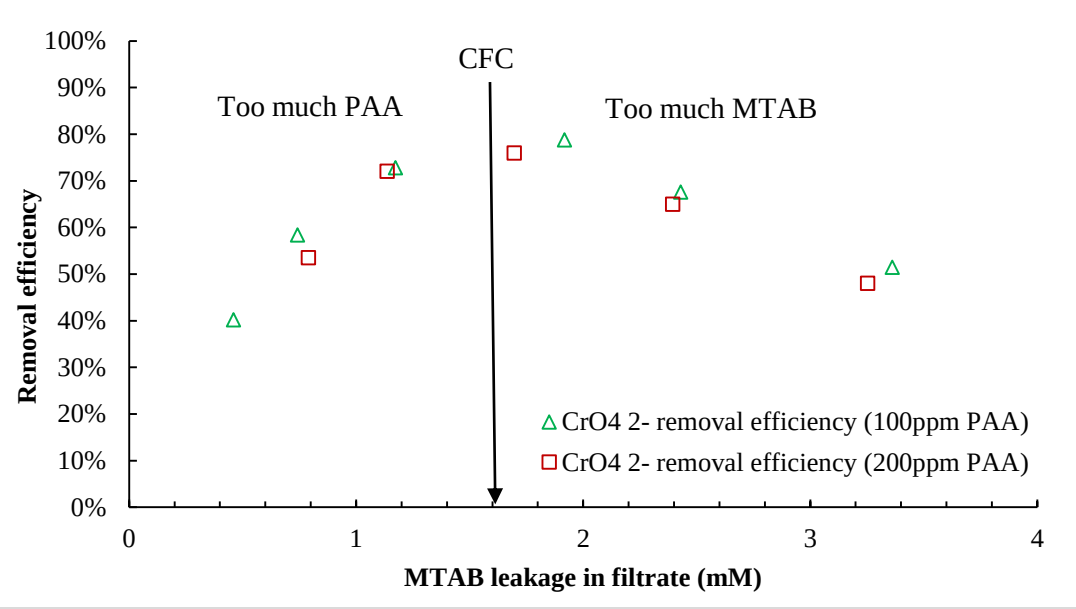

Figure 6.6: Correlations between the MTAB leakage in the filtrate and the CrO_4^{2-} removal efficiency at 100/200 ppm PAA at a pH of 5.3.

To further confirm that the extra amount of PSAs has little effect on the chromate removal above a certain level, the removal efficiencies are plotted against the concentration of leaked MTAB in the filtrate (Figure 6.6). From conductivity measurements in Chapter 3, the CFC of MTAB in 200 ppm PAA is approximately 1.6mM (Figure 3.30), which is around the concentration of leaked MTAB at the highest removal efficiency for both 100 ppm and 200 ppm PAA systems. Assuming the change in MTAB monomer concentration across the coarse filter is negligible, the concentration of leaked MTAB should be equal to the concentration of bulk MTAB. Thus, at the highest removal

efficiency, the amount of MTAB is just enough to saturate most of the PAA to form PSAs, and the monomer concentration should equal the CFC (1.6mM), as highlighted in Figure 6.6. This also explains the interpretation of the change of increase of conductivity for the PAA-MTAB system.

When the MTAB leakage is lower than the CFC, the excessive amount of PAA forms polymer–surfactant complexes, which consume the MTAB that may leak into the filtrate. It is worth noting that even when the leaked MTAB concentration is slightly below the CFC, PSAs can still form when the local concentration (near the PAA chain) of MTAB is above the CFC under the electrostatic and hydrophobic interactions. At lower MTAB concentrations than this, the interactions become too weak to allow this. Therefore, some of the chromate is removed when the leaked MTAB concentration is lower than its CFC, and the removal efficiency decreases with decreasing MTAB leakage. On the other hand, when the leakage is higher than the CFC, the excessive amount of MTAB leaks directly into the filtrate, and the decreasing chromate removal efficiency is probably a result of the increasing ionic strength from the counter ions of the extra MTAB and an inefficient flocculation due to negative repulsion between PSAs.

In conclusion, an extra amount of PSAs above a critical amount does not promote the removal efficiency of chromate, and the high removal is mainly due to binding with the PSAs, rather than the precipitation with MTAB.

6.3.2. Filtration method

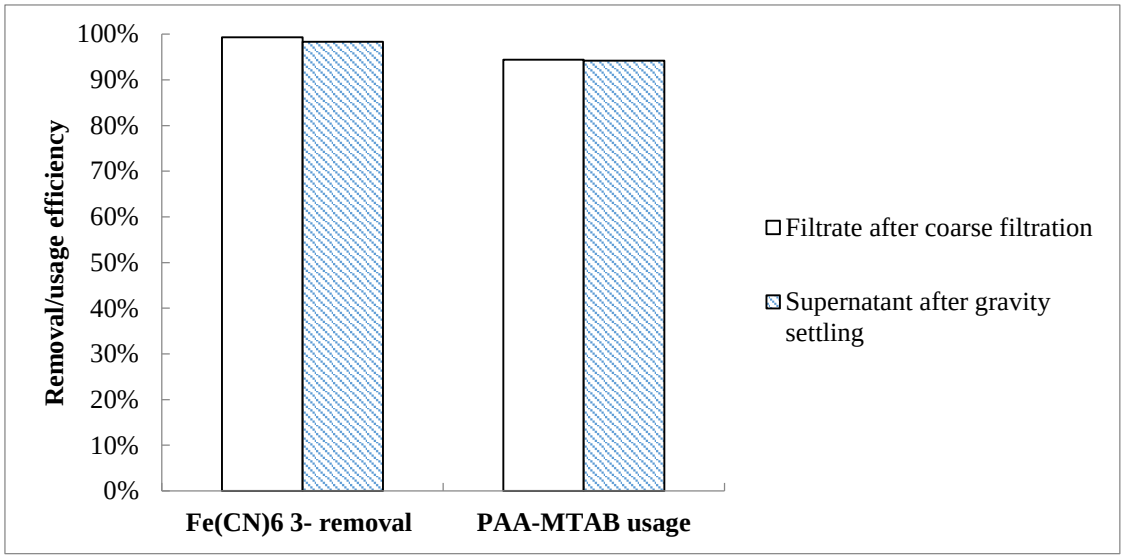

Figure 6.7: Effects of coarse filtration on $Fe(CN)_6^{3-}$ removal and PAA-MTAB usage efficiencies at the optimum dosage (350 ppm PAA+ 1 mM MTAB).

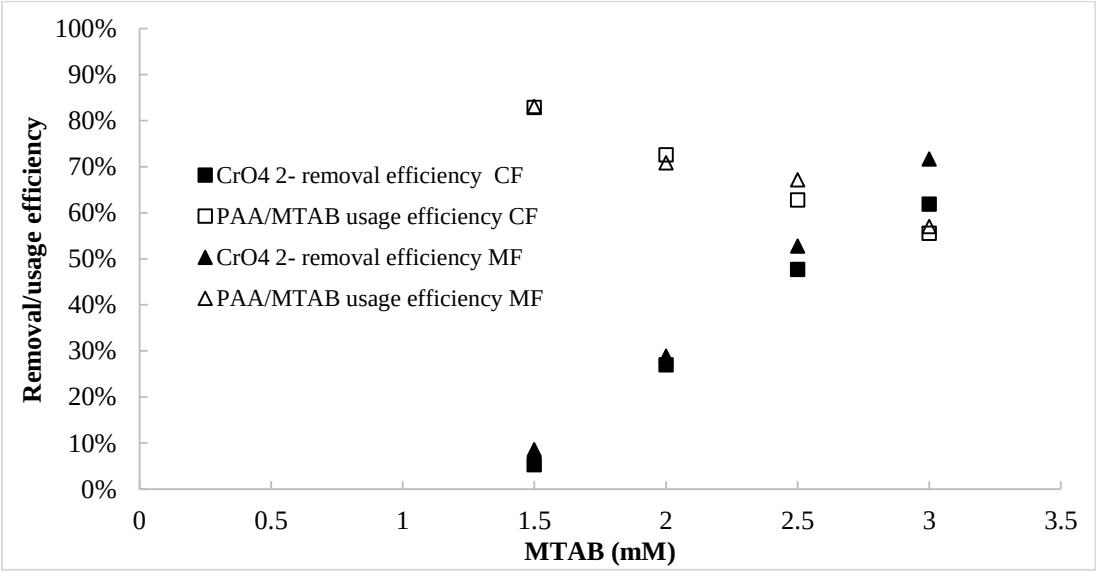

Figure 6.8: Effects of microfiltration (MF) and coarse filtration (CF) on the removal efficiency of 0.2 mM K_2CrO_4 and the usage efficiency of 100 ppm PAA and varying amounts of MTAB.

The treatment outcome for removing $Fe(CN)_6^{3-}$ is almost the same for the after coarse filtration and gravity settling (Figure 6.7). Thus, the coarse filtration is a method of speed

up the gravity settling. The $Fe(CN)_6^{3-}$ ions have a high charge density. This allows them to be removed effectively as a targeted component, and enhance the speed and effectiveness of the flocculation of PSAs. This synergistic effect can obviate the need for a filtration, which further increases the speed of the process, and subsequently increases the treatment capacity.

Regarding the chromate removal, owing to the relatively low charge density, the synergistic effect in the chromate system is weak. The chromate flocculated solutions are filtered by both micro-filtration and coarse filtration, respectively. In Figure 6.8, the results show there is little difference in removal and usage efficiencies for the two filtration methods due to the highly effective self-flocculation of PSAs. Furthermore, a coarse filter is capable of separating the flocs and/or colloids from the solution with less filtration time than using microfiltration. In short, the use of either coarse filtration or gravity settling for rapid separation depends upon the charge density of anions.

6.3.3. Removal limit and capacity

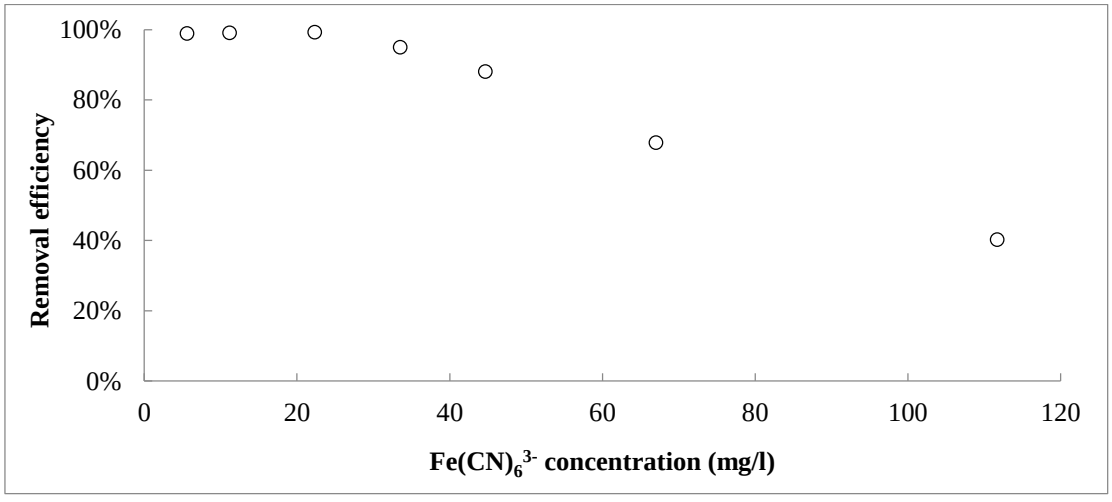

Figure 6.9: $Fe(CN)_6^{3-}$ adsorption capacities of the PSAs at the optimum dosage (350 ppm PAA + 1 mM MTAB).

With regard to the $Fe(CN)_6^{3-}$-PAA-MTAB system, the removal efficiency of $Fe(CN)_6^{3-}$ starts to decrease as the $Fe(CN)_6^{3-}$ concentration rises slightly above 20mg/l, and gradually decreases with increasing $Fe(CN)_6^{3-}$ concentration (Figure 6.9). This suggests that the adsorption capacity of PSAs at the optimum dosage is limited. From the $Fe(CN)_6^{3-}$ concentration in the filtrate, the PSAs can effectively remove $Fe(CN)_6^{3-}$ down to concentration of 10 ppb.

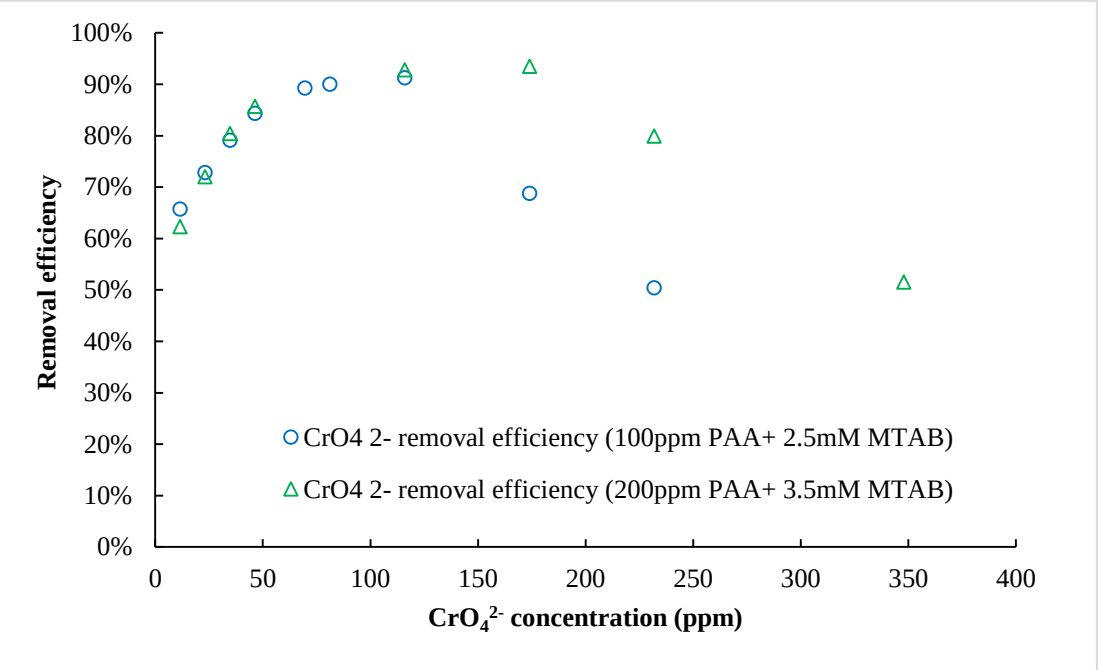

Figure 6.10: Removal efficiency of K_2CrO_4 at two optimum dosages of PAA and MTAB with increasing concentrations of K_2CrO_4.

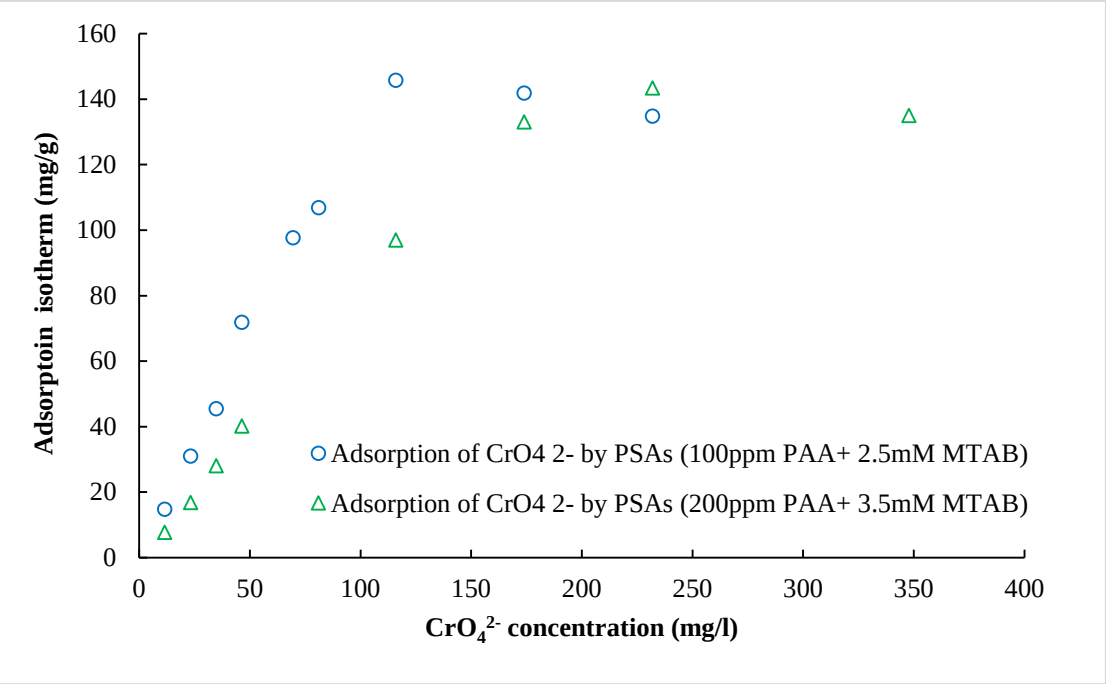

Figure 6.11: Adsorption isotherm of CrO_4^{2-} at two optimum dosages of PAA and MTAB with increasing concentrations of K_2CrO_4.

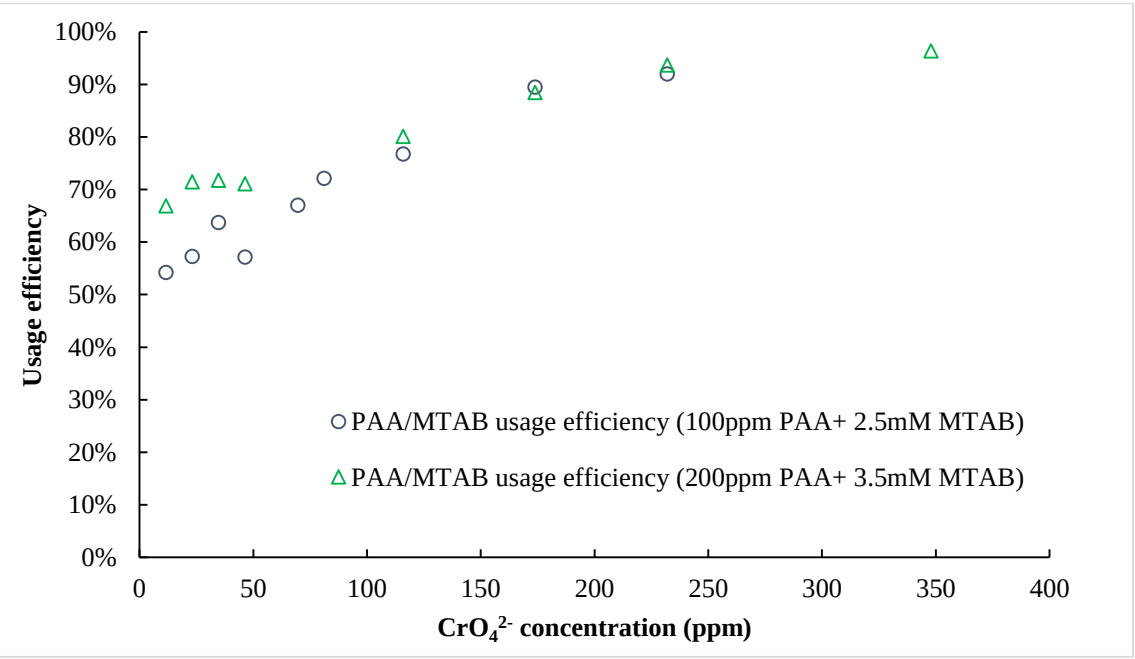

Figure 6.12: Usage efficiency of PAA and MTAB at two optimum dosages of PAA and MTAB with increasing concentrations of K_2CrO_4.

With regard to the K_2CrO_4-PAA-MTAB system, the overall trend in the low CrO_4^{2-} concentration range is rather different to that for $Fe(CN)_6^{3-}$ (Figure 6.10). The chromate removal efficiency at 100ppm PAA increases to above 90% with increasing chromate concentration until levelling off at 70mg/l. The subsequent level and then decreasing removal efficiency is due to the limited adsorption capacity of the PSAs. This capacity can limit the removal efficiency at a high concentration of metallic ions, but at a low concentration, the removal limits play an important role, which is defined as the minimum concentration of metallic ions can be treated down to in the filtrate. As chromate has a relatively low charge density, the removal limit of PSAs for chromate is relatively high (7 ppm) when compared with 10 ppb for the $Fe(CN)_6^{3-}$. Given the relatively high removal limit, at a low chromate feed concentration (< 70 mg/l), the available binding sites in PSAs are not fully saturated. Thus, before reaching the saturation point, the increase of removal efficiency is a result of the increasing amount of chromate that saturates the PSA with constant concentration in the filtrate at the removal limit.

In Figure 6.10, the removal efficiency for the 200ppm PAA system continues to increase until the chromate feed concentration reaches ~174 mg/l, which is about twice as high as the adsorption amount in the 100 ppm PAA system. This is also supported by the adsorption isotherm (Figure 6.11). The results show that both 100ppm and 200ppm PAA systems level off at the same amount of chromate adsorption per gram of PSA (~140 mg/g), and the 100 ppm PAA curve reaches the plateau first, which indicates the PSAs are saturated first. This is useful for determining the polymer and surfactant dosages to remove a certain amount of metallic anions, which are mainly based on the linear relationship between the polymer dosage and ion concentration, and the surfactant dosage should be just enough to saturate the polymer to form PSAs.

Another important change with increasing K_2CrO_4 concentration is the increase of ionic strength, which increases the polymer surfactant usage efficiency (Figure 6.12). At a higher ionic strength, the screening of electrostatic repulsive forces between monomers in aggregates promotes the formation of PSAs at a lower MTAB concentration, which is in the same way that the CMC is lowered by increasing ionic strength. Therefore, the polymer surfactant usage efficiency may be higher in real waste streams than in the deionised water, as a result of a higher ionic strength.

6.3.4. pH

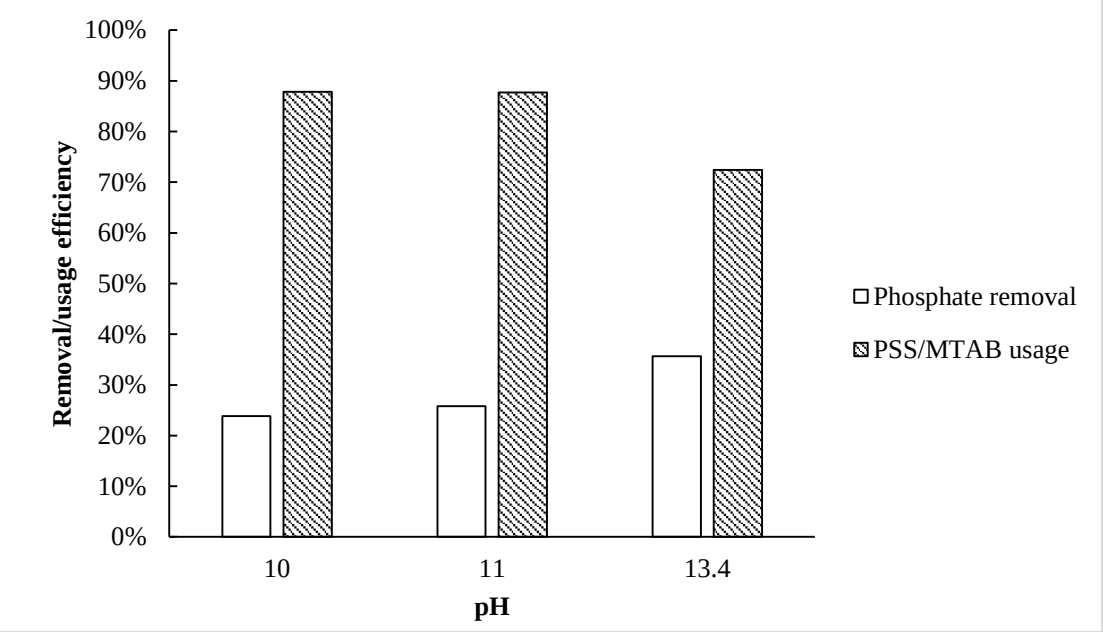

Figure 6.13: Phosphate removal and PSS-MTAB usage efficiencies at the optimum dosage (350 ppm PSS+ 1.5 mM MTAB) at several pH values.

Phosphate is one of the primary concerns when discharging the wastewater into environment. It may cause the eutrophication, and subsequently consumes the dissolved oxygen in the receiving water, resulting serious effects on the aquatic plants and animals.

To face the concern, the PSAs are proposed to bind phosphate, and then separated together from solution by coarse filtration. According to a phosphoric acid speciation, phosphate exist primarily in the $H_2PO_4^-$ form at a pH of 6; with increase of pH value, the composition of phosphate shifts to multivalent forms (HPO_4^{2-} and PO_4^{3-}): almost 100% of phosphate exists as HPO_4^{2-} at a pH of 10, and PO_4^{3-} is the predominant form at a pH of 14. At the pH values in between, it comprises a combination of $H_2PO_4^-$, HPO_4^{2-} and PO_4^{3-}, (e.g. at a neutral pH, theoretically, the solution contains half $H_2PO_4^-$ and half HPO_4^{2-}), and the average valence increases with the pH values.

Owing to the electrostatic bindings between PSAs and monovalent ions are relatively weak, approximately 15% of total 0.1 mM phosphate (i.e. 30% of HPO_4^{2-}) is removed at a pH of 7 from the solution. With increasing pH, the proportion of multivalent phosphate is increased as expected, but the removal efficiency does not increase as fast as the proportion of multivalent phosphate (Figure 6.13). The reason may be that the addition of OH^- screens the charges of the PSAs and compete with some of the phosphate for binding sites on the PSA. Therefore, with increasing pH value, the proportion of multivalent phosphate increases, but the solution environment becomes less and less favourable for removing the phosphate. In Figure 6.13, it seems not easy to identify a compromised pH to remove a cost justifiable amount of multivalent phosphate from dilute aqueous solutions.

The $Fe(CN)_6^{3-}$ has not been tested over the whole range of pH. The health and safety reason is that cyanide gas could be released from $Fe(CN)_6^{3-}$, when it contacts with strong acids.

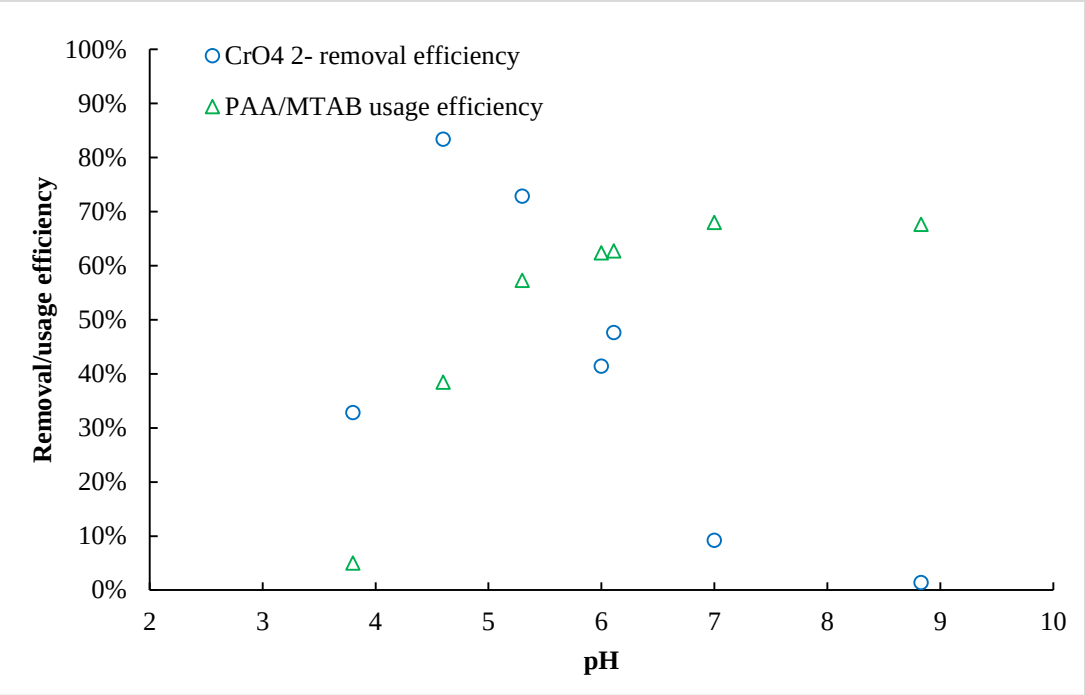

Figure 6.14: Removal efficiency of 0.2 mM K_2CrO_4 and the usage efficiency of 100 ppm PAA and 2.5 mM MTAB at different pH values.

The effective pH range for chromate removal in the PAA-MTAB system is relatively narrow (pH of 4.5-6 see Figure 6.14). As a consequence of adding 100 ppm PAA, the natural pH of the original solution is approximately 4. To enhance the formation of PSAs, hydroxide ions are added to promote the disassociation of PAA, and subsequently increase the charge percentage of PAA. The added hydroxide ions, however, also compete with the chromate ion to bind with the PSAs.

As chromate ions have a relatively low charge density, the changes in removal and polymer surfactant usage efficiencies are strongly related to the charge percentage of PAA. Increasing the pH to 6.2 means 99% of the PAA is theoretically disassociated. Therefore, the polymer surfactant usage efficiency reaches its highest value (~70%). Beyond this pH, further increasing the pH has little effect on the usage efficiency and formation of PSAs

(Figure 6.14). Although the usage efficiency increases by 5% from pH 5.3 to 6.2, the removal efficiency is compromised by 20%. The reason is that the undesired competing effect of hydroxide on chromate binding is stronger than the desired disassociation of PAA, leading to displace the weakly bound chromate ions by the hydroxide ions. Therefore, upon further increasing the pH to 7 and beyond, less than 5% chromate is removed.

In conclusion, due to the relatively low charge density of chromate ions, in order to achieve a high removal efficiency, a fine balance between the extra formation of PSAs and the lower removal of chromate must be made by adjusting the pH. In addition, pH adjustment can generate salt and increase the ionic strength, which may have some effects on the treatment outcome.

6.3.5. Ionic strength and organic contaminants

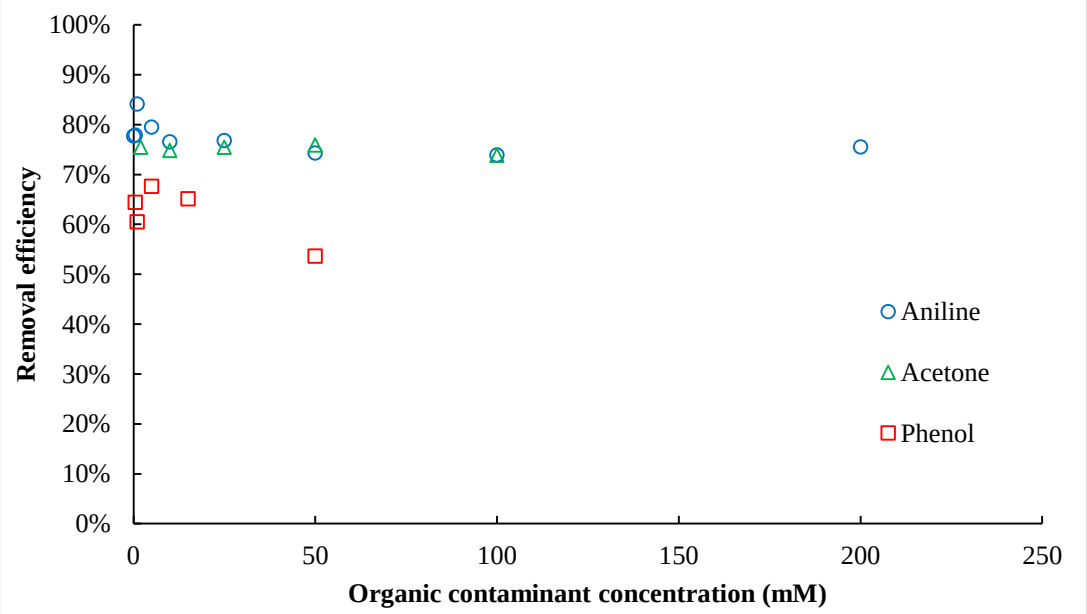

Figure 6.15: Removal efficiencies of CrO_4^{2-} at the optimum dosage of PAA and MTAB in the presence of various organics at different concentrations.

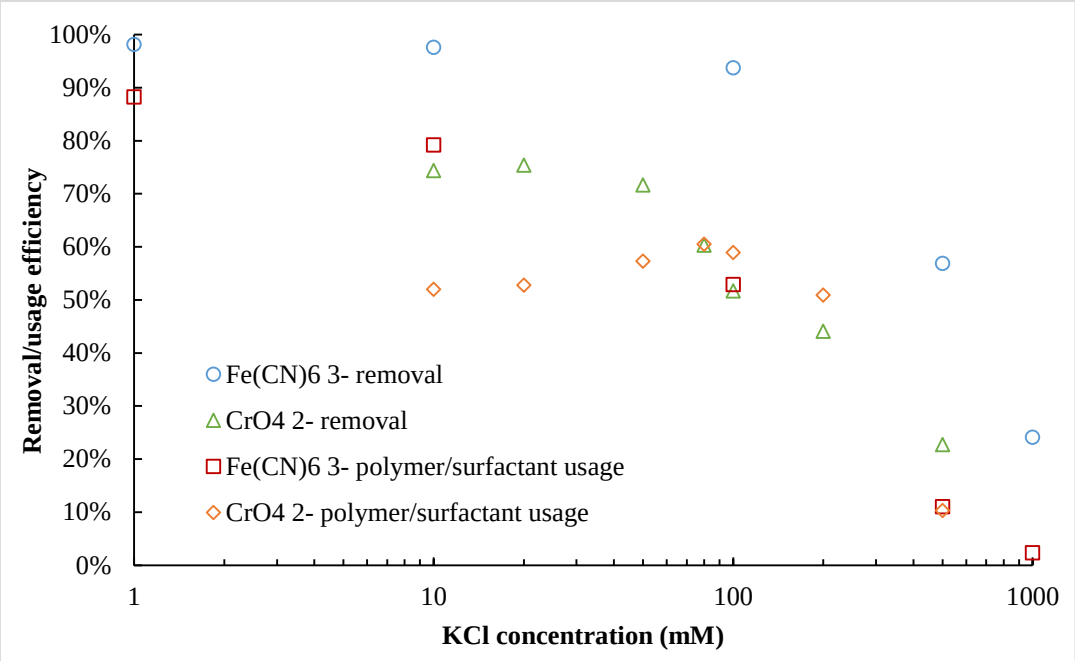

Figure 6.16: Removal and polymer surfactant usage efficiencies of $Fe(CN)_6^{3-}$ (no pH adjustment) and CrO_4^{2-} (at a pH of 5.3) in the presence of different KCl concentrations at their optimum dosages (300 ppm PSS+ 1.5 mM MTAB+ 0.1 mM $Fe(CN)_6^{3-}$; 100 ppm PAA+ 2.5 mM MTAB+ 0.2 mM CrO_4^{2-}, respectively).

The effects of salinity and organic contaminants on the treatment performance are studied. Organic contaminants such as acetone and aniline have little effect on the process (Figure 6.15). However, a 20% decrease in the removal efficiency is caused by the addition of phenol and the solution did not return to a clear state from a turbid one even after prolonged agitation.

The KCl is used as an example salt in the solution, and the concentration is studied up to 1M KCl which is relatively high for industrial effluents. In the $Fe(CN)_6^{3-}$ system, the polymer surfactant usage efficiency decreases rapidly above 50 mM KCl, but the removal efficiency only starts to drop around 100 mM KCl (Figure 6.16). The delayed decrease in the removal efficiency may be caused by the unbound surfactant monomers forming

$Fe(CN)_6^{3-}$-MTAB precipitates at higher salinity. In the chromate system, the removal efficiency starts to decrease around 50 mM KCl, so the chromate system is less resistant to salinity effects than the $Fe(CN)_6^{3-}$ system. Interestingly, the usage efficiency increases slightly until 100mM, before decreasing with further addition of KCl. This initial increase is probably due to the decrease of the CFC in a solution of moderate ionic strength, which promotes the formation of PSAs at a lower surfactant concentration. In summary, the $Fe(CN)_6^{3-}$ possesses a higher charge density than the chromate, and this leads to a relatively high tolerance to the ionic strength environment.

In conclusion, the PSA process works effectively for removing anions in the presence of moderate ionic strength and organic contaminants, and the tolerance of environment increase with the charge density of the targeted anion.

6.3.6. Temperature

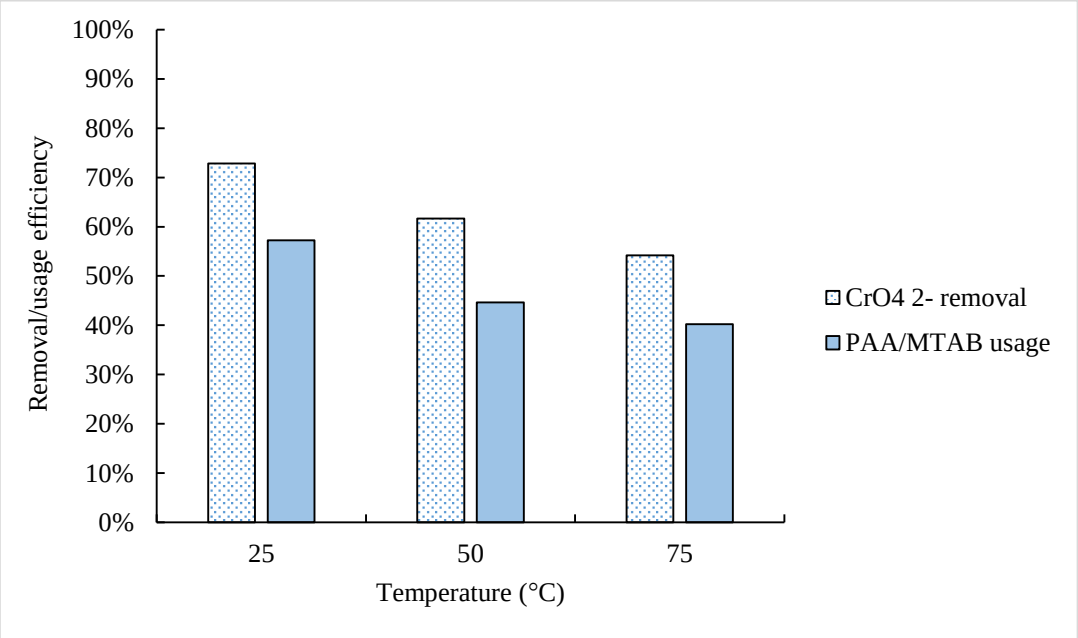

Figure 6.17: Temperature effects on the chromate removal and PAA-MTAB usage efficiencies at the optimum dosage. (100 ppm PAA+ 2.5 mM MTAB+ 0.2 mM K_2CrO_4)

The performance and robustness of PSA treatment at different solution temperatures are studied. In Figure 6.17, with increasing temperature, both the chromate removal and usage efficiencies decrease. This is probably caused by the exothermic nature of the formation of PSAs and their binding with chromate ions, so that higher temperature moderately inhibits both. Most importantly, the performance of PSA treatment is still high at room temperature (25 °C), and the extent of decrease with increasing temperature is small. The process may thus have a slightly better performance during the winter season. In conclusion, the treatment process is robust over a moderate temperature range (25-50 °C).

6.4. Studies of metallic anion selectivity

Table 6.1: PSA binding selectivity between $K_3Fe(CN)_6$ and K_2CrO_4 in the PAA-MTAB system without pH adjustment.

PAA (ppm)	**MTAB (mM)**	**$K_3Fe(CN)_6$ (mM)**	**K_2CrO_4 (mM)**	**$Fe(CN)_6^{3-}$ removal efficiency %**	**CrO_4^{2-} removal efficiency %**	**$Fe(CN)_6^{3-}$ selectivity coefficient**
350	1	0.1	0.00	99.2	N/A	N/A
350	1	0.1	0.05	98.7	0.8	128.3
350	1	0.1	0.10	98.9	5.2	19.1
350	1	0.1	0.20	99.0	6.5	15.1
350	1	0.1	0.30	98.3	8.0	12.3
350	1	0.1	0.50	97.6	8.4	11.6

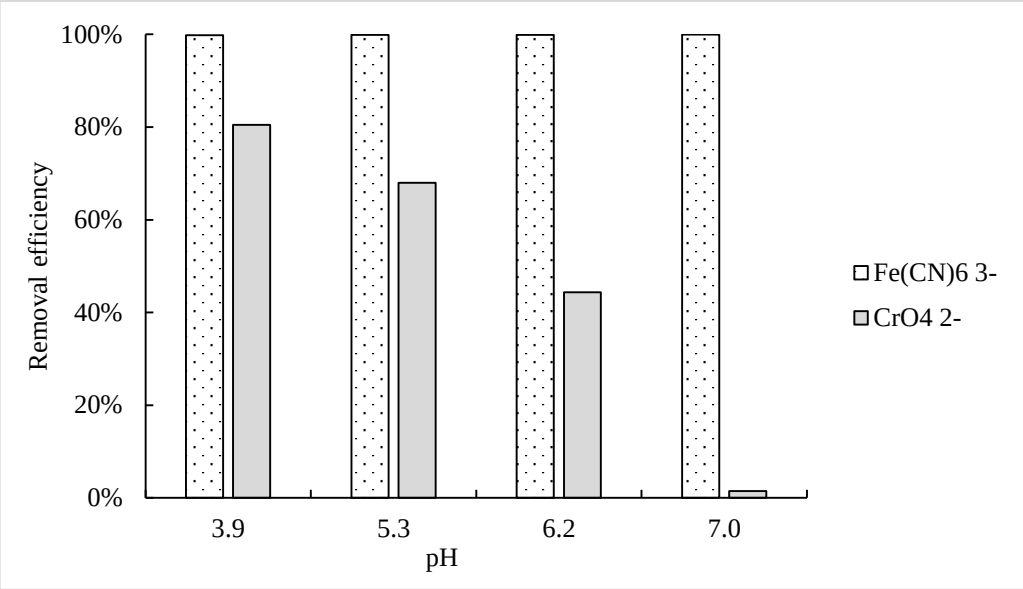

Figure 6.18: PSA binding selectivity between 0.2 mM $K_3Fe(CN)_6$ and 0.2 mM K_2CrO_4 in the PAA-MTAB system at different pH values (100 ppm PAA+ 2.5 mM MTAB).

Having obtained the results for the removal of single metallic anion species, the mixtures of them are studied to understand the binding selectivity of PSA. The selectivity is important for industrial applications, which allows the process to remove and subsequently recover the desired components into a relative pure solution. The solution can be reused or purified with little further treatment. Two approaches have been studied to enhance the selectivity: reducing the PSA usage and adjusting the solution environment.

The rationale of the first approach is that at a fixed amount of metallic anions, the anions with higher charge density can preferably bind with a limited amount of PSAs, so that adding a limited amount of PSAs may selectively remove the highest charge density anions first, and the rest can be removed in the order of charge density in the next cycles, if they are the targeted species. In Table 6.1, the optimum dosage for 0.1 mM $Fe(CN)_6^{3-}$ is used to treat mixtures of $Fe(CN)_6^{3-}$ (fixed 0.1 mM) and CrO_4^{2-} (increasing concentration). A strong selectivity is found at a low concentration of chromate, but with

increase of its concentration, the selectivity coefficient (Equation 6.3) decrease slowly because of the competitive displacement from a high concentration of chromate. Overall, the selectivity remains at a high level with a low dosage of PSAs.

The second approach is to increase the ionic strength of the solution; in this case, the pH is increased to displace the relatively weak charge density chromate from PSAs, and maintain the binding between PSA and $Fe(CN)_6^{3-}$. In Figure 6.18, as a consequence, at the same anion molar concentration, almost 100% $Fe(CN)_6^{3-}$ is removed over a wide range of pH, but the chromate removal efficiency decreases dramatically with increasing pH value. At a pH of 7, less than 5% of the chromate is removed, and the $Fe(CN)_6^{3-}$ is still completely removed. This suggests that a minor adjustment of pH can lead to a major improvement in the selectivity between anions with difference valences.

6.5. Discussion and summary

Multivalent anions can be effectively removed by PSAs. The notion of anion removal in this chapter is very similar with the cation removal in Chapter 4. In both processes, the charge of polymers are pH-sensitive and the opposite of the permanently charged surfactants. The polymer at the removal stage can be also be permanently charged, if the regeneration of the polymer and surfactant is unnecessary in some cases. As an electrostatic driven removal process, the charge of both polymer and surfactant in the anion treatment are reversed compared with the cation treatment process. Another difference is in the length of carbon chain of surfactant. The cationic MTAB contains 14-carbon compared with 12-carbon chain in the anionic SDS for the cation process. A 12-carbon chain cationic surfactant, namely dodecyl trimethyl ammonium bromide, is also

available for approximately 30 times more expensive than that for the MTAB. This 12-carbon chain surfactant has a lower hydrophobicity than the 14-carbon surfactant. As a consequence, the CAC of the 12-carbon surfactant is higher than the MTAB, which will lead to severe surfactant leakage into the filtrate.

To reduce the leakage, a surfactant containing 16-carbon chain is investigated, but the CMC is also lowered. The low CMC value allows the surfactant to form micelles directly under a low surfactant concentration, which lead to less amount of surfactant to form aggregates on the polymer chain. Both micelles and aggregates can bind to anions, but the mechanism is rather different. In the presence of micelles, the anions may bind to micelles, and then they are coagulated and flocculated by polymer. The aggregates, however, form on the polymer chains, and the whole structure (i.e. PSA) bind to the anions. Therefore, the 16-carbon surfactant is not in the scope of the thesis due to the different removal mechanisms and the CMC level of surfactant leakage into the filtrate. In addition, the high cost of the 16-carbon surfactant also discourage its industrial applications. Thus, MTAB is used as an example of permanently charged surfactant in the anion process.

Apart from the differences in the use of removal agent, there are some similarities and differences between the actual treatment processes. Both processes are capable of removing dilute target metallic ions over wide ranges of pH, salinity and organic contaminants. The tolerance of extreme solution environment largely depends on the charge density of the targeted ions. In general, the higher the charge density is, the higher resistance toward the extreme solution environment.

Much research work could be investigated in the process, in particular reducing the surfactant leakage in the filtrate and improving the selectivity between divalent ions. The

permanently charged polymer PSS has a lower level of surfactant leakage (approximately 30ppm MTAB) than the pH-sensitive polymer PAA, the latter has approximately 300 ppm MTAB leaks in the filtrate. The PAA system may seem to have a high surfactant leakage, but the leakage in a similar process called micellar enhanced ultrafiltration is equivalent to its CMC level: approximately 1500 ppm MTAB. As previously noted, the reason for using PAA instead of PSS is to recover and recycle the polymer and surfactant, which is discussed in the next chapter.

The sustainability and economic viability of the process can be significantly improved by minimising the leakage with the use of different pH-sensitive polymers or surfactants. Alternatively, addition of a small amount of non-ionic surfactant may well reduce the CAC, and consequently reduce the surfactant leakage. To enhance the selectivity between divalent ions, a polymer modification could be a possible solution. For example, adding some functional groups on the polymer chains to allow specific interactions with targeted ions.

In conclusion, the metallic anions can be effectively removed using PSAs, and this process has the potential to be applied in industrial effluent treatment.

Chapter 7

Investigation of the Recovery of Metallic Anions and Recycle Removal Agent in the Polymer–Surfactant Aggregate Process

7.1. Introduction

With the development of industrialisation, the use of anions has increased dramatically. Chromate as one example is commonly used in the pigment and painting industries. Some of the effluent containing chromate will contaminate the water body and usually in a low concentration, but it can accumulate in organs and cause disorders. Apart from contaminating the water body, this is also an inefficient way of using resources. Thus, a separation and purification process is needed to treat the industrial effluent and turn the waste into a valuable resource. However, treating a dilute wastewater cost–effectively still remains as a challenge.

To overcome challenge, the polymer–surfactant aggregate (PSA) process has been developed and applied to remove metallic anions from dilute aqueous solutions. In this chapter, a reverse order of the cation recovery process is described and applied. It uses basification to recover and concentrate the anions, and then uses acidification to regenerate and recycle the PAA and MTAB (i.e. removal agent). The concentrated anions can be a valuable resource to recycle back into the manufacturing process stream or sell as a by-product. The regenerated polymer and surfactant are recycled to the next cycle, with a small addition of surfactant to make up the surfactant leakage at the removal stage. The whole anion treatment process is presented, and the important process variables including pH, concentration factor and residence time are investigated and optimised. Finally, the treatment mechanism, performance, procedure and application between the cation and anion treatment process are compared and contrasted.

7.2. Materials and methods

7.2.1. Materials and the removal stage

Poly(acrylic acid) (PAA) solutions were prepared by diluting stock PAA solution (Sigma Aldrich, average MW <100,000, 35 wt.% in H_2O). Sodium dodecyl sulphate (SDS) (purity ≥ 99.9%) and myristyl trimethyl ammonium bromide (MTAB) (purity ≥ 99%) were obtained directly from Sigma Aldrich. Potassium chromate and potassium chloride were purchased from Fisher Scientific (all purity ≥ 99%). Sulphuric acid (ACS reagent, 95-98%) and sodium hydroxide (reagent grade, ≥ 98%, pellets) were obtained from Sigma Aldrich. 20 μm nylon filters were obtained from Millipore.

All the methods for the solution preparation, filtration method, total carbon, MTAB and anion concentration measurements follow the protocols in Chapter 6 (Section 6.2.).

7.2.2. Anion recovery by basification

A calculated amount of 0.03M NaOH solution was added to the flask and then stirred at 200 rpm to recover the anion from the flocs until the colour of flocs becomes white, which usually took 15 min. The NaOH solution in the flask was then decanted into the filtration cell, and stirred at 200 rpm for another 15 min before starting the filtration by lowering the outlet from a high position. The filtration was stopped when all solution had passed through the 20μm filter under gravity. For the residence time experiments, a basic solution was stirred in the flask for a desired period, and then decanted into the filtration cell to stir for the same period before the filtration was started, in order to study the kinetics of the anion desorption process. The pH experiments were carried out by adding the base at various pH values at a concentration factor of 5 for 15 min residence time. The concentration factor is defined in Equation 5.1. The recovery filtrate was analysed directly by total organic carbon analyser (TOC–VCPH, Shimadzu) and two-phase mixed indicator titration. The filtrate solution was then diluted by deionised water before measuring the anion concentrations. The anion recovery efficiency was calculated from Equation 7.1.

$$\text{Anion recovery efficiency} = \frac{C_{\text{recovered ion}}(\text{mg/l}) \times V_{\text{filtrate}}(\text{ml})}{C_{\text{original effluent}}(\text{mg/l}) \times V_{\text{effluent}}(\text{ml})} \times 100\% \qquad (7.1)$$

Equation 7.1: Calculation of the anion recovery efficiency.

7.2.3. Polymer and surfactant recovery by acidification

After the basification, some of the flocs remained in the original removal flask and the rest was retained in the filtration cell. A calculated amount of 0.05M H_2SO_4 solution was

added to the original flask and then stirred at 200 rpm for 15 min until all the flocs in the flask were dissolved. The solution was then poured into the filtration cell, and stirred at 200 rpm for another 15 min to regenerate the polymer and surfactant in the cell. The filtration started when all the flocs had dissolved to speed up the draining process. The filtration was stopped when all solution had passed through the 20μm filter. The methods for the residence time, pH and concentration factor experiments are the same as for the anion recovery by basification (Section 7.2.2). The recovery filtrate was analysed directly by atomic adsorption spectrometry and UV–Vis spectrometry, and was diluted before analysis by total organic carbon analyser and two-phase mixed indicator titration. The polymer–surfactant recovery efficiencies were calculated from Equation 7.2.

$$\text{Polymer} - \text{surfactant recovery efficiency} = \frac{\text{Total carbon}_{\text{recovered}}(\text{ppm}) \times V_{\text{2nd filtration filtrate}}(\text{ml})}{\text{Total carbon}_{\text{added removal agent}}(\text{ppm}) \times V_{\text{effluent}}(\text{ml})} \times 100\%$$

$$\text{Surfactant recovery efficiency} = \frac{C_{\text{recovered SDS}}(\text{mM}) \times V_{\text{2nd filtration filtrate}}(\text{ml})}{C_{\text{added SDS}}(\text{mM}) \times V_{\text{effluent}}(\text{ml})} \times 100\% \quad (7.2)$$

Equation 7.2: Calculations of the polymer and surfactant recovery efficiencies.

7.2.4. Polymer and surfactant recycle

The regenerated PAA–MTAB acidic solution was directly recycled back into the feed solution as a batch process, and then the pH was adjusted by adding NaOH. After stirring the solution overnight, the next cycle was performed by repeat of the filtration (Section 6.2), basification (Section 7.2.2) and acidification (Section 7.2.3) procedures.

7.3. Development of the recovery method for the treatment process

Table 7.1: Direct addition of acid and base solutions in the PSS–MTAB flocs with anions

Direct addition	PSS + MTAB + Metallic anions	PSS–MTAB recovery efficiency	$K_3Fe(CN)_6$ recovery efficiency
0.05 M H_2SO_4	300 ppm + 1.5 mM (no anions)	5%	N/A
0.1 M NaOH	300 ppm + 1.5 mM (no anions)	15%	N/A
2 M NaOH	300 ppm + 1.5 mM (no anions)	38%	N/A
2 M NaOH	300 ppm + 1.5 mM + 0.1mM $K_3Fe(CN)_6$	27%	32%

Table 7.2: Direct addition of acid and base solutions in the PolyDADMAC–SDS flocs

Direct addition	PolyDADMAC + SDS	PolyDADMAC–SDS recovery efficiency
0.05 M H_2SO_4	162 ppm + 1 mM	23%
0.1 M NaOH	162 ppm + 1 mM	5%
2 M NaOH	162 ppm + 1 mM	50%

To recover either metallic ions or polymer and surfactant, the direct addition of acid or base solution is studied in both of the anion and cation treatment processes. In both of the processes, two types of polymer, namely permanently charged and pH-sensitive, are tested with permanently charged surfactants. With regard to the permanently charged polymer and surfactant system, less than half of the polymer and surfactant is recovered, even at extreme pH solutions (Table 7.1 and Table *7.2*). For instance, only 15% PSAs is recovered using a 0.1M hydroxide ion solution, and using the same concentration of hydrogen ion solution, even less (5%) PSAs is recovered (Table 7.1). This indicates that it is kinetically less favoured to displace the cationic MATB by hydrogen ions than the anionic PSS by hydroxide ions. Increasing the concentration of hydroxide ion to 2M, 38%

of the PSAs are dissolved (Table 7.1). Under the same hydroxide concentration, with the addition of $K_3Fe(CN)_6$, the PSS–MTAB recovery efficiency decreases from 38% to 27%. This decrease suggests that the flocculation of PSAs is hard to reverse even in extreme pH solutions, and the bridge effects from $K_3Fe(CN)_6$ enhance the strength of interactions between PSAs, which makes them even harder to be reversed.

The molecular interactions between PSS–MTAB–$K_3Fe(CN)_6$ are shown in Figure 7.1. Strong and stable electrostatic bindings exist in the both ends of the MTAB aggregates (PSS–MTAB; MTAB–$Fe(CN)_6^{3-}$), which also explains the difficulties in dissolving the flocs.

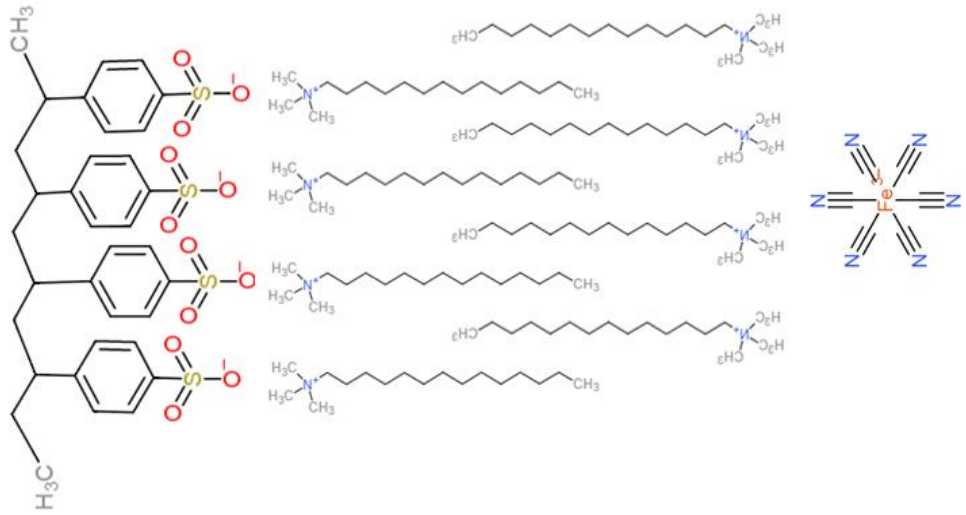

Figure 7.1: PSS, MTAB and $K_3Fe(CN)_6$ interactions at a molecular level.

In the permanently charged polyDADMAC and SDS system, the similar results are measured. The polyDADMAC is easier to be displaced (23%) than that for surfactant (5%) (Table 7.2). At the extreme base condition, half flocs is dissolved. Thus, the electrostatic bindings in both systems of permanently charged polymer and surfactant have high resistance towards pH shift, even in the extreme pH solutions, resulting the flocs that only partially dissolve in extreme pHs. In other words, the system of

permanently charged polymer and surfactant is not suitable for regeneration using pH adjustment method. However, it is necessary to use a permanently charged surfactant in order to maintain a strong binding with the oppositely charged ions for removing them from dilute solutions.

Two pH-sensitive polymers, namely PAA and PEI, are used for the later regeneration. In an acidic solution, the PAA acts as a neutral polymer because the disassociation of the carboxylic acid groups is inhibited. In a basic solution, however, the disassociation is promoted, so the PAA becomes a negatively charged polymer, and the charge percentage increases with pH values. In the cation treatment process, the amine groups in the PEI can either be protonated in an acidic solution to acquire a positive charge or be deprotonated and neutralised in a basic solution.

The molecular interactions between PEI–SDS–Zn(II) are shown in Figure 7.2. At an acid pH, the electrostatic interactions between PEI and SDS are strengthened, but the bound zinc ions are displaced by the excess hydrogen ions. Once the zinc ions are displaced, i.e. recovered, a base solution can be applied to weaken the PEI–SDS interactions, consequently regenerate the PEI and SDS.

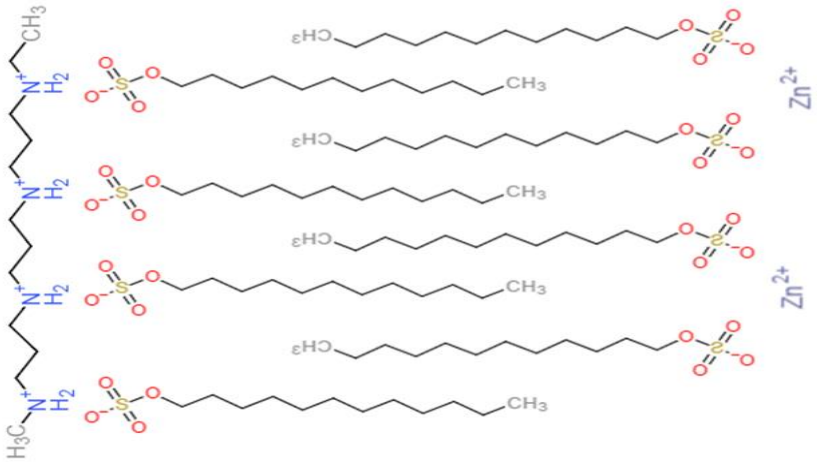

Figure 7.2: PEI, SDS and zinc interactions at a molecular level.

Table 7.3: Direct addition of acid and base in the PAA–MTAB flocs with anions

Direct addition	PAA + MTAB + Metallic anions	PAA–MTAB recovery efficiency	Anion recovery efficiency
0.05 M H_2SO_4	350 ppm + 1 mM (no anions)	90%	N/A
0.1 M NaOH	350 ppm + 1 mM (no anions)	38%	N/A
2 M NaOH	350 ppm + 1 mM (no anions)	48%	N/A
			$K_3Fe(CN)_6$
0.1 M NaOH	350 ppm + 1 mM + 0.1 mM $K_3Fe(CN)_6$	42%	15%
1 M NaOH	350 ppm + 1 mM + 0.1 mM $K_3Fe(CN)_6$	51%	2%
2 M NaOH	350 ppm + 1 mM + 0.1 mM $K_3Fe(CN)_6$	54%	2%
			K_2CrO_4
0.1 M NaOH	100 ppm + 2.5 mM + 0.2 mM K_2CrO_4	20%	97%
0.05 M H_2SO_4	100 ppm + 2.5 mM + 0.2 mM K_2CrO_4	77%	1%

It is worth noting that 90% of the PAA–MTAB are recovered at a pH of 1 in the absence of anions, which is much higher than the 5% recovery for the PSS and MTAB system under the similar conditions (Table 7.1 and Table *7.3*). Interestingly, in the extreme base solution, the recovery efficiency of PAA–MTAB is much lower than in the extreme acid solution, which is the opposite trend in the PSS and MTAB system. This is due to the increasing charge percentage of PAA that enhances the binding with MTAB, which inhibit the dissociation of PAA and MTAB in the extreme acid solution to some extent. In extreme base conditions (0.1M and 2M NaOH), when PAA is fully charged, the

recovery efficiency of PAA–MTAB is higher than that of PSS–MTAB (Table 7.1 and Table *7.3*), because the charge density of PSS is higher than that of PAA.

Another example is the PEI and SDS system, a negligible amount of PEI/PolyDADMAC and SDS is recovered at pH 1 (Table 7.2 and Table *7.4*). This indicates that most of the PEI are protonated at a pH of 1, and the resulting PEI has a high charge density like polyDADMAC. In the base solution, thanks to the complete deprotonantion at a pH of 13, 99% PEI–SDS are recovered, which is higher than the 90% in the PAA–MTAB. Therefore, the protonation of amine groups in the PEI is more pH sensitive than the disassociation of carboxylic acid groups in the PAA.

Table 7.4: Direct addition of acid and base in the PEI–SDS flocs with metal ions

Direct addition	PEI + SDS + Metal ions	PEI–SDS recovery efficiency
0.05 M H_2SO_4	80 ppm + 0.8 mM (no metal ions)	3%
0.1 M NaOH	80 ppm + 0.8 mM (no metal ions)	99%
0.1 M NaOH	80 ppm + 0.8 mM + 0.3 mM $ZnSO_4$	36%
2 M NaOH	80 ppm + 0.8 mM + 0.3 mM $ZnSO_4$	76%

As previously noted, in the presence of multivalent ions, the recovery efficiency of polymer and surfactant decreases generally (Table 7.1, 7.3 and 7.4), because the multivalent ions hold the PSAs together via bridging that increases the size and rigidness of the flocs. It is important to eliminate the effect of bridging for the regeneration of polymer and surfactant, thus the multivalent ions should be recovered first. Another advantage for recovering the ion first is that the ions can be recovered in a relatively pure and concentrated form that usually requires little further treatment. After the ion recovery, the polymer and surfactant can be regenerated by displacing the surfactants from polymer chains. The resulting polymer and surfactant mixture can co-exist in the acidic/basic

solution, because the polymer is present in a neutral form.

In conclusion, in the anion treatment process, anions in the flocs can be recovered first into a relatively pure and concentrated form by basification, and then the PAA–MTAB can be regenerated by acidification, which is the reverse order of pH adjustment in the cation treatment process.

7.4. Variables in the recovery of anions via basification

7.4.1. pH

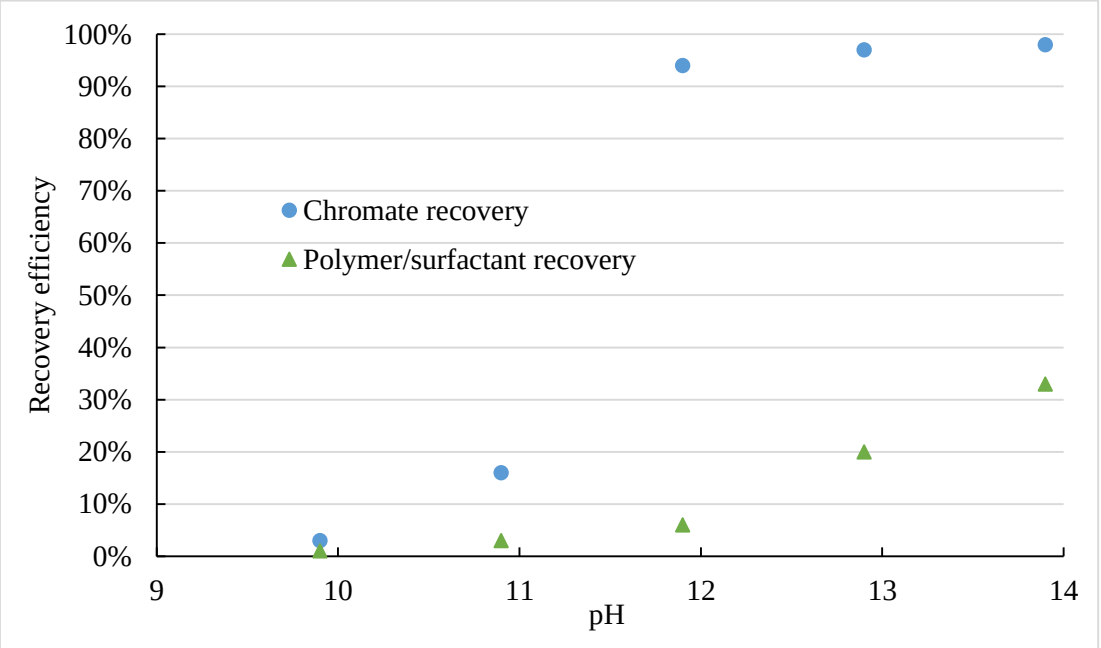

Figure 7.3: pH effects on the chromate and PAA–MTAB recovery efficiencies at the basification step with a concentration of 5 and 5 min residence time.

As a mirror-image pH adjustment method to the cation recovery method, a base solution is applied first to displace the bound chromate ion from the flocs. In Figure 7.3, with increasing pH values, the chromate and polymer-surfactant recovery efficiencies increase because hydroxide ions can effectively displace the bound chromate and PAA

from MTAB. The MTAB monomers form aggregates on the PAA chains, and the aggregates also bind with chromate. To some extent, MTAB aggregates act as interlinks between negatively charged PAA and negatively charged chromate via electrostatic binding. Once the concentration of hydroxide ions increases, the PAA or chromate ions are competitively displaced via hydroxide ions. This displacement effect results in the recovery of most of the chromate and a little PAA, because the disassociation of PAA is promoted when the pH value increases. The aggregates have a relatively stronger binding strength with the highly charged PAA chains than with the chromate (Figure 7.3). Owing to the loss of PAA from flocs, which serves as the backbone for MTAB aggregates, some of the MTAB is also dissolved into the basic solution.

However, a relatively pure chromate recovery solution is desired that requires little further treatment before reuse. To maximise the chromate recovery and minimise the impurity from PAA and MTAB, a pH of 12 is selected as the optimum recovery pH because it sits between the dissociation of CrO_4^{2-}–MTAB and PAA–MTAB. At this pH, the results show that 94% chromate with only 6% PAA–MTAB is recovered in the basic solution (Figure 7.3). There is still some room for improvement between pH 11-12 to lower the percentage of PAA–MTAB recovery and maintain a high chromate recovery efficiency.

7.4.2. Concentration factor

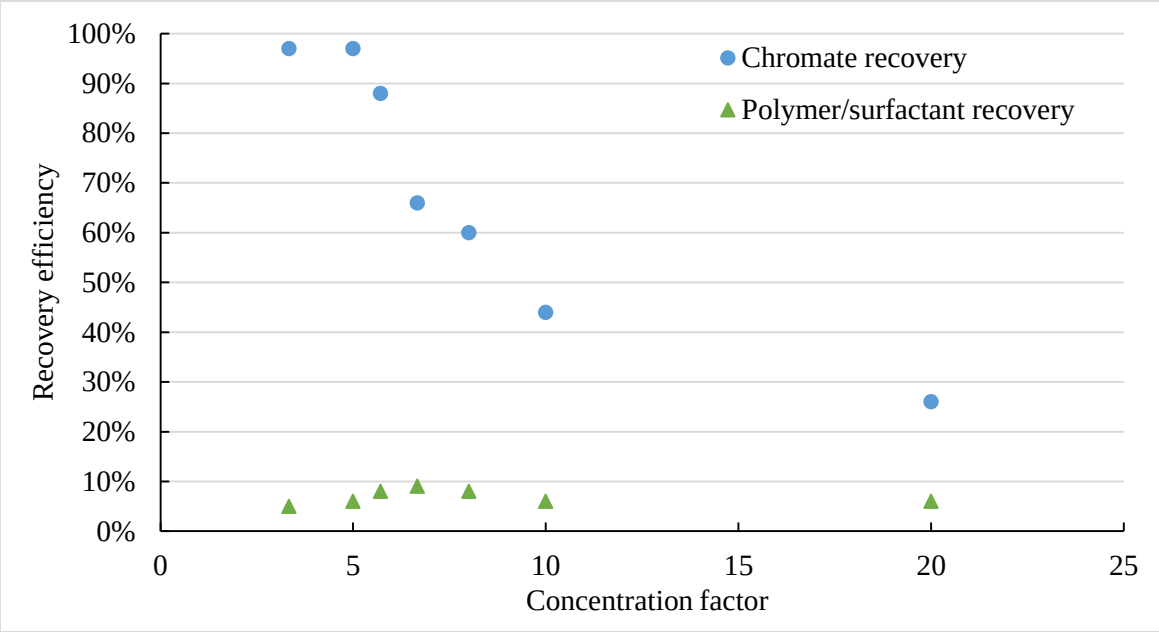

Figure 7.4: Concentration factor effects on the chromate and PAA–MTAB recovery efficiencies at the basification step (at a pH of 12) in 15 min residence time.

As the optimum recovery pH is 12 as determined from Figure 7.3, the effects of the volume of base solution used, i.e. concentration factor, on the recovery efficiency are also studied to minimise the usage of the base solution and maximise the concentration of recovered chromate. However, it is important to balance between the recovered concentration in the solution and the recovery efficiency. Thus, various concentration factors are applied to recover the flocculated chromate to determine the balance point. It is no surprise that the recovery efficiency remains at 98% when the concentration factor increases to 5, and then the efficiency of chromate decreases dramatically with increasing concentration factor (Figure 7.4). The possible reason for decreasing efficiency is that the concentration of chromate in the basic solution approaches the saturation point at room temperature. Consequently, the equilibrium of the recovery step for chromate slows down, resulting in a smaller amount of recovered chromate under the same residence time (i.e. a slowing dissolution rate).

7.4.3. Residence time

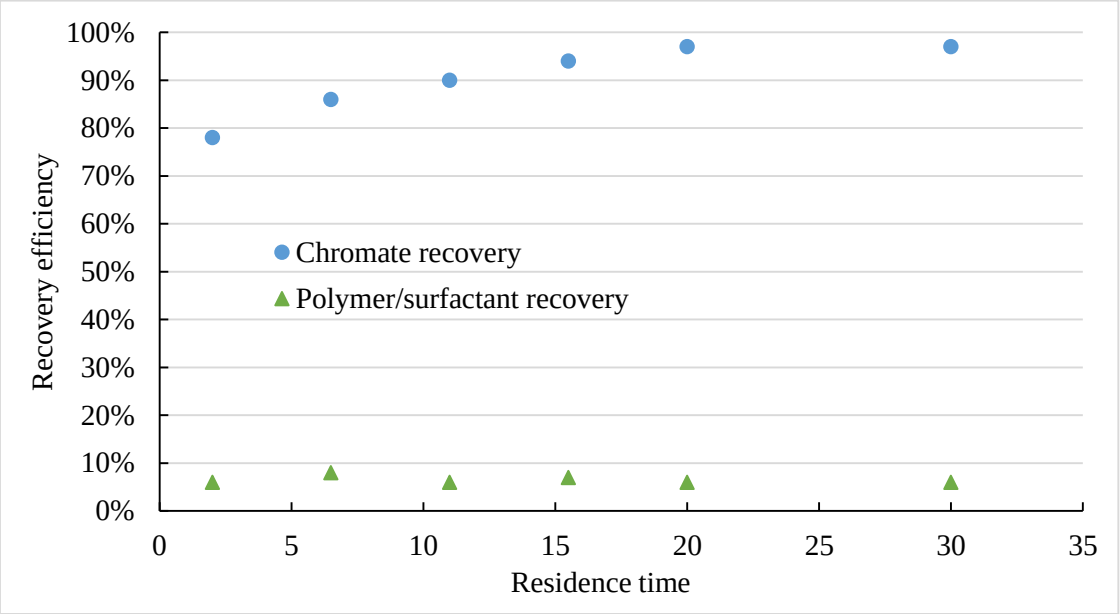

Figure 7.5: Residence time effects on the chromate and PAA–MTAB recovery efficiencies at the basification step at a pH of 12 and a concentration factor of 5.

The kinetics of the chromate recovery step is relatively fast. In the first 2 min, about 80% of the bound chromate has been recovered. After that, the dissolution rate slows downs dramatically. After 20 min, 97% of the bound chromate and 6% of the flocculated PAA–MTAB are recovered in a basic solution (Figure 7.5). The results indicate that at a relatively moderate pH and concentration factor, the chromate can be quickly recovered into a concentrated solution with a small residue of polymer and surfactant. With the same treatment capacity, for instance, a shorter residence time can reduce the capital cost of building extra reaction tanks and the space volume they occupy. Alternatively, it can increase the total treatment rate with the same equipment. In addition, a higher concentration factor could be applied given a longer residence time, because the rate of recovering is finite. Thus, there is another balance to be made between the speed of operation and the concentration of recovered anions.

7.5. Variables in the regeneration of PAA and MTAB via acidification

7.5.1. pH

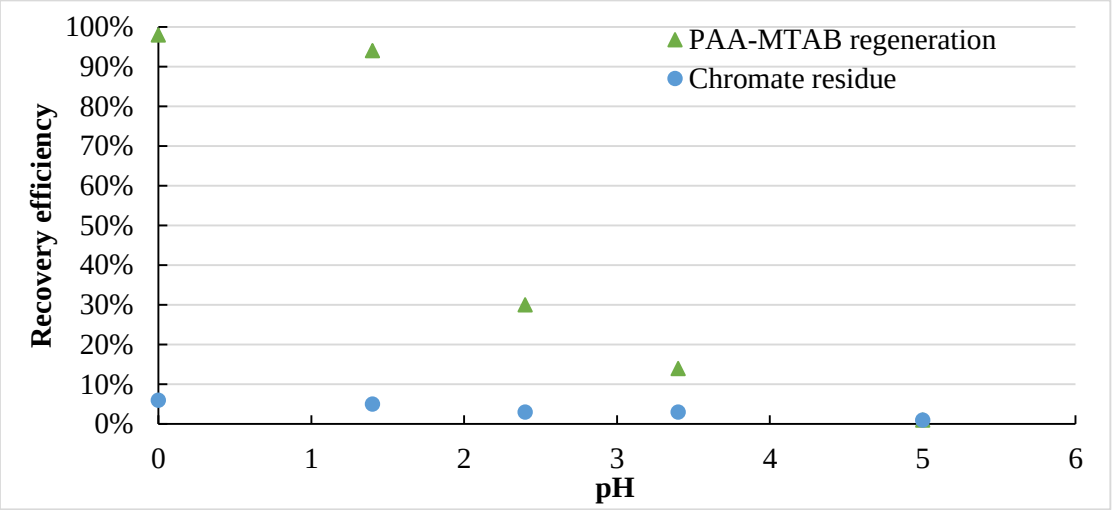

Figure 7.6: pH effects on the chromate and PAA–MTAB regeneration efficiencies at the acidification step in 15 min residence time with a concentration factor of 5.

After the basification, a small volume of acid solution is added to dissolve the chromate leached flocs and subsequently regenerate the PAA and MTAB. The acid solution neutralises the PAA and displaces the MTAB from the PAA chains. The regenerated PAA–MTAB contains a small chromate residue left from the previous step. At a pH of 0, 98% of the flocculated PAA–MTAB is regenerated, but a slightly lower regeneration (94%) is achieved at a relatively moderate pH of 1.4. Although this might still be considered an extreme pH, it is nevertheless sensible to trade-off 4% of the regeneration efficiency while reducing the acid usage more than 30 times. This reduction can significantly save chemical costs and improve health and safety during the operation. Further increasing the pH value to 2.5, the regeneration efficiency declines to 30%, which is too low to achieve a sustainable operation and generates unnecessary sludge from the undissolved removal agent that needs further treatment or landfill. Therefore, a pH of 1.5

is used as the optimum pH for the PAA–MTAB regeneration.

7.5.2. Concentration factor and residence time

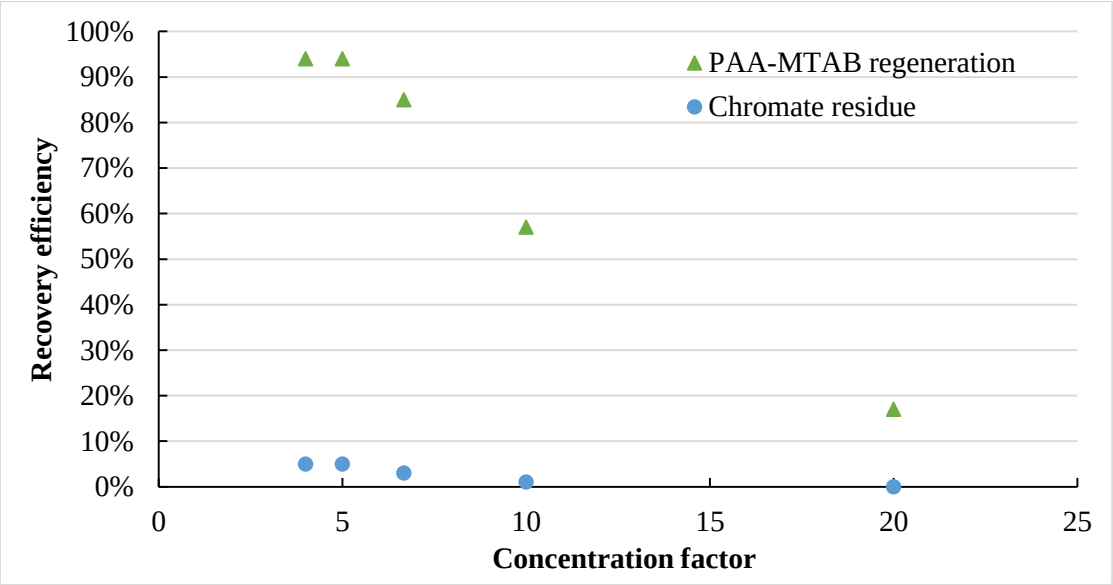

Figure 7.7: Concentration factor effects on the chromate and PAA–MTAB regeneration efficiencies at the acidification step (a pH of 1.5) in 15 min residence time.

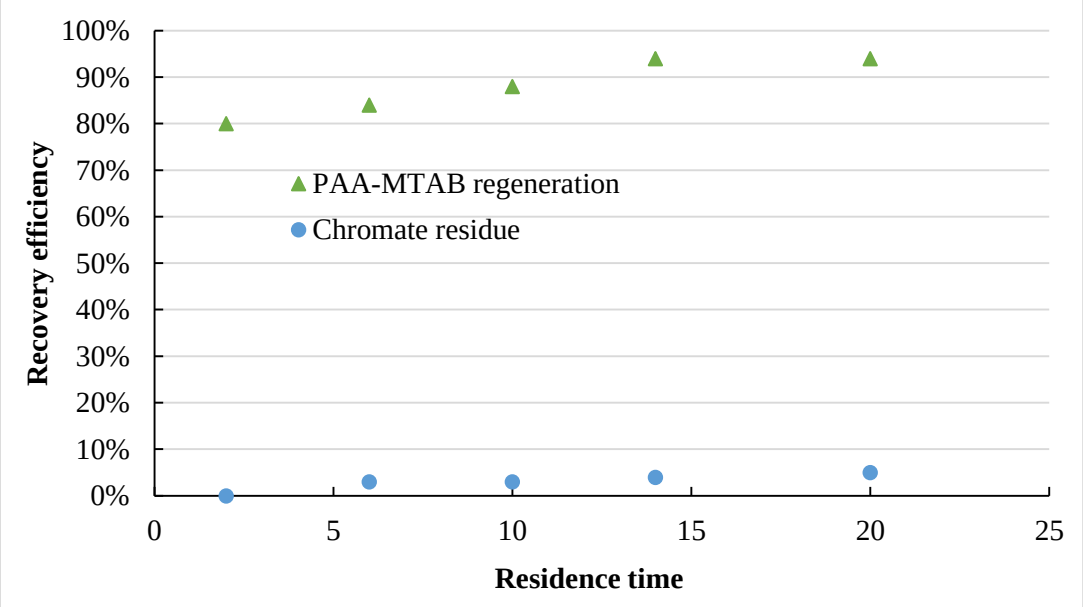

Figure 7.8: Residence time effects on the chromate and PAA–MTAB regeneration efficiencies at the acidification step (a pH of 1.5) with a concentration factor of 5.

At the PAA–MTAB regeneration step, the concentration factor and residence time have been also studied. The results for the concentration factor in Figure 7.7 are rather similar to those in Figure 7.4, which may also result from the kinetics and equilibrium of the regeneration process. There is a subtle difference, however, between these two figures: the PAA–MTAB regeneration efficiency is constantly about 5% higher than the chromate recovery for the same concentration factor and residence time. One of the reasons is probably that the surface of the flocs are dissolved with time and fresh surface is created and exposed to the acidic solution. The base solution, however, needs to penetrate inside the tortuous floc structure to recover some of the anions, which then takes a longer time to contact with the same surface area. For the same reason, the PAA–MTAB regeneration efficiencies remain almost constant after 15 min residence time, which is 5 min shorter than that for the chromate recovery (Figure 7.8). In conclusion, the optimum conditions for PAA–MTAB regeneration are at a pH of 1.5, a concentration factor of 5 and 15 min residence time.

7.6. PAA and MTAB recycle

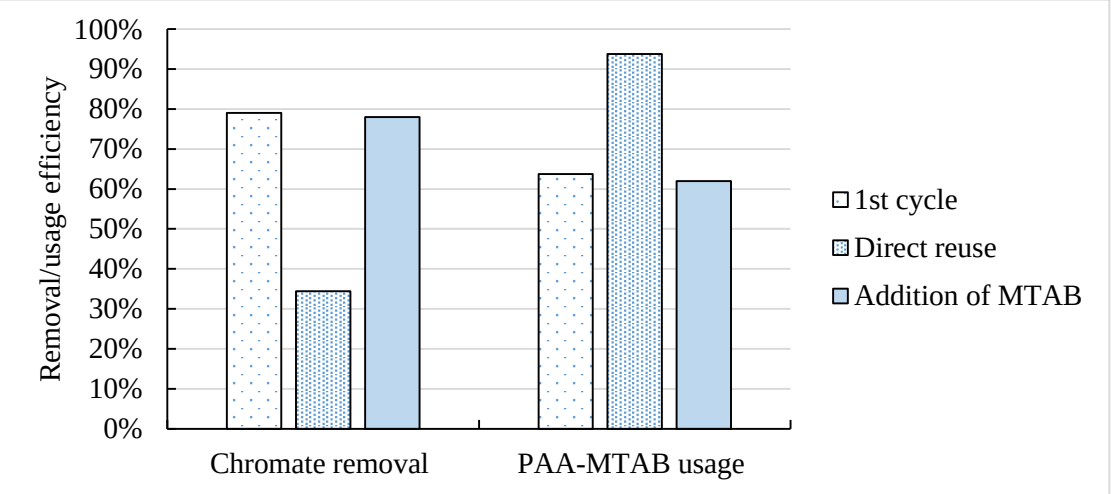

Figure 7.9: Chromate removal and PAA–MTAB usage efficiencies in the first treatment

cycle, after direct reuse of the regenerated PAA–MTAB and after reuse of the PAA–MTAB with the make-up of leaked MTAB at the removal stage (all solutions are adjusted to a pH of 5.3 before stirring).

To reduce the total usage of removal agent and improve the sustainability of the process, the regenerated PAA and MTAB are recycled back into the next cycle of the process. They are added directly into the feed solution, and then the pH of the solution is adjust to the optimum removal pH of 5.3. In this case, some flocs are still observed in the solution with 94% of PAA–MTAB usage efficiency, but only 30% of chromate is removed (Figure 7.9). This probably results from the leaked MTAB at the removal stage, which shifts the PAA–MTAB dosage ratio away from the optimum. Thus, under sub-optimal MTAB condition, some of the PAA forms polymer–surfactant complexes instead of the PSAs. The formation of polymer–surfactant complexes is based mainly on a one to one polymer and surfactant neutralisation, so they are not effective in binding the chromate. Hence, the limited amount of PSAs in the solution results in the low removal efficiency of chromate.

To shift the dosage ratio back to the optimum range, the amount of leaked MTAB (~1mM, i.e. about 40% of the added MTAB) is replenished in the next cycle. As a consequence, the performance reaches almost the same level as in the first cycle (Figure 7.9). The results suggest that the regenerated PAA and MTAB performs as well as fresh removal agent, and also confirm that the removal of chromate is mainly due to PSAs – the optimum dosage is required to form the PSAs. In conclusion, the regeneration and recycle step can reduce the total usage of removal agent in the process, but a small amount of make-up MTAB is required to offset the MTAB leakage during the removal stage.

Having developed the anion recovery and PAA–MTAB recycle stages, the whole anion treatment process is completed. It is a mirror-image process to the cation treatment

process. The PSA process is this capable of treating both anionic and cationic species from dilute aqueous solutions.

7.7. Overview of the whole anion treatment process

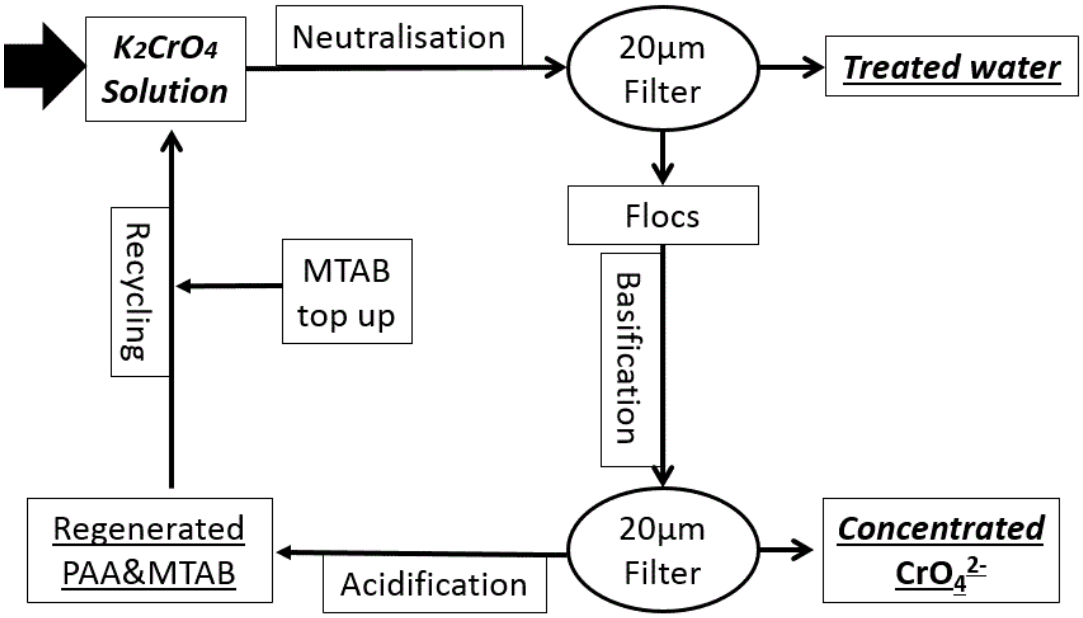

Figure 7.10: Flow sheet of the whole anion treatment process.

A flow sheet of the whole anion treatment process is shown in Figure 7.10, including three stages: removal, recovery and recycle. The chromate is used as an example anion in the process. At the removal stage, which is reported in Chapter 6, the PAA and MTAB are added at the optimum dosage ratio (100 ppm PAA and 2.5 mM MTAB) to bind with dilute chromate and form yellow flocs. The flocs are then separated from the treated water by a coarse filter, which is a faster alternative to gravity settling. After the filtration, a small amount of base solution is added to leach out the bound chromate from the flocs. Consequently, the flocs turn white since the yellow chromate ions are recovered and

concentrated into the base solution. The white flocs are further treated in an acid solution to regenerate the PAA and MTAB. Finally, the regenerated PAA and MTAB solution is recycled into the next process cycle with a small amount of make-up of MTAB before neutralising to the optimum removal pH of 5.3. The treatment process then starts again.

In summary, the whole treatment is a closed loop process that only a small amount of MTAB make-up in each cycle and consumes small amounts of acid and base solutions requires to produce a concentrated anion solution and treated clean water. In short, the process turns wastewater into valuable resources.

7.8. Discussion and summary

This chapter has described the recovery part of the anion treatment process, which is developed as the mirror-image of the recovery part in the cation treatment process. The reason for developing such a mirror-image process is to extend the application range of PSAs for treating dilute negatively charged components using a combination of reverse charged polymers and surfactants. The cation and anion (mirror-image) treatment processes have many in common.

7.8.1. Similarities between the cation and anion treatment processes

The mechanism, overall procedure and performance of the treatment are the three major similarities between the cation and anion treatment processes. For the treatment mechanism, metallic ions are removed by the PSAs, which work well on most of the multivalent ions. The mechanisms in both processes are mainly the electrostatic binding and hydrophobic interactions, though a fraction of metal ions may bind onto polymer

chains via chelation. At the same time that the ions are binding with the PSAs, the intermolecular associations between the PSAs promote the formation of large flocs. The bound multivalent ions can form bridges between PSAs, and even small flocs, to further enlarge the flocs. Hence, the size of flocs becomes large enough to be retained by a coarse filter, and even settle down under gravity. At the recovery stage, the mechanisms of bound ion recovery and polymer–surfactant regeneration in both processes are also similar. Both processes use pH-sensitive polymers and permanently charged surfactants with the charge opposite to that of the polymer. The PSAs, formed by the polymers and surfactants, remain undissolved during the step of bound ion recovery, because the pH-sensitive polymer chains nevertheless remain fully charged and have strong associations with the oppositely charged surfactant aggregates. The benefit of this is that relatively little amount of polymer and surfactant is reported in the recovered filtrate, so that a relatively pure and concentrated form of the targeted ions can be obtained, with little further treatment needed before reuse.

For the overall procedure of treatment, both processes contain three stages: removal, recovery and recycle. At the removal stage, the dilute charged species is removed by the PSAs with the polymer possessing the same charge as the targeted ions and the opposite charge to the surfactant aggregates. At the recovery stages, the bound ions are recovered first, and then the polymer and surfactant are regenerated. At the recycle stage, the polymer and surfactant are recycled without a deterioration of function into the next cycle with a small make-up of surfactant.

The final common point is the treatment performance in terms of the removal and recovery efficiencies, selectivity, and the optimum operation conditions, such as pH, concentration factor and residence time. Both processes are capable of removing above

80% of metallic ions from dilute aqueous solutions, and recovering more than 90% of them into a concentrated form. The selectivity at the removal stage generally follows the order of the charge density of targeted ions in both processes, because the removal is mainly an electrostatically driven process. To achieve effective recovery, the concentrations of applied acid or base are above 0.01 M and their optimum concentrations increase with increase of the charge density of targeted ions, polymers and surfactant aggregates. Most of the ions that bind onto the PSAs can be recovered in 30 min residence time. The kinetic and equilibrium behaviour are the main limitations for a higher concentration factor in both processes.

7.8.2. Summary

A new application of the polymer–surfactant aggregate process was previously presented to remove anions from dilute aqueous solutions. According to the recovery method for the cation treatment process, a parallel anion recovery and polymer–surfactant recycle method has been developed. This method uses a small volume of base solution to recover the anions from the flocculated PSAs, and then coarse filters separate the highly concentrated anion solution from the flocs. After this, the anion unloaded flocs are completely dissolved in an acid solution to regenerate PAA and MTAB, which is recycled into the next process cycle with a small addition of MTAB to make up the leakage at the removal stage. Finally, the pH of the solution is adjusted by adding a small amount of NaOH to optimise the formation of PSAs in the next cycle.

The removal and recovery performance of anions using regenerated PAA and MTAB are also studied. The results suggest that a pH of 12, a concentration factor of 5, and 15 min residence time are the operational conditions for optimal anion recovery, which can

recover about 94% of bound anions into a concentrated basic solution. This solution can be either recycled back into a manufacturing process or sold directly. Most importantly, the anion removal and recovery efficiencies remain almost the same for the second cycle involving recycle of the regenerated PEI and SDS and make-up of the leaked amount of MTAB. These recovery and recycle stages, therefore, complete the whole anion treatment process, and significantly save the chemical usage and enhance the sustainability of the process.

In short, cationic and anionic components from dilute aqueous solution can be removed and recovered using PSAs. Thus, such a process can treat the industrial effluents sustainably, and turn waste into valuable resources. This process opens up a range of potential applications in the wastewater treatment, precious metal/anion recovery, fine chemical processing, pesticide, semiconductor and pharmaceutical industries.

Chapter 8

Conclusions and future work

8.1. Concluding remarks

The main objective of this project is to develop a novel process to effectively recover dilute metallic ions from industrial process and effluent streams using recyclable polymer–surfactant aggregates (PSAs). PSAs are formed through an interplay of electrostatic and hydrophobic forces. They can remove the oppositely charged species via electrostatic interactions and chelation, resulting in the formation of flocs that settle out. The bound ions in the flocs are recovered as a concentrated salt before the polymer and surfactant are recycled using pH adjustment method. This process is simple, uses low energy and is essentially generable with little material loss or discharge.

There are two key parts in this project: firstly, to elucidate the mechanisms involved in the removal process and secondly, to develop the whole treatment process (removal of metallic ions, recovery of the constituents in the PSAs and recycling of the polymer and surfactant involved in the removal).

8.1.1. Removal of metallic ions and mechanisms

Through surface tension and electrical conductivity measurements, it is shown that the formation of PSAs is not influenced by metallic ions present in solution at mM concentrations. By correlating the surface tension and conductivity measurements with the removal efficiency of metallic ions, it is shown that the removal efficiency increases with the formation of PSAs. The removal efficiency reaches the peak when most of the polymer forms PSAs, and then declines when the polymer–surfactant ratio shifts away from the optimum for the formation of PSAs. These correlations suggest that the PSAs are responsible for removing the metallic ions.

Having developed an understanding of the removal mechanism, the PSAs are used to remove both cations and anions from dilute aqueous solutions. The PSA contains both positive and negative charges, which allows it to bind the oppositely charged ions onto the surfactant aggregates as well as bind with other PSAs to form large flocs at the same time. Since the interaction is mainly electrostatic in nature, the binding strength between monovalent ions and the surfactant aggregates is relatively weak, thus the PSAs only works effectively in removing multivalent ions. The bound multivalent ions also act as bridges that interlink the PSAs and even small flocs so that the speed and effectiveness of flocculation are enhanced. It is shown that the flocs containing the bound ions can be settled by gravity within a reasonable time scale (a few hours), but a coarse filter is used to accelerate the separation process.

Due to the fact that the PSAs form at relatively low concentrations of polymer and surfactant in a nanometre size (a high surface-volume ratio), it can effectively scavenge the multivalent ions from dilute aqueous solutions (< 0.1 mM). It is shown that ability to

scavenge ions at such low concentrations could be influenced by the solution environment, e.g. pH, temperature, ionic strength and the presence of organics. For example, the cation removal process works effectively within a pH range of 5-9, NaCl concentrations up to 1M and several organic contaminants up to 0.1M, such as acetone, aniline and ethanol. In the anion removal process, the working range for pH is 4.5-6, for KCl up to 0.1M and for organics up to 0.05M, which are all narrower than that in the cations. A possible explanation is that with the same valence, anions investigated have a larger ionic radius than the cations, which leads to a relatively low charge density for the anions. The charge density of the ions is positively related to the binding strength/stability. Thus, the cations can be removed at a wider range of solution conditions than the anions investigated. In addition, the strong removal selectivity between trivalent and divalent ions is a promising feature for industrial applications, which allows the recovered ions to report as a relatively pure salt. In short, the removal of metallic ions from dilute solutions through PSA interactions is robust and reliable in various solution environments.

8.1.2. Recovery of the constituents in the PSAs

At the recovery stage, the key is the use of pH-sensitive polymers: PEI for the cation treatment process and PAA for the anions. These polymers contain functional groups that can be protonated or deprotonated repeatedly via pH adjustment in order to manipulate the charge percentage of polymer to a desired level. By adding acid, the positive charge of PEI is enhanced due to the protonation of the amine groups, when ~98% of the scavenged cations are displaced by hydrogen ions. Thus, the interactions between PEI and SDS are strengthened while recovering the cations, resulting in a highly concentrated cation solution with little impurities from the polymer and surfactant. This relatively pure

and concentrated solution can be either recycled back into the manufacturing process or sold as a revenue stream. After the cation recovery, all white PEI–SDS flocs are rapidly dissolved in a small amount of base solution, because the hydroxide ions neutralise the PEI and displace the SDS. The regenerated PEI and SDS can be recycled back directly into the next treatment cycle before neutralising the pH of effluent.

In the anion treatment process, the two major differences compared with the cation process are that the charge of the polymer and surfactant and the order of pH adjustment are reversed. In this case, the cationic MTAB monomers form PSAs on the anionic PAA chains. The PSAs remove anions and forms flocs, and subsequently settle out. A base solution is used to displace ~98% of the bound anions first, and then an acid solution is applied to regenerate the PAA and MTAB for recycling.

Another difference between the cation treatment and anion treatment processes is the pH values of the acid and base added. The investigated anions have a lower charge density than the cations, and the change densities and hydrophobic forces in the polymer and surfactant aggregate are similar. As a result, the applied pH values in the anion process are more moderate than that in the cations. For instance, during the recovery of bound ions, the optimum pH for the anion is approximately 12, and for the cation is approximately 1.5. The optimum concentration of hydrogen ions used in the cation recovery is more than 3 times higher than that of the hydroxide ions for the anions. With regard to the polymer–surfactant regeneration, the optimum pH for the PAA–MTAB is approximately 1.5, and the same concentration but for hydroxide ions (a pH of 12.5) is the optimum for the PEI–SDS regeneration. Thus, the binding strength for the pH-sensitive polymer and permanently charged surfactant in both of the processes is similar, and for the metallic ions depend mainly on their charge densities.

Due to the salt accumulation from pH adjustment, the salt effects on the recovery efficiency are studied. No effect is found when the concentration of Na_2SO_4 reaches 0.5M, beyond which the recovery efficiency of metal ions decreases from 95% to 80%. Apart from salt effects, the residence time and concentration factor are equally important for the recovery stage. In both processes, the added acid or base solution is stirred for about 15 min to achieve approximately 95% recovery. The usage of acid or base can be reduced by applying a high concentration factor, and subsequently obtain a highly concentrated recovered metallic ions or polymer–surfactant. However, the above limit of concentration factor is restricted by the kinetics and equilibrium of the recovery process.

8.1.3. Recycle of polymer and surfactant

The final key feature in the treatment process is the capability of recycling polymer and surfactant without a deterioration of the removal ability in the next cycle. The PEI and SDS recycles up to 6 times in the cation process without any make-up. This feature significantly reduces the polymer–surfactant usage and chemical costs, and enhances the sustainability of the process. In a sense, the process uses a small amount of acid and base to recover dilute metallic ions from industrial effluents, and turn them into valuable resources: cleaned effluent and concentrated cation or anion salt.

In conclusion, the PSA process is a simple, inexpensive and effective treatment process for sustainably removing the metallic ions from dilute aqueous effluents and recovering these ions into a concentrated salt. The process contains three stages: removal, recovery and recycle. The estimated chemical cost is less than 1 penny per tonne for treating dilute effluents. Finally, the removal efficiencies of the process are above 99% for cations and about 80% for anions with a high selectivity towards ions with difference valences. The

recovery efficiency for targeted ions and polymer–surfactant are all above 98%. Such a process thus has a wide range of applications in industrial effluent treatment.

8.2. Consideration for industrial applications

To date, applications have been explored in treating heavy metal ions (textile and electroplate industries), precious metals (semiconductor and catalyst industries) and some metallic anions (pigment and plating industries). The potential applications, however, are not limited to these ions and industries. It is shown in the thesis that the process is robust and effective for treating many multivalent ions in dilute aqueous solutions under different conditions. For example, the process may treat dilute arsenic in the ground water, which is a major problem in some regions, like Bangladesh. It could also be applied to remove and recover industrial leakage in the ground water and washing water from heavy metal contaminated soil, even recover the valuable ions from used solvent in laboratory. Despite treating inorganic species, it may also treat organic species by dissolving into the hydrophobic inter core of the aggregates. Exploring the treatment of organic species can open up many possible applications in pharmaceutical and pesticide industries.

The process, nevertheless, does not work effectively in treating monovalent ions, such as potassium and chloride. The reason is that these ions possess a low charge density, resulting weak electrostatic interactions with PSAs. The solution environments can influence the effectiveness of the process. For example, in a high salinity solution, the anion treatment process probably would not work effectively, but the cation process may still work. Finally, the treatment requirements for effluent are an important criterion for

selecting a suitable process. The process is not suitable for producing ultrapure water due to the surfactant leakage in the treated water.

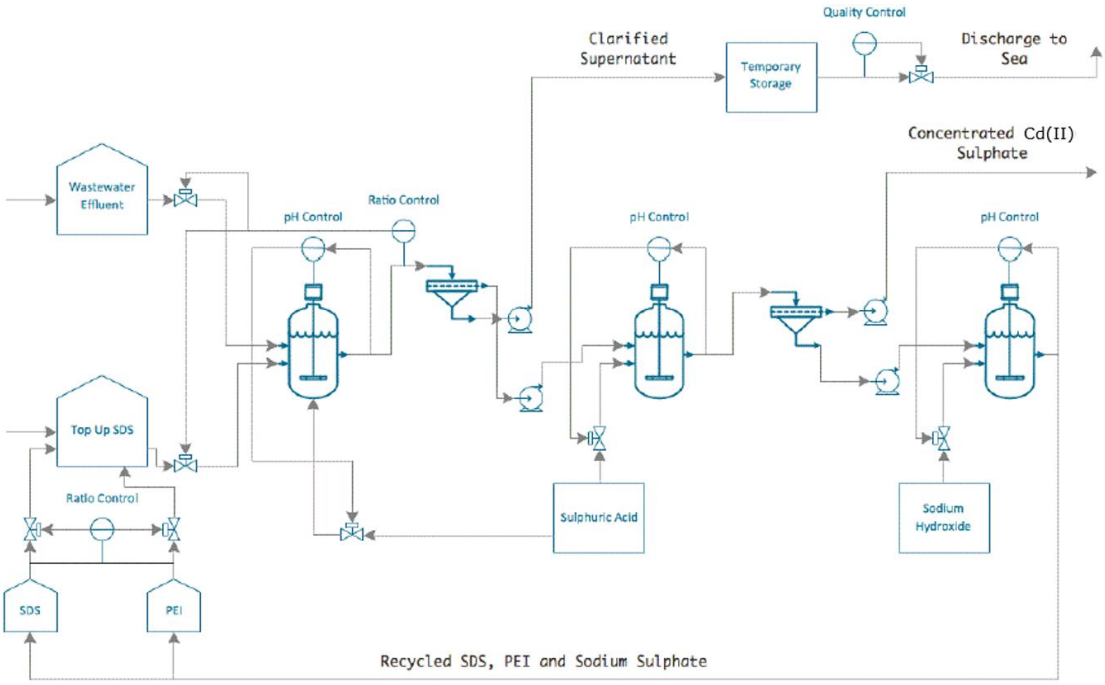

Figure 8.1: Process flow diagram for effluent treatment pilot scale process.

Table 8.1: Mass balance for the first cycle of the PSA process

Stream **Unit: g/hour**	**H_2O**	**Cd(II)**	**SDS**	**PEI**	**NaOH**	**H_2SO_4**	**Na_2SO_4**
Feed effluent	1000	0.0112	0	0	0	0	0
Feed PEI-SDS	0	0	0.144	0.04	0	0	0
Feed acid	20	0	0	0	0.0005	0	0
Feed base	20	0	0	0	0	0.0005	0
Neutralisation	1	0	0	0	0	0.0005	0
Treated effluent	1000	0.00004	0.02	0	0	0	0
Cd(II) recovery	20	0.01116	0	0	0	0.0005	0
PEI-SDS recovery	20	0	0.124	0.04	0.0005	0	0
Into the next cycle							
Feed used PEI-SDS	21	0	0.124	0.04	0	0	0.001

Mass balance and economic analysis are also the important aspects for industrial applications. During the operation, the polymer and most of the surfactant are recycled in the operation loop (Table 8.1). Therefore, the feed are industrial effluent, acid and base solutions and occasionally surfactant for make-up; the throughputs are the recovered ion solution and treated effluent containing a small amount of salt and surfactant. In order to improve the treatment performance, the salt accumulation and surfactant leakage should be minimised by maintaining a high concentration factor and purge percentage, and other scientific improvements are discussed in Section 8.3. A simple pilot-scale process flow diagram is shown in Figure 8.1.

Some preliminary cost estimations are made regarding the continuous operation of the described water treatment process. The main assumptions are that the sales of recovered ions is the only revenue stream, its concentration in the original contaminated solution is 10 ppm and the polymer and surfactant are recycled 20 times, whereas only the costs of chemicals are included in the variable costs. Prices of the chemicals are based on quotes from Alibaba.

Table 8.2: Economic analysis for the chemical cost of the PSA process.

	Unit price (£/kg)	**Concentration (g/m^3)**	**Number of recycles**	**Cost (£/m^3)**
Polymer	2	40	20 cycles	0.004
Surfactant	0.5	140	20 cycles	0.0035
Pure acid	0.2	0.5	1 cycle	0.0001
Pure base	0.2	0.5	1 cycle	0.0001
Total				0.0077
				Revenue (£/m^3)
Rh	20,000	10		200
Cd	0.5	10		0.005

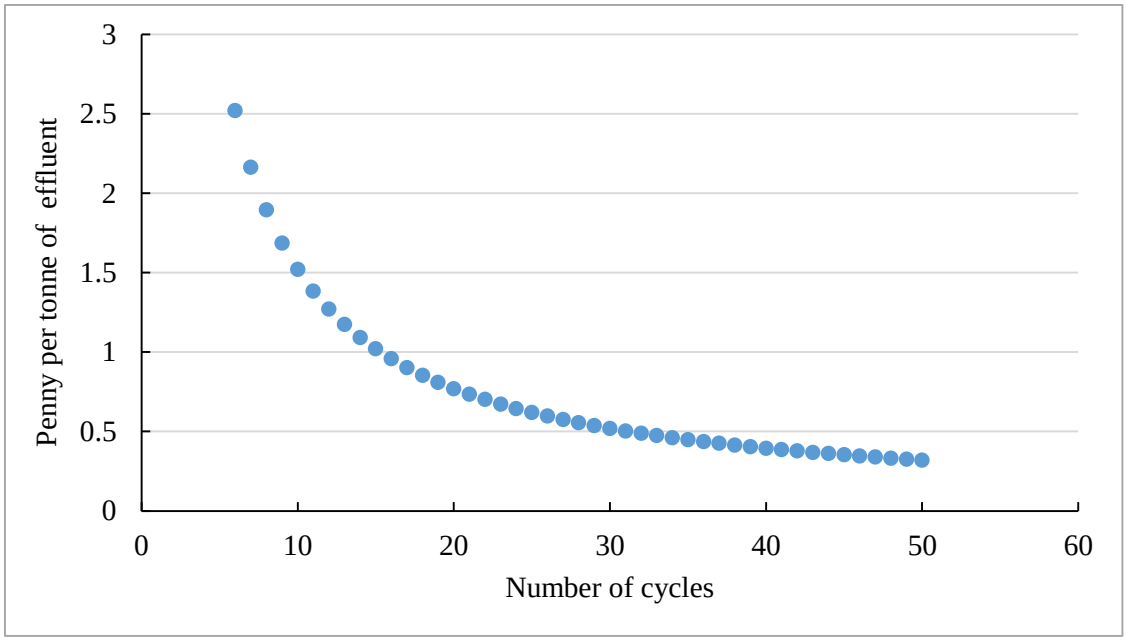

Figure 8.2: Effect of number of cycles for polymer and surfactant on the chemical cost of treatment.

In Table 8.2, the wastewater treatment plant runs a loss of about 0.3 penny/m^3 of throughput for treating Cd(II). This is primarily due to the low selling price of cadmium. Assuming the system has been optimised and the feed conditions do not change, the process can only improve profitability if a different target metal is chosen. The selling price of the chosen metal species has to be above £0.8/kg in order for the process to break even. It is also important to note that the estimation assumes the recovered is sold as the price of pure cadmium, but further purification is needed.

The number of cycle is a key variable affect the chemical cost (Figure 8.2). The metal removal and recovery efficiencies remain at high levels after 6 process cycles involving recycle of the regenerated PEI and SDS without any make-up. The reason of only using 6 cycles is that a proportion of the regenerated PEI–SDS solution is consumed by analytical measurements and no make-up is added, so that the total amount of the PEI and

SDS in the process was reduced after each cycle. Based on this, without the analytical measurements, 20 cycle times of the polymer–surfactant is assumed.

The estimation has only taken account of the cost of chemicals, other variable costs including utilities and selling expenses are going to inflate the variable costs further. Thus, the treatment technology should be targeting metal species possessing high values, such as platinum group metals (Rh: £20,000/kg). The profit generated from these high value ions can potentially be used to pay back the fixed cost of the treatment plant like agitators, clarifiers and control instrumentations.

8.3. Future work

The future research can be investigated in both science and engineering aspects. Colloid science behind the polymer and surfactant mixtures has not fully been researched. The leakage of surfactant, particularly in the anion treatment process, should be minimised, if the CAC of surfactant is lowered. A low CAC surfactant usually has a long hydrophobic carbon chain. The cost and availability of surfactant are also essential to consider when testing other possible surfactants. Apart from changing the surfactant, adding a non-ionic surfactant can also decrease the overall CAC, but the charge density of the resulting aggregates is reduced, which might cause a decline in the removal efficiency or possible improvement to the selectivity towards target ions. The selectivity can also be improved using a pH-sensitive surfactant because its charge density is manipulated via pH adjustment. Both methods may also decrease the concentrations of applied hydrogen or hydroxide ions for the ion recovery and polymer–surfactant regeneration. Modification of polymer by attaching various functional groups may also

increase the selectivity through other binding mechanisms, such as chelation and complexation.

As regards extending the engineering applications, there are four possible directions: treatment of valuable charged species, treatment of organics, real industrial effluent and pilot plant studies. Firstly, recovering the targeted ions as a by-product is a key revenue stream; it could become more lucrative, if the by-product has a higher market value, such as rare earth or precious metals. Secondly, the charged surface of aggregates in the PSAs is used to bind the oppositely charged ions, but the inner hydrophobic core has not been used at all. The adsorption capacity may not as large as the micelles, but it might work for dilute organic contaminants, such as trace amounts of pesticide residuals in the water body, which becomes a raise problem in recent years. Thirdly, testing the process with real industrial effluents would be extremely beneficial for understanding the applicability of the process and identifying potential improvement. Much more targeted work will be proposed based on the feedback from industries. Finally, the PSA process has only been investigated in a bench scale, therefore, a continuous treatment setup, scaling up and detail design of the reaction tanks and process flow sheet could be another step towards commercialising.

Abbreviations

AC	admicellar chromatography
AMF	adsorptive micellar flocculation
CAC	critical aggregation concentration
CF	coarse filtration
CFC	critical formation concentration
CMC	critical micellar concentration
LM-MEUF	ligand modified – micellar enhanced ultrafiltration
MEUF	micellar enhanced ultrafiltration
MF	micro filtration
MTAB	myristyl trimethyl ammonium bromide
MW	molecular weight
PAA	poly(acrylic acid)
PEI	poly(ethyleneimine)
PEUF	polymer enhanced ultrafiltration
PolyDADMAC	poly(diallyl dimethyl ammonium chloride)
PPB	part per billion
PPM	part per million
PSA	polymer surfactant aggregate
PSS	poly(sodium 4-styrenesulfonate)
RMP	revolution per minute
SDS	sodium dodecyl sulphate
UF	ultra filtration
UHQ	ultra-high quality

References

Adak, A. and Pal, A. 2006. Removal Kinetics and Mechanism for Crystal Violet Uptake by Surfactant-Modified Alumina, *Journal of Environmental Science and Health, Part A* 41(10), 2283-2297.

Adak, A., Bandyopadhyay, M. and Pal, A. 2005a. Adsorption of Anionic Surfactant on Alumina and Reuse of the Surfactant-Modified Alumina for the Removal of Crystal Violet from Aquatic Environment, *Journal of Environmental Science and Health, Part A*, 40(1), 167-182.

Adak, A., Bandyopadhyay, M. and Pal, A. 2005b. Removal of crystal violet dye from wastewater by surfactant-modified alumina, *Separation and Purification Technology* 44(2), 139-144.

Ajjabi, L. C. and Chouba, L. 2009. Biosorption of Cu^{2+} and Zn^{2+} from aqueous solutions by dried marine green macroalga Chaetomorpha linum, *Journal of Environment Management* 90 (11), 3485-3489.

Ajmal, M., Rao, R. A. K., Ahmad, R. and Ahmad, J. 2000. Adsorption studies on Citrus reticulata (fruit peel of orange): removal and recovery of Ni (II) from electroplating wastewater, *Journal of Hazardous Materials* 79(1), 117-131.

Ajmal, M., Rao, R. A. K., Anwar, S., Ahmad, J. and Ahmad, R. 2003. Adsorption studies on rice husk: removal and recovery of Cd (II) from wastewater, *Bioresource Technology* 86(2), 147-149.

Akita, S., Yang, L. and Takeuchi, H. 1997. Micellar-enhanced ultrafiltration of gold(III) with nonionic surfactant, *Journal of Membrane Science* 133(2), 189-194.

Allen, H. E. and Chen, P. H. 1993. Remediation of metal contaminated soil by EDTA incorporating electrochemical recovery of metal and EDTA, *Environmental Progress* 12(4), 284-293.

Almeida, T. D. O. and Talens-Alesson, F. I. 2006. Removal of phenylamine and catechol by adsorptive micellar flocculation, *Colloids and Surfaces A: Physicochemical and Engineering Aspects* 279(1), 28-33.

Almutairi, F. M., Williams, P. M. and Lovitt, R. W. 2011. Polymer enhanced membrane filtration of metals: retention of single and mixed species of metal ions based on adsorption isotherms, *Desalination and Water Treatment* 28(1-3), 130-136.

Alyüz, B. and Veli, S. 2009. Kinetics and equilibrium studies for the removal of nickel and zinc from aqueous solutions by ion exchange resins, *Journal of Hazardous Materials* 167(1-3), 482-488.

Ananthapadmanabhan, K. P., Leung, P. S. and Goddard, E. D. 2011. Fluorescence and solubilization studies of polymer–surfactant systems, *Colloids and Surfaces* 13(0), 63-72.

Anthony, O. and Zana, R. 1996. Interactions between Water-Soluble Polymers and Surfactants: Effect of the Polymer Hydrophobicity. 1. Hydrophilic Polyelectrolytes, *Langmuir* 12(8), 1967-1975.

Anthony, S. and Talens-Alesson, F. 2007. Effect of an electrolyte on Adsorptive Micellar Flocculation (I): Increased selectivity in the presence of monovalent–monovalent electrolyte, *Colloids and Surfaces A: Physicochemical and Engineering Aspects* 301(1), 1-7.

Apiratikul, R. and Pavasant, P. 2008. Batch and column studies of biosorption of heavy metals by Caulerpa lentillifera, *Bioresource Technology* 99(8), 2766-2777.

Aroua, M. K., Zuki, F. M. and Sulaiman, N. M. 2007. Removal of chromium ions from aqueous solutions by polymer-enhanced ultrafiltration, *Journal of Hazardous Materials* 147(3), 752-758.

Athanasiadis, K. and Helmreich, B. 2005. Influence of chemical conditioning on the ion exchange capacity and on kinetic of zinc uptake by clinoptilolite, *Water Research* 39, 1527-1532.

Bacchin, P., Aimar, P. and Field, R. W. 2006. Critical and sustainable fluxes: theory, experiments and applications, *Journal of membrane science* 281(1), 42-69.

Baek, K. and Yang, J. W. 2004. Simultaneous removal of chlorinated aromatic hydrocarbons, nitrate, and chromate using micellar-enhanced ultrafiltration, *Chemosphere* 57(9), 1091-1097.

Barakat, M. and Schmidt, E. 2010. Polymer-enhanced ultrafiltration process for heavy metals removal from industrial wastewater, *Desalination* 256(1), 90-93.

Barton, J., Fitzgerald, T., Lee, C., O'Rear, E. and Harwell, J. 1988. Admicellar chromatography: separation and concentration of isomers using two-dimensional solvents, *Separation Science and Technology* 23(6-7), 637-660.

Bayer, E., Spivakov, B. Y. and Geckeler, K. 1985. Poly (ethyleneimine) as complexing agent for separation of metal ions using membrane filtration, *Polymer Bulletin* 13(4), 307-311.

Belfort, G., Davis, R. H. and Zydney, A. L. 1994. The behavior of suspensions and macromolecular solutions in crossflow microfiltration, *Journal of Membrane Science* 96(1), 1-58.

Bell, C. G., Breward, C. J. W., Howell, P. D., Penfold, J. and Thomas, R. K. 2007. Macroscopic Modeling of the Surface Tension of Polymer−Surfactant Systems, *Langmuir* 23(11), 6042-6052.

Berglund, K. D., Truong, M. T., Przybycien, T. M., Tilton, R. D. and Walker, L. M. 2004. Rheology of transient networks containing hydrophobically modified cellulose, anionic surfactant and colloidal silica: role of selective adsorption, *Rheologica acta* 43(1), 50-61.

Bolto, B. A. 1995. Soluble polymers in water purification, *Progress in Polymer Science* 20(6), 987-1041.

Bolto, B. and Gregory, J. 2007. Organic polyelectrolytes in water treatment, *Water research* 41(11), 2301-2324.

Boonyasuwat, S., Chavadej, S., Malakul, P. and Scamehorn, J. F. 2003. Anionic and cationic surfactant recovery from water using a multistage foam fractionator, *Chemical Engineering Journal* 93(3), 241-252.

Boukhalfa, C. 2010. Sulfate removal from aqueous solutions by hydrous iron oxide in the presence of heavy metals and competitive anions: Macroscopic and spectroscopic analyses, *Desalination* 250(1), 428-432.

Bulpin, P.V., Cutler, A.N. and Lips, A. 1987. Cooperative binding of sodium myristate to amylose, *Macromolecules* 20(1), 44-49.

Camarillo, R., Llanos, J., García-Fernández, L., Pérez, Á. and Canizares, P. 2010. Treatment of copper (II)-loaded aqueous nitrate solutions by polymer enhanced ultrafiltration and electrodeposition, *Separation and Purification Technology* 70(3), 320-328.

Campbell, R. A., Angus-Smyth, A., Yanez Arteta, M., Tonigold, K., Nylander, T. and Varga, I. 2010. New perspective on the cliff edge peak in the surface tension of oppositely charged polyelectrolyte/surfactant mixtures, *Journal of Physical Chemistry Letters* 1(20), 3021-3026.

Canizares, P., Perez, A., Camarillo, R. and Villajos, M. T. 2005. Improvement and modelling of a batch polyelectrolyte enhanced ultrafiltration process for the recovery of copper, *Desalination* 184(1-3), 357-366.

Cañizares, P., Pérez, Á., Llanos, J. and Rubio, G. 2008. Preliminary design and optimisation of a PEUF process for Cr(VI) removal, *Desalination* 223(1–3), 229-237.

Chan, K., Liu, T., Matsuura, T. and Sourirajan, S. 1984. Effect of shrinkage on pore size and pore size distribution of cellulose acetate reverse osmosis membranes. *Industrial & engineering chemistry product research and development* 23(1), 124-133.

Charerntanyarak, L. 1999. Heavy metals removal by chemical coagulation and precipitation, *Water Science Technology* 39(10-11) 135-138.

Chu, D.Y. and Thomas, J. K. 1986. Effect of cationic surfactants on the conformation transition of poly(methacrylic acid), *Journal of the American Chemical Society* 108(20), 6270-6276.

Darnall, D. W., Greene, B., Henzl, M. T., Hosea, J. M., McPherson, R. A., Sneddon, J. and Alexander, M. D. 1986. Selective recovery of gold and other metal ions from an algal biomass, *Environmental Science & Technology* 20(2), 206-208.

Das, A. K., Saha, S., Pal, A. and Maji, S. K. 2009. Surfactant-modified alumina: An efficient adsorbent for malachite green removal from water environment, *Journal of Environmental Science and Health, Part A* 44(9), 896-905.

Deng, S. and Ting, Y. P. 2005. Polyethylenimine-Modified Fungal Biomass as a High-Capacity Biosorbent for Cr(VI) Anions: Sorption Capacity and Uptake Mechanisms, *Environmental Science & Technology* 39(21), 8490-8496.

Deriszadeh, A., Harding, T. G. and Husein, M. M. 2009. Improved MEUF removal of naphthenic acids from produced water, *Journal of Membrane Science* 326(1), 161-167.

Dorra, E. J., Mourad, B. S. and Mahmoud, D. 2010. Retention of cadmium and zinc from aqueous solutions by poly (acrylic acid)-assisted ultrafiltration, *International Journal of Chemical Reactor Engineering* 8(1), 133.

Dubin, P. L. and Davis, D. 1985. Stoichiometry and coacervation of complexes formed between polyelectrolytes and mixed micelles, *Colloids and surfaces* 13, 113-124.

Dunn Jr, R. O., Scamehorn, J. F. and Christian, S. D. 1985. Use of micellar-enhanced ultrafiltration to remove dissolved organics from aqueous streams, *Separation Science and Technology* 20(4), 257-284.

El-Abbassi, A., Khayet, M. and Hafidi, A. 2011. Micellar enhanced ultrafiltration process for the treatment of olive mill wastewater, *Water research* 45(15), 4522-4530.

El-Samrani, A.G., Lartiges, B.S. and Villiéras, F. 2008. Chemical coagulation of combined sewer overflow: Heavy metal removal and treatment optimization, *Water Research* 42(4–5), 951-960.

Ennigrou, D. J., Ali, M. B. S. and Dhahbi, M. 2014. Copper and Zinc removal from aqueous solutions by polyacrylic acid assisted-ultrafiltration, *Desalination* 343, 82-87.

Everett, D. H. 1988. Basic principles of colloid science, Chapter 1. *Royal Society of Chemistry*.

Fegyver, E. and Mészáros, R. 2015. Complexation between Sodium Poly (styrenesulfonate) and Alkyltrimethylammonium Bromides in the Presence of Dodecyl Maltoside, *The Journal of Physical Chemistry B* 119(16), 5336-5346.

Fillipi, B.R., Brant, L.W., Scamehorn, J.F. and Christian, S.D. 1999. Use of Micellar-Enhanced Ultrafiltration at Low Surfactant Concentrations and with Anionic–Nonionic Surfactant Mixtures, *Journal of Colloid and Interface Science* 213(1), 68-80.

Fu, F. and Wang, Q. 2011. Removal of heavy metal ions from wastewaters: A review, *Journal of Environmental Management* 92 (3), 407-418.

Fuguet, E., Ràfols, C., Rosés, M. and Bosch, E. 2005. Critical micelle concentration of surfactants in aqueous buffered and unbuffered systems, *Analytica Chimica Acta* 548(1–2), 95-100.

Geckeler, K. E. and Volchek, K. 1996. Removal of hazardous substances from water using ultrafiltration in conjunction with soluble polymers, *Environmental Science & Technology* 30(3), 725-734.

Ghezzi, L., Robinson, B. H., Secco, F., Tinè, M. R. and Venturini, M. 2008. Removal and recovery of palladium (II) ions from water using micellar-enhanced ultrafiltration with a cationic surfactant, *Colloids and Surfaces A: Physicochemical and Engineering Aspects* 329(1), 12-17.

Goddard, E. 2002. Polymer/surfactant interaction: interfacial aspects, *Journal of colloid and Interface Science* 256(1), 228-235.

Goddard, E.D. and Hannan, R.B. 1976. Cationic polymer/anionic surfactant interactions, *Journal of Colloid and Interface Science* 55 (1), 73-79.

Goddard, E.D. and R.B. Hannan, 1977. Polymer/surfactant interactions, *Journal of the American Oil Chemists' Society* 54(12), 561-566.

Goddard, E.D. 1986. Polymer–surfactant interaction part II. Polymer and surfactant of opposite charge, *Colloids and Surfaces* 19 (2–3), 301-329.

Goldraich, M., Schwartz, J. R. Burns, J. L. and Talmon, Y. 1997. Microstructures formed in a mixed system of a cationic polymer and an anionic surfactant, *Colloids and Surfaces A: Physicochemical and Engineering Aspects* 125(2–3), 231-244.

Gözmen, B., Oturan, M. A., Oturan, N. and Erbatur, O. 2003. Indirect Electrochemical Treatment of Bisphenol A in Water via Electrochemically Generated Fenton's Reagent, *Environmental Science & Technology* 37(16), 3716-3723.

Guo, W., Uchiyama, H., Tucker, E. E., Christian, S. D. and Scamehorn, J. F. 1997. Use of polyelectrolyte-surfactant complexes in colloid-enhanced ultrafiltration, *Colloids and Surfaces A: Physicochemical and Engineering Aspects* 123, 695-703.

Gzara, L. and Dhahbi, M. 2001. Removal of chromate anions by micellar-enhanced ultrafiltration using cationic surfactants, *Desalination* 137(1–3), 241-250.

Hafiane, A., Lemordant, D. and Dhahbi, M. 2000. Removal of hexavalent chromium by nanofiltration, *Desalination* 130(3), 305-312.

Halacheva, S. S., Penfold, J. Thomas R. K. and Webster. J. R. P. 2012. Effect of Architecture on the Formation of Surface Multilayer Structures at the Air–Solution Interface from Mixtures of Surfactant with Small Poly(ethyleneimine)s, *Langmuir* 28(15), 6336-6347.

Hankins, N. P., Lu, N. and Hilal, N. 2006. Enhanced removal of heavy metal ions bound to humic acid by polyelectrolyte flocculation, *Separation and Purification Technology* 51(1), 48-56.

Hankins, N., Hilal, N., Ogunbiyi, O. O. and Azzopardi, B. 2005. Inverted polarity micellar enhanced ultrafiltration for the treatment of heavy metal polluted wastewater, *Desalination* 185(1–3), 185-202.

Hansson, P. and Almgren, M. 1996. Interaction of CnTAB with Sodium (Carboxymethyl) cellulose: Effect of Polyion Linear Charge Density on Binding Isotherms and Surfactant Aggregation Number, *The Journal of Physical Chemistry* 100(21), 9038-9046.

Higgins, I. R. 1973. Ion exchange. Present and future use, *Environmental Science & Technology* 7(13), 1110-1114.

Hilal, N., Busca, G., Hankins, N. and Mohammad, A. W. 2004. The use of ultrafiltration and nanofiltration membranes in the treatment of metal-working fluids, *Desalination* 167, 227-238.

Hilal, N., Busca, G., Rozada, F. and Hankins, N. 2005. Use of activated carbon to polish effluent from metalworking treatment plant: comparison of different streams, *Desalination* 185(1), 297-306.

Inglezakis, V. J., Zorpas, A. A., Loizidou M. D. and Grigoropoulou H. P. 2005. The effect of competitive cations and anions on ion exchange of heavy metals, *Separation and Purification Technology* 46 (3), 202-207.

Islamoglu-Kadioglu, S., Yilmaz, L. and Onder-Ozbelge, H. 2009. Estimation of binding constants of Cd (II), Ni (II) and Zn (II) with polyethyleneimine (PEI) by polymer enhanced ultrafiltration (PEUF) technique, *Separation Science and Technology* 44(11), 2559-2581.

İslamoğlu, S. and Yılmaz, L. 2006. Effect of ionic strength on the complexation of polyethyleneimine (PEI) with Cd^{2+} and Ni^{2+} in polymer enhanced ultrafiltration (PEUF), *Desalination* 200(1), 288-289.

Jellinek, H. H. G. and Sangal, S. P. 1972. Complexation of metal ions with natural polyelectrolytes (removal and recovery of metal ions from polluted waters), *Water Research* 6(3), 305-314.

Jiang, J. S., Vane, L. M. and Sikdar, S. K. 1997. Recovery of VOCs from surfactant solutions by pervaporation, *Journal of Membrane Science* 136(1), 233-247.

Jones, M. N. 1967. The interaction of sodium dodecyl sulfate with polyethylene oxide, *Journal of Colloid and Interface Science* 23 (1), 36-42.

Jorgensen, T. C. and Weatherley, L. R. 2003. Ammonia removal from wastewater by ion exchange in the presence of organic contaminants, *Water Research* 37(8), 1723-1728.

Juang, R. S., Xu, Y. Y. and Chen, C. L. 2003. Separation and removal of metal ions from dilute solutions using micellar-enhanced ultrafiltration, *Journal of Membrane Science* 218(1), 257-267.

Jung, J., Yang, J. S., Kim, S. H. and Yang, J. W. 2008. Feasibility of micellar-enhanced ultrafiltration (MEUF) or the heavy metal removal in soil washing effluent, *Desalination* 222(1), 202-211.

Katsumata, H., Kaneco, S., Kasai, H., Itoh, K., Masuyama, K., Suzuki, T., Funasaka, K. and Ohta, K. 2004. Removal of humic substances and their metal complexes by adsorption, *Environmental Engineering Science* 21(3), 341-348.

Kim, H. J., Baek, K., Kim, B. K. and Yang, J. W. 2005. Humic substance-enhanced ultrafiltration for removal of cobalt, *Journal of Hazardous Materials* 122(1), 31-36.

Kim, H., Baek, K., Lee, J., Iqbal, J. and Yang, J. W. 2006. Comparison of separation methods of heavy metal from surfactant micellar solutions for the recovery of surfactant, *Desalination* 191(1), 186-192.

Komesvarakul, N., Do, L. D., Nguyen, T. T. and Scamehorn, J. F. 2005a. Colloid-Enhanced Ultrafiltration of Chlorophenols in Wastewater: Part IV. Effect of Added Salt on the Surfactant Leakage in Surfactant Solutions and Surfactant–Polymer Mixtures, *Separation Science and Technology* 40(12), 2463-2478.

Komesvarakul, N., Nguyen, T. T., Do, L. D. and Scamehorn, J. F. 2005b. Colloid-enhanced ultrafiltration of chlorophenols in wastewater: Part V. simultaneous removal of a chlorophenol and a metal ion, *Separation Science and Technology* 40(14), 2803-2818.

Komesvarakul, N., Scamehorn, J. F. and Gecol, H. 2003. Purification of phenolic-laden wastewater from the pulp and paper industry by using colloid-enhanced ultrafiltration, *Separation Science and Technology* 38(11), 2465-2501.

Komesvarakul, N., Scamehorn, J. F. and Taylor, R. W. 2004. Colloid-enhanced ultrafiltration of chlorophenols in wastewater: Part II. Apparent acid dissociation constants of chlorophenols in colloid solutions at different ionic strengths and effect of pH on solubilization of phenolic compounds, *Separation Science and Technology* 39(14), 3169-3191.

Komesvarakul, N., Scamehorn, J. F. and Taylor, R. W. 2004. Colloid-enhanced ultrafiltration of chlorophenols in wastewater: Part III. Effect of added salt on solubilization in surfactant solutions and surfactant–polymer mixtures, *Separation Science and Technology* 39(14), 3193-3214.

Korkish, J. 1989. Handbook of Ion Exchange Resins: Their Application to Inorganic Analytical Chemistry, CRC Press: *Boca Raton*, FL.

Korus, I. and Rumińska, M. 2014. UV spectrophotometric studies of Cu (II) ions separation by ultrafiltration enhanced with poly (sodium acrylate), *Desalination and Water Treatment* (ahead-of-print), 1-7.

Ku, Y. and Jung, I. L. 2001. Photocatalytic reduction of Cr(VI) in aqueous solutions by UV irradiation with the presence of titanium dioxide, *Water Research* (35)135-142.

Kurniawan, T. A., Chan, G. Y., Lo, W. H. and Babel, S. (2006). Physico–chemical treatment techniques for wastewater laden with heavy metals, *Chemical Engineering Journal* 118(1), 83-98.

Lee, J., Yang, J. S., Kim, H. J., Baek, K. and Yang, J. W. 2005. Simultaneous removal of organic and inorganic contaminants by micellar enhanced ultrafiltration with mixed surfactant, *Desalination* 184(1), 395-407.

Lee, S. W., Song, T. S., Jo, M. C. and Park, S. J. 2000. Separation of o-Cresol Using Polymer/Surfactant Complexes, *Journal of Industrial and Engineering Chemistry* 6(1), 53-58.

Lekkerkerker, H. N. and Tuinier, R. 2011. Colloids and the depletion interaction, Chapter 1. (Vol. 833). *Springer*.

Leung, P. S., Goddard E. D., Han C. and Glinka C. J. 1985. A study of polycation—anionic-surfactant systems, *Colloids and Surfaces* 13(0), 47-62.

Li, C. W., Cheng, C. H., Choo, K. H. and Yen, W. S. 2008. Polyelectrolyte enhanced ultrafiltration (PEUF) for the removal of Cd (II): Effects of organic ligands and solution pH, *Chemosphere* 72(4), 630-635.

Li, X., Zeng, G. M., Huang, J. H., Zhang, C., Fang, Y. Y., Qu, Y. H., Luo, F., Lin, D. and Liu, H. L. 2009. Recovery and reuse of surfactant SDS from a MEUF retentate containing Cd^{2+} or Zn^{2+} by ultrafiltration, *Journal of Membrane Science* 337(1), 92-97.

Liu, C. K. and Li, C. W. 2004. Simultaneous recovery of copper and surfactant by an electrolytic process from synthetic solution prepared to simulate a concentrate

waste stream of a micellar-enhanced ultrafiltration process. *Desalination* 169(2), 185-192.

Liu, Y. and Fang, H. H. 2003. Influences of extracellular polymeric substances (EPS) on flocculation, settling, and dewatering of activated sludge, *Critical Reviews in Environmental Science and Technology* 33(3), 237-273.

Llanos, J., Pérez, Á. and Cañizares, P. 2008. Copper recovery by polymer enhanced ultrafiltration (PEUF) and electrochemical regeneration, *Journal of Membrane Science* 323(1), 28-36.

Loukidou, M. X., Matis, K. A., Zouboulis, A. I. and Liakopoulou-Kyriakidou, M. 2003. Removal of As(V) from wastewaters by chemically modified fungal biomass, *Water Research* 37(18), 4544-4552.

Lubal, P., Široký, D., Fetsch, D. and Havel, J. 1998. The acidobasic and complexation properties of humic acids: Study of complexation of Czech humic acids with metal ions, *Talanta* 47(2), 401-412.

Luo, F., Zeng, G. M., Huang, J. H., Zhang, C., Fang, Y. Y., Qu, Y. H., Li, X., Lin, D. and Zhou, C. F. 2010. Effect of groups difference in surfactant on solubilization of aqueous phenol using MEUF, *Journal of Hazardous Materials* 173(1), 455-461.

Miretzky, P. and Cirelli, A. F. 2009. Hg (II) removal from water by chitosan and chitosan derivatives: a review, *Journal of Hazardous Materials* 167(1), 10-23.

Mohan, D. and Chander, S. 2006. Removal and recovery of metal ions from acid mine drainage using lignite—a low cost sorbent. *Journal of Hazardous Materials* 137(3), 1545-1553.

Mólgora, C. C., Domínguez, A. M., Avila, E. M., Drogui, P. and Buelna, G. 2013. Removal of arsenic from drinking water: A comparative study between electrocoagulation-microfiltration and chemical coagulation-microfiltration processes, *Separation and Purification Technology* 118 (1), 645-651.

Montgomery, M. A. and Elimelech, M. 2007. Water and sanitation in developing countries: including health in the equation, *Environmental Science &* Technology 41(1), 17-24.

Najafi, M., Yousefi, Y. and Rafati, A. A. 2012. Synthesis, characterization and adsorption studies of several heavy metal ions on amino-functionalized silica nano hollow sphere and silica gel, *Separation and Purification Technology* 85 (1), 193-205.

Nayyar, S. P., Sabatini, D. A. and Harwell, J. H. 1994. Surfactant adsolubilization and modified admicellar sorption of nonpolar, polar, and ionizable organic contaminants, *Environmental Science & Technology* 28(11), 1874-1881.

Neyens, E., Baeyens, J. and Dewil, R. 2004. Advanced sludge treatment affects extracellular polymeric substances to improve activated sludge dewatering, *Journal of Hazardous Materials* 106(2), 83-92.

Nguyen, Q. T., Jyline, Y. and Neel, J. 1981. Concentration of cupric and nickel ions by complexation-ultrafiltration. Synergic effect of succinic acid, *Desalination* 36(3), 277-283.

Nizri, G. and Magdassi, S. 2005. Solubilization of hydrophobic molecules in nanoparticles formed by polymer–surfactant interactions, *Journal of Colloid and Interface Science* 291(1), 169-174.

Nizri, G., Lagerge, S. Kamyshny, A. Major D. T. and Magdassi, S. 2008. Polymer–surfactant interactions: Binding mechanism of sodium dodecyl sulfate to poly(diallyldimethylammonium chloride), *Journal of Colloid and Interface* Science 320(1), 74-81.

Ohbu, K., Hiraishi, O. and Kashiwa, I. 1982. Effect of quaternary ammonium substitution of hydroxyethylcellulose on binding of dodecyl sulphate, *Journal of the American Oil Chemists' Society* 59(2), 108-112.

Onsosyen, E. and Skaugrud, O. 1990. Metal recovery using chitosan, *Journal of Chemical Technology and Biotechnology* 49(4), 395-404.

Ostroski, I. C., Barros, M. A. S. D., Silvab, E. A., Dantas, J. H., Arroyo, P. A. and Lima, O. C. M. 2009. A comparative study for the ion exchange of Fe(III) and Zn(II) on zeolite NaY, *Journal of Hazardous Materials* 161 1404-1412.

Paton, P. and Talens-Alesson, F. 2001. Effect of pH on the flocculation of SDS micelles by Al^{3+}, *Colloid and Polymer Science* 279(2), 196-199.

Paton-Morales, P. and Talens-Alesson, F. 2000. Flocculation of anionic surfactant micelles in the presence of hydrocarbons, *Colloid and Polymer Science* 278(7), 697-700.

Paton-Morales, P. and Talens-Alesson, F. 2002. Effect of competitive adsorption of Zn^{2+} on the flocculation of lauryl sulfate micelles by Al^{3+}, *Langmuir* 18(22), 8295-8301.

Penfold, J., Thomas, R. and Taylor, D. 2006. Polyelectrolyte/surfactant mixtures at the air–solution interface, *Current Opinion in Colloid & Interface Science* 11(6), 337-344.

Penfold, J., Thomas, R. K. and Taylor, D. J. F. 2007b. The Interaction between Sodium Alkyl Sulfate Surfactants and the Oppositely Charged Polyelectrolyte, polyDMDAAC, at the Air−Water Interface: The Role of Alkyl Chain Length and Electrolyte and Comparison with Theoretical Predictions, *Langmuir* 23(6), 3128-3136.

Penfold, J., Tucker, I., Thomas, R. K. and Zhang, J. 2005. Adsorption of Polyelectrolyte/Surfactant Mixtures at the Air−Solution Interface: Poly(ethyleneimine)/Sodium Dodecyl Sulfate, *Langmuir* 21(22), 10061-10073.

Penfold, J., Tucker, I., Thomas, R. K., Taylor, D. J. F., Zhang, J. and Zhang, X. L. 2007a. The Impact of Electrolyte on the Adsorption of Sodium Dodecyl Sulfate/Polyethyleneimine Complexes at the Air−Solution Interface, *Langmuir* 23(7), 3690-3698.

Petkov, J. T., Tucker, I. M. Penfold, J. Thomas, R. K. Petsev, D. N. Dong, C. C. Golding, S. and Grillo, I. 2010. The Impact of Multivalent Counterions, Al^{3+}, on the Surface Adsorption and Self-Assembly of the Anionic Surfactant Alkyloxyethylene Sulfate and Anionic/Nonionic Surfactant Mixtures, *Langmuir* 26(22), 16699-16709.

Petzold, G. and Schwarz, S. 2006. Dye removal from solutions and sludges by using polyelectrolytes and polyelectrolyte–surfactant complexes, *Separation and Purification Technology* 51(3), 318-324.

Petzold, G., Schwarz, S., Mende, M. and Jaeger, W. 2007. Dye flocculation using polyampholytes and polyelectrolyte-surfactant nanoparticles, *Journal of Applied Polymer Science* 104(2), 1342-1349.

Porras, M. and Talens, F. 1999. Removal of 2, 4-D from aqueous solutions by micellar flocculation, *Separation Science and Technology* 34(13), 2679-2684.

Porras, M. and Talens, F. 2000. Removal of 2, 4-D from aqueous solutions by micellar flocculation with α-olefinsulfonates, *Separation Science and Technology* 35(12), 1973-1978.

Pramauro, E., Prevot, A. B., Pelizzetti, E., Marchelli, R., Dossena, A. and Biancardi, A. 1992. Quantitative removal of uranyl ions from aqueous solutions using micellar-enhanced ultrafiltration, *Analytica Chimica Acta* 264(2), 303-310.

Rether, A. and Schuster, M. 2003. Selective separation and recovery of heavy metal ions using water-soluble N-benzoylthiourea modified PAMAM polymers, *Reactive and Functional Polymers*, 57(1), 13-21.

Ritacco, H., Kurlat, D. and Langevin D. 2003. Properties of Aqueous Solutions of Polyelectrolytes and Surfactants of Opposite Charge: Surface Tension, Surface Rheology, and Electrical Birefringence Studies, *The Journal of Physical Chemistry B* 107(34), 9146-9158.

Rivas, B. L. and Geckeler, K. E. 1992. Synthesis and metal complexation of poly (ethyleneimine) and derivatives. Polymer Synthesis Oxidation Processes, *Springer*: 171-188.

Rivas, B. L., Pooley, S. A., Pereira, E. D., Cid, R., Luna, M., Jara, M. A. and Geckeler, K. E. 2005. Water-soluble amine and imine polymers with the ability to bind metal ions in conjunction with membrane filtration, *Journal of Applied Polymer Science* 96(1), 222-231.

Roach, J. D. and Zapien, J. H. 2009. Inorganic ligand-modified, colloid-enhanced ultrafiltration: A novel method for removing uranium from aqueous solution, *Water Research* 43(18), 4751-4759.

Roach, J. D., Christian, S. D., Tucker, E. E., Taylor, R. W. and Scamehorn, J. F. 2003. Ligand-modified colloid enhanced ultrafiltration. Use of nitrilotriacetic acid

derivatives for the selective removal of lead from aqueous solution, *Separation Science and Technology* 38(9), 1925-1947.

Rubio, J., Souza, M. L. and Smith, R. W. 2002. Overview of flotation as a wastewater treatment technique, *Minerals Engineering* 2002 (15)139-155.

Saeed, A., Iqbal, M. and Akhtar, M. W. 2005. Removal and recovery of lead (II) from single and multimetal (Cd, Cu, Ni, Zn) solutions by crop milling waste (black gram husk), *Journal of Hazardous Materials,* 117(1), 65-73.

Saiano, F., Ciofalo, M., Cacciola, S. O. and Ramirez, S. 2005. Metal ion adsorption by Phomopsis sp. biomaterial in laboratory experiments and real wastewater treatments, *Water Research* 39(11), 2273-2280.

Saitoh, T., Fukushima, K. and Miwa, A. 2014. Combined use of surfactant-induced coagulation of poly (allylamine hydrochloride) with peroxidase-mediated degradation for the rapid removal of estrogens and phenolic compounds from water, *Separation and Purification Technology* 128, 11-17.

Samper, E., Rodr ǵuez, M., De la Rubia M. A. and Prats. D. 2009. Removal of metal ions at low concentration by micellar-enhanced ultrafiltration (MEUF) using sodium dodecyl sulfate (SDS) and linear alkylbenzene sulfonate (LAS). *Separation and Purification Technology* 65(3), 337-342.

Sasaki, K. J., Burnett, S. L., Christian, S. D., Tucker, E. E. and Scamehorn, J. F. 1989. Polyelectrolyte ultrafiltration of multivalent ions. Removal of copper (2+) by sodium poly (styrenesulfonate), *Langmuir* 5(2), 363-369.

Sato, Y., Kang, M., Kamei, T. and Magara, Y. 2002. Performance of nanofiltration for arsenic removal, *Water Research* 36(13), 3371-3377.

Scamehorn, J. F., Christian, S. D., Tucker, E. E. and Tan, B. I. 1990. Concentration polarization in polyelectrolyte-enhanced ultrafiltration, *Colloids and Surfaces* 49, 259-267.

Shadizadeh, S. B., Taylor, R. W., Scamehorn, J. F., Schovanec, A. L. and Christian, S. D. 1999. Use of Ligand-Modified Micellar-Enhanced Ultrafiltration to Selectively Remove Copper from Water, *ACS Symposium Series* 716, 280-293.

Shafiquzzaman, M., Azam, M. S., Nakajima, J. and Bari, Q. H. 2011. Investigation of arsenic removal performance by a simple iron removal ceramic filter in rural households of Bangladesh, *Desalination* 265(1–3), 60-66.

Shen, L. C., Nguyen, X. T. and Hankins, N. P. 2015. Removal of heavy metal ions from dilute aqueous solutions by polymer–surfactant aggregates: A novel effluent treatment process, *Separation and Purification Technology*, 152, 101-107.

Shkinev, V., Spivakov, B. Y., Geckeler, K. and Bayer, E. 1989. Anion exchange extraction and enrichment from aqueous solutions by quarternary ammonium reagents, *Solvent Extraction and Ion Exchange* 7(3), 499-510.

Shkinev, V., Vorob'eva, G., Spivakov, B. Y., Geckeler, K. and Bayer, E. 1987. Enrichment of arsenic and its separation from other elements by liquid-phase polymer-based retention, *Separation Science and Technology* 22(11), 2165-2173.

Sokolov, E. L., Yeh, F. Khokhlov A. and Chu. B. 1996. Nanoscale Supramolecular Ordering in Gel−Surfactant Complexes: Sodium Alkyl Sulfates in Poly(diallyldimethylammonium Chloride), *Langmuir* 12(26), 6229-6234.

Soponvuttikul, C., Scamehorn, J. F. and Saiwan, C. 2003. Aqueous dispersion behavior of barium chromate crystals: Effect of cationic polyelectrolyte, *Langmuir* 19(10), 4402-4410.

Staples, E., Tucker, I., Penfold, J., Warren, N., Thomas, R. K. and Taylor, D. J. F. 2002. Organization of Polymer−Surfactant Mixtures at the Air−Water Interface: Sodium Dodecyl Sulfate and Poly(dimethyldiallylammonium chloride), *Langmuir* 18(13), 5147-5153.

Staples, I. T., Penfold, J., Warren, N. and Thomas, R. K. 2000. The structure and composition of surfactant-polymer mixtures of sodium dodecyl sulphate, hexaethylene glycol monododecyl ether and poly-(dimethyldialyl ammonium chloride) adsorbed at the air-water interface, *Journal of Physics: Condensed Matter* 12, 6023-6038.

Sun, H., Hankins, N., Azzopardi, B., Hilal, N. and Almeida, C. 2008. A pilot-plant study of the adsorptive micellar flocculation process: Optimum design and operation, *Separation and Purification Technology* 62(2), 273-280.

Svab, M., Müllerová, M. and Raschman, R. 2008. Adsorptive micellar flocculation as an efficient method for processing soil extracts containing both surfactant and polychlorinated biphenyls: practical demonstration, *Water Environment Research* 80(1), 26-31.

Tabatabai, A., Scamehorn, J. F. and Christian, S. D. 1995. Water softening using polyelectrolyte-enhanced ultrafiltration, *Separation Science and Technology* 30(2), 211-224.

Taffarel, S.R. and Rubio, J. 2009. On the removal of Mn2. ions by adsorption onto natural and activated Chilean zeolites, *Minerals Engineering* (22) 336-343.

Talens-Alesson, F. I. 2001. Binding of pesticide 2, 4-D to SDS and AOS micellar flocculates, *Colloids and Surfaces A: Physicochemical and Engineering Aspects* 180(1), 199-203.

Talens-Alesson, F. I., Anthony, S. and Bryce, M. 2004. Complexation of organic compounds in the presence of Al^{3+} during micellar flocculation, *Water Research* 38(6), 1477-1483.

Talens-Alesson, F. I., Anthony, S. and Bryce, M. 2006. Removal of phenol by adsorptive micellar flocculation: multi-stage separation and integration of wastes for pollution minimisation, *Colloids and Surfaces A: Physicochemical and Engineering Aspects* 276(1), 8-14.

Talens-Alesson, F. I., Hall, S. T., Hankins, N. P. and Azzopardi, B. J. 2002. Flocculation of SDS micelles with Fe^{3+}, *Colloids and Surfaces A: Physicochemical and Engineering Aspects* 204(1–3), 85-91.

Talens-Alesson, F., Svabova, M. and Svab, M. 2010. The role of mixing in high performance Adsorptive Micellar Flocculation, *Colloids and Surfaces A: Physicochemical and Engineering Aspects* 355(1), 16-22.

Tangvijitsri, S., Saiwan, C., Soponvuttikul, C. and Scamehorn, J. F. 2002. Polyelectrolyte-enhanced ultrafiltration of chromate, sulfate, and nitrate, *Separation Science and Technology* 37(5), 993-1007.

Taylor, D. J. F., Thomas, R. K. and Penfold, J. 2002. The Adsorption of Oppositely Charged Polyelectrolyte/Surfactant Mixtures: Neutron Reflection from Dodecyl Trimethylammonium Bromide and Sodium Poly(styrene sulfonate) at the Air/Water Interface, *Langmuir* 18(12), 4748-4757.

Taylor, D. J. F., Thomas, R. K., Li, P. X. and Penfold, J. 2003. Adsorption of Oppositely Charged Polyelectrolyte/Surfactant Mixtures. Neutron Reflection from Alkyl Trimethylammonium Bromides and Sodium Poly(styrenesulfonate) at the Air/Water Interface: The Effect of Surfactant Chain Length, *Langmuir* 19(9), 3712-3719.

Taylor, D. J. F., Thomas, R. K. and Penfold, J. 2007. Polymer/surfactant interactions at the air/water interface, *Advances in Colloid and Interface Science* 132(2), 69-110.

Tharapiwattananon, N., Scamehorn, J. F., Osuwan, S., Harwell, J. H. and Haller, K. J. 1996. Surfactant recovery from water using foam fractionation, *Separation Science and Technology* 31(9), 1233-1258.

Tuncay, M., Christian, S. D., Tucker, E. E., Taylor, R. W. and Scamehorn, J. F. 1994a. Ligand-modified polyelectrolyte-enhanced ultrafiltration with electrostatic attachment of ligands. 1. Removal of Cu (II) and Pb (II) with expulsion of Ca (II), *Langmuir* 10(12), 4688-4692.

Tuncay, M., Christian, S. D., Tucker, E. E., Taylor, R. W. and Scamehorn, J. F. 1994b. Ligand-modified polyelectrolyte-enhanced ultrafiltration with electrostatic attachment of ligands. 2. Use of diethylenetriaminepentaacetic acid/cationic polyelectrolyte mixtures to remove both cations and anions from aqueous streams, *Langmuir* 10(12), 4693-4697.

Uchiyama, H., Christian, S. D., Tucker, E. E. and Scamehorn, J. F. 1994a. Solubilization and separation of p-tert-butylphenol using polyelectrolyte/surfactant complexes in colloid-enhanced ultrafiltration, *Journal of Colloid and Interface Science* 163(2), 493-499.

Uchiyama, H., Christian, S. D., Tucker, E. E. and Scamehorn, J. F. 1994b. Solubilization of trichloroethylene by polyelectrolyte/surfactant complexes, *AIChE journal* 40(12), 1969-1975.

Uludag, Y., Özbelge, H. Ö. and Yilmaz, L. 1997. Removal of mercury from aqueous solutions via polymer-enhanced ultrafiltration, *Journal of Membrane Science* 129(1), 93-99.

Vaaramaa, K. and Lehto, J. 2003. Removal of metals and anions from drinking water by ion exchange, *Desalination* 155(2), 157-170.

Van den Hoop, M. A., Porasso, R. D. and Benegas, J. C. 2002. Complexation of heavy metals by humic acids: analysis of voltammetric data by polyelectrolyte theory, *Colloids and Surfaces A: Physicochemical and Engineering Aspects* 203(1), 105-116.

Van der Bruggen, B., Mänttäri, M. and Nyström, M. 2008. Drawbacks of applying nanofiltration and how to avoid them: a review, *Separation and Purification* Technology 63(2), 251-263.

Vane, L. M. and Alvarez, F. R. 2002. Full-scale vibrating pervaporation membrane unit: VOC removal from water and surfactant solutions, *Journal of Membrane Science* 202(1), 177-193.

Voisin, D. and Vincent, B. 2003. Flocculation in mixtures of cationic polyelectrolytes and anionic surfactants, *Advances in Colloid and Interface Science* 106(1–3), 1-22.

Volchek, K., Keller, L., Velicogna, D. and Whittaker, H. 1993. Selective removal of metal ions from ground water by polymeric binding and microfiltration, *Desalination* 89(3), 247-262.

Von Wandruszka, R. 2000. Humic acids: Their detergent qualities and potential uses in pollution remediation, *Geochemical Transactions* 1(1), 10-15.

Winnik, M. A., Bystryak, S. M., Chassenieux, C., Strashko, V., Macdonald, P. M. and Siddiqui, J. 2000. Study of Interaction of Poly(ethylene imine) with Sodium Dodecyl Sulfate in Aqueous Solution by Light Scattering, Conductometry, NMR, and Microcalorimetry, *Langmuir* 16(10), 4495-4510.

Witek, A., Kołtuniewicz, A., Kurczewski, B., Radziejowska, M. and Hatalski, M. 2006. Simultaneous removal of phenols and Cr^{3+} using micellar-enhanced ultrafiltration process, *Desalination* 191(1), 111-116.

Wu, B., Christian, S. and Scamehorn, J. (1998). Recovery of surfactant from micellar-enhanced ultrafiltration using a precipitation process. Horizons 2000–aspects of colloid and interface science at the turn of the millenium, *Springer*: 60-73.

Xia, J., Zhang, H., Rigsbee, D. R., Dubin P. L. and Shaikh, T. 1993. Structural elucidation of soluble polyelectrolyte-micelle complexes: intra- vs interpolymer association, *Macromolecules* 26(11), 2759-2766.

Xu, K., Zeng, G. M., Huang, J. H., Wu, J. Y., Fang, Y. Y., Huang, G. H., Li, J. B., Xi, B. D. and Liu, H. L. 2007. Removal of Cd 2+ from synthetic wastewater using micellar-enhanced ultrafiltration with hollow fiber membrane, *Colloids and Surfaces A: Physicochemical and Engineering Aspects* 294(1), 140-146.

Xu, Y.H., Nakajima, T. and Ohki, A. 2002. Adsorption and removal of arsenic(V) from drinking water by aluminum-loaded Shirasu-zeolite, *Journal of Hazardous Materials* 92(3), 275-287.

Yurlova, L., Kryvoruchko, A. and Kornilovich, B. 2002. Removal of Ni (II) ions from wastewater by micellar-enhanced ultrafiltration, *Desalination* 144(1), 255-260.

Zahrim, A., Tizaoui, C. and Hilal, N. 2011. Coagulation with polymers for nanofiltration pre-treatment of highly concentrated dyes: a review, *Desalination* 266(1), 1-16.

Zemaitaitiene, R. J., Zliobaite, E., Klimaviciute, R. and Zemaitaitis, A. 2003. The role of anionic substances in removal of textile dyes from solutions using cationic flocculant, *Colloids and Surfaces A: Physicochemical and Engineering Aspects* 214(1), 37-47.

Zhang, J., Thomas, R. K. and Penfold, J. 2005. Interaction of oppositely charged polyelectrolyte-ionic surfactant mixtures: adsorption of sodium poly(acrylic acid)-dodecyl trimethyl ammonium bromide mixtures at the air-water interface, *Soft Matter* 1(4), 310-318.